Molecular Pathomechanisms of Amyotrophic Lateral Sclerosis Caused by *FUS* mutations

Haiyan An

January 2020

A thesis submitted to Cardiff University for the degree of Doctor of Philosophy

Summary

Amyotrophic lateral sclerosis (ALS) is the most common type of motor neuron disease affecting both upper and lower motor neurons. About 10% of ALS cases run in families with known genetic background, and mutations in the Fused in Sarcoma (*FUS*) gene are responsible for about 5% of the fALS cases (ALS-FUS). Despite normal FUS is a predominantly nuclear protein, mutant FUS is found to accumulate and aggregate in the cytoplasm of affected neurons and glial cells in ALS-FUS. It is generally believed that mutations are the primary cause of FUS protein mislocalisation, and additional stresses are required to trigger the formation of insoluble FUS aggregates (FUSopathy). However, no clear consensus has been achieved on many important questions. For instance, what are the consequences of FUS protein mutation for its nuclear function and how do they contribute to ALS-FUS development? What is the nature of the stress that promotes the massive protein accumulation and inclusion formation in the cytoplasm? This thesis attempts to address these questions using novel cellular models with targeted modifications of the *FUS* gene. It is demonstrated that the presence of endogenous mutant FUS protein in the nucleus causes hyper-assembly of structurally and functionally abnormal paraspeckles - nuclear bodies assembled on the long non-coding RNA called Nuclear Paraspeckle Assembly Transcript 1 (NEAT1). Dysfunctional paraspeckles together with accumulation of NEAT1 outside paraspeckles might contribute to the disease severity. Stresses capable of triggering cytoplasmic FUS aggregates are also investigated, and as a result, antiviral immune response has emerged as a potent stress promoting formation of persistent cytoplasmic FUS-positive assemblies. In addition, type I interferon expressed during antiviral response is found to cause FUS protein accumulation by increasing FUS mRNA stability. I propose a multi-step model where antiviral immune response serves as the "second hit" provoking FUSopathy. This thesis offers novel insights into the cellular and molecular events leading to the initiation and progression of ALS-FUS, which should help inform the development of therapeutic strategies in the future.

Acknowledgements

I gratefully acknowledge the international student scholarship and full tuition fees scholarship awarded by China Scholarship Council and Cardiff University. The project was also supported by the Medical Research Foundation and Motor Neurone Disease Association.

I would like to express my sincere gratitude to my supervisors Professor Vladimir Buchman and Dr. Tatyana Shelkovnikova for guiding me all the way through my PhD course with great enthusiasm and patience. I am truly lucky to become one of their students. Special thanks to Dr. Tatyana Shelkovnikova who has provided me with excellent technical support and professional guidance during the planning and development of the research project. My grateful thanks also extend to Dr. Natalia Ninkina for always being so kind and considerate.

I would like to thank former lab members Dr. Michael Kukharsky, Dr. Andrei Roman and Dr. Tatiana Tarasova for their kindness and friendship.

I am particularly thankful to my best friend Miss Isabel García Martín for always being there for me and giving me reasons to cheer.

I am deeply grateful to Darong Jin for being such a wonderful, appreciating, and understanding husband. I also give thanks to my beautiful little daughter Shuyan Jin for all the joy and happiness she has brought to me.

I owe my parents Tianyi An and Meiyu Bu a debt of gratitude for their unconditional love and trust over the years. I am also grateful for the generous support from my parents-in-law Chengzhu Jin and Huizi Jin. Many thanks to my sister Haiyue An for her continuous support and encouragement. Last but not least, I would like to thank my brother Qinghe Xu for his generous financial and moral support when I desperately needed it.

Contents

List of Figures

List of Tables

Abbreviations

ALS	amyotrophic lateral sclerosis
ADARB2	adenosine deaminase RNA specific B2
ASO	antisense oligonucleotide
C9orf72	chromosome 9 open reading frame 72
CC3	cleaved caspase 3
CNS	central nervous system
DAPI	4,6-diamidino-2-phenylindole
DMEM	Dulbecco's Modified Eagle's Medium
DPR	dipeptide repeat protein
DRB	5,6-dichloro-1-beta-D-ribofuranosylbenzimidazole
DSB	double-strand DNA break
dsRNA	double-stranded RNA
DTT	dithiothreitol
eIF2α	eukaryotic translation initiation factor 2α
endoFA	endogenous FUS aggregate
endoFG	endogenous FUS granule
ER	endoplasmic reticulum
ES	embryonic stem cell
exoFA	exogenous FUS aggregate
exoFG	exogenous FUS granule
FA	FUS aggregate
fALS	familial amyotrophic lateral sclerosis
FBS	fetal bovine serum
FG	FUS granule
FPKM	fragments per kilobase of transcript per million mapped reads
FTLD	frontotemporal lobar degeneration
FUS	fused in sarcoma
G3BP1	RAS GTPase-activating protein SH3 domain-binding protein 1
GFP	green fluorescent protein
gRNA	guide RNA

HBSS	Hank's Balanced Salt Solution
HDR	homology directed repair
HERV	human endogenous retrovirus
IDR	intrinsically disordered domain
IFN	interferon
IFNAR1	interferon alpha/beta receptor alpha chain
iPSC	induced pluripotent stem cell
KO	knockout
lncRNA	long non-coding RNA
NEAT1	Nuclear Paraspeckle Assembly Transcript 1
NHEJ	non-homologous end joining
NLS	nuclear localisation signal
NMD	nonsense-mediated mRNA decay
NONO	non-POU domain containing octamer binding
NPC	nuclear pore complex
ORF	open reading frame
PAM	protospacer adjacent motif
PAT	poly(A) tail-length assay
PBS	phosphate-buffered saline
PBS-T	phosphate-buffered saline with Tween-20
PCR	polymerase chain reaction
PKR	protein kinase R
PLA	proximity ligation assay
poly(I:C)	polyinosinic:polycytidylic acid
qPCR	quantitative polymerase chain reaction
RBP	RNA-binding protein
RGG	Arg–Gly–Gly-rich motif
RNA-FISH	RNA Fluorescence In Situ Hybridisation
RNP	ribonucleoprotein
RRM	RNA-recognition motif
SA	sodium arsenite
sALS	sporadic amyotrophic lateral sclerosis
SDS-PAGE	sodium dodecyl sulfate polyacrylamide gel electrophoresis
SFPQ	splicing factor proline and glutamine rich

SG	stress granule
SNE	soluble nuclear extract
snRNP	small nuclear ribonucleoprotein
SOD1	superoxide dismutase 1
STAT1	signal transducer and activator of transcription 1
TARDBP	TAR DNA Binding Protein
TBS-T	Tris-buffered saline with Tween 20
TIA1	T cell-restricted intracellular antigen 1
TIAR	T cell-restricted intracellular antigen 1-related protein
TNPO1	transportin 1
UPS	ubiquitin-proteasome system
ZnF	zinc-finger motif

Chapter 1. General Introduction

1.1. Amyotrophic Lateral Sclerosis (ALS)

1.1.1. Motor neuron diseases and ALS

1.1.1.1. Clinical features of ALS

Amyotrophic lateral sclerosis (ALS) is the most common motor neuron disease, primarily affecting the upper and/or lower motor neurons in the motor cortex, brainstem and spinal cord. The degeneration of the lower motor neurons results in the denervation of muscles causing fasciculation, cramps, muscle wasting, and weakness. The degeneration of the upper motor neurons affects fine motor control of the lower motor neuron system, causing spastic paresis (Volk *et al.* 2018). The symptoms typically begin focally from one motor unit and gradually propagates to adjacent ones (Taylor *et al.* 2016). ALS commonly affects people in their mid-adulthood (Hardiman *et al.* 2017). Male to female ratios with ALS are 2.5 and 1.4 before and after the age of 50, respectively (Manjaly *et al.* 2010). Death occurs, in most cases, typically within 5 years since the disease onset, mainly due to the respiratory failure, although there are exceptions with patients surviving longer (Taylor *et al.* 2016). The incidence of ALS varies across the continents, with 1.89 and 0.83 per 100,000 in North Europe and East Asia respectively, suggesting a possible link between ancestry, environment and ALS incidence (Marin *et al.* 2017).

Up to 50% of ALS patients show various degrees of cognitive impairment, with 14% meeting definite diagnosis of Frontotemporal lobar degeneration (FTLD) (Phukan *et al.* 2012). FTLD is a neurodegenerative disorder characterised by progressive decline of behavioural, language and cognitive function, is the second common cause of dementia among people under the age of 65. Importantly, FTLD and ALS share striking overlaps on clinical, genetic and neuropathological levels. Mutations in chromosome 9 open reading frame 72 (*C9orf72),* fused in sarcoma *(FUS)* and TAR DNA binding protein (*TARDBP)* together with some other rare genes have been found to be associated with both ALS and FTLD (Sreedharan *et al.* 2008, Van Langenhove *et al.* 2010, DeJesus-Hernandez *et al.* 2011, Karch *et al.* 2018). In addition, development of ubiquitin-positive inclusions with TDP-43 (protein encoded by *TARDBP* gene) as major component is the pathological hallmark of a subset of ALS and

FTLD brain (Neumann *et al.* 2006). Primary lateral sclerosis and progressive muscular atrophy, which affect only upper and lower motor neurons respectively, although initially categorised in an independent disease group, are now considered as ALS variants (Turner and Swash 2015). Taken together, diseases categorised under ALS is expanding with primary lateral sclerosis/progressive muscular atrophy and FTLD being the two extreme ends of this disease spectrum (Figure 1.1).

Currently only two drugs, Riluzole and Edaravone, have been approved by the United States Food and Drug Administration (FDA), with very limited benefits on survival. Riluzole acts to ameliorate the glutamate excitotoxicity, one of the proposed pathomechanisms of ALS (Trotti *et al.* 1999), but it only extends life expectancy by 3 months (Riviere *et al.* 1998). Edaravone is a free-radical scavenger that acts against the oxidative stress (Nagase *et al.* 2016), and it may slow down the disease progression by 33% only in a selected subgroup of ALS patients (Writing Group 2017). As there are no medications that can reverse the disease, the contemporary treatment of ALS is to alleviate the related symptoms and to ameliorate the progressive degeneration.

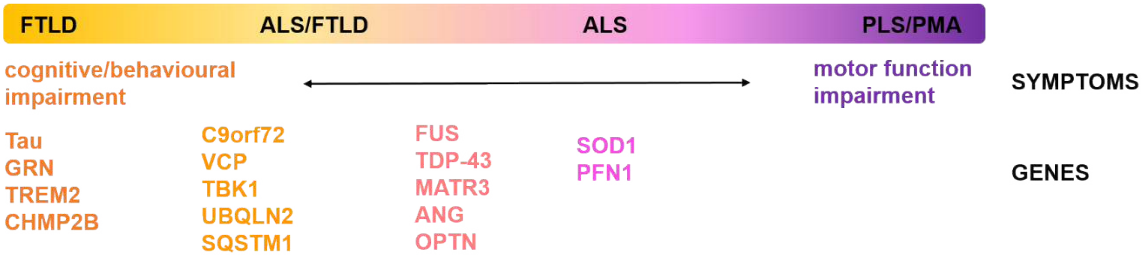

Figure 1.1 Disease spectrum of ALS/FTLD.
ALS is currently considered to be a group of diseases with primary lateral sclerosis (PLS) and progressive muscular atrophy (PMA) and FTLD as two extreme ends of the disease spectrum. Genes associated with corresponding phenotypic groups along the spectrum are indicated. This figure is adapted from (Radford *et al.* 2015).

1.1.1.2. Histopathology of ALS/FTLD

Motor neuron loss and gliosis in affected brain areas (spinal cord, frontal and temporal cortex, hippocampus, cerebellum, etc.) are the major

neuropathological features of ALS and FTLD. Residual neurons and surrounding oligodendrocytes contain cytoplasmic and/or nuclear, morphologically variable (skein-like or Lewy body-like) inclusions that are positive for ubiquitin and composed of misfolded proteins (Forman *et al.* 2004). Ultrastructural observation revealed filamentous aggregates covered with electron dense granules within the inclusions (Lin and Dickson 2008).

In 2006, a ground-breaking discovery was made by Neumann and her colleagues that TDP-43, a highly abundant, ubiquitously expressed nuclear protein, is the major component of pathological inclusions found in ALS and FTLD patients (Neumann *et al.* 2006). Redistribution of TDP-43 and concomitant nuclear clearance are frequently observed in the neurons containing inclusions, suggesting a possible loss-of-function mechanism contributing to the disease pathogenesis. Biochemical analysis has revealed that this pathological TDP-43 component is present predominantly in the form of cleaved C-terminal fragments of ~25 kDa and ~35 kDa, together with a high molecular weight smear on western blots, and these protein species are abnormally ubiquitinated and hyper-phosphorylated. Slightly different TDP-43 variants are detected among different ALS/FTLD subtypes, which might explain differences of inclusion distribution within brain regions and clinical manifestations among these subtypes (Neumann *et al.* 2006).

In addition to TDP-43, a whole range of other proteins encoded by disease-associated genes usually become the prominent component of ubiquitin-positive inclusions found in corresponding mutation carriers, such as SOD1, FUS, optineurin, ubiquilin-2, ataxin-2, C9orf72 (encoded by *SOD1, FUS, OPTN, UBQLN, ATXN2, C9orf72* gene, respectively), among others (Blokhuis *et al.* 2013). Importantly, these proteins can be found in pathological inclusions of non-mutation carriers, suggesting shared molecular mechanisms that might underlie both familial and sporadic ALS/FTLD (Blokhuis *et al.* 2013). Other protein components of neuronal inclusions are ribonucleoprotein (RNP) granule markers, such as T cell-restricted intracellular antigen 1 (TIA1), poly(A) binding protein cytoplasmic 1 (PABP1), eukaryotic translation initiation factor 4 gamma 1 (eIF4G) and non-POU domain containing octamer binding (NONO), most likely incorporated into protein aggregates by sequestration

mechanism (Dormann *et al.* 2010, Liu-Yesucevitz *et al.* 2010, Shelkovnikova *et al.* 2014b). Such sequestration and subsequent clearance from the sites of function would inevitably result in downstream effects that might contribute to disease onset and/or progression.

There are also other types of inclusions found in degenerating neurons of ALS. Bunina bodies are small, round, eosinophilic inclusions that are negative for ubiquitin. Ultrastructurally, Bunina bodies appear to be amorphous electron-dense material surrounded by tubules and vesicles (Okamoto *et al.* 2008). Another type of inclusions are found at axonal hillock of affected neurons containing neurofilaments, usually located close to ubiquitin-positive inclusions (Blokhuis *et al.* 2013). Other non-specific pathological changes of ALS/FTLD are mitochondrial vacuolisation, fragmentation of Golgi apparatus and neuromuscular junction abnormalities (Jaarsma *et al.* 2000, Blokhuis *et al.* 2013, Sundaramoorthy *et al.* 2015).

1.1.2. ALS subtypes and genes associated with the disease

ALS is a genetically heterogeneous disorder with monogenic forms as well as complex genetic aetiology. In about 10% cases, the disease runs in the family (familial ALS, fALS) (Mitchell and Borasio 2007), and a monogenic cause can be identified in 70% of fALS (Renton *et al.* 2014, Volk *et al.* 2018). The remaining 90% cases appear to be sporadic (sALS), nevertheless mutations in genes implicated in fALS can also be found in 10% of sALS patients (Renton *et al.* 2014, Volk *et al.* 2018). Among over 30 genes reported to date, the most frequently identified genes are *C9orf72* and *SOD1,* together accounting for nearly half of fALS cases (Volk *et al.* 2018) (Table 1.1). Mutations in *TDP-43* and *FUS*, although less prevalent than above genes, are found in about 10% of fALS cases, and have been studied extensively (Lagier-Tourenne and Cleveland 2009) (Table 1.1). Therefore, I will focus on these four genes in the following sections.

1.1.2.1. *C9orf72*

A hexanucleotide (GGGGCC-) repeat expansion in the non-coding region between exons 1a and 1b of *C9orf72* gene is the most frequent genetic cause

of fALS and FTLD in Europe and North America, corresponding to about 35% of fALS and 12% of familial FTLD (DeJesus-Hernandez *et al.* 2011, Renton *et al.* 2011, Zou *et al.* 2017). Although the exact cut-off between normal and pathological repeat length is unclear, patients with an expanded allele usually have several hundred to thousand repeats, and healthy individuals usually have less than 20 repeats (DeJesus-Hernandez *et al.* 2011). Long hexanucleotide repeat of *C9orf72* is inherited in an autosomal dominant manner, and also linked to other neurodegenerative disease including Parkinson's disease, Huntington's disease-like disorders and Alzheimer's disease (Cooper-Knock *et al.* 2014).

Three mutually non-exclusive mechanisms that might explain disease pathogenesis have been suggested for ALS associated with C9orf72 mutation (ALS-C9 hereafter): i) haploinsufficiency of C9orf72 protein; ii) toxic gain of function from C9orf72 repeat RNA; and iii) toxic gain of function from dipeptide repeat proteins (DPRs) (Balendra and Isaacs 2018). Firstly, protein product of C9orf72, whose exact function is still under investigation, is found to be decreased in ALS/FTLD patient motor neurons (DeJesus-Hernandez *et al.* 2011, Belzil *et al.* 2013), suggesting a possible loss of function mechanism. Secondly, the toxic effect of hexanucleotide repeats may arise from its RNA and protein product. In this case, the expanded repeats are transcribed bidirectionally into RNA molecules before they accumulate and form sense and antisense RNA foci within the nuclei of neurons and glial cells, which sequester numerous RNA-binding proteins (RBPs) (Gendron *et al.* 2013, Mizielinska *et al.* 2013, Zu *et al.* 2013). Finally, these repeat sequences-containing RNA can be translated into six different DPRs through repeat-associated non-ATG translation, which further aggregate to form inclusions in affected neurons (Ash *et al.* 2013, Gendron *et al.* 2013, Mori *et al.* 2013a, Mori *et al.* 2013b, Zu *et al.* 2013). These inclusions often contain more than one type of DPR and are positive for the ubiquitin-binding protein p62 but negative for TDP-43 (Mori *et al.* 2013a).

1.1.2.2. *SOD1*

Superoxide dismutase 1 *(SOD1)* gene is the first gene identified as an ALS-causing gene and the second most frequently identified gene in ALS,

accounting for 15% and 2% of fALS and sALS cases, respectively (Rosen *et al.* 1993, Zou *et al.* 2017). Up to date, more than 160 different mutations have been identified, and most of them are missense mutations, although small deletions and truncation mutations are also detected. It is inherited in autosomal dominant or recessive manner (Andersen and Al-Chalabi 2011). SOD1 protein is a ubiquitously expressed enzyme that catalyses the reduction of superoxide anions to oxygen and hydrogen peroxide. Misfolding and aggregation of mutant SOD1 protein, rather than the loss of its enzymatic activity, is thought to be the central pathomechanism of ALS linked with *SOD1* (Sibilla and Bertolotti 2017).

1.1.2.3. *TARDBP*

Although TDP-43 deposition in neuronal inclusions is a pathological hallmark of ALS and FTLD, *TARDBP* mutations have been identified in only 4% of fALS and 1% of sALS cases and rarely in FTLD (Zou *et al.* 2017). More than 60 mutations have been identified, with the majority being missense mutations clustered within the prion-like domain of the protein (Lattante *et al.* 2013). TDP-43 is an RBP involved in many aspects of RNA biology, including splicing, miRNA biogenesis, RNA transport and translation (reviewed in (Buratti and Baralle 2012)). TDP-43 is a predominantly nuclear protein, which can also shuttle between the cytoplasm and the nucleus (Ayala *et al.* 2008), and mutant TDP-43 has been shown to mislocalise to the cytoplasm (Barmada *et al.* 2010). Although the exact pathological mechanism of ALS caused by TDP-43 mutation is largely unknown, both gain-of-function in the cytoplasm and loss-of-function in the nucleus are believed to underlie ALS pathology caused by TDP-43 mutations.

1.1.2.4. *FUS*

FUS gene was initially identified as a fusion oncogene causing human liposarcoma (Crozat *et al.* 1993, Rabbitts *et al.* 1993), and hence named as Fused in Sarcoma (FUS). *FUS* gene mutations have been found to be causative in a subset of fALS in 2009 (Kwiatkowski *et al.* 2009, Vance *et al.* 2009). Later on, FUS mutations have also been identified in sALS and FTLD (Corrado *et al.* 2010, Van Langenhove *et al.* 2010, Deng *et al.* 2014a). FUS mutations are responsible for about ~5% of fALS and 1% sALS cases, and are

very rare in FTLD (Zou *et al.* 2017, Volk *et al.* 2018). FUS mutations are inherited in an autosomal dominant manner in most cases, with a few exceptions, where autosomal recessive mode and *de novo* mutations were also reported (Kwiatkowski *et al.* 2009, Volk *et al.* 2018). Over 50 *FUS* gene mutations have been identified, and the majority are missense mutations but rare truncation/frameshift mutations have also been found (Deng *et al.* 2014a). Most of the mutations affect the nuclear localisation signal (NLS) of FUS protein on its C-terminus, therefore, mutant proteins exhibit impaired nuclear targeting leading to their cytoplasmic mislocalisation (Deng *et al.* 2014a). FUS mutations are frequently associated with early onset and rapid progressive ALS, with the youngest reported victim developed the disease at the age of 13 (Suzuki *et al.* 2010b, Yan *et al.* 2010, Gromicho *et al.* 2017). Different mutations affect the nuclear targeting of FUS protein differently and the extent to which FUS mutants mislocalise to the cytoplasm correlates with the disease severity (Bosco *et al.* 2010, Dormann *et al.* 2010). For example, patients with FUS R495X mutation, which deletes the entire NLS, exhibit relatively severe disease phenotype compared with missense mutation carriers (Bosco *et al.* 2010).

Inclusions containing FUS protein in the spinal motor neurons are a pathological hallmark of ALS caused by *FUS* gene mutation (ALS-FUS hereafter) (Kwiatkowski *et al.* 2009, Vance *et al.* 2009). FUS-positive inclusions can also be found in Tau-negative and TDP-negative FTLD cases, and these cases are subcategorised as FTLD-FUS (Neumann *et al.* 2009). Contrary to TDP-43, complete nuclear clearance of FUS is rarely observed in affected human spinal motor neurons (Kwiatkowski *et al.* 2009, Vance *et al.* 2009).

FUS is an abundant nuclear DNA/RNA binding protein playing important roles in multiple cellular processes such as cell proliferation, DNA repair and RNA metabolism (Deng *et al.* 2014a). Nuclear loss/gain of function and cytoplasmic gain of function by FUS have been implicated in the disease pathogenesis. This will be discussed further in section 1.1.4.

1.1.2.5. Other genes implicated in ALS

During the past 10 years, thanks to the advances in next-generation sequencing technology, there has been an explosive increase in the number of ALS-causitive genes identified (Chia *et al.* 2018). A list of these genes and their functional implications in ALS is given in Table 1.1. Although mutations in the most of newly identified genes are rare, some genes are found mutated relatively frequently and therefore are studied more intensively, such as *TBK1* and *MATR3*.

TBK1 gene, which encodes TANK-binding kinase 1, a multiplayer in the autophagic process and inflammatory signalling (Weidberg and Elazar 2011), has been found to be mutated in a number of fALS pedigrees (Freischmidt *et al.* 2015) and in several sALS patients (Cirulli *et al.* 2015). To date, more than 50 mutations have been reported, representing 4% of fALS cases among Caucasians, although meta analysis showed lower prevalence (Cui *et al.* 2018). Remarkable similarity has been found between the neuropathology in ALS-TBK1 patients and ALS-C9 patients, both characterised by TDP-43-positive perinuclear inclusions in affected neurons (Freischmidt *et al.* 2015). Optineurin and p62 are both substrates of TBK1 in autophagy, and are coincidentally also ALS-associated genes (Maruyama *et al.* 2010, Fecto *et al.* 2011). Therefore *TBK1* mutations suggest the important mechanistic role of autophagy in ALS development.

MATR3 gene encodes an RNA/DNA-binding protein matrin 3 that interacts with TDP-43, and *MATR3* mutations are found in about 1% of fALS and sALS cases (Johnson *et al.* 2014, Therrien *et al.* 2016). Nuclear accumuation and mild cytoplasmic distribution of Matrin 3 is observed in the spinal cord neurons of mutation carriers, yet no neuronal inclusions containing Martrin 3 are found in these patients (Johnson *et al.* 2014). Importantly, Matrin 3 is occasionally found in the pathological inclusions in ALS-C9 patients (Johnson *et al.* 2014), and recently, it was also identified in the cytoplamsic TDP-43-positive inclusions in the spinal motor neurons of sALS patients (Tada *et al.* 2018). Identification of MATR3 mutations further strengthens the role of dysregulated RNA metabolism in ALS aetiology.

Table 1.1 A summary of ALS-associated genes and their functions implicated in ALS

Gene	Protein	Mode of inheritance	Prevalence fALS/sALS	Protein functions relevant to ALS	Number of mutations	References
C9orf72	C9orf72	AD	35% / 8%	Intracellular transport, autophagy, protein degradation	Intronic GGGGCC repeat	(DeJesus-Hernandez *et al.* 2011, Renton *et al.* 2011)
SOD1	Cu/Zn superoxide dismutase	AD, AR	15% / 2%	Neurotoxicity	>150	(Rosen *et al.* 1993)
FUS	FUS/TLS	AD, AR	5% / 1%	RNA metabolism	>50	(Kwiatkowski *et al.* 2009, Vance *et al.* 2009, Van Langenhove *et al.* 2010)
TARDBP	TDP-43	AD, AR	4% / 1%	RNA metabolism	>40	(Gitcho *et al.* 2008, Kabashi *et al.* 2008, Sreedharan *et al.* 2008)

CCNF	G2/mitotic-specific cyclin-F	AD	4% / 2%	Protein degradation	10	(Williams *et al.* 2016)
VCP	Valosin-containing protein	AD	1% / 1%	Protein degradation	7	(Johnson *et al.* 2010)
UBQLN2	Ubiquilin-2	XL	<1% / <1%	Protein degradation	5	(Deng *et al.* 2011)
VAPB	Synaptobrevin-associated membrane protein B	AD	N/A	Protein degradation	3	(Nishimura *et al.* 2004)
TBK1	TANK-binding kinase 1	AD	3% / <1%	Autophagy, inflammation	>50	(Cirulli *et al.* 2015, Freischmidt *et al.* 2015)
SQSTM1	p62	AD	1% / <1%	Autophagy, inflammation	12	(Fecto *et al.* 2011)
OPTN	Optineurin	AD, AR	<1% / <1%	Autophagy, inflammation	11	(Maruyama *et al.* 2010)

GRN	Granulin	AD	<1% / <1%	Autophagy, inflammation	4	(Schymick *et al.* 2007)
FIG4	Sac3	AD, AR	<1% / <1%	Autophagy	10	(Chow *et al.* 2009)
MATR3	Matrin 3	AD	<1% / <1%	RNA metabolism	15	(Johnson *et al.* 2014)
HNRNPA1	hnRNPA1	AD	N/A	RNA metabolism	3	(Kim *et al.* 2013)
HNRNPA2B1	hnRNPA2	AD	N/A	RNA metabolism	1	(Kim *et al.* 2013)
SETX	Senataxin	AD	N/A	RNA metabolism	4	(Chen *et al.* 2004)
ATXN2	Ataxin-2	AD	N/A	RNA metabolism	Intermediate-length polyQ expansions	(Elden *et al.* 2010)
TAF15	TATA-Box Binding Protein Associated Factor 15	AR, AD	1% / 1%	RNA metabolism	8	(Ticozzi *et al.* 2011)
EWSR1	Ewing sarcoma breakpoint region 1	AD	1% / 1%	RNA metabolism	3	(Couthouis *et al.* 2012)
GLE1	Nucleoporin GLE1	AD	<1% / <1%	RNA metabolism	3	(Kaneb *et al.* 2015)

NEK1	NIMA-related kinase 1	AD, AR	2% / 2%	Cytoskeletal organisation	4	(Kenna *et al.* 2016)
ANG	Angiogenin	AD	N/A	Cytoskeleton organisation, angiogenesis	>20	(Greenway *et al.* 2006)
PRPH	Peripherin	AD	<1% / <1%	Cytoskeleton organisation	10	(Gros-Louis *et al.* 2004)
PFN1	Profilin-1	AD	<1% / <1%	Cytoskeleton organisation, axonal transport	8	(Wu *et al.* 2012)
TUBB4A	α-tubulin	AD	<1% / <1%	Cytoskeleton organisation, axonal transport	7	(Smith *et al.* 2014)
NEFH	Neurofilament heavy polypeptide	AD	N/A	Axonal transport	5	(Tomkins *et al.* 1998, Al-Chalabi *et al.* 1999)
KIF5A	Kinesin family member 5A	AD	<1% / <1%	Axonal transport	12	(Nicolas *et al.* 2018)
DCTN1	Dynactin	AD	N/A	Axonal transport	10	(Puls *et al.* 2003)

CHMP2B	Charged multivesicular protein 2B	AD	N/A	Vesicular trafficking	3	(Parkinson *et al.* 2006)
ALS2	Alsin	AR	N/A	Vesicular trafficking	5	(Hadano *et al.* 2001, Yang *et al.* 2001)
SS18L1	SS18-like protein 1	AD	N/A	Dendritic outgrowth	4	(Chesi *et al.* 2013)
SPAST	Spastin	AD	N/A	Axonal growth	2	(Meyer *et al.* 2005)
CHCHD10	Coiled-coil-helix-coiled-coil-helix domain containing 10	AD	<1% / <1%	Mitochondrial function	10	(Bannwarth *et al.* 2014)
SIGMAR1	Sig-1R	AR	<1% / <1%	Mitochondrial function	3	(Al-Saif *et al.* 2011)
DAO	D-amino acid oxidase	AD	<1% / <1%	Neurotoxicity	2	(Mitchell *et al.* 2010)
SPG11	Spatacsin	AR	<1% / <1%	DNA damage	2	(Orlacchio *et al.* 2010)

AD autosomal-dominant, AR autosomal-recessive, XL X-linked, N/A not available

The top four most common genes are given in the order of frequency, and the rest are sorted by the primary functions relevant to ALS

1.1.3. Molecular mechanisms underlying ALS pathogenesis

Since the identification of the first ALS-causing gene *SOD1*, whose mutant protein product is known to form abnormal aggregates in affected neurons, impaired protein homeostasis has been extensively studied as the central mechanism underlying ALS pathogenesis. After over two decades of study, along with the ever-growing number of ALS-causative genes being discovered, a plethora of cellular mechanisms involving almost every aspect of neuronal biology has been suggested to be involved in ALS development and progression. Among them, perturbed proteostasis, dysregulation in RNA metabolism and altered axonal transport are believed to be the most prominent mechanisms, as evidenced by the convergence of the majority of disease-associated genes within these categories (Ling *et al.* 2013, Taylor *et al.* 2016) (Table 1.1).

1.1.3.1. Protein quality control and proteostasis

Cells produce misfolded proteins throughout their lifespan due to various internal processing errors and environmental stresses, which, if not managed promptly, would lead to protein aggregation, toxicity, and cell death. Cells have evolved three main strategies to precisely maintain their proteostasis – re-folding, degradation and sequestration. Among them, protein degradation is the most effective strategy to eliminate potentially deleterious species and recycle amino acids when the upstream correction has failed. There exist two major pathways for protein degradation in eukaryotic cells: the ubiquitin-proteasome system (UPS) and autophagy (Chen *et al.* 2011, Webster *et al.* 2017). The protein quality control systems of eukaryotic cells are described in detail in Figure 1.2. The ability of cells to preserve the stability of proteome declines with age (Morimoto and Cuervo 2009), and this is more deleterious for the long-living, post-mitotic cells like neurons, which are not able to dilute the accumulated misfolded proteins via cell division (Son *et al.* 2012).

Inclusions containing misfolded proteins in the degenerating neurons and surrounding glial cells are the most common pathological hallmark of ALS. These inclusions are mainly composed of ubiquitinated proteins (Neumann *et al.* 2006, Dormann *et al.* 2010), and very often contain proteasome- and autophagy- related proteins such as p62 and molecular chaperons (Basso *et*

al. 2009, King *et al.* 2011). Experimental inhibition of UPS or autophagy results in accumulation and aggregation of TDP-43 protein in cultured cells (Urushitani *et al.* 2010, Wang *et al.* 2010). Taken together, these findings suggest that impaired proteostasis is involved in the disease aetiology in ALS.

Several ALS-associated proteins contribute to protein degradation pathways (see Table 1.1). For example, misfolded proteins marked with ubiquitins are brought to proteasome for degradation by ubiquilin-2 and p62 (Moscat and Diaz-Meco 2012), whereas valosin-containing protein (VCP) extracts misfolded proteins from the endoplasmic reticulum (ER) and targets them for degradation via the proteasome (Wojcik *et al.* 2006). p62 and optineurin serve as adaptor proteins for targeting substrates to autophagy, and TBK1 regulates autophagy by directly phosphorylating p62 and optineurin (Wild *et al.* 2011, Heo *et al.* 2015). Finally, TBK1, CHMP2B and FIG4 are required for autophagosome maturation (Pilli *et al.* 2012, Ling *et al.* 2013). ALS-causing mutations in some of these genes have been proven to affect protein clearance pathways to a different extent eventually leading to the accumulation of substrates for degradation (reviewed in (Webster *et al.* 2017)).

Cytoplasmic aggregation coupled with nuclear clearance of TDP-43 is frequently observed in motor neurons of ALS patients. TDP-43 nuclear loss-of-function is known to affect the expression of protein degradation pathway components, such as CHMP2B, FIG4, optineurin, VAPB, and VCP (Polymenidou *et al.* 2011). In addition, TDP-43 silencing is shown to result in decreased autophagosome numbers and impaired autophagosome delivery to lysosomes, due to the downregulation of Atg7 and dynactin 1 expression, respectively (Bose *et al.* 2011, Xia *et al.* 2016). Similarly, FUS is also shown to bind to the transcripts encoding optineurin, ubiquilin-2, VAPB and VCP (Ling *et al.* 2013).

In SOD1 mouse models, mutant SOD1 shows increased interaction with chaperones, which may result in a depletion of the chaperone pool and impaired protein folding (Tummala *et al.* 2005, Ganesan *et al.* 2008). Moreover, ALS-causing mutant SOD1 has been shown to interact with an ER

protein Derlin-1 which is essential for ER-associated degradation (ERAD), causing impaired ERAD response and cellular toxicity (Nishitoh *et al.* 2008).

C9orf72 is also known to play important roles in autophagy (Farg *et al.* 2014). C9orf72 regulates autophagy by forming a complex with SMCR8-C9orf72 complex subunit (SMCR8) and WD repeat domain 41 (WDR41) proteins (Sellier *et al.* 2016, Sullivan *et al.* 2016, Xiao *et al.* 2016). Depletion of C9orf72 in primary cortical neurons results in impaired autophagy and TDP-43 and p62 aggregation (Sellier *et al.* 2016).

Protein misfolding and aggregation are considered to crucially contribute to motor neuron degeneration, and clearance of these toxic species heavily relies on protein degradation pathways. However, once the balance of protein homeostasis is disrupted due to a primary mutation or many secondary factors, a feedforward loop is initiated, leading to a snowballing effect that would eventually cause inclusion formation and neuronal degeneration (Webster *et al.* 2017).

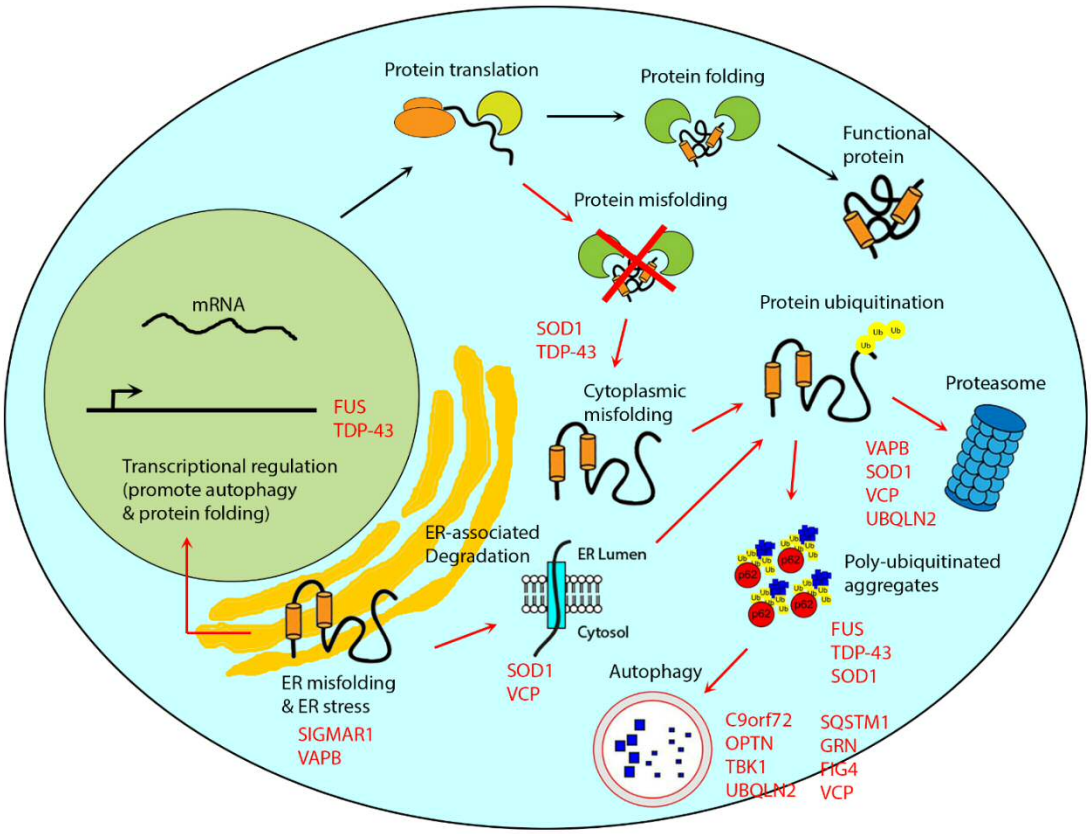

Figure 1.2 Protein quality control systems of eukaryotic cells and ALS-associated proteins.

Protein folding happens co-translationally, which continues in the cytoplasm and the ER lumen with the assistance of molecular chaperones. Misfolding can be corrected by chaperones during this process. However, chronic misfolding leads to the overload of chaperones therefore requires the UPS and autophagy pathways for the clearance of the misfolded proteins. Cytoplasmic misfolded proteins are ubiquitinated and targeted to the UPS, and when the system is overloaded, poly-ubiquitinated aggregates form, which, if not cleared by autophagy, may lead to cell death. Chronic misfolding in ER triggers unfolded protein response, which upregulates ER-associated degradation (ERAD) and autophagy by altering gene expression. Failure to maintain the proteostasis can lead to aggregate formation. A large number of ALS-associated proteins (indicated in red) are indirectly or directly involved in this network. This figure is adapted from (Webster *et al.* 2017).

1.1.3.2. RNA metabolism

TDP-43 and FUS, whose dysregulation and aggregation accounts for the majority of ALS cases, are both ubiquitously expressed, abundant nuclear RBPs with important functions across many aspects of RNA biology. Remarkably, TDP-43 and FUS are known to bind to over 6,000 and 5,500 RNA targets respectively in the human brain, which is about 30% of the total transcriptome, regulating every stage of RNA life cycle including transcription, splicing, stability, transport and beyond (reviewed in (Ling *et al.* 2013)). In addition, apart from *FUS* and *TDRDBP*, a number of other ALS-associated genes, including *hnRNPA1, hnRNPA2B1, RGNEF, SETX, ANG, TAF15, EWSR1, TIA-1* and *MATR3,* encode RBPs that have important functions in RNA metabolism. Moreover, a variety of RBPs are found to be sequestered in the protein inclusions found in the central nervous system (CNS) of ALS and FTLD patients, which might result in downstream consequences due to the depletion of their functional pool.

i Transcription and splicing

TDP-43 and FUS play critical roles in the regulation of RNA transcription and pre-mRNA splicing, actively participating in splicing events in the mouse brain and in human neuronal cells (Polymenidou *et al.* 2011, Tollervey *et al.* 2011). Knockdown of TDP-43 or FUS in adult mouse brain changed the expression levels as well as splicing patterns of hundreds of mRNAs, with surprisingly little overlap with each other (Lagier-Tourenne *et al.* 2012). Transcripts downregulated both by TDP-43 and FUS knockdown tend to have exceptionally long introns and encode proteins essential for neuronal integrity (Lagier-Tourenne *et al.* 2012). In line with this experimental evidence, studies of post-mortem tissues of ALS patients revealed decreased number of Gemini of Cajal bodies (Gems), nuclear bodies responsible for the biogenesis of uridine-rich small nuclear RNA (U snRNA), a component of the splicing machinery, in spinal motor neurons (Ishihara *et al.* 2013, Tsuiji *et al.* 2013). Furthermore, recent studies using mouse models with endogenous TDP-43 or FUS mutations also suggest that splicing abnormalities are a major consequence of these mutations (Fratta *et al.* 2018, White *et al.* 2018). Very recently, Klim and his colleagues found that the expression level of stathmin 2

(STMN2), a microtubule regulator that mediates motor neuron growth and repair, is extremely sensitive to TDP-43 knockdown in human motor neurons differentiated from induced pluripotent stem cells (iPSCs), and this change is due to altered splicing of STMN2 transcripts. Importantly, the same change was also found in the motor neurons derived from iPSCs generated from ALS patients carrying TDP-43 mutations, as well as in ALS patients' post-mortem spinal cord samples (Klim *et al.* 2019). This study, for the first time, provides a clear link between altered splicing pattern caused by TDP-43 depletion and motor neuron degeneration.

ii miRNA biogenesis and function

Mounting clinical and laboratory evidence points to altered miRNA system as a possible contributor to ALS pathogenesis. Global downregulation of miRNA levels has been observed in ALS motor neurons and serum (Cloutier *et al.* 2015, Emde *et al.* 2015), and it has been suggested as a common molecular feature in fALS and sALS (Emde *et al.* 2015). Loss of miRNA biogenesis by knocking out Dicer, an enzyme in a multi-protein complex that processes pre-miRNA into mature miRNA, in motor neurons is sufficient to cause spinal motor neuron degeneration in mouse models (Haramati *et al.* 2010). Moreover, enhancing Dicer activity by enoxacin has shown beneficial effects on neuromuscular function in two independent ALS mouse models (SOD1 and TDP-43) (Emde *et al.* 2015).

TDP-43 and FUS are known to participate in miRNA biogenesis and function by associating with various protein complexes at several stages of miRNA life cycle. For example, TDP-43 associates with the Microprocessor (Ling *et al.* 2010), a complex that processes pri-miRNAs into pre-miRNAs, and Dicer complex (Kawahara and Mieda-Sato 2012); FUS binds to miRNA-induced silencing complex (miRISC) component Argonaute-2 as well as miRNAs and their target transcripts (Zhang *et al.* 2018b) (Figure 1.3). Consistently, reduced miRNA biogenesis was observed in iPSC-derived human motor neurons from TDP-43 or FUS mutation carriers (Zhang *et al.* 2013b, De Santis *et al.* 2017).

FUS and TDP-43 are also components of the paraspeckle, a nuclear body whose role in ALS pathomechanisms has become increasingly appreciated. Interestingly, paraspeckles have recently been suggested to have profound

effect on miRNA biogenesis on a global scale through orchestrating efficient pri-miRNA processing by spatially organising multiple RBPs within the Microprocessor (Jiang *et al.* 2017).

Key components of multi-protein complexes participating in the miRNA biogenesis and function also interact with the pathways involving stress response and stress granule (SG) assembly, one of the major mechanisms underlying ALS pathology. For example, Dicer and its co-factors play roles in the stress response (Emde and Hornstein 2014), and its loss-of-function results in impaired stress tolerance and shortened life span in *C. elegans* (Mori *et al.* 2012). In addition, various stress-signalling cascades are known to regulate Argonaute-2 activity by altering its stability, post-translational modifications and its recruitment into SGs (Leung *et al.* 2006, Shen *et al.* 2013).

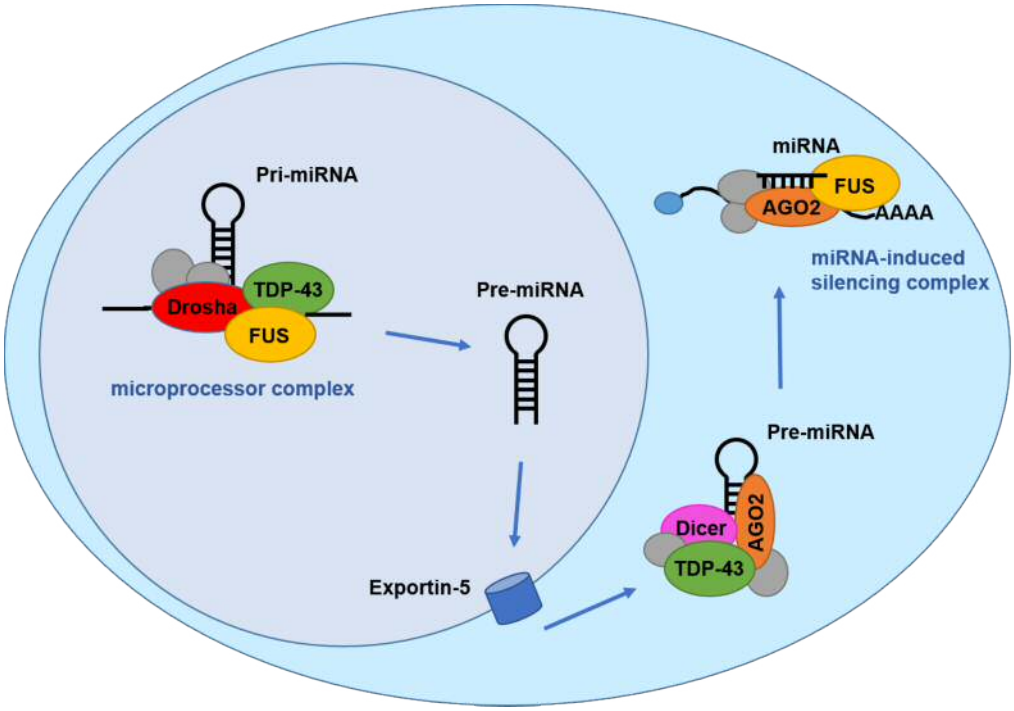

Figure 1.3 miRNA biogenesis and ALS-associated proteins.
Generation of mature miRNA in mammalian cells involves the processing of pri-miRNA to pre-miRNA by microprocessor complex in the nucleus as well as further cleavage by Dicer in the cytoplasm. Mature single-stranded miRNA forms miRNA-induced silencing complex (RISC) with a member of Argonaute (Ago) protein families to repress translation of target mRNA. ALS-associated proteins TDP-43 and FUS

participate in miRNA biogenesis as components of key macromolecular complexes at multiple critical miRNA processing steps. This figure is modified from (Volonte *et al.* 2015).

iii Translation

TDP-43 is known to be associated with the translation machinery by interacting with the ribosomal protein receptor for activated C kinase 1 (RACK1), and increased cytoplasmic TDP-43 level resulted in the global suppression of protein synthesis (Russo *et al.* 2017). Indeed, knockdown of TDP-43 homologue TBPH in *D. melanogaster* reduced the expression of Futsch, a neuronal microtubule associated protein, and resulted in altered neuromuscular junction organisation (Romano *et al.* 2016). Similarly, inclusions containing mutant FUS are enriched in proteins related to translation in the overexpression cellular models, and the presence of mutant FUS impaired global protein translation by ~ 30% in the fibroblasts derived from ALS-FUS patients (Kamelgarn *et al.* 2018). Reduced protein synthesis has detrimental effects on the neuronal function and survival (Holt and Schuman 2013).

Apart from its roles in global translation, FUS also regulates local translation of specific mRNAs at the distal ends of neuronal axons. As a component of the adenomatous polyposis coli (APC)-RNP complex, which targets mRNAs to cell protrusions for expression, FUS promotes translation preferentially within the protrusions (Yasuda *et al.* 2013). In the cytoplasmic aggregates formed by mutant FUS, a small group of mRNA is translated, and this ectopic protein expression is suggested to cause local protein imbalance and synaptic dysfunction (Yasuda *et al.* 2013, Yasuda and Mili 2016).

iv Stability and degradation

TDP-43 also regulates the stability of mRNAs. TDP-43 is found to stabilise the neurofilament light chain (NFL) mRNA by directly binding to its 3' UTR (Strong *et al.* 2007, Volkening *et al.* 2009), and reduced NFL mRNA level has been reported in the motor neurons of sALS patients (Wong *et al.* 2000). Very recently, a profound instability of hundreds of mRNAs was reported in the

fibroblasts and iPSCs derived from sALS and ALS-C9, and this phenotype can be recapitulated by TDP-43 overexpression in control iPSCs. Destabilised transcripts encode ribosomal and mitochondrial components, and reduction of oxidative phosphorylation is detected in the CNS of ALS patients (Tank *et al.* 2018).

Mutant FUS also contributes to the hyper-activation of nonsense-mediated mRNA decay (NMD) pathway by upregulating the pro-NMD factors while decreasing molecular brake of NMD (Kamelgarn *et al.* 2018). However, others demonstrated that enhancing NMD by overexpressing pro-NMD factor UPF1 RNA helicase and ATPase (UPF1) can protect cells against FUS or TDP-43 mediated toxicity (Barmada *et al.* 2015, Jackson *et al.* 2015). Therefore, increased NMD activity can be pathogenic, or alternatively, it can be a protective response of cells against protein overload.

1.1.3.3. Cytoskeletal defects and altered axonal transport

In humans, although axons of motor neurons can extend for more than a meter, therefore, active axonal transport is crucial for maintaining function and survival of neurons (Hirokawa 2006). Interestingly, it has been reported that in SOD1 mice models, retardation in axonal transport and dismantling of neuromuscular junction precedes the degeneration of neurons and the onset of first symptoms (Williamson and Cleveland 1999, Fischer *et al.* 2004, Bilsland *et al.* 2010).

Interestingly, many novel ALS-associated genes encode proteins involved in the cytoskeletal maintenance and axonal transport (see Table 1.1). α-tubulin, profilin-1, neurofilament heavy chain and peripherin encoded by *TUBA4A, PFN1, NEFH, and PRPH,* respectively, are building blocks of the cellular scaffold and axonal transport machinery, and their mutations are shown to significantly compromise cytoskeletal organisation and axonal transport (reviewed in (Chia *et al.* 2018)). For example, ALS-causing mutations in TUBA4A have been shown to destabilise microtubule network in primary motor neurons by affecting tubulin dimerisation (Smith *et al.* 2014).

TDP-43 is a component of RNP granules that undergo bidirectional, microtubule-dependent transport in neurons (Fallini *et al.* 2012), and ALS-

associated TDP-43 mutants impair axonal trafficking of transport granules in *D*. *melanogaster* ALS models and in human motor neurons obtained from iPSCs carrying a TDP-43 mutation (Alami *et al.* 2014, Baldwin *et al.* 2016). As mutations investigated in this study are located in the prion-like domain of TDP-43, which are important for the assembly of RNA granules, it is speculated that abnormal assembly of transport granules could be the main cause of the transport defects. A more recent study reported that an ALS-associated TDP-43 mutant has a compromised affinity to mRNA cargoes thereby causing impaired mRNA transport (Ishiguro *et al.* 2016). FUS is also a component of RNA transport granules (Fujii *et al.* 2005), and ALS-associated mutant FUS is shown to induce axonal defects in primary motor neurons (Groen *et al.* 2013). In addition, FUS is a binding partner of IGF2 mRNA-binding protein 1 (IMP1), a protein involved in axonal transport, and IMP1 is found sequestered in the cytoplasmic inclusions containing mutant FUS (Kamelgarn *et al.* 2016). This sequestration could also lead to the defects in axonal transport.

Mutant SOD1 is known to interact with the dynein-dynactin complex, the essential machinery for intercellular transport, in motor neurons, and SOD1 transgenic mice displayed significantly impaired axonal transport, which was correlated with disease progression (Ligon *et al.* 2005, Zhang *et al.* 2007). In line with this, depletion of mitochondria in axons due to the deficit in axonal transport is found in cultured motor neurons and murine models with SOD1 mutation (De Vos *et al.* 2007, Vande Velde *et al.* 2011). Importantly, similar findings have also been reported in various model systems with TDP-43, FUS and C9orf72 mutations (Magrane *et al.* 2014, Baldwin *et al.* 2016, Chen *et al.* 2016).

Together, these data strongly suggest that the defective cytoskeleton integrity and axonal transport are important mechanisms in ALS onset and/or progression.

1.1.4. *FUS* gene, protein and FUSopathy

1.1.4.1. *FUS* gene and protein

FUS gene is located on chromosome 16 in humans and contains 15 exons, encoding a protein of 526 amino acids (Deng *et al.* 2014a). FUS protein belongs to the FET protein family, which also includes Ewing Sarcoma (EWS) protein and TATA binding associated factor 15 (TAF15) (Tan and Manley 2009). FUS protein has a Gln–Gly–Ser–Tyr (QGSY)-rich region, several RNA/DNA recognition/binding domains such as RNA-recognition motif (RRM), Arg–Gly–Gly-rich motif (RGG) and zinc-finger motif (ZnF), a nuclear export signal and an NLS (Figure 1.4). QGSY-rich domain possesses prion-like properties that confer aggregation-prone nature to the protein. NLS is responsible for targeting FUS to the nucleus through interaction with the nuclear transport receptor transportin 1 (Iko *et al.* 2004, Dormann *et al.* 2010, Dormann *et al.* 2012).

FUS is mainly localised in the nucleus under physiological conditions, but it can also shuttle between nucleus and cytoplasm (Zinszner *et al.* 1997). FUS plays important roles in DNA damage response and repair (Mastrocola *et al.* 2013, Wang *et al.* 2013, Rulten *et al.* 2014), which is supported by the finding that mouse embryonic fibroblasts derived from FUS knockout (KO) mice showed significant chromosomal instability and increased sensitivity to the radiation (Hicks *et al.* 2000, Kuroda *et al.* 2000).

FUS is also known to regulate gene expression in the nucleus by binding to a variety of molecular targets including nuclear hormone receptors, gene-specific transcription factors, transcription initiation factors and RNA polymerase II. It can also bind to the promoter region of some genes to regulate their expression (Deng *et al.* 2014a).

Regulation of mRNA splicing and maturation is another well-known function of FUS. Importantly, FUS is shown to regulate alternative splicing of some transcripts whose protein products are involved in pathological aggregate formation in neurodegeneration. For example, knockout of FUS promotes inclusion of exons 2, 3 and 10 into tau transcripts, which would result in increased production of tau isoforms containing four amino acid repeats

(Orozco and Edbauer 2013). Such change in tau isoform composition is known to be associated to ALS-FUS and FTLD-FUS (Orozco *et al.* 2012).

FUS is an essential structural component of a nuclear body paraspeckle, which is a highly organised nuclear RNP granule (Naganuma *et al.* 2012, Shelkovnikova *et al.* 2014b). Absence of FUS causes loss of paraspeckles, and compromised paraspeckle assembly is thought to be a pathogenic factor in FUSopathy (Shelkovnikova *et al.* 2014b) (discussed further in section 1.2). In addition, as a component of the Microprocessor complex (Gregory *et al.* 2004), FUS contributes to miRNA biogenesis facilitating co-transcriptional Drosha recruitment to specific pri-miRNA sites (Gregory *et al.* 2004, Morlando *et al.* 2012).

FUS gene expression is subject to autoregulation attributable to the suppressive effect of FUS protein on its own pre-mRNA splicing. FUS protein binds to the region of exon 7 and its flanking introns of FUS pre-mRNA and promotes exon 7 skipping. The transcripts lacking exon 7 are degraded through NMD, resulting in downregulation of FUS protein (Zhou *et al.* 2013).

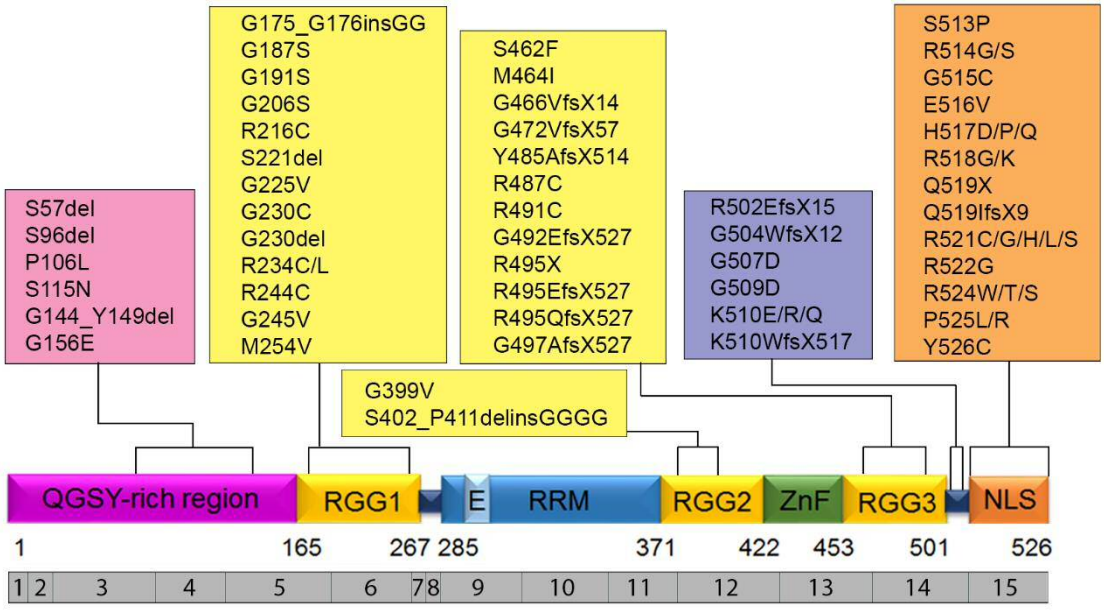

Figure 1.4 Schematic illustration of FUS protein functional domains with gene mutations identified in patients with ALS.

The grey bar on the bottom represents the FUS transcript, which is shown to indicate the corresponding coding region for each protein domain. SYGQ: Ser–Tyr–Gly–Gln;

RGG: Arg–Gly–Gly-rich motifs; E: nuclear export signal; RRM: RNA-recognition motif; ZnF: zinc-finger motif; NLS: nuclear localisation signal. The figure was modified from (Deng *et al.* 2014a).

1.1.4.2. FUSopathy

Mutations in the *FUS* gene were identified in a subset of fALS cases in 2009, reported by two independent research groups (Kwiatkowski *et al.* 2009, Vance *et al.* 2009). Up to date, more than 50 ALS-associated *FUS* mutations, mostly missense mutations, have been reported, and there are two regions in the *FUS* gene where mutations occur most frequently: exons 12-15 encoding ZnF, RGG2, RGG3 and NLS account for 2/3 of mutations, and exons 3-6 encoding QGSY-rich domain and RGG1 account for the rest 1/3 known mutations (Deng *et al.* 2014a) (Figure 1.4). Of note, mutations found in exons 12-15 are often found in fALS cases with high penetrance whereas those found in exons 3-6 are mainly identified in sALS cases or in fALS with incomplete penetrance (Deng *et al.* 2014a).

Formation of FUS immunoreactive cytoplasmic or nuclear inclusions in affected neurons and glial cells is the pathological hallmark of ALS-FUS and FTLD associated with FUS protein dysregulation (collectively called FUSopathy). It is worth mentioning that extremely high degree of heterogeneity is an important feature of FUSopathy. Firstly, FUS-positive inclusions are different in terms of morphology, components, ultrastructure and regional distribution (Mackenzie *et al.* 2010a, Mackenzie *et al.* 2010b). For instance, FUS-containing inclusions found in FTLD are also positive for Transportin 1, whereas ALS-FUS inclusions are Transportin 1-negative (Troakes *et al.* 2013). Secondly, even within ALS-FUS or FTLD-FUS, pathological and clinical heterogeneity among different missense mutation carriers has been described. For example, in FUS p.P525L cases, round, basophilic neuronal cytoplasmic inclusions have been identified, whereas in FUS p.R521C cases, tangle-like neuronal and oligodendroglial cytoplasmic inclusions are typical. The former cases showed early onset, severe clinical manifestations while the latter mutation is found in late onset, slowly progressing cases (Mackenzie *et al.* 2011). Finally, it was also reported that

FUSopathy takes different forms even among individuals with the same mutation (Mackenzie *et al.* 2010b). Taken together, the complexity of molecular mechanisms leading to FUSopathy might exceed our estimation, where each mutant FUS protein interacts with a specific subset of molecules eventually resulting in neurodegeneration via different pathogenic pathways.

1.2. RNP granules in ALS pathophysiology

1.2.1. RNP granules and their physiological functions

At any stage of the mRNA life cycle, mRNAs are often bound to a set of RBPs to form RNP particles. These RNP particles could further cluster and interact to form dynamic membraneless compartments called RNP granules, which is considered to be a conserved cellular mechanism to concentrate specific cellular components to increase efficiency of biological processes (Protter and Parker 2016). RNP granules include nucleolus, Cajal bodies and paraspeckles in the nucleus as well as SGs and processing bodies (P bodies) in the cytoplasm (Spector 2006), each of which serves as a distinct molecular hub for RNA storage and processing.

Physiological functions of RNP granules cover a broad range of mRNA-related processes as well as many other cellular processes and pathways that are important for basal cellular metabolism and stress response alike. The nucleolus is the primary site for the ribosomal RNA transcription, maturation and initial assembly of ribosomes (Pederson 2011). Cajal bodies are the main sites for processing, assembly, modification and maturation of spliceosomal small nuclear ribonucleoproteins (snRNPs) and recycling of spliceosome components (Wang *et al.* 2016). Paraspeckles are relatively recently identified nuclear bodies whose structure and physiological roles are just beginning to emerge. SGs and P bodies are two conserved RNP granules that are essential for cytoplasmic mRNA metabolism under stress conditions. When mRNAs in the cytoplasm are not engaged in translation, they are recruited into either P bodies or into SGs. P bodies contain translation repressors and mRNA decay machinery, and SGs contain mRNAs stalled in translation initiation and various translation initiation factors (Anderson and Kedersha 2009a). When they disassemble, stored mRNAs can return to translation. Excessive SG formation and/or their disrupted clearance are considered to be one of the central mechanisms underlying ALS/FTLD pathogenesis. A surprisingly strong association between paraspeckles and neurodegenerative diseases, and ALS in particular, will be discussed further in the following sections.

1.2.2. Paraspeckles

1.2.2.1. Long non-coding RNA NEAT1

Nuclear Paraspeckle Assembly Transcript 1, initially named as Nuclear Enriched Abundant Transcript 1 (NEAT1), is one of the most abundant long non-coding RNAs (lncRNAs) in the mammalian nucleus (Hutchinson *et al.* 2007). It is transcribed from the *familial tumour syndrome multiple endocrine neoplasia (MEN) type I* gene on human chromosome 11 (Guru *et al.* 1997). Two NEAT1 isoforms – 3.7 kb NEAT1_1 and 23 kb NEAT1_2 are generated from the gene locus. The primary NEAT1 transcript synthesised by RNA polymerase II is cleaved and polyadenylated through a canonical RNA processing pathway to generate NEAT1_1. In contrast, the tRNA-like structure at the 3'-end of the primary transcript is recognised and cleaved by RNase P, giving rise to a much longer NEAT1_2 with a triple helix structure at its 3'-end, which stabilises the transcript (Sunwoo *et al.* 2009, Brown *et al.* 2012, Wilusz *et al.* 2012) (Figure 1.5). Hereafter, NEAT1 refers to both NEAT1_1 and NEAT1_2.

In vitro, both NEAT1 isoforms are expressed in the majority of cultured cells except embryonic stem cells (Chen and Carmichael 2009). *In vivo*, while NEAT1_1 is ubiquitously expressed in the majority of adult organs and tissues, NEAT1_2 is only present in certain types of cells, such as epithelial cells in the digestive tract (Nakagawa *et al.* 2011). Both isoforms are hardly detectable in the developing mouse embryo, suggesting their limited function during mammalian embryogenesis (Nakagawa *et al.* 2011).

Human and mouse postmitotic neurons cultured *in vitro* express a very low level of NEAT1_2, and NEAT1_2 is barely expressed in the adult nervous system (Nakagawa *et al.* 2011, Bluthgen *et al.* 2017, Shelkovnikova *et al.* 2018). Therefore, the bulk of *NEAT1* gene expression in the nervous system is attributable to NEAT1_1. NEAT1 levels are low in the progenitors of neurons or oligodendrocytes, however, as they differentiate, NEAT1 becomes upregulated (Mercer *et al.* 2010).

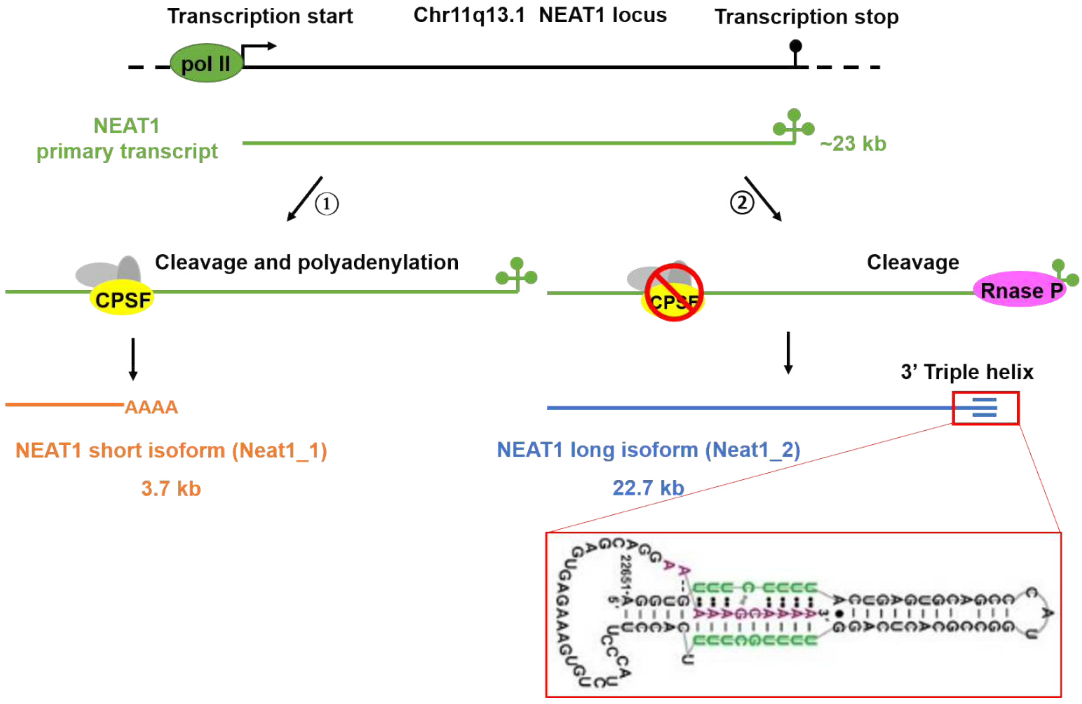

Figure 1.5 *NEAT1* gene produces two NEAT1 isoforms.
A schematic illustration of *NEAT1* gene and two transcript isoforms generated from it. NEAT1 primary transcript transcribed from NEAT1 locus gives rise to two isoforms through two distinct processing pathways: NEAT1_1 is generated through canonical cleavage and polyadenylation, whereas NEAT1_2 is generated by Rnase P cleavage. A triple helix structure at the 3' end of NEAT1_2 stabilises the transcript. The triple helical structure is enlarged to show how two U-rich motifs (green) and A-rich tract (purple) interact to form triple helix (Brown *et al.* 2012).

1.2.2.2. Paraspeckles

What makes lncRNA NEAT1 truly unique is that it has a nuclear body of its own – the paraspeckle. Paraspeckles are located in the interchromatin space, usually adjacent to the splicing speckles (Andersen *et al.* 2002, Fox *et al.* 2002). NET1_2 is an essential component of paraspeckles, and multiple copies of NEAT1_2 transcripts line up to build a scaffold for protein and RNA components (Clemson *et al.* 2009, Fox and Lamond 2010, Naganuma *et al.* 2012, Yamazaki and Hirose 2015) (Figure 1.6). Paraspeckle assembly is strictly dependent on RNA polymerase II transcription of NEAT1_2 and on the binding of paraspeckle proteins to NEAT1_2 (Mao *et al.* 2011). Although not essential, NEAT1_1 is also a component of paraspeckles and is hardly

present outside these structures (Naganuma *et al.* 2012). Nevertheless, since NEAT1_1 is highly expressed in the cell types devoid of paraspeckles (Nakagawa *et al.* 2011), it likely has a range of paraspeckle-independent functions.

More than 60 paraspeckle proteins have been identified, and the majority are RBPs (Naganuma *et al.* 2012). Some of them bind to NEAT1_2 to stabilise it (SFPQ, NONO, RBM14), and some maintain secondary structure of paraspeckles (FUS, DAZAP1), whereas others (CPSF6, NUDT21) regulate the ratio of the two NEAT1 isoforms. Presence of prion-like domain is the common feature of paraspeckle proteins important for liquid-liquid phase separation (LLPS), a phenomenon when a mixture of molecules forms a network of multivalent weak interactions. These molecules concentrate and separate from the surrounding molecules to form a distinct phase (Protter and Parker 2016). Prion-like domains are important for paraspeckle formation (Hennig *et al.* 2015, Yamazaki *et al.* 2018). For example, disruption of the prion-like domain of FUS or RBM14 is sufficient to disassemble paraspeckles (Shelkovnikova *et al.* 2014b, Hennig *et al.* 2015).

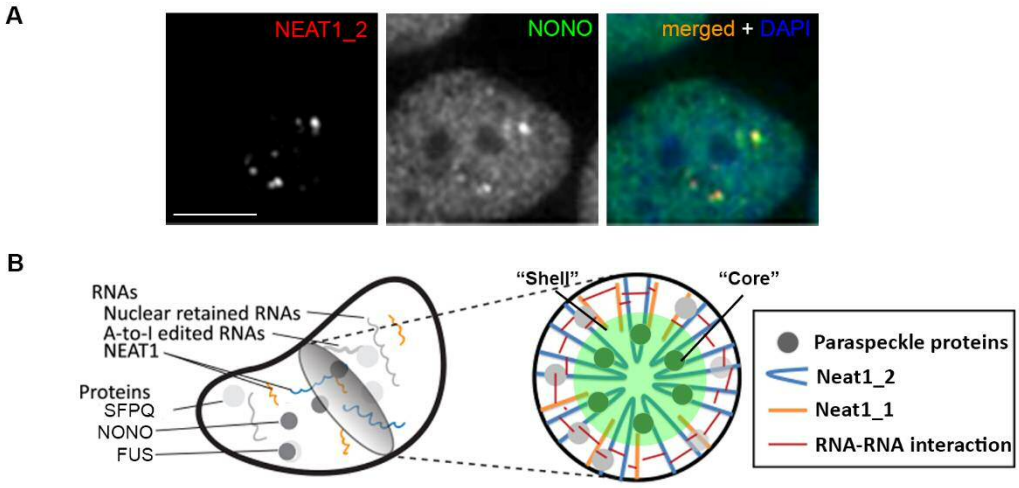

Figure 1.6 Paraspeckles

A) NEAT1_2 and an essential paraspeckle protein NONO colocalise within the paraspeckles. The average size of paraspeckles is 0.5–1 μm in diameter. The scale bar is 5 μm. B) Structural organisation of paraspeckles. On the cross section, NEAT1_2 transcripts folded end-to-end are arranged in a circle to form the scaffold for other paraspeckle components. The middle region of NEAT1_2 transcripts and essential paraspeckle proteins comprise the stable "core", while the 3' and 5'-ends of

NEAT1_2, together with NEAT1_1 and other paraspeckle components, make up the more labile “shell”. This figure was adapted from (Lin *et al.* 2018).

Compared to the paraspeckle proteome, less is known about its RNA components. In addition to NEAT1_1, which is the second most abundant paraspeckle RNA following NEAT1_2, two classes of RNA species have also been reported to be enriched within paraspeckles, namely Adenosine-to-Inosine (A-to-I hereafter) edited transcripts (Chen *et al.* 2008) and miscellaneous AG-rich RNAs (West *et al.* 2016). Recently, mRNAs encoding mitochondrial proteins (Wang *et al.* 2018b) as well as pri-miRNAs being processed by the Microprocessor (Jiang *et al.* 2017) have also been found to be retained in the paraspeckles.

Studies using electron and super-resolution microscopy have revealed the 3D arrangement of NEAT1_2 within paraspeckles and the characteristic “core-shell” structure of paraspeckles (Souquere *et al.* 2010, West *et al.* 2016, Fox *et al.* 2018) (Figure 1.6). Computational analysis has suggested that long-range interactions, but not sequence conservation, are required for the structural function of NEAT1_2 (Lin *et al.* 2018), with the repeat-rich middle region of NEAT1_2 being essential for paraspeckle assembly (Yamazaki *et al.* 2018).

Paraspeckles are stress-responsive nuclear bodies and various physiological and pathological stimuli, such as viral infection (Saha *et al.* 2006), differentiation (Sunwoo *et al.* 2009) and proteasome inhibition (Hirose *et al.* 2014), can upregulate NEAT1_2 expression, and increase paraspeckle number and size. The physiological functions of paraspeckles discovered so far are as follows: i) Retention of A-to-I hyper-edited RNAs within the nucleus and rapidly release them to the cytoplasm for translation during stress, thereby regulating stress response (Prasanth *et al.* 2005, Chen *et al.* 2008, Chen and Carmichael 2009); ii) transcriptional regulation by sequestering important regulatory factors, such as splicing factor proline and glutamine rich (SFPQ) (Hirose *et al.* 2014, Imamura *et al.* 2014); iii) modulation of pri-miRNA processing (Jiang *et al.* 2017).

1.2.3. Paraspeckles and ALS

1.2.3.1. Evidence of paraspeckle dysregulation in ALS

Post-mortem studies in ALS/FTLD patients have demonstrated that neurodegeneration in ALS is accompanied by altered NEAT1 and paraspeckle abundance. The first report on NEAT1 dysregulation in ALS was published in 2013, when paraspeckles were detected in spinal motor neurons in a subset of sALS patients (Nishimoto *et al.* 2013). Considering the fact that motor neurons are generally devoid of NEAT1_2 under physiological conditions (Nakagawa *et al.* 2011), this finding was somewhat unexpected. Subsequently, a study in a different cohort of sALS patients also confirmed hyper-assembly of paraspeckles in spinal motor neurons (Shelkovnikova *et al.* 2018). Moreover, this phenomenon was also observed in ALS-C9 and ALS-TDP cases, suggesting that paraspeckle hyper-assembly is a common pathological feature of ALS cases with different aetiology (Shelkovnikova *et al.* 2018).

Genetic evidence also points to the strong association between NEAT1/paraspeckles and ALS pathogenesis. Among ~25 proteins genetically linked to ALS/FTLD, eight proteins, namely, FUS, TDP-43, SFPQ, hnRNPA1, EWS, TAF15, CREST and matrin3, are paraspeckle proteins, and some of them regulate NEAT1 levels and paraspeckle assembly (Naganuma *et al.* 2012, Shelkovnikova *et al.* 2014b, Banerjee *et al.* 2017, Shelkovnikova *et al.* 2018) (Table 1.2).

TDP-43 is known to bind NEAT1 (Polymenidou *et al.* 2011, Tollervey *et al.* 2011) and its depletion in cultured cells stimulates NEAT1_2 accumulation and paraspeckle assembly (Shelkovnikova *et al.* 2018). TDP-43 protein cytoplasmic aggregation and concomitant nuclear depletion occur in about 95% of sALS cases, thus enhanced paraspeckle assembly in the spinal cord of ALS patients is most likely caused by TDP-43 loss of function in the nucleus (Shelkovnikova *et al.* 2018). Similarly, FUS protein loss of function in the nucleus, due to the mutations and/or abnormal aggregation in the cytoplasm, also affects paraspeckle functions by perturbing their higher-order structure (West *et al.* 2016).

ALS-associated mutant proteins also compromise paraspeckle structure and function through a gain of function mechanism. Pathological aggregates formed by mutant FUS are found to sequester paraspeckle proteins that can directly regulate NEAT1 levels, such as NONO (Shelkovnikova *et al.* 2014b). Likewise, nuclear aggregates containing mutant CREST can entrap FUS (Kukharsky *et al.* 2015). Moreover, pathological nuclear RNA foci formed by C9orf72 hexanucleotide repeat expansions also retain paraspeckle proteins, such as TDP-43, hnRNPK and EWS (Lee *et al.* 2013).

Compared to ALS, evidence of NEAT1 dysregulation in FTLD is scarce. Two research groups reported upregulated NEAT1 levels in the brain of FTLD patients (Tollervey *et al.* 2011, Tsuiji *et al.* 2013). According to the unpublished observations of our group, unlike in ALS spinal cord, NEAT1_2 upregulation and paraspeckle formation is not typical for the frontal cortex in FTLD.

Table 1.2 Paraspeckle proteins genetically associated with ALS

Protein	Importance for paraspeckle assembly	Regulation of NEAT1_2 levels	Role in ALS	Role in other neurodegenerative diseases
FUS	Essential, >75% loss upon knockdown (Naganuma *et al.* 2012, Shelkovnikova *et al.* 2014b)	No or minimal	>50 mutations in fALS and sALS (Deng *et al.* 2010, Lattante *et al.* 2013)	FTLD (FTLD-FUS) (Neumann *et al.* 2009)
TDP-43	Depletion enhances paraspeckle assembly (Shelkovnikova *et al.* 2018)	Yes (more NEAT1_2 upon TDP-43 depletion)	>60 mutations in fALS and sALS; TDP-43 proteinopathy in cases with TDP-43 mutations and in 95% of all sALS cases (Neumann *et al.* 2006, Mackenzie *et al.* 2010b, Lattante *et al.* 2013)	FTLD (FTLD-TDP) (Neumann *et al.* 2006); AD (Wilson *et al.* 2011)
TAF15	Important, 30-75% loss upon knockdown (Naganuma *et al.* 2012)	No	6 mutations in 6 unrelated sALS cases and 2 mutations – in 2 fALS cases (Couthouis *et al.* 2011, Ticozzi *et al.* 2011)	FTLD (FTLD-FUS) (Neumann *et al.* 2011)

EWS	Important, 30-75% loss upon knockdown (Naganuma, Nakagawa et al. 2012)	yes	2 mutations in 2 unrelated sALS cases (Couthouis, Hart et al. 2012)	FTLD (FTLD-FUS) (Neumann, Bentmann et al. 2011)
hnRNPA1	Important, 30-75% loss upon knockdown (Naganuma *et al.* 2012)	No	2 mutations in fALS cases; 2 rare variants (Kim *et al.* 2013, Liu *et al.* 2016)	Multisystem proteinopathy (MSP) (Kim *et al.* 2013)
CREST**	ND	ND	4 mutations in 4 unrelated sALS cases (Chesi, Staahl et al. 2013, Teyssou, Vandenberghe et al. 2014)	N/A
MATR3	Depletion enhances paraspeckle assembly (Banerjee *et al.* 2017)	Yes (more NEAT1_2 upon MATR3 depletion)	~10 mutations in fALS and sALS cases (Johnson *et al.* 2014, Leblond *et al.* 2016)	Initially diagnosed myopathy with vocal cord paralysis, diagnosis changed to 'ALS' (Senderek *et al.* 2009)
SFPQ	Essential, >75% loss upon knockdown (Naganuma *et al.* 2012)	Yes	2 mutations in 2 sALS cases (Thomas-Jinu *et al.* 2017)	N/A

** CREST is a neuro-specific protein, therefore its effect on paraspeckles in stable cell lines could not be tested.

1.2.3.2. Paraspeckles and ALS pathomechanisms

i Proteasome dysfunction

Collapse of proteostasis is the most apparent pathological mechanism underlying ALS/FTLD, and dysfunctional UPS and autophagosome-lysosome systems are the main culprits responsible. Proteasome inhibition is a well-known trigger of NEAT1 upregulation and paraspeckle hyper-assembly (Hirose *et al.* 2014). Both NEAT1 isoforms increased in cells treated with proteasome inhibitors, such as bortezomib or MG132. Paraspeckle enlargement causes excessive protein retention within the structure, resulting in up to 50% depletion of the nuclear pool of paraspeckle proteins, many of which are transcription regulators. Therefore, the augmented paraspeckle assembly under these conditions could potentially have a profound effect on the gene expression profile. However, how exactly the dysfunctional proteasome system signals to NEAT1 and paraspeckles is not clear. NEAT1 is known to have a heat shock responsive element within its promoter region, and induction of heat shock transcription factor 1 (HSF1) has been shown to upregulate NEAT1 expression (Lellahi *et al.* 2018). Therefore, accumulation of HSF1 due to its impaired clearance (Raychaudhuri *et al.* 2014) can at least partly explain the NEAT1 upregulation under proteasome inhibition.

ii miRNA biogenesis

Altered miRNA expression in the CNS is known to contribute to neuronal damage. Several paraspeckle proteins, such as SFPQ, NONO, FUS, TDP-43, and EWS, have established functions in the regulation of the miRNA pathway (Kawahara and Mieda-Sato 2012, Morlando *et al.* 2012, Bottini *et al.* 2017, Ouyang *et al.* 2017). A recent study reported that paraspeckle components, NEAT1 and SFPQ-NONO heterodimer, act to enhance global miRNA biogenesis by binding to pri-miRNA molecules and attracting the Microprocessor complexes (Jiang *et al.* 2017). The role for NEAT1_1 in this process is less known, however, it may potentiate NEAT1_2 function. It remains to be established whether NEAT1_1, in the absence of NEAT1_2, contributes to miRNA biogenesis in neurons.

iii Neuroinflammation

Neuroinflammation, caused by the activation and proliferation of resident immune cells in the nervous system, is believed to play a role in ALS/FTLD. Initially discovered as a virus-inducible RNA in the brain (Saha *et al.* 2006), NEAT1 is heavily involved in the antiviral immunity (Zhang *et al.* 2013a, Imamura *et al.* 2014). During RNA virus infection, paraspeckles sequester SFPQ away from the promoters of genes encoding cytokines and chemokines, such as interleukin 8 (IL8) or C-C motif chemokine ligand 5 (CCL5), thereby alleviating the inhibitory effect of SFPQ upon these genes (Imamura *et al.* 2014). Endogenous double-stranded RNA (dsRNA) accumulation can also induce NEAT1 upregulation and paraspeckle assembly in cultured cell lines (Shelkovnikova *et al.* 2018). NEAT1 responds to foreign DNAs as well. Upon double-stranded (dsDNA) exposure, NEAT1 activates cGAS-STING-IRF3 pathway and interferon signalling through its binding to the HEXIM P-TEFb complex subunit 1 (HEXIM1) protein (Morchikh *et al.* 2017). Bacterial infection can also stimulate NEAT1 expression, which promotes the expression of chemokines and cytokines, such as interleukin 6 (IL6) and C-X-C motif chemokine ligand 10 (CXCL10), in human monocytic cells (Zhang *et al.* 2017).

iv Cell death

Programmed cell death including apoptosis and necroptosis is the primary cause of neuron loss in ALS/FTLD (Su *et al.* 2000, Sathasivam *et al.* 2001, Re *et al.* 2014). NEAT1 knockout in mouse fibroblasts rendered them more sensitive to cell death upon proteasome inhibition (Hirose *et al.* 2014). Similarly, downregulation of NEAT1 potentiated dsRNA toxicity in human cells (Shelkovnikova *et al.* 2018). Furthermore, NEAT1 protected cells against apoptosis under oxygen and/or glucose deprivation (Choudhry *et al.* 2015, Zhong *et al.* 2017). These studies suggested that paraspeckle assembly downstream of increased NEAT1_2 expression is responsible for the protection against cell death by sequestrating transcription factors to regulate gene expression (Hirose *et al.* 2014, Choudhry *et al.* 2015) or by regulating miRNA biogenesis (Shelkovnikova *et al.* 2018). Whether upregulated NEAT1_1 also plays anti-apoptotic roles or is merely a bystander needs

further investigation. The levels of p53 protein, which is one of the key factors in cellular apoptosis, are increased in affected regions of the CNS both in patients and in disease models of neurodegenerative diseases, including ALS (Martin 2000, Chang *et al.* 2012). Interestingly, NEAT1 expression can be stimulated by p53 (Adriaens *et al.* 2016, Mello *et al.* 2017). While much is known on the interplay between p53 and NEAT1 in the context of cancer, limited information is available on their interaction in the CNS. Precise molecular mechanisms that underlie the co-operation of NEAT1 and apoptotic pathways still remain to be elucidated.

v Neuronal excitability

Increased excitability in upper and lower motor neurons is one of the early disease signs in ALS (Vucic *et al.* 2008), and has been considered as a possible disease mechanism (Saxena and Caroni 2011). NEAT1 expression in human brain is activity-dependent – it is expressed in the high-spiking "active" regions in the CNS and it is responsive to neuronal depolarisation (Lipovich *et al.* 2012, Barry *et al.* 2017). NEAT1 depletion in cultured human neurons resulted in significant increase in the expression of ion channel components, suggesting that NEAT1 might negatively regulate neuronal excitability by controlling transcription of this class of genes (Barry *et al.* 2017). In addition, NEAT1 can also directly bind to potassium voltage-gated channel subfamily A regulatory beta subunit 2 (KCNAB2), a potassium channel-interacting protein that is important in controlling excitability of neurons (Barry *et al.* 2017). Upon depolarisation, NEAT1 is acutely downregulated to aid the cytoplasmic translocation of KCNAB2, where the latter modulates excitatory response via interacting with membrane channels (Barry *et al.* 2017).

1.2.4. Stress granules

1.2.4.1. Stress granules: structure

SGs are large cytoplasmic RNP granules that form in response to translational arrest due to various cellular stresses (Anderson and Kedersha 2009b, Buchan and Parker 2009). In mammalian cells, their size ranges from 0.1 to 0.2 μm, and their main components include polyadenylated mRNA, PABP, translation initiation factors, small ribosome subunits and a number of RBPs

(Loschi *et al.* 2009). Protein composition of SGs depends on many factors including cell type and the nature and duration of stress (Anderson and Kedersha 2009b). Stressors known to induce SG assembly are oxidative stress, ER stress, viral infection, hyperosmolarity, heat shock, hypoxia, UV irradiation, among others. Some physical stresses, such as X-irradiation and DNA-damaging agents, do not induce SGs (Anderson and Kedersha 2009b).

When the stress is sensed by one of four kinases, namely protein kinase R (PKR), heme-regulated eIF2α kinase (HRI), general control nonderepressible 2 (GCN2), and PKR-like ER kinase (PERK), the kinase becomes activated, and its activated form phosphorylates eukaryotic translation initiation factor 2α (eIF2α), thereby initiating the molecular cascade leading to SG assembly (McCormick and Khaperskyy 2017). Different stress types activate different kinases. For example, dsRNA, ER stress, oxidative stress and nutrient starvation activate PKR, PERK, HRI and GCN2, respectively (Anderson and Kedersha 2009b). Phosphorylation of eIF2α results in translation arrest by blocking the recruitment of large ribosomal subunit, leading to the accumulation of stalled 48S mRNPs. This exposes polysome-free mRNAs to RBPs, such as TIA1, TIA1-related protein (TIAR) and RAS GTPase-activating protein SH3 domain-binding protein 1 (G3BP1) (McCormick and Khaperskyy 2017). These proteins and many other SG proteins are known to possess low-complexity, intrinsically disordered domains (IDRs), and binding to RNA triggers their rapid aggregation. Small mRNP aggregates further and fuse to form mature, large SGs that concentrate hundreds of proteins and RNAs (Tourriere *et al.* 2003, Gilks *et al.* 2004, Kedersha *et al.* 2013). There also exists an eIF2α-independent way of inducing translational arrest through inhibition of the mammalian target of rapamycin (mTOR), which blocks the formation of translation initiation complex. However, translation arrest induced by this pathway does not promote stress granule formation (McCormick and Khaperskyy 2017).

SGs that are induced by different stresses assemble through different pathways, and therefore their composition varies. For example, self-interaction of G3BP1 and a closely related protein G3BP2 is important in SG assembly upon oxidative stress. However, they are not required for SG formation under

osmotic stress (Tourriere *et al.* 2003, Kedersha *et al.* 2016). Similarly, yeast proteins Gtr1, Rps1b and Hgb1 promote SG formation under glucose starvation, whereas under heat shock conditions they suppress SG assembly (Yang *et al.* 2014).

SGs could also be induced by pharmacologically inhibiting translation initiation or by depleting translation initiation factors or even by overexpressing certain RBPs (Anderson and Kedersha 2008). For example, overexpression of TIA1 and TIAR induces SG assembly in the absence of stress (Kedersha *et al.* 1999).

Since persistence of SGs requires constant influx of translationally stalled mRNPs, drugs like cycloheximide and emetine that inhibit translation elongation and thus trap mRNA in polysomes, dissolve SGs (Kedersha *et al.* 2000, Brengues *et al.* 2005, McCormick and Khaperskyy 2017).

SGs are highly dynamic structures that exhibit liquid-like behaviour – they "flow" freely in the cytoplasm, undergo fusion like liquid droplets and continuously and rapidly exchange components with the rest of the cytoplasm. SGs disassemble very quickly after stress is removed, which typically takes 20 – 60 min (Kedersha *et al.* 2005, Buchan and Parker 2009, McCormick and Khaperskyy 2017). These properties are found to be dependent on adenosine triphosphate (ATP), as impaired ATP production is shown to eliminate SG movement and diminish the recovery of G3BP1 after photobleaching (Jain *et al.* 2016).

Studies using super-resolution microscopy have revealed the complex 3D structure of SGs. Instead of being a uniform structure, each SG is composed of a cluster of sub-structures, where a dense and less dynamic core is surrounded by a relatively loose and more dynamic shell (Jain *et al.* 2016). These cores can be biochemically purified, and proteomic analysis has found that over half of SG core proteins are RBPs (Jain *et al.* 2016). Due to the dynamic and liquid-like biophysical properties of SGs, it is plausible that they are formed, at least partly, by LLPS. Although it is still unclear whether intermolecular interactions or LLPS is the main force driving SG assembly, currently the widely accepted model is as follows: In the cytoplasm, translationally stalled mRNPs first concentrate into core structures through

strong RNA-protein, protein-protein interactions as described previously. Subsequently, as these cores grow by joining of other cores, the high local concentration of IDRs within these structures trigger LLPS, thereby forming the dynamic shell structure surrounding the cores (Jain *et al.* 2016).

Once the stress is resolved, SGs disappear either by passive disassembly or by autophagic clearance (Buchan *et al.* 2013). Persistence of SGs due to their increased stability or impaired autophagy is believed to increase the susceptibility of IDR-containing protein components to aggregation. These persistent granules might become seeds for non-reversible protein deposits causative for neurodegenerative diseases, including ALS and FTLD (Li *et al.* 2013, Ramaswami *et al.* 2013).

1.2.4.2. Stress granules: function

As a conserved protective mechanism of eukaryotic cells against environmental stress, SGs play central roles in cell survival and recovery. Cells expressing mutant form of eIF2α that is non-phosphorylatable cannot form SGs in response to sodium arsenite-induced oxidative stress and show increased sensitivity to low doses of arsenite (Anderson and Kedersha 2009b).

During stress, bulk protein synthesis shut-off helps limit energy consumption, however, mRNAs encoding proteins that play key roles in survival still must be translated. SGs help re-programme protein expression towards cell survival by sequestering 'housekeeping' transcripts for silencing while excluding mRNAs that encode molecular chaperones and repair enzymes to allow their preferential translation (Anderson and Kedersha 2009b). For example, transcripts that encode heat shock proteins (HSP), such as HSP70 and HSP90, are selectively excluded from SGs (Kedersha and Anderson 2002). In addition, SGs facilitate cell survival by recruiting pro-apoptotic proteins, including Receptor For Activated C Kinase 1 (RACK1), 2-Oxoglutarate And Iron Dependent Oxygenase Domain Containing 1 (OGFOD1), as well as cell growth regulators angiogenin and caprin-1 (Droppelmann *et al.* 2014).

SGs also participate in dynamic RNA triage under stress conditions by interacting with P bodies. P bodies are constitutive RNP granules that are

further induced by stress. Unlike SGs, P bodies represent sites of mRNA degradation by mediating mRNA decay including NMD and RNA interference (Jain and Parker 2013). The ultimate purpose of SG and P body assembly in eukaryotic cells is to collect untranslated mRNAs that exceed the capacity of the translation and/or decay machineries (Anderson and Kedersha 2009b). SGs and P bodies are found to actively interact to facilitate the exchange of RNA and protein components. This interaction helps to sort RNA molecules for storage, translation or degradation, thereby maintaining RNA homeostasis during stress attack (Anderson and Kedersha 2008, Li *et al.* 2013) (Figure 1.7).

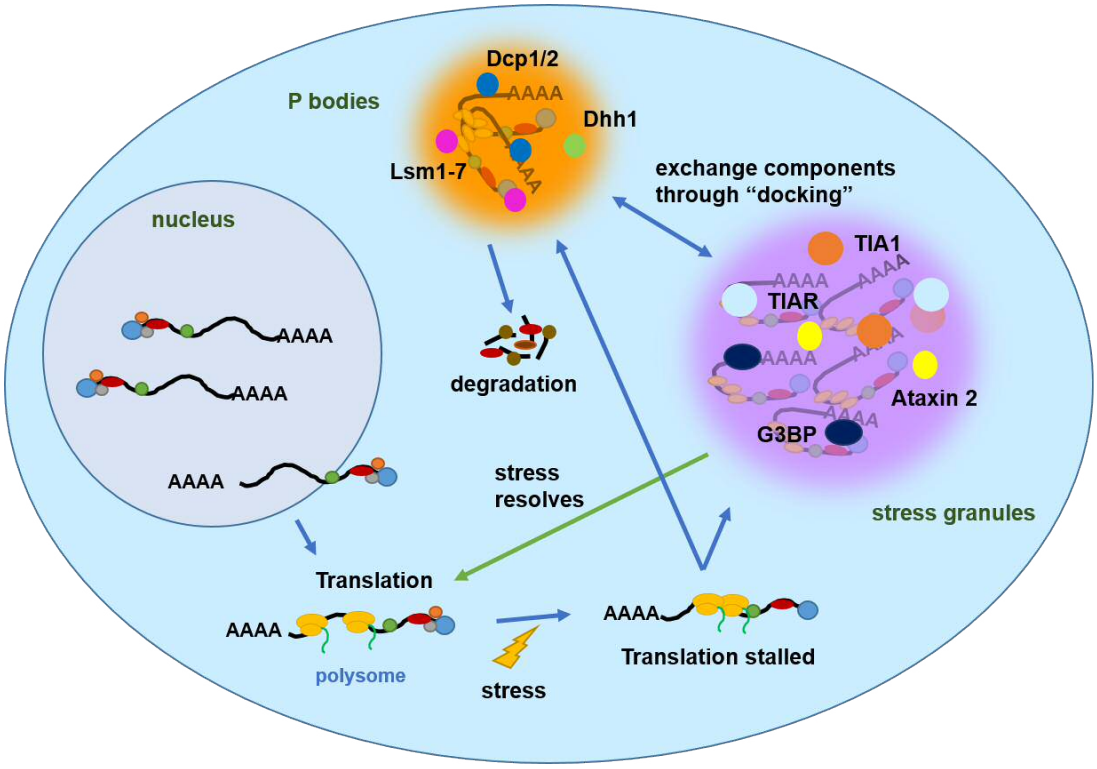

Figure 1.7 Stress granules and P bodies participate in RNA triage during stress
Stress granules and P bodies play important roles for RNA sorting, storage and degradation during stress and recovery. When stress triggers translation arrest, non-translating mRNAs are recruited into stress granules and P bodies. Although formed and regulated independently, stress granules and P bodies often exchange components through "docking" to each other. RNAs recruited into P bodies are targeted for degradation. When stress resolves, mRNAs in stress granules are released for translation. This figure is modified from (Li *et al.* 2013).

SGs exert their functions via two routes: i) by bringing together various SG components, it helps shift the equilibriums of interacting molecules towards associated states, thus, facilitates their interactions; ii) by sequestering various proteins and RNAs leading to their depletion from the sites of their normal function (Protter and Parker 2016). These mechanisms of action can be illustrated very well using the case of viral infection.

Antiviral immunity is one of the most studied functions of SGs. Their assembly blocks viral replication and helps cells fight against the virus while supporting cell survival. Firstly, translation arrest provides very early protection by blocking viral protein synthesis before the expression of antiviral genes of infected cells commences (McCormick and Khaperskyy 2017). Secondly, SGs recruit viral sensors and signalling proteins thereby modulating host signalling cascade. On one hand, it provides a platform to enhance virus recognition and antiviral signal transduction by putting together innate immune sensors and RNA/protein ligands (Onomoto *et al.* 2012). On the other hand, it suppresses the pro-apoptotic signalling cascade downstream of tumour necrosis factor (TNF) activation by sequestering TNF receptor-associated factor 2 (TRAF2) to prevent cell death (Kim *et al.* 2005). Finally, SGs could also trap viral factors preventing them from participating in the normal viral replication cycle (McCormick and Khaperskyy 2017).

Proteomic analysis of biochemically purified SG cores found that non-RNA binding SG proteins include post-translational modification enzymes, metabolic enzymes, and protein/RNA remodelling complexes, i.e. the key components of signalling pathways (Jain *et al.* 2016). SGs also contain the Argonaute family proteins and miRNAs, mRNA-editing enzymes and RNAs and proteins required for transposon activity, such as RNA from LINE1 retrotransposons and its protein product ORF1 as well as reverse transcriptase (Anderson and Kedersha 2009a, Anderson and Kedersha 2009b).

1.2.5. Stress granules and ALS molecular pathology

SGs and ALS pathology are strongly linked. Firstly, pathological inclusions found in neurons and glial cells of ALS and FTLD patients show immunoreactivity for core SG proteins, such as TIAR or TIA1 (Liu-Yesucevitz *et al.* 2010). Secondly, 70% of ALS-associated genes encode proteins that are recruited into SGs upon stress, such as TDP-43, FUS, hnRNPA1, hnRNPA2, TAF15 and VCP (reviewed in (Aulas and Vande Velde 2015)). Finally, pathogenic mutant proteins encoded by some of ALS-associated genes could form constitutive cytoplasmic assemblies containing SG proteins in cultured cells in the absence of cellular stress (Liu-Yesucevitz *et al.* 2010, Wolozin 2012, Shelkovnikova *et al.* 2014a).

As already mentioned, TDP-43 and FUS are among the most frequently dysregulated proteins in ALS and FTLD pathology. Although they are predominantly nuclear proteins, they shuttle rapidly between the nucleus and cytoplasm for the transport of mRNA (Zinszner *et al.* 1997). Interestingly, upon various cellular stresses, a small amount of nuclear TDP-43 and FUS shuttle to the cytoplasm and incorporate into SGs. When the stress is resolved and SGs disassemble, they return to the nucleus (Ayala *et al.* 2008, Dormann *et al.* 2010). Therefore, TDP-43 and FUS are normal SG components and their recruitment is a physiological and reversible process.

However, cells expressing mutant TDP-43 show attenuated SG assembly and increased propensity to form abnormal SGs (Liu-Yesucevitz *et al.* 2010, McDonald *et al.* 2011). Moreover, TDP-43 mutation can cause persistent cytoplasmic aggregation and/or SGs after the stress is resolved (Liu-Yesucevitz *et al.* 2010). Similarly, cells expressing FUS mutants display delayed SG formation under oxidative stress, and the extent of delay is correlated with the cytoplasmic level of mutant FUS. Mutant FUS incorporation also increases the size and abundance of SGs, and alters the dynamics of the SGs. However, unlike TDP-43, mutant FUS accelerates SG disassembly following removal of stress (Baron *et al.* 2013). Existing experimental evidence supports two non-mutually exclusive models of the effect ALS mutants have on SGs.

The gain of function model implies that ALS-linked mutant proteins acquire a novel toxic function within SGs. According to this model, as mutant TDP-43 and FUS are more prone to localise to SGs than their WT forms (Bosco *et al.* 2010, Dormann *et al.* 2010), their excessive localisation within SGs results in increased local concentration of IDRs, raising the risk of insoluble fibrillary aggregates formation (Bosco *et al.* 2010, Dormann *et al.* 2010, Liu-Yesucevitz *et al.* 2010, Wolozin 2012). In addition, incorporation of mutant proteins might change the protein-protein and protein-RNA interaction network within SGs, which would further lead to changes in SG dynamics and function. For example, abnormal SGs interfere with the localisation of mRNPs that are required for RNA sorting and processing, resulting in compromised RNA homeostasis during stress (Johnson *et al.* 2009, Sun *et al.* 2011, Baron *et al.* 2013). Moreover, altered SGs might also diminish the localisation of internal ribosome entry site (IRES)-containing mRNAs thereby inhibiting translation of anti-apoptotic factors and proliferative factors essential for cell survival (Li *et al.* 2013). Intriguingly, mutant TDP-43 and FUS that are incompetent in RNA binding show significantly reduced toxicity without affecting their aggregation (Elden *et al.* 2010, Voigt *et al.* 2010, Sun *et al.* 2011, Daigle *et al.* 2013), suggesting that protein aggregation alone is not sufficient to cause cellular toxicity. Interacting with RNA might cause TDP-43 or FUS change their conformation to a toxic form that will aggregate more. Alternatively, RNA-binding activity of TDP-43 and FUS may allow entrapment of RNAs and proteins that are essential for cell survival.

The loss of function model argues that absence of normal TDP-43 or FUS disrupts SG assembly and turnover. Knockdown of TDP-43 by siRNA in HeLa cells and neuroblastoma cells affected SG assembly and disassembly as evidenced by delayed formation, reduced average size, decreased stability and quicker disassembly upon the removal of stress, partly resembling the phenotype caused by mutant TDP-43 expression (McDonald *et al.* 2011, Aulas *et al.* 2012). Therefore, it is possible that ALS-linked mutations in TDP-43 impair protein-protein or protein-RNA interactions of SG components, which are essential for SG formation, maintenance, clearance and, ultimately function. In contrast, knockdown of FUS in HeLa cells or in HEK-293 cells had

no impact on SG assembly under oxidative stress (Aulas *et al.* 2012), suggesting that FUS might not be an essential SG component.

In conclusion, ALS-associated mutant proteins can alter dynamics and function of SGs, and persistent SGs and possibly inadequate stress response are important mechanisms underlying ALS pathogenesis.

1.2.6. Stress granules vs. pathological RNP granules formed by mutant FUS

As described above, persistent SGs are thought to be the “seeds” of pathological inclusions found in degenerating neurons in ALS. However, for FUS, it has been shown that when mutated, this protein can initiate the assembly of a novel type of RNP granule, distinct from the SG.

Mutant FUS accumulated in the cytoplasm can form small granules (termed FUS granules, or FGs) spontaneously when FUS level reaches a certain threshold (Shelkovnikova *et al.* 2014a). This was shown both in non-neuronal cultured cell lines and in primary neurons. When the cells are exposed to stress, unlike diffuse FUS protein that are recruited into SGs, preformed FGs further cluster to form large aggregates (FUS aggregates, FAs), which also contain SG proteins and require RNA as a structural component. However, high-resolution microscopy showed that while SGs are characterised by compact appearance with “smooth” surface, FAs appear as non-compact, irregularly shaped collection of small granules. Furthermore, FAs often undergo further aggregation to form larger structures, which is not typical for mature SGs. Importantly, a subset of FAs are negative for SG proteins that are essential for SG formation, suggesting that they are dispensable during FA biogenesis. Moreover, the ribosomal protein S6, a component of pre-initiation complex which builds SGs, is absent from FAs (Shelkovnikova *et al.* 2014a). Therefore, mutant FUS can form a pathological RNP granule different from SGs in composition, organisation and dynamics.

Interestingly, since RNA is essential for FA maintenance, depletion of free RNA due to the transcriptional arrest resulted in their disassembly. However,

upon prolonged transcriptional repression, solubilised mutant FUS reassembled into insoluble aggregates that do not require free RNA (Shelkovnikova *et al.* 2014a). Likewise, it has been reported that C-terminally truncated FUS protein lacking RNA-binding domains can spontaneously assemble into aggresomes under basal condition (Shelkovnikova *et al.* 2013b). These aggresomes morphologically resemble FAs formed under persistent transcriptional arrest described above. In agreement with these findings, it has been reported recently that high RNA concentration keeps RBPs, including FUS, soluble while depletion of RNA promotes excessive phase separation (Maharana *et al.* 2018). In a nutshell, cytoplasmically mislocalised FUS protein, if accumulated beyond a certain threshold, can form irreversible aggregates when free RNA is not available or the protein is incapable of RNA binding. Importantly, RNA binding and subsequent recruitment into SGs is shown to prevent cytoplasmic FUS from forming aggresomes (Shelkovnikova *et al.* 2013b), suggesting that SG assembly is a protective mechanism against the development of FUSopathy. It is observed in cultured cells that the presence of FGs or FAs perturbs the assembly of SGs by competing for their shared protein and RNA components, which will compromise the protective SG function.

1.3. Aims

Our understanding of the pathomechanisms underlying ALS-FUS has increased greatly since the discovery of the causative link between *FUS* gene mutation and ALS. Now it is clear that mutant FUS protein mislocalises to the cytoplasm where it forms insoluble aggregates – a pathological hallmark of FUSopathy. Both nuclear loss of function and cytoplasmic gain of function of FUS protein are considered to contribute to the disease development, hence understanding the behaviour of mutant FUS protein both in the nucleus and in the cytoplasm is crucial in understanding the disease mechanisms.

As described in the previous chapter, FUS is an important component of nuclear paraspeckles, a structure deeply implicated in ALS. Although it is known that FUS knockout compromises paraspeckle integrity, it is not clear how mutant FUS present in the nucleus (as in ALS-FUS patient cells) affect their structure and function. Since NEAT1 level is very sensitive to FUS protein levels, existing cellular models overexpressing mutant FUS protein is not ideal for paraspeckle studies. The advent of CRISPR/Cas9 gene editing technology has allowed us to study paraspeckles in the cells expressing mutant FUS at physiological levels. Therefore, the aims of the first part of the thesis are:

1) Generate and characterise stable human cell lines with *FUS* gene modifications (Chapter 3).
2) Investigate the pathological impact of mutant FUS protein on paraspeckle structure and function using cellular models generated (Chapter 4).

To achieve the first aim, a region of *FUS* gene encoding NLS domain of FUS protein, where most ALS-causing mutations occur, was deleted (or completely disrupted) by CRISPR/Cas9. Single-cell clones with desired modifications were generated and characterised in terms of FUS gene sequence, FUS protein subcellular localisation, FUS mRNA and protein expression levels *etc*..

For the second aim, NEAT1 levels and paraspeckle formation, the interaction between FUS protein and core paraspeckle components as well as paraspeckle function were studied in mutant FUS clones established above.

Results obtained from the cellular models were confirmed in fibroblasts and spinal cord tissues from ALS-FUS patients.

In addition to the pathological behaviour of mutant FUS protein in the nucleus, the thesis also explored the possible stresses that could possibly trigger the formation of insoluble FUS aggregates in the patient neurons. Since overexpressed FUS is highly prone to aggregate spontaneously, FUS clones expressing physiological levels of mutant FUS protein can be extremely valuable in this study. Therefore, the third aim of the thesis is:

3) Investigate the possible triggers of FUSopathy using cellular models generated (Chapter 5).

For this, several neurodegeneration-relevant stresses were tested on FUS clones for their ability to trigger persisting FUS-positive cytoplasmic assemblies. Antiviral immune response induced by poly (I:C), a synthetic molecule mimicking viral dsRNA, emerged as a promising environmental trigger and other aspects of virus-induced FUSopathy were further studied.

Finally, the thesis also aimed to study FUS truncation mutations focusing on the C-terminal peptide “tails” resulted from frameshift.

4) Investigate pathological roles of C-terminal peptide “tails” generated from FUS truncation mutations.

To this end, FLAG-tagged truncated FUS proteins with or without a “tail” were expressed in human SH-SY5Y neuroblastoma cells as well as in mouse hippocampal primary neurons to compare their subcellular distribution and aggregation. This is a preliminary study of a currently ongoing project in the lab, which should yield interesting results when studied further.

Overall, this thesis aimed to provide important insight into the pathological functions of mutant FUS protein in the nucleus as well as into the nature of the environmental stress that could trigger or exacerbate FUSopathy.

Chapter 2. Materials and Methods

2.1. Generation of stable cell lines with targeted modification of the *FUS* gene

2.1.1. Construction of plasmids carrying guide RNA sequence

pX330-U6-Chimeric_BB-CBh-hSpCas9 vector (pX330) (Addgene), which allows simultaneous expression of human codon-optimised SpCas9 and a chimeric guide RNA (gRNA), was selected, and the cloning was performed following the protocol provided by Addgene (https://www.addgene.org/), with modifications. The vector map, structure of the chimeric gRNA and gRNA cloning site are shown in Figure 2.1. Locations of gRNA target sequences and how they have been selected are described in detail in section 3.2.1.

Briefly, pX330 vector was linearised with FastDigest BbsI (ThermoScientific) and purified from the agarose gel using QIAquick Gel Extraction Kit (Qiagen) following the manufacturer's instructions. Double-stranded DNA insertions containing gRNA sequence were synthesised (Sigma) as instructed by Addgene, and these insertions contained overhangs complementary to the overhangs on the digested pX330 vector. Ligation reaction was performed between digested vector and DNA insertions in the molar ratio of 1:10 using T4 DNA ligase (New England Bioloabs, NEB).

The ligated plasmids were delivered into chemically competent E. coli cells (NEB #C2987H) through transformation (protocol see below) and ampicillin-resistant positive colonies were further amplified. Plasmid DNA from each positive colony was sequenced to verify the correct insertion of the target sequence using U6 primer. All the sequencing services for this project were provided by Eurofins and all the sequence analysis was carried out using ApE software.

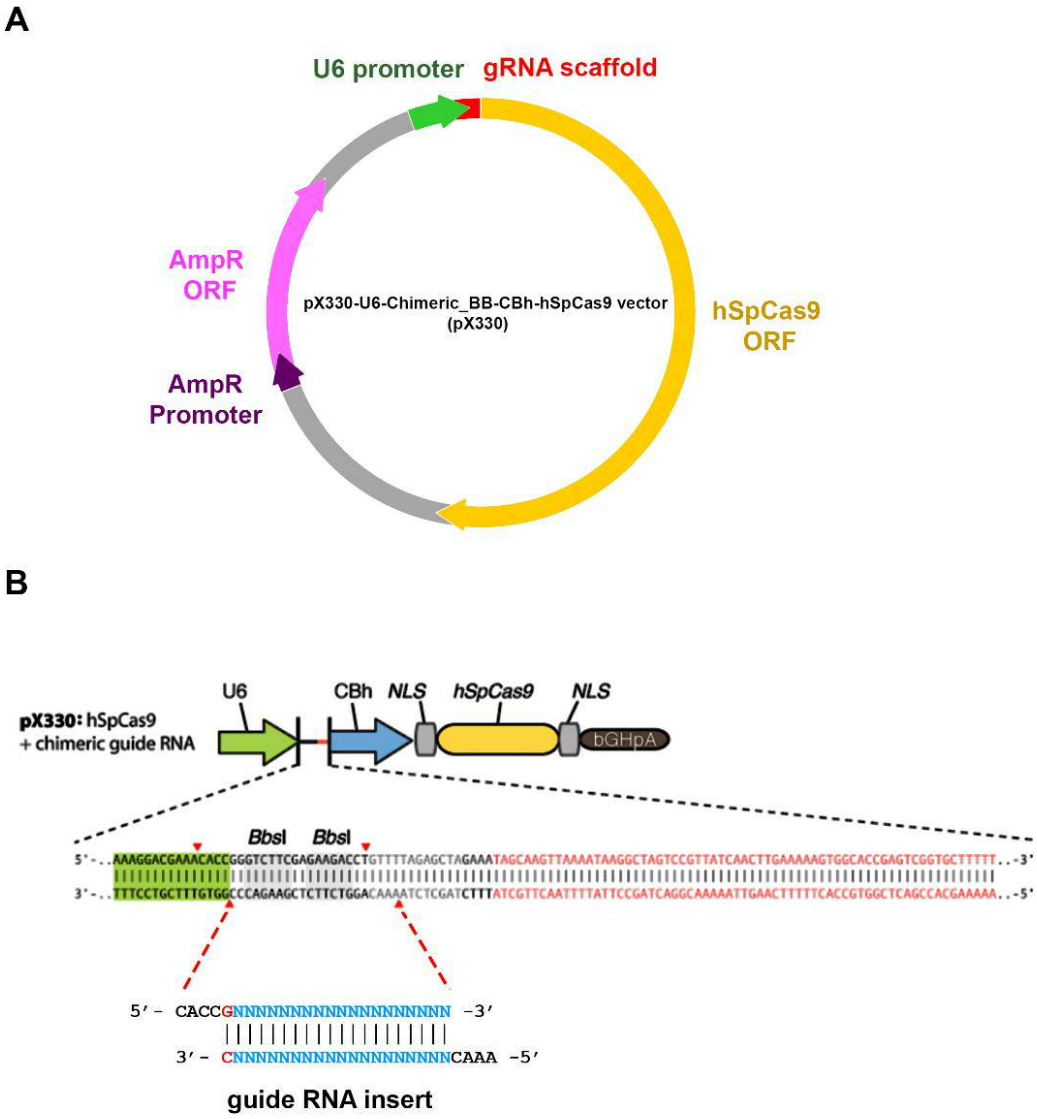

Figure 2.1 Construction of pX330 plasmid carrying guide RNA (gRNA) sequence.

A) Simplified map of pX330 vector. This vector can express both gRNA and humanized S.pyogenes Cas9 (hSpCas9) under U6 promoter. **B)** The sequence of chimeric gRNA and its location in the pX330 vector is shown. gRNA is inserted into the site created by BbsI restriction endonuclease. CBh: chicken beta-actin promoter; NLS: nuclear localisation signal; bGHpA: bovine growth hormone polyadenylation signal.

2.1.2. Transfection and stable single-cell clone generation

Calcium phosphate transfection was used to deliver pX330 constructs into human neuroblastoma SH-SY5Y cells (ATCC line, Sigma). SH-SY5Y cells were chosen for their human origin, neuron-like properties and ease of maintenance. The day before transfection, SH-SY5Y cells were plated onto a 35 mm dish at 50-60% density, and the culture medium was replaced by fresh medium 1 h prior to the transfection.

Reagents used for calcium transfection are given in Table 2.1. Solution A was 90 µl 2X HEPES buffered saline (HBS), and solution B was a 90 µl mixture containing 3.6 µg pX330 constructs and 245 mM $CaCl_2$. Solution B was added to solution A dropwise while the mixture was continuously agitated, and the mixture was applied on the surface of the culture medium evenly as small droplets. The dish was returned to the incubator overnight.

Table 2.1 Components of the calcium phosphate transfection reagents

Solutions	Components	Final concentration
$CaCl_2$ *	$CaCl_2 \cdot 2H_2O$	2 M
	H_2O	N/A
2X HBS (solution A) ** (pH=7.05)	HEPES	50 mM
	NaCl	280 mM
	$Na_2HPO_4 \cdot 7H_2O$	1.5 mM
	H_2O	N/A

* filtered through 0.22 µm filter, stored at 4 °C.

** filtered through 0.22 µm filter, stored at -20 °C, and defrosted at room temperature before use.

The culture medium was replaced by fresh medium at 24 h post-transfection, and cells were allowed to recover for 4 h. Cells were split onto 10 cm culture dishes at a density of ~ 200 cells/dish. After 2 weeks, single cell-derived colonies were picked by sterile 200p pipette tips, and transferred to 96-well plates for further expansion. When the cells reached ~ 70-80% confluency, colonies were screened by polymerase chain reaction (PCR) and immunostaining. Primers flanking the deleted region were used for PCR screening, and therefore, the presence of shorter PCR product relative to that from WT cells indicated gene editing (section 3.2.2). Immunostaining of FUS

protein showed cytoplasmic mislocalisation due to the deletion/disruption of NLS or FUS protein absence, in FUS ΔNLS clones and FUS KO clones, respectively. Positive clones were further expanded and stored in liquid nitrogen in BAMBANKER™ serum free cell freezing medium (Lymphotec Inc). Schematic illustration of this protocol is available in Figure 2.2.

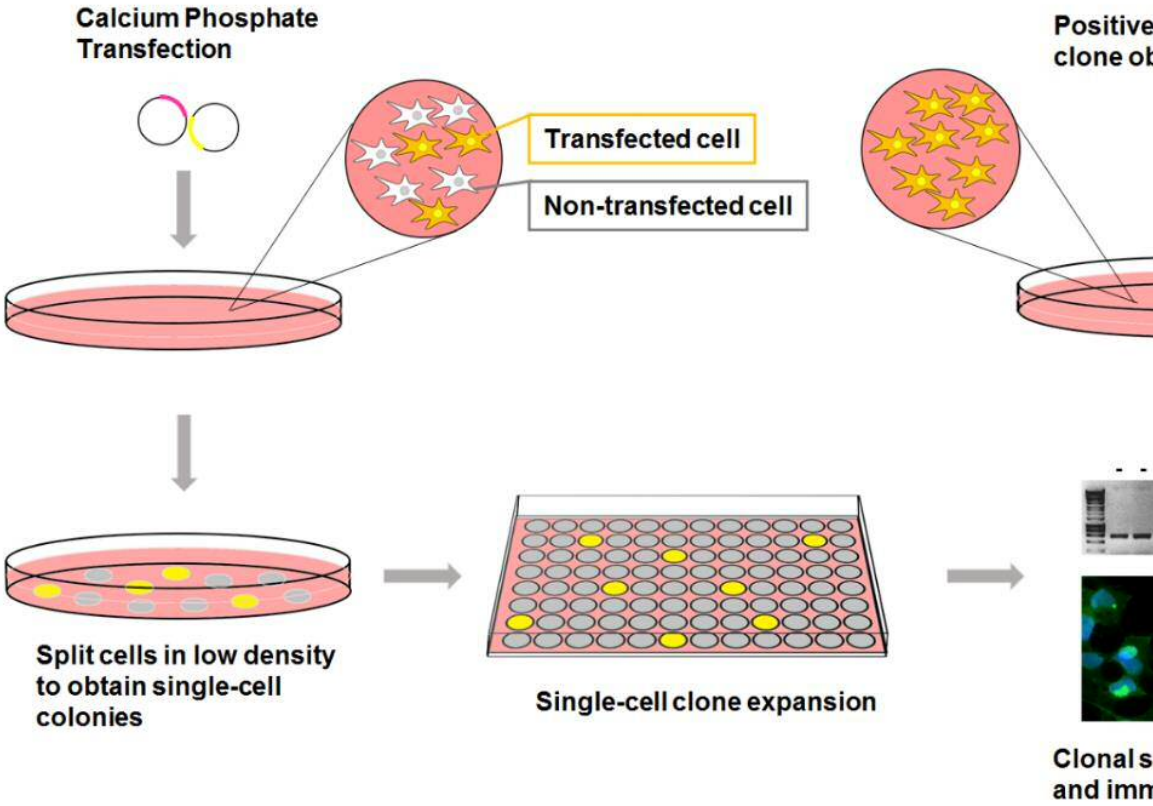

Figure 2.2 Generation of stable single-cell-derived clones with *FUS* gene mo

dNTP (Sigma). Blunt-ended PCR product was cloned into TOPO® vector following the manufacturer's instructions. Cloned vectors were delivered into chemically competent E. coli by transformation and the plasmid DNA was extracted from bacteria colonies. After confirming the insertion by EcoR I endonuclease (Thermo Scientific) digestion, positive plasmids were sent for sequencing.

2.2.1.2. Plasmid cloning for protein expression

pFLAG-CMV-4 vector (Sigma) was used for the construction of plasmids expressing N-terminal FLAG-tagged truncated FUS proteins with/without a C-terminal "tail". Human WT cDNA synthesised from WT SH-SY5Y cells served as the PCR template for the amplification of DNA fragments that code for the proteins of desired peptide sequences. The primers were therefore designed to contain sequence alterations that would introduce frameshift mutations to the protein products (Table 2.2). A list of truncated FUS proteins produced and details about the C-terminal "tail" are shown in Chapter 6. Primers also contained restriction digest sites for asymmetric sub-cloning. After TOPO cloning and sequence verification, PCR fragments were excised from the TOPO® plasmid by restriction endonuclease digestion (HindIII and BamHI, both from NEB). Purified PCR fragments were then cloned into pFLAG-CMV-4 vectors using T4 DNA ligase, with the vector and insert molar ratio of 1:3. Ligated constructs were expanded in the E.coli and correct insertions were confirmed by sequencing.

Table 2.2 Primer sequences used for cloning fragments of truncated *FUS* gene with a frames

Construct	Reverse primer sequence
FUS466fs	5'-CGGGATCCCTAATTAATACGGCCTCTCCCTGCGATCCTGTCTGTGCTCACCC
FUS491	5'- CGGGATCCTTAACGGTCCCCGCCGCGGCCCCGGTAG -3'
FUS491tail	5'- CGGGATCCTTAATTAATACGGCCTCTCCCTGCGATCCTGTCTGTGCTCACCC GCCAAAGCCACCTCTGTCCCCACCACCCCACGGTCCCCG -3'
FUS503	5'- CGGGATCCTTATCTGTCCCCACCACCCCGGC -3'
FUS503tail	5'- CGGGATCCTTACCCCTGGAATCCATCTTGCCAGGGCCAAAGCCATCTGTCC
FUS514tail	5'- CGGGATCCTTACCTTCCTGATCGGGACATCGATCTGGAATCCATCTTGCCAG
FUS513tail2	5'- CGGGATCCTTACAAAATAACGAGGGTAACACTGGGTACAGGACAAAAAGCTC TGCAGAATTCGA -3'
	Common forward primer sequence
All constructs	5'- GCTAAAGCAGCTATTGACTG -3'

2.2.2. Bacterial cell transformation and plasmid purification

The bacterial cell transformation was optimised from the protocol provided by NEB. Briefly, one vial of 5-alpha competent E.coli cells were mixed with 2 µl plasmid DNA (10 ng), and were incubated on ice 15 min. Cells were subjected to heat shock at 42°C for 45 sec, followed by 5 min cooling on ice. Cells were resuspended in S.O.C Outgrowth Medium (NEB) and kept shaking for 1 h at 37°C. Cells were plated on a 1% selective agar plate containing 50 µg/ml ampicillin or kanamycin and incubated at 37°C overnight. Positive colonies grown on the plate were inoculated into 2.5% Luria Broth media (Invitrogen) supplemented with 50 µg/ml ampicillin or kanamycin and incubated overnight in a shaker at 37 °C. Plasmid DNA was purified from overnight culture using QIAGEN Plasmid Miniprep kit as instructed by the manufacturer.

2.2.3. Genomic DNA extraction and PCR

A made in-house digest buffer, which contains 100 mM NaCl, 50 mM Tris Buffer (pH 8.0), 2 mM ethylenediaminetetraacetic acid (EDTA) and 2 mg/ml proteinase K (all Sigma), was used for genomic DNA extraction from cultured mammalian cells. Cells washed with phosphate-buffered saline (PBS) were pelleted down, resuspended in digest buffer and then incubated at 55 °C for 2 h. After inactivating proteinase K by incubating the samples at 85 °C for 15 min, clear supernatants, which contain genomic DNA, were obtained by centrifugation at 13,000 rpm for 15 min.

The PCR, for the purpose of either PCR-based single-cell screening (explained in section 2.1.2) or molecular cloning, was performed in a 50 µl reaction volume containing 0.75 µl of each primer (forward, reverse, 10 µM stock), 2 µl of genomic DNA sample (100~500 ng/µl), 0.25 µl of Taq DNA polymerase (NEB) and 5ul 10X Standard Taq Reaction buffer. Parameters of PCR program were as follows. 95°C for 2 min, (95°C for 15 s, 58°C for 45 s, 68°C for 45 s) X 35 cycles, 68°C for 2 min 30 s, but they were adjusted for different targets amplification – annealing temperature was adjusted depending on primer melting temperature and elongation time was adjusted depending on the product size. PCR products were separated by

electrophoresis in 1 - 3% agarose gel and visualised and imaged using Gel Doc™ EZ system (Bio-Rad). Primer sequences are given in Table 2.3.

Table 2.3 Primer sequences for PCR and PAT assay.

Target	Forward primer sequence	Reverse primer sequence
FUS*	5'-TGGGGACAGAGGTGGCT TTG -3'	5'-CCTTCCTGATCGGGACATC G -3'
FUS**	5' ACCATTTGAGAAAGGCAC GCT -3'	5'-CACGGATTAGGACACTTCCA GT -3'
FUS***	5'- GTCCAGCCCATGTGAGA CTT -3' (p1)	5'-AACCTCCAGCATAAAAGGG CT -3' (p2)

* for FUS ΔNLS clone screening; ** for FUS KO clone validation by sequencing; *** for PAT assay.

2.2.4. RNA extraction, cDNA synthesis, and qPCR

Total RNA was extracted from mammalian cells either using GenElute™ Total RNA Purification Kit (Sigma) or using QIAzol (Qiagen) following the manufacturers' instructions. When extracting RNA using RNA purification kit, DNase I (Qiagen) on-column treatment was performed to eliminate DNA contamination. NEAT1_2 transcripts are known to be "semi-extractable", which means that heating or shearing step must be included in the standard Acid Guanidinium Thiocyanate-Phenol-Chloroform (AGPC)-based RNA purification methods to extract them efficiently (Chujo *et al.* 2017). Therefore, an additional heating step was introduced to the standard QIAzol RNA extraction protocol in semi-extractability analysis. For that, cell lysates in QIAzol reagent were incubated at 55 °C for 10 min. The purity and concentration of RNA were measured using NanoDrop™ 1000 Spectrophotometer (Thermo Fisher Scientific) and RNA concentration was was diluted to the same concentration within each set for first strand cDNA synthesis.

First strand cDNA was synthesised using SuperScript™ IV Reverse Transcriptase (Invitrogen). The reaction was performed in 20 µl volume containing 300 – 500 ng RNA, 1 µl random primers (Promega, 500 µg/ml), 1 µl dNTP mixture (Sigma, 10 mM), 1 µl DTT (Invitrogen, 0.1 M), 1 µl reverse transcriptase and 4 µl 5X buffer. Solutions containing RNA, random primers and dNTPs were incubated at 68 °C for 5 min to break RNA secondary structure before adding the rest of reagents followed by the incubation at room temperature for 5 min to allow annealing of random primers to the targets. Reverse transcription was performed at 55 °C for 15 min followed by the inactivation step at 85 °C for 10 min. First strand cDNA was diluted 5 times in nuclease-free water for qPCR.

Quantitative PCR (qPCR) reaction was performed using TrueStart Hot Start Taq DNA Polymerase (Thermo Scientific) following the manufacturer's instruction. Each reaction contained 2 µl cDNA, 0.2 µl dNTP mixture (Sigma, 10 mM), 0.1 µl forward primer, 0.1 µl reverse primer (Sigma, 10 µM), 2 µl $MgCl_2$ (Thermo Scientific, 25 mM), 0.2 µl SYBR Green (Bio-Rad), 0.2 µl ROX reference dye (Thermo Scientific), 0.125 µl Taq DNA polymerase, 2 µl 10X buffer and nuclease-free water up to 20 µl. A two-step PCR was performed on Applied Biosystems StepOne™ system with the settings as follows: 95 °C for 10 min, (95 °C 15 s, 60 °C for 1 min) X 40 cycles. Primer sequences used are shown in Table 2.4.

For miRNA measurement, first strand cDNA was prepared using miScript II RT (Qiagen), following the manufacturer's instruction. miRNA levels were measured by qPCR using forward miRNA-specific primer and the universal reverse primer (unimiR). The primer sequences are given in Table 2.4.

2.2.5. Poly(A) tail-length (PAT) assay

Poly(A) tail length was measured using USB® Poly(A) Tail-Length Assay Kit (Thermo Scientific) following the manufacturer’s instructions (Figure 2.3). A stretch of guanosine and inosine residues (G/I tail) was added on the 3’-ends of RNA molecules by poly(A) polymerase. Tailed RNAs were then reverse transcribed into cDNAs using the G/I tails as the priming sites. PCR

amplification was carried out from the cDNAs using two primer sets: first primer pair was designed upstream of the polyadenylation start site, and it was used as a control for the gene-of-interest (p1 and p2 in Figure 2.3); the second primer pair was the gene-specific forward primer and the universal reverse primer recognising the tail region (p1 and p3 in Figure 2.3), and this pair amplifies poly(A) tail of the gene. PCR products were run on 3% agarose gel for the comparison of poly(A) tail lengths. The primer sequences are given in Table 2.3.

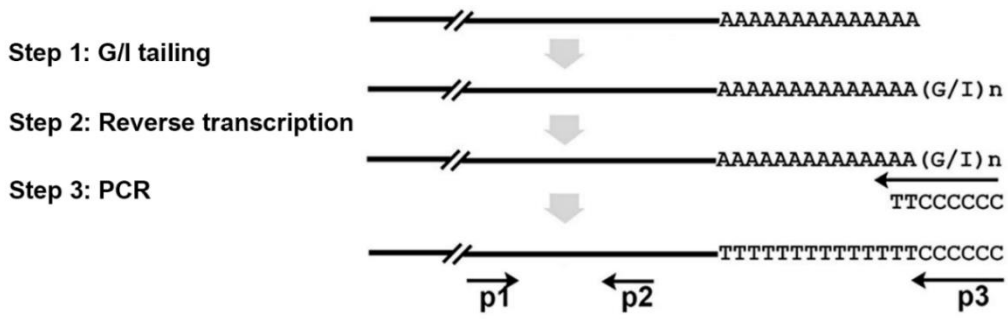

Figure 2.3 The principle behind poly(A) tail-length assay.

p1 and p2 are gene-specific primers. p3 is the universal primer provided with the kit.

Table 2.4 Primer sequences for qPCR.

Target	Forward primer sequence (5' - 3')	Reverse prime
GAPDH	5'- TCGCCAGCCGAGCCA -3'	5'- GAGTTAAAAGCAG
FUS WT	5'- GTGAGCACAGACAGGATCGC -3'	5'- GAGGGTAACACTC
FUS ex7-	5'- CAGAGGTGGCATGGGGC -3'	5'- TGTAACATTCTCA
FUS total	5'- GGAACTCAGTCAACTCCCCA -3'	5'- TACCGTAACTTCC
NEAT1 total	5'- CTCACAGGCAGGGGAAATGT -3'	5'- AACACCCACACCC
NEAT1_2	5'- AGAGGCTCAGAGAGGACTGTAACCTG -3'	5'- TGTGTGTGTAAAA
MALAT1	5'- GGATCCTAGACCAGCATGCC -3'	5'- AAAGGTTACCATA
NEAT1_1 pA	5'- TCACGCATGTATGGGGAAGT -3'	5'- ACCATACAGAGCA
ADARB2	5'- ATATTCGTGCGGTTAAAAGAAGGTG -3'	5'- ATCTCGTAGGGAC
miR-18a_for	5'- CATCATCGGTAAGGTGCATC -3'	5'- GAATCGAGCACCA
miR-19b_for	5'- GCACTGACATGTGCAAATCC -3'	unimiR
miR-20a_for	5'- CGCACGACTAAAGTGCTTATAG -3'	unimiR
miR-92a_for	5'- GAGTCTATTGCACTTGTCCC -3'	unimiR
miR-105_for	5'- TCAAATGCTCAGACTCCTGTGGT -3'	unimiR
miR-106a_for	5'- AAAAGTGCTTACAGTGCAGGTAG -3'	unimiR
STAT1	5'- CTGTGCGTAGCTGCTCCTTT -3'	5'- GGTGAACCTGCTC
CHOP	5'- TTAAAGATGAGCGGGTGGC -3'	5'- GCTTTCAGGTGTG
FUS pre-mRNA	5'- GAACCACCTCCAGAAAGGGG -3'	5'- TGGGGCAAACCC
FUS pre-mRNA	5'- GAAGCCGCGGAGAAGAGTAA -3'	5'- AAGAAAAGACTTC

2.2.6. RNA sequencing

For RNA-Seq and gene expression analysis, total RNA from cells was extracted using PureLink total RNA extraction kit (Life Technologies) and possible DNA contamination was removed using RNase free DNase kit (Qiagen). RNA-Seq analysis was performed at School of Biosciences Genomics Research Hub. Libraries were prepared using the TruSeq stranded mRNA kit (Illumina) and single-end sequencing was performed on Illumina NextSeq500 (read length: 75 bp; coverage ~20 million reads/sample). Reads were aligned to the human reference genome (GRCh38) using STAR (Dobin et al, 2013) and FPKM values were obtained using DESeq2 (Love, Huber et al. 2014). Reads were viewed in the IGV browser (Thorvaldsdottir, Robinson et al. 2013).

2.2.7. Protein extraction and western blot

Total protein lysates were obtained from cells or tissues by lysing them in 2X Laemmli buffer supplemented with 5% 2-mercaptoethanol. Lysates were heated up to 95 °C for 10 min before being used for sodium dodecyl sulfate polyacrylamide gel electrophoresis (SDS-PAGE).

Protein samples was loaded to SDS-PAGE gel (8%, 10% or 16% depending on the molecular weight of the protein of interest) and proteins with different molecular weights were separated by electrophoresis, which was followed by semi-dry transfer onto Hybond- polyvinylidene fluoride (PVDF) membrane (Amersham). Membranes were blocked in 4% milk prepared with Tris-buffered saline with Tween 20 (TBS-T) for 1 h at room temperature and then incubated in primary antibodies diluted in 4% milk/TBS-T at 4 °C overnight. On the following day, the membranes were washed with TBS-T and incubated in HRP-conjugated secondary antibodies (Amersham) diluted in 4% milk/TBS-T (1:3000) at room temperature for 1.5 h. WesternBright enhanced chemiluminescence (ECL) horseradish peroxidase (HRP) substrate (Advansta) was used for detection on an X-ray film (CL-XPosure, Thermo Scientific). Membranes were re-probed for beta-actin. The list of primary antibodies are given in Table 2.5.

For puromycin labelling of nascent polypeptides, puromycin (Sigma) was added to the culture medium 30 min before lysis at the final concentration of 10 µg/ml. For negative control, cycloheximide (Sigma) was added to a final concentration of 10 µg/ml together with puromycin. Puromycilated proteins were detected by western blot using an antibody recognising puromycin.

Table 2.5 Antibodies used for immunostaining and western blot

Targets	Type	Dilution (immunostaining)	Dilution (western blot)	Manufacturer	Product code
FUS (full)	r. pol.	1:1000	1:1000	Proteintech	11570-1-AP
FUS (NT)	r. pol.	1:500	1:1000	Abcam	ab84078
FUS (mid)	m.mono.	1:1000	1:1000	Santa Cruz	sc-47711
FUS (CT)	r. pol.	N/A	1:1000	Bethyl	A300-294A
G3BP1	m.mono.	1:1000	N/A	BD Biosciences	611126
TIAR	m.mono.	1:1000	N/A	BD Biosciences	610352 610352
CC3	r. pol.	1:500	N/A	Cell Signaling	9661
IFNAR1	r. pol.	N/A	1:1000	Bethyl	A304-290A
OPTN	r. pol.	1:500	1:1000	Bethyl	A301-829A
puromycin	m.mono	N/A	1:1000	Merck Millipore	MABE343
eIF2α	r. pol.	N/A	1:1000	Cell Signalling	9722
p-eIF2α (Ser51)	r. pol.	N/A	1:1000	Abcam	ab32157
Nup107	r. pol.	1:500	N/A	Proteintech	19217-1-AP
Nup98-Nup96	r. pol.	1:500	N/A	Proteintech	12329-1-AP
KPNA2	r. pol.	1:500	N/A	Proteintech	10819-1-AP

TNPO1	r. pol.	1:500	N/A	Proteintech	20679-1-AP
Beta-III-tubulin	r. pol.	1:500	N/A	Sigma	T2200
beta-actin	m.mono.	N/A	1:1000	Sigma	A5441
FLAG tag	r. pol.	1:500	N/A	Sigma	F7425
SFPQ	r. pol.	1:500	1:1000	Abcam	ab177149
SFPQ	r. pol.	1:500	1:1000	Bethyl	A301-322A
NONO	r. pol.	1:500	1:1000	Sigma	N8664

* r.pol.: rabbit polyclonal antibody; m.mono.: mouse monoclonal antibody; N/A: not applicable.

2.2.8. Subcellular fractionation

Subcellular fractionation was carried out as described (Suzuki *et al.* 2010a). Briefly, WT SH-SY5Y cells and mutant FUS clones were grown as monolayers in 6 cm culture dishes to 80-90% confluency (~4 x 10^6 cells). Cells were washed with ice-cold PBS (pH 7.4) and scraped from the surface on ice and collected in 1.5 ml Eppendorf tubes containing 1 ml ice-cold PBS. After brief centrifugation, supernatant was removed and the cell pellet was resuspended in 900 µl of ice-cold 0.1% NP40 (Calbiochem) solution in PBS. After pipetting the solution using p1000 pipette for 5 times, 300 µl of the lysate was moved to a separate Eppendorf tube as “total cell lysate” and 100 µl 4X Laemmli buffer was added to it, then kept on ice. The rest of 600 µl lysate was centrifuged at 800xg for 5 min and 300 µl supernatant was moved to a separate Eppendorf tube as “cytosolic fraction” and was kept on ice after adding 100 µl 4X Laemmli buffer. The remaining 300 µl supernatant was removed and the pellet was resuspended in 1 ml of ice-cold 1% NP40 and centrifuged for at 800xg for 1 min. After removing the supernatant, the pellet was mixed in 180 µl 2X Laemmli buffer and labelled as “nuclear fraction”. Subcellular fraction samples were boiled at 95°C for 5 min for western blot.

2.2.9. Preparation of soluble nuclear extract

Soluble nuclear extract (SNE) was prepared following the protocol by Werner and Ruthenburg (Werner, Ruthenburg, 2015). WT SH-SY5Y cells and mutant FUS clones were grown as monolayers in 10 cm culture dishes to 80-90% confluency (~9 x 10^6 cells). Cells were scraped into 15 ml centrifugation tubes (Corning) containing 10 ml ice-cold PBS and centrifuged at 1500 rpm for 1 min. The cell pellet was resuspended in 200 µl ice-cold lysis buffer composed of 0.15% NP-40, 10mM Tris buffer (pH 7.5) and 150 mM NaCl using p1000 pipette, followed by 5 min incubation on ice. The lysate was layered onto 500 µl 24% sucrose buffer prepared in 10mM Tris buffer (pH 7.5) containing 150mM NaCl, and centrifuged at 13,000 rpm for 10 min at 4°C. After removing the supernatant, the nuclear pellet was gently resuspended using p200 pipette in 200 µl 50% glycerol buffer prepared with 20 mM Tris (pH 7.9) containing 75

mM NaCl, 0.5 mM EDTA, and 0.85 mM dithiothreitol (DTT). After that, 200 µl ice-cold buffer composed of 20 mM 4-(2-hydroxyethyl)-1-piperazineethanesulfonic acid (HEPES) (pH 7.6), 7.5 mM $MgCl_2$, 0.3M NaCl, 1% NP-40, 1M urea, 1mM DTT and 0.2 mM EDTA was added to the samples. Pulse vortexing was applied to the samples followed by centrifugation at 13,000 rpm for 2 min at 4°C. The supernatant was kept and used as the SNE.

2.3. Tissue culture and differentiation

2.3.1. Cell culture, transfection and treatment

SH-SY5Y neuroblastoma cells and human fibroblast cells were maintained in 1:1 mixture of Dulbecco's Modified Eagle's Medium (DMEM) and F12 medium supplemented with 10% fetal bovine serum (FBS), 50 U/ml penicillin-streptomycin, and 500 µM L-glutamine (all Invitrogen). The medium was replaced every 3 or 4 days, and when cells reach ~90% confluency, they were split into ~25% confluency.

Lipofectamine™ 2000 Transfection Reagent (Thermo Scientific) was used for the transfection following the manufacturer's instruction. 200 ng of plasmid DNA or 250 ng of polyinosinic:polycytidylic acid (poly (I:C)) (Sigma) or 250 ng of siRNA (NEAT1 Silencer Select® from Life Technologies, or STAT1 from Sigma) were used per well in a 24-well plate (~1.5 x 10^5 cells). DNA/siRNA-Lipofectamine complexes were applied onto the cells for 4h, after which an equal amount of full medium was added. Medium was replaced with fresh medium on the following day.

All chemicals used in the studies are listed in table 2.6.

Table 2.6 Chemical compounds used for cell treatment.

Chemical compound	Final concentration	Manufacturer
Actinomycin D	5 µg/ml	Sigma
Cycloheximide	10 µg/ml	Sigma
DRB	25 µg/ml	Sigma
DTT	1 mM	Sigma
Interferon beta	1X10^4 IU	Sigma
MG132	50 µM	Calbiochem
Pifithrin-µ	5 µM	Enzo Life Sciences, UK
Puromycin	10 µg/ml	Sigma
Sodium arsenite	0.5 mM	Sigma

2.3.2. Mouse hippocampal neuron preparation and culture

Hippocampi were obtained from mice on postnatal day 1, washed with cold Hank's Balanced Salt Solution (HBSS) twice and digested for 40 min at 37°C in 0.1% trypsin diluted with HBSS. Digested hippocampi tissue was dissociated by pipetting up and down in Neurobasal A medium containing 100 U/ml penicillin/streptomycin, 0.2% 2-mercaptoethanol, 500 µM L-Glutamine and 10% horse serum. Cell pellet was collected from these tissue suspensions by centrifuging at 1,500 rpm for 5 min. The pellet was resuspended in fresh medium and plated on dishes or coverslips coated with poly-L-lysine. On the following day, the medium was replaced by serum-free medium containing B27 supplement. All the reagents used in this preparation were from Invitrogen.

Transfections or treatments on the mixed neuronal/glial cells were done 5 days after plating, after the neurite network was formed. Transfection was performed using Lipofectamine2000 following the standard protocol (see section 2.3.1), except that complexes were left on cells for 1 h and replaced with fresh full medium after that.

2.3.3. Human motor neuron differentiation from embryonic stem cells

The human embryonic stem cells (ES) H9 cell line was maintained in mTESR2 media (Stemcell Technologies) on Matrigel® (Corning)-coated dishes. Confluent hES H9 cells were switched to the differentiation medium composed of advanced DMEM/F12 (ADF) supplemented with 500 µM GlutaMax (Gibco), 50 U/ml penicillin-streptomycin (Gibco) and 10 µM SB431542 (Abcam). On day 4, 1 µM purmophamine (Cayman Chemicals) and 0.1µM retinoic acid (Sigma) were added to the above medium. Cells were split in a 1:2 ratio on day 8. On day 16, neuronal progenitors were detached from the culture surface using Accutase® (Sigma) and plated on poly-L-lysine/Matrigel® -coated dishes and cultured in ADF medium supplemented with 500 µM GlutaMax, 50 U/ml penicillin-streptomycin, 2% B27 supplement

(Gibco), 1% N2 supplement (Gibco) and 10 ng/ml BDNF (Miltenyi). On day 23, differentiated neurons were dissociated with Accutase and plated onto poly-L-lysine/laminin (Sigma)-coated dishes or coverslips and maintained in the same medium described above, except that 50:50 mixture of ADF/Neurobasal A (Gibco) was used instead of ADF medium until day 40.

2.4. Staining and imaging

2.4.1. Immunocytochemistry

Cells grown on coverslips were washed once with cold PBS and fixed with 4% cold paraformaldehyde for 15 min at room temperature. After washing with PBS, cells were treated with cold methanol for 5 min to permeabilise membranes followed by two washing steps with PBS to remove residual methanol. Cells were incubated in primary antibodies diluted with phosphate-buffered saline with Tween-20 (PBS-T) containing 5% goat serum at room temperature for 2 h or at 4 °C overnight (dilution rate of antibodies see Table 2.5). Cells were washed with PBS and incubated in the fluorochrome conjugated secondary antibodies (AlexaFluor, Life Technologies) diluted to 1:1000 in PBS-T at room temperature for 1.5 h. Cells were kept away from light from this step henceforth. After washing with PBS, nuclei were stained with 1:10,000 4′,6-diamidino-2-phenylindole (DAPI) solution (Sigma,10mg/ml stock) for 2 min at room temperature, and coverslips were mounted on the glass slides using Immu-Mount media (Thermo Scientific).

2.4.2. Immunohistochemistry

Human spinal cord paraffin sections (7 µm thick) from a group of clinically and histopathologically characterised ALS cases and neurologically healthy individuals were obtained from the Medical Research Council (MRC) London Neurodegenerative Diseases Brain Bank and Sheffield Brain Tissue Bank. Consent was obtained from all subjects for autopsy, histopathological assessment, and research was performed in accordance with local and national Ethics Committee approved donation. Immunohistochemistry was

performed using Elite plus kits (Vector laboratories) and 3,3' – diaminobenzidine (DAB) (Sigma) as a substrate. Human spinal cord paraffin sections mounted on the glass slides were deparaffinised in xylene, and rehydrated through a series of ethanol with decreasing percentage. Slides were boiled in microwave in 10 mM sodium citrate buffer (pH 6) for 10 min for antigen retrieval, and cooled down to room temperature. Tissues were incubated in 3% hydrogen peroxide in methanol at 4°C for 30 min to quench the background oxidase activity. After blocking with 10% goat serum/PBS-T for 30 min at room temperature, tissues were incubated in the primary antibodies diluted in the blocking solution at 4°C overnight (dilution rate of antibodies see Table 2.5). The following day, tissues were washed with PBS and then incubated in the biotinylated secondary antibodies (Vector Laboratories) diluted to 1:1000 in PBS-T at room temperature for 1 h. After washing with PBS, Avidin-biotin HRP complexes (Vector Laboratories) were applied to the slides for 45 min followed by washing with PBS. Tissues were incubated in 10 mg/ml DAB solution for around 5 min until a dark brown pigment developed, and then slides were washed with water and dehydrated through a series of ethanol solutions with increasing concentration. Slides were incubated in xylene and mounted in DPX mounting medium (Thermo Fisher).

2.4.3. RNA Fluorescence In Situ Hybridisation (ISH) and RNAscope® ISH

For RNA Fluorescence In Situ Hybridisation (RNA-FISH) cells grown (1~2 x 10^4 cells) on coverslips were fixed in 4% cold paraformaldehyde for 15 min at room temperature, which was followed by membrane permeabilisation in cold methanol for 5 min at room temperature. After washing with PBS, cells were kept in 70% ethanol solution at 4 C overnight. Human spinal cord tissues were deparaffinised, re-hydrated and antigen-retrieved the same way as for immunohisgology. Coverslips/slides were washed in 2X Saline Sodium Citrate (SSC) solution prepared with diethylpyrocarbonate (DEPC)-treated water at room temperature three times. Coverslips/slides were then incubated in

hybridisation buffer (10% formamide/2XSCC) for 10 min at room temperature. Commercially available NEAT1 probes, either against 5' or middle region of human NEAT1 (Stellaris® Quasar® 570-labelled, Biosearch Technologies), or oligo(dT)30 probe that was targeting polyA+RNA (Cy5-labelled, Sigma), were diluted in the hybridisation buffer (2 µl probe in 100 µl buffer). Coverslips/slides were incubated with the probe overnight at 37 C in a humidified chamber. On the following day, coverslips/slides were washed with 2XSSC, incubated in DAPI for nuclei staining and then mounted. Where RNA-FISH was used in combination with immunocytochemistry, the second day after overnight incubation in the RNA probes, cells were incubated in primary antibody diluted in PBS for 30 min and then Alexa488-conjugated secondary antibody diluted to 1:1000 in PBS for 30 min before proceeding to DAPI staining and mounting.

RNAscope® ISH, a novel RNA ISH technology which relies on a unique probe design strategy that allows simultaneous signal amplification and background suppression to achieve single-molecule visualization while preserving tissue morphology, was used for paraspeckle detection in human spinal cord tissues (Wang *et al.* 2012). Hs-NEAT1-long (411541) probe (Advanced Cell Diagnostics) was used in conjunction with RNAscope® 2.5 HD Detection Brown kit according to manufacturer's instructions.

All the solutions used in these experiments were prepared with DEPC-treated water to prevent RNA degradation.

2.4.4. Proximity Ligation Assay

To detect the interaction between endogenous FUS and a paraspeckle protein (NONO or SFPQ) in situ, Proximity Ligation Assay (PLA) is performed. The principle of PLA is shown in figure 2.4. Briefly, FUS and SFPQ (or NONO) are detected by two primary antibodies raised in different species. A pair of secondary antibodies labelled with oligonucleotide (PLA probes) then binds to the primary antibodies. Next, connector oligos and DNA ligase are introduced to join the PLA probes forming circular DNA template only if they are in close proximity to each other. These circular DNA template is then amplified through

a rolling-circle amplification using PLA probe as a primer generating concatemer which is still tethered to the PLA probe. This allows up to 1000-fold signal amplification. Finally, labelled oligos with complementary sequence with concatemer were introduced to visualise the amplicon, which appear as individual spots under microscope.

Here, PLA was performed using Duolink® In Situ Orange Starter Kit Mouse/Rabbit (Sigma) using anti-FUS (mouse monoclonal, Santa Cruz) antibody in combination with rabbit anti-NONO (Sigma) or anti-SFPQ (Bethyl) antibody. The assay was carried out strictly following manufacturer's instructions.

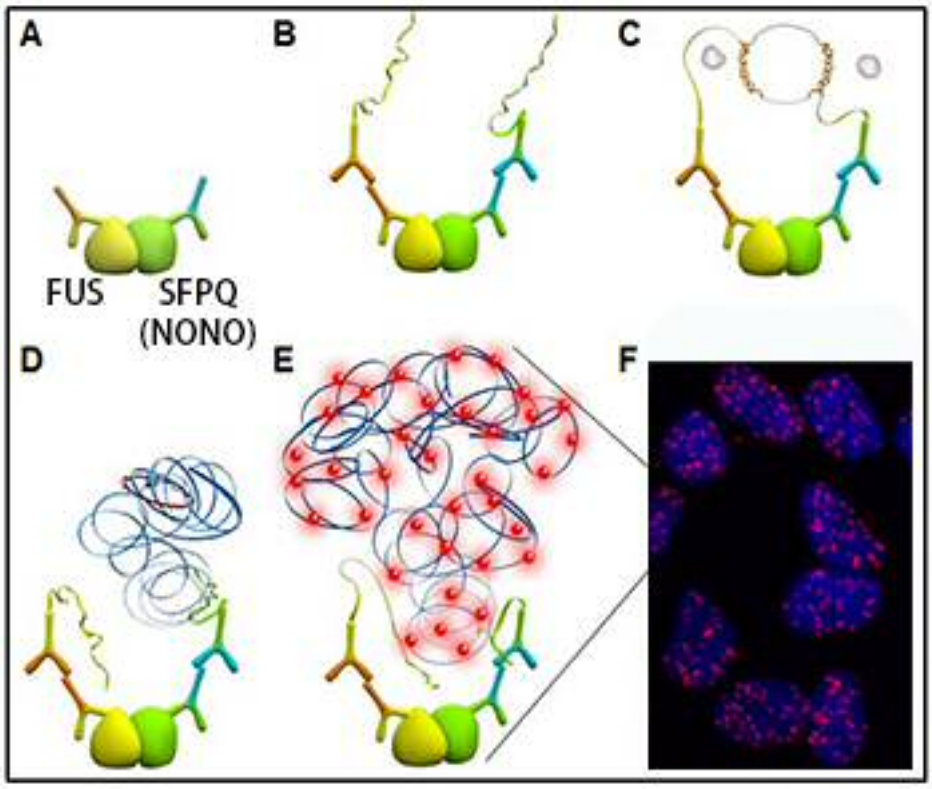

Figure 2.4 Schematic of PLA.
(A) Primary antibodies recognise FUS and SFPQ. (B) PLA probes bind to the primary antibodies. (C) When the probes are in close proximity, connector oligos join the PLA probes generating circular DNA. (D) Circular DNA template becomes amplified by DNA polymerase. (E) Fluorescently labelled detection oligos hybridize to the amplicons. (F) PLA signals under fluorescent microscope. This image is modified from the original chematic available from manufacturer's website.

2.4.5. Imaging of fixed cells and image processing

Fluorescent images were taken using BX61 fluorescent microscope equipped with F View Soft Imaging digital camera and Cell F software (all Olympus). Confocal fluorescent images were taken using the Airyscan LSM880 upright confocal microscope with ZEN software (Zeiss). Bright-field images of human spinal cord tissues were taken using Olympus X53 microscope. Plot profiles and surface profiles were generated using the plot profile function and interactive 3D surface plot plugin in Image J, respectively. Figures were prepared using Photoshop CS3 or PowerPoint 2016 software.

2.4.6. Live imaging

To observe FUS aggregate formation dynamically, SH-SY5Y cells were plated on glass-bottomed culture dishes (Mattek) and transfected with a plasmid expressing GFP-tagged FUS R522G. After 24 h, cells were transfected with poly(I:C) before the live imaging. Imaging was conducted under a Leica TCS SP2 MP confocal microscope using Fluotar L 63 x 1.4 oil objective. Cells were maintained in the HEPES-buffered medium, and kept in the on-scope incubator during the imaging for temperature control. A stack of images were taken every 7 min for 12 hours, deconvoluted and compiled into a movie using Leica Application Suite AF software.

2.5. Data analysis

Statistical analysis was performed using GraphPad Prism 7 software. Distribution of normality was tested using D'Agostino & Pearson normality test, and when $p>0.05$, the corresponding data set is considered to be normal distribution. For the comparison of two data sets with normal distribution, the Student's t test was used to compare their means, and for the comparison of three or more data sets with normal distribution, the One-way ANOVA test and Tukey's multiple comparison test were used. For the data sets that failed to pass the normality test, non-parametric tests were performed instead. For two data sets comparison, Mann-Whitney U test was used, whereas for three or

more data sets comparison, Kruksal-Wallis test and Dunn’s multiple comparison test were used. The specific statistical tests used for each data set were indicated in the figure legends.

Chapter 3. Characterisation of stable cell lines with *FUS* gene modification

3.1. Overview

Establishing cellular models that can closely recapitulate FUSopathy would be of enormous benefit in developing effective therapeutic strategies against diseases caused by FUS malfunction. Most of the cellular models that are commonly used nowadays rely on transient over-expression of mutant FUS proteins in various cell lines or primary neurons. These models recapitulate FUSopathy to some extent, and have helped provide us with valuable information on the underlying molecular mechanisms of the disease. Nevertheless, FUS protein over-abundance is certainly not a physiological feature of the cells, and therefore should be avoided when possible. Fibroblasts and iPSCs derived from patients carrying FUS mutations are good options, yet they are not readily available and relatively costly to establish and maintain. Recent advances in CRISPR/Cas9 technology allowed us to generate better cellular models that express physiological level of FUS protein through targeted *FUS* gene modification in human neuroblastoma SH-SY5Y cell line. A panel of stable sub-clones have been generated through the plasmid transfection and colony screening procedure described in the Materials and Methods chapter. These clones will be used to study pathological effects of mutant FUS protein on paraspeckles (Chapter 4) as well as potential triggers of FUSopathy (Chapter 5). This chapter aims to give detailed characteristics of each sub-clones, such as *FUS* gene sequence at the site of modification, FUS protein subcellular distribution, FUS mRNA and protein expression levels.

3.2. Results

3.2.1. Target sequence selection in the *FUS* gene

A *FUS* gene region spanning from the end of exon 14 to the end of exon 15 (Figure 3.1), which encode NLS domain of the protein, was selected for deletion. All potential CRISPR/Cas9 target sequences flanked by a NGG protospacer adjacent motif (PAM) sequence at the 3' end were screened using Feng Zhang lab's Target Finder (http://crispr.mit.edu/) within this region.

Top three or four sequences that were predicted to have the lowest chance of off-target effects on each end of the target region were shortlisted for further evaluation. All possible editing outcomes, such as changes in mRNA splicing causing transcript degradation and consequent protein modifications, generated by each combination of upstream and downstream target sequences were examined, under the assumption that Cas9 would cleave 3-4 nt upstream of PAM sequence and minor errors may occur during non-homologous end joining (NHEJ) DNA repair process. One pair of sequences that showed the highest possibility to generate the desired deletion was finally selected (Figure 3.1).

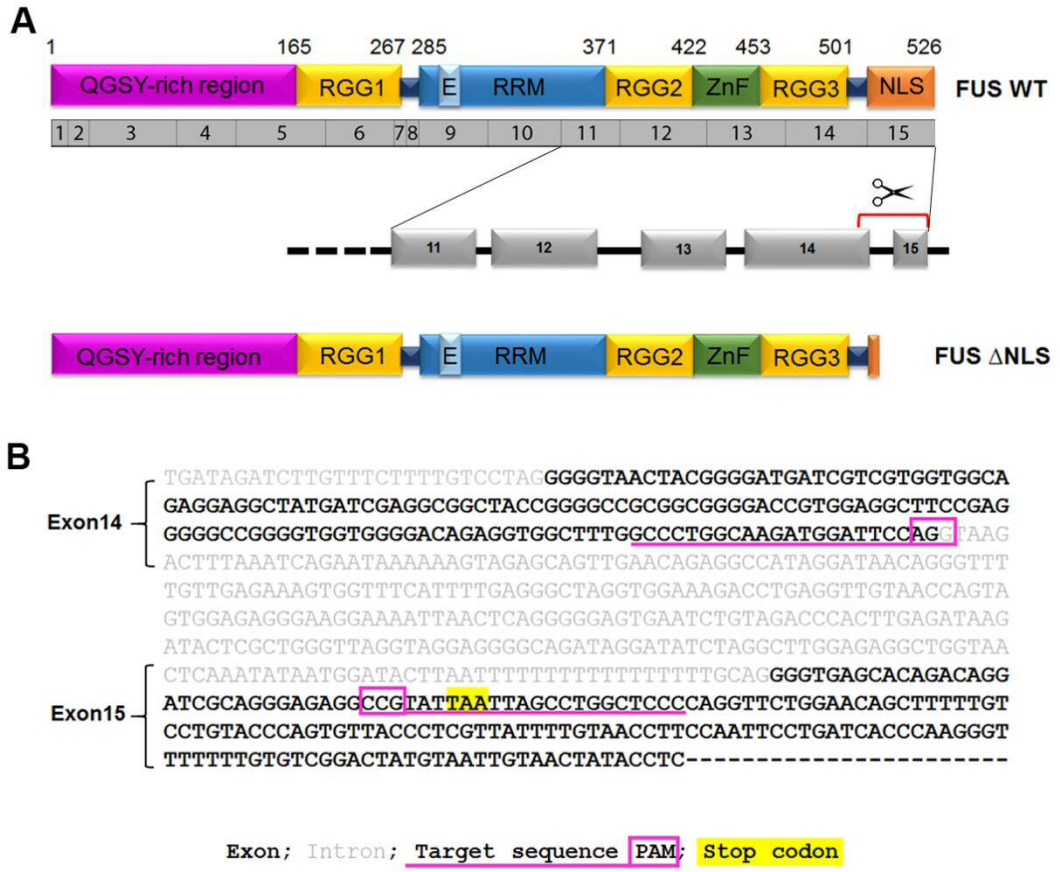

Figure 3.1 Selection of the CRISPR/Cas9 target sequences in the *FUS* gene.

A) Schematic illustration of the editing strategy for the deletion of the NLS domain of FUS protein. A grey bar under FUS WT protein diagram shows *FUS* gene exons corresponding to protein domains. *FUS* gene region targeted for deletion is indicated with a red line. **B)** Partial *FUS* gene sequence with gRNA target sequences is indicated. Exons and introns are in bold and regular letters, respectively; target

sequences are marked with pink lines; PAM sequences are boxed; stop codon is highlighted in yellow.

3.2.2. *FUS* gene sequences and predicted protein sequences of stable clones

The region of the *FUS* gene spanning the sites of gene modification was amplified from the genomic DNA extracted from all stable ΔNLS clones (Figure 3.2A). The pair of primers used for PCR should produce a fragment of 595 bp from WT *FUS* gene, whereas the edited form of FUS, only when the gene editing worked as expected, should give rise to an amplicon of 265 bp. According to the PCR results, most of the clones appeared to be 'heterozygous', where only one copy of *FUS* gene has been edited (Figure 3.2B). Two clones, ΔNLS4 and ΔNLS7, were homozygous, with both of *FUS* alleles edited. Figure 3.2C shows RNA sequencing result, which was carried out later in the project on a panel of selected clones. Compared to the WT cells, ΔNLS8 heterozygous clone had a significantly decreased number of reads in exons 14 and 15, which corresponded to the deletion area, whereas in ΔNLS4 homozygous clone, almost no reads were present in this region. Two clones, ΔNLS5 and ΔNLS10, did not show the shorter fragment in the PCR. This is explained in Figure 3.4 below. These clones were obtained during the sub-cloning of 'mixed clones', which showed the shorter fragment in the initial round of PCR screening, but appeared to be mixtures of two or more clones with different FUS protein subcellular localisation pattern by immunostaining; presumably they originated from two or more cells with different gene modifications. The 'mixed clones' were passed through the single-cell selection procedure again, and the sub-clones were screened by FUS immunostaining to identify 'pure' clones. ΔNLS5 and ΔNLS10 clones were obtained in this immunostaining screening process.

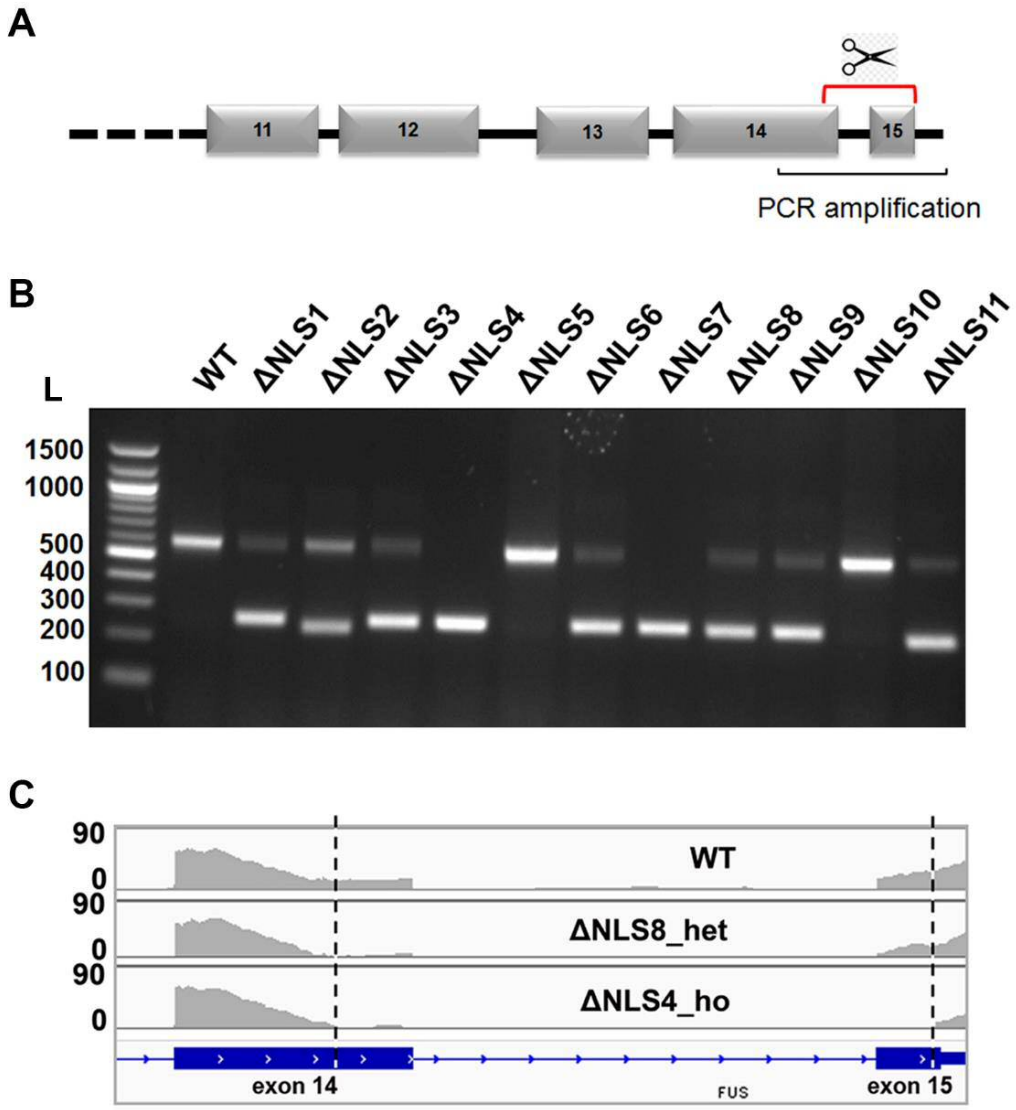

Figure 3.2 Validation of the *FUS* gene editing.

A pair of primers flanking the region to be deleted was used to amplify *FUS* gene from a series of single cell-derived stable ΔNLS clones. **A)** A fragment of human *FUS* gene is given with the region to be deleted indicated using a red line. The *FUS* gene region amplified in the PCR is indicated with a black line. **B)** An agarose gel image showing results of PCR screening in all ΔNLS clones. Clones were named according to the order of establishment. L, DNA ladder. **C)** RNA sequencing result for selected clones. The deleted region is indicated with two vertical dashed lines on both ends. Y axis indicates the number of reads.

Sequencing of the PCR fragments (both long and short) revealed the exact outcome of the *FUS* gene modifications, which covered a diverse range of results that could arise during DNA recovery through the NHEJ pathway (Figure 3.3). The most frequent result was the removal of the intermediate sequence and direct joining of exons 14 and 15, and this accounted for 50% (11/22) of all outcomes. Among these cases, small indels of single or multiple nucleotides could be found at the junction at the frequency of 27% (3/11). For example, in ΔNLS8 allele 2, a single nucleotide adenosine (A) was deleted at the junction; in ΔNLS2 allele 2, 20 nucleotides were missing from the junction (Figure 3.4). In about 18% (4/22) of all alleles sequenced, small indels at the upstream and/or downstream Cas9 cleavage sites were the only modifications that could be found in the region ("scarring"), such as allele 2 of ΔNLS5 clone, where a 2-nucleotide insertion and a 4-nucleotide deletion were found at the upstream and downstream Cas9 cleavage sites, respectively (Figure 3.4). About 14% of alleles (3/22) showed the re-insertion of the excised fragment but in the opposite orientation, such as ΔNLS1 allele 2, where the fragment between the two target sites to be deleted was inverted and re-inserted to its original site (Figure 3.4). Due to the undesirable DNA repair outcomes described above, different degrees of frameshifts were caused in most cases, and therefore a stretch of novel amino acids ('tail') with FUS-unrelated sequence was added to the C-terminus of FUS protein, replacing its normal NLS sequence. Only four clones out of 11 (ΔNLS2, ΔNLS8, ΔNLS10 and ΔNLS11) were confirmed to be true heterozygotes by sequencing (Figure 3.4).

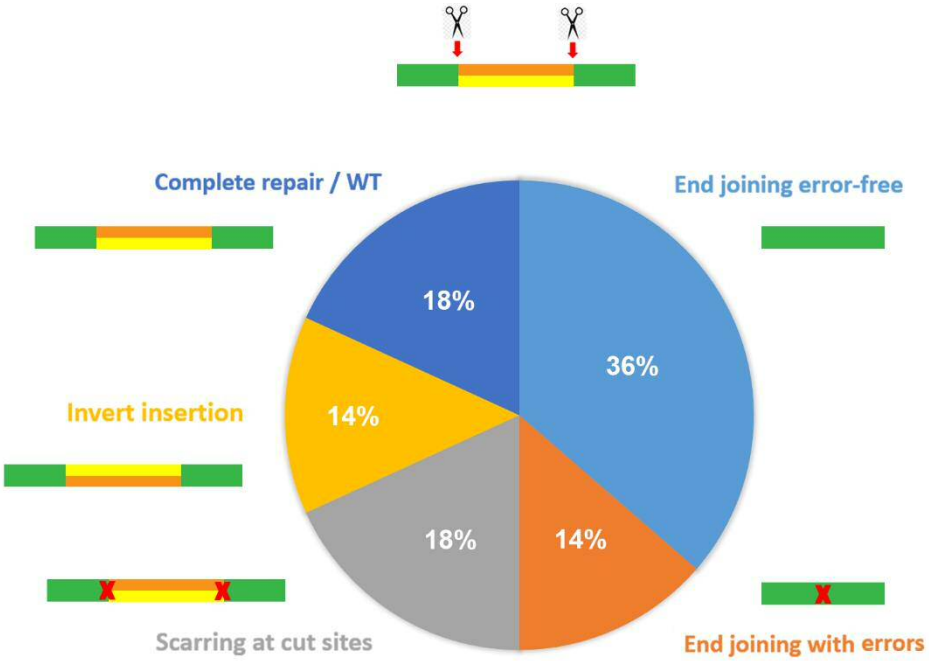

Figure 3.3 A summary of the outcomes of *FUS* gene modification in ΔNLS clones.

This summary is from a total of 11 FUS ΔNLS clones (22 FUS alleles) analysed. The red arrows indicate Cas9 cleavage sites. DNA fragment between two arrows is coloured in orange and yellow in order to distinguish between top and bottom strands. The red crosses indicate small indel mutations.

WT FUS gene sequence

```
GCGGCGGGGACCGTGGAGGCTTCCGAGGGGGCCGGGGTGGTGGGGACAGAGGTGGCTTTG
GCCCTGGCAAGATGGATTCCAGGTAAGACTTTAAATCAGAATAAAAAAGTAGAGCAGTTG
AACAGAGGCCATAGGATAACAGGGTTTTGTTGAGAAAGTGGTTTCATTTTGAGGGCTAGG
TGGAAAGACCTGAGGTTGTAACCAGTAGTGGAGAGGGAAGGAAAATTAACTCAGGGGGAG
TGAATCTGTAGACCCACTTGAGATAAGATACTCGCTGGGTTAGGTAGGAGGGGCAGATAG
GATATCTAGGCTTGGAGAGGCTGGTAACTCAAATATAATGGATACTTAATTTTTTTTTTT
TTTTTTGCAGGGGTGAGCACAGACAGGATCGCAGGGAGAGGCCGTATTAATTAGCCTGGC
TCCCCAGGTTCTGGAACAGCTTTTTG----------TCGATGTCCCGATCAGGAAGG
```

ΔNLS1 clone FUS gene sequence allele 1

```
GCGGCGGGGACCGTGGAGGCTTCCGAGGGGGCCGGGGTGGTGGGGACAGAGGTGGCTTTG
GCCCTGGCAAGATGGATTAATTAGCCTGGCTCCCCAGGTTCTGGAACAGCTTTTTG----
---------TCGATGTCCCGATCAGGAAGG
```

ΔNLS1 clone FUS gene sequence allele 2

```
GCGGCGGGGACCGTGGAGGCTTCCGAGGGGGCCGGGGTGGTGGGGACAGAGGTGGCTTTG
GCCCTGGCAAGATGGATATACGGCCTCTCCCTGCGATCCTGTCTGTGCTCACCCCTGCAA
AAAAAAAAAAAAAAATTAAGTATCCATTATATTTGAGTTACCAGCCTCTCCAAGCCTAGA
TATCCTATCTGCCCCTCCTACCTAACCCAGCGAGTATCTTATCTCAAGTGGGTCTACAGA
TTCACTCCCCCTGAGTTAATTTTCCTTCCCTCTCCACTACTGGTTACAACCTCAGGTCTT
TCCACCTAGCCCTCAAAATGAAACCACTTTCTCAACAAAACCCTGTTATCCTATGGCCTC
TGTTCAACTGCTCTACTTTTTTATTCTGATTTAAAGTCTTACCTGGATAATTAGCCTGGC
TCCCCAGGTTCTGGAACAGCTTTTTG----------TCGATGTCCCGATCAGGAAGG
```

ΔNLS2 clone FUS gene sequence allele 1 (WT)

WT FUS protein sequence

```
MASNDYTQQA.....FRGGRGGGDRGGFGPGKMDSRGEHRQDRRERPY*
▲                                ▲                ▲
1                               512              526
```

Predicted mutant FUS protein sequence

```
MASNDYTQQA.....FRGGRGGGDRGGFGPGKMD*
▲                                ▲
1                               512
```

```
MASNDYTQQA.....FRGGRGGGDRGGFGPGKMDIRPLPAILSVLTPA
▲                                ▲
1                               512
KKKKKIKYPLYLSYQPLQA*
                 ▲
                545
```

ΔNLS2 clone FUS gene sequence allele 2

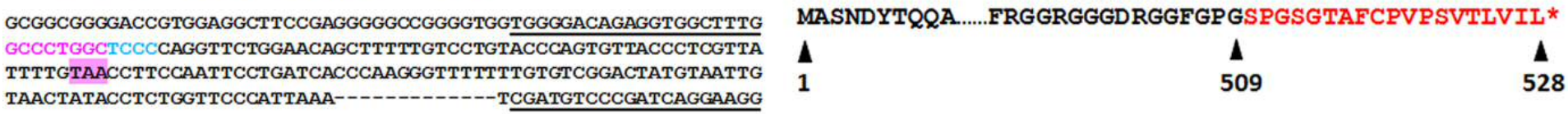

ΔNLS3 clone FUS gene sequence allele 1 (same as ΔNLS1 allele 1)

ΔNLS3 clone FUS gene sequence allele 2

ΔNLS4 clone FUS gene sequence allele 1

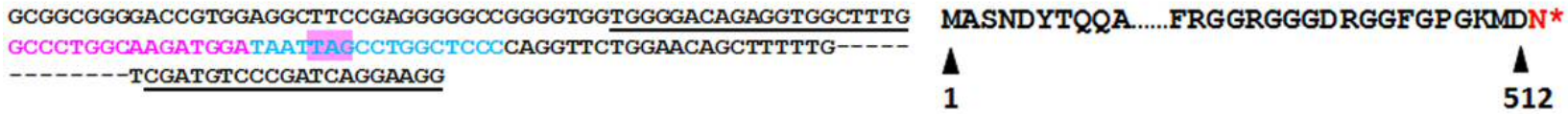

ΔNLS4 clone FUS gene sequence allele 2 (same as ΔNLS1 allele 1)

ΔNLS5 clone FUS gene sequence allele 1 (same as ΔNLS3 allele 2)

ΔNLS5 clone FUS gene sequence allele 2

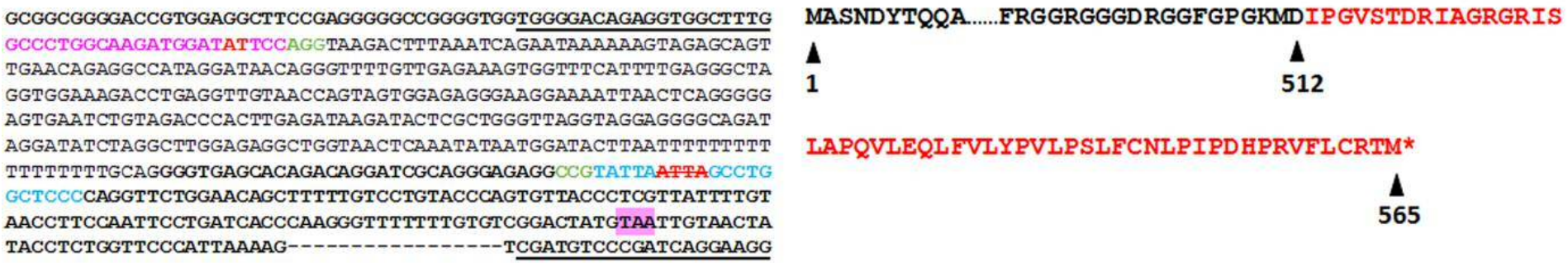

ΔNLS6 clone FUS gene sequence allele 1 (same as ΔNLS4 allele 1)

ΔNLS6 clone FUS gene sequence allele 2 (same as ΔNLS1 allele 2)

ΔNLS7 clone FUS gene sequence allele 1 (same as ΔNLS4 allele 1)

ΔNLS7 clone FUS gene sequence allele 2 (same as ΔNLS4 allele 2)

ΔNLS8 clone FUS gene sequence allele1 (WT)

ΔNLS8 clone FUS gene sequence allele 2

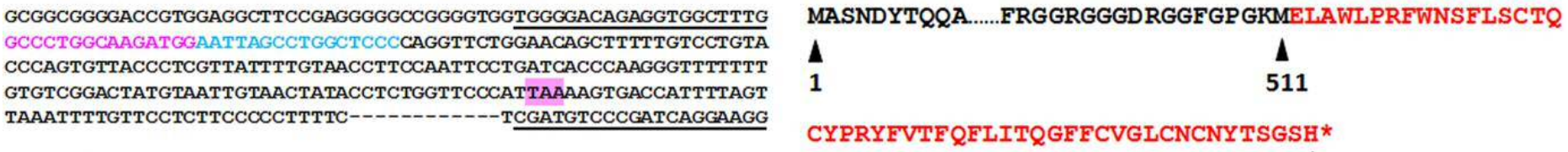

ΔNLS9 clone FUS gene sequence allele 1 (same as ΔNLS4 allele 1)

ΔNLS9 clone FUS gene sequence allele 2

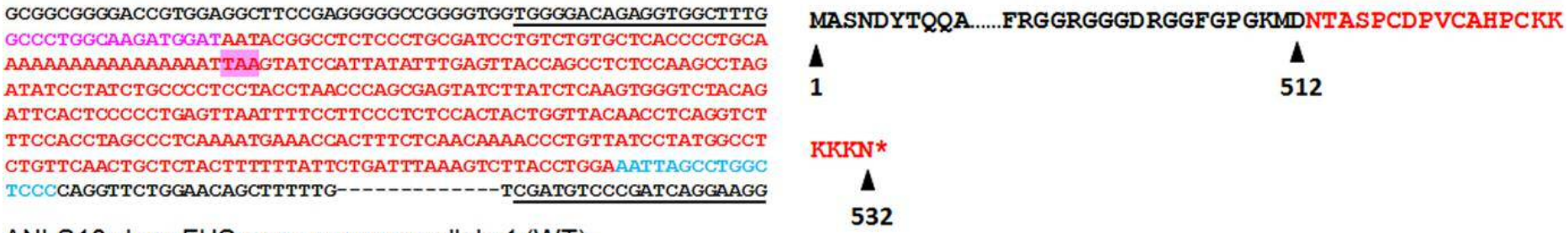

ΔNLS10 clone FUS gene sequence allele 1 (WT)

ΔNLS10 clone FUS gene sequence allele 2

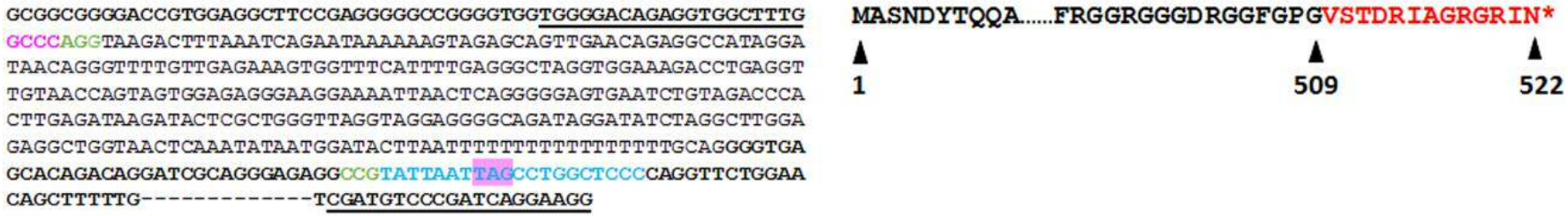

ΔNLS11 clone FUS gene sequence allele 1 (WT)

ΔNLS11 clone FUS gene sequence allele 2 (same as ΔNLS2 allele 2)

Figure 3.4 Partial *FUS* gene sequences of all the ΔNLS clones and their predicted protein sequences.

WT *FUS* gene sequence of the same region and partial WT FUS protein sequence are given for comparison. Exons are in bold letters and introns are in regular letters. Upstream and downstream CRISPR/Cas9 target sequences are in pink and blue respectively, and PAM sequences are in green. Original stop codons are highlighted in yellow, and the alternative stop codons in pink. Single or double nucleotide insertions are indicated using red letters (e.g. ΔNLS3 allele 2), and nucleotides deletions are indicated with red letters with a strikethrough (e.g. ΔNLS5 allele 2). Re-insertion of excised fragments inverted is indicated with red letters (e.g. ΔNLS1 allele 2). Primers used for PCR are underlined. Novel peptide sequences caused by the frameshift are indicated using red letters. Numbers below the protein sequence indicate the order of the amino acid pointed on the FUS protein. Asterisks mark the end of the protein sequence.

In addition to FUS ΔNLS clones, a FUS KO clone was also generated. This clone is obtained during my initial attempt to generate clones expressing mutant FUS proteins with larger FUS C-terminal truncation, which removes all domains downstream of RRM (protein domain see Figure 3.1). For this, target sequences were selected on exon 11 and exon 15. However this attempt did not yield cells with desired modification. Instead, I obtained a clone expressing no visible FUS protein either by immunostaining or by western blot. Sequencing of the target site on exon 11 revealed that both alleles in the FUS KO clone have a single nucleotide insertion at the Cas9 cleavage site, which was inserted during the DSB repair through the NHEJ pathway. This caused frameshift and therefore a pre-mature stop codon on exon 11 (Figure 3.5A), which eventually led to FUS mRNA degradation through the NMD pathway. It should be noted that modified FUS mRNAs in ΔNLS clones, such as ΔNLS1 allele 2, also possess a pre-mature stop codon, but escaped NMD surveillance and produce mutant proteins (Figure 3.4). Figure 3.5B illustrates the mechanism underlying this discrepancy. NMD is triggered when a pre-mature stop codon is found upstream of the last exon-exon junction. In contrast, when no exon-exon junction is present downstream of a pre-mature stop codon, the mRNA is regarded as normal. In FUS KO clone, FUS mRNA was degraded because its pre-mature stop codon was located upstream of the last stop codon. However, in ΔNLS1 clone, mRNA was preserved because the last exon-exon junction (between exons 14 and 15) was destroyed due to the intron14 retention, which rendered the pre-mature stop codon to be located downstream to the last exon-exon junction (between exon 13 and 14).

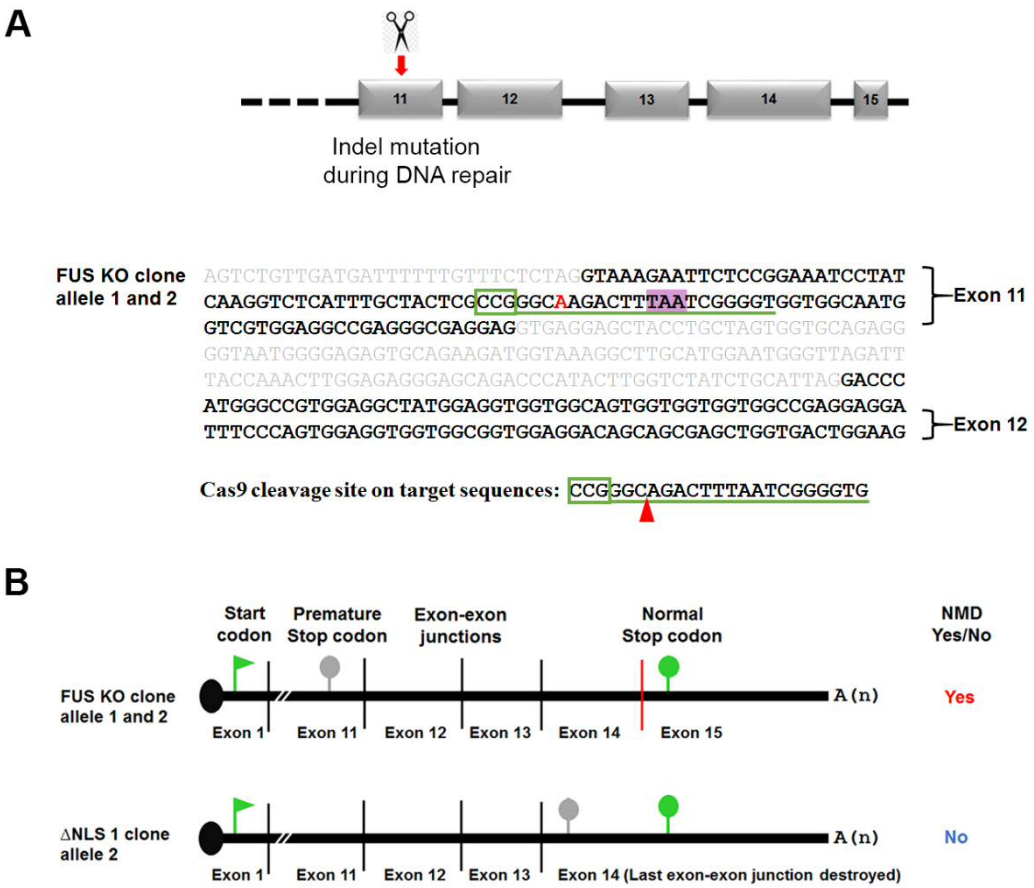

Figure 3.5 Generation of the FUS KO clone using CRISPR/Cas9 gene editing.

A) Sequencing across the CRISPR target site in exon 11 of *FUS* gene of the FUS KO clone revealed an indel mutation on the Cas9 cleavage site, which caused a frameshift and therefore mRNA degradation. Single nucleotide insertion is indicated in red, and the pre-mature stop codon is highlighted in pink. CRISPR/Cas9 target sequence in underlined and the PAM sequence is boxed. **B)** A schematic illustration describing the mechanism underlying the selective degradation of FUS mRNA through NMD in FUS KO clone, but not in certain ΔNLS clones that also possess pre-mature stop codons. Vertical lines indicate exon-exon junctions, and the last exon-exon junction is marked in red. Green flag and green pin indicate start codon and normal stop codon, respectively. Grey pin indicates premature stop codon. The red vertical line indicates the last exon-exon junction.

3.2.3. FUS protein subcellular distribution

Distribution of FUS in all clones was visualised using an antibody detecting the N-terminus of the protein (Abcam). While FUS was mainly detectable in the nucleus in WT SH-SY5Y cells, mutant FUS in heterozygous clones (ΔNLS_het hereafter) exhibited mild to moderate cytoplasmic mislocalisation (Figure 3.6 upper panel). Compared to ΔNLS_het clones, homozygous clones (ΔNLS_ho hereafter) displayed more pronounced FUS cytoplasmic mislocalisation (Figure 3.6 lower panel). In line with the previous report, where cytoplasmic FUS showed strong affinity to SGs (Dormann *et al.* 2010), mutant FUS in these clones was also readily recruited into SGs induced by sodium arsenite (SA) (Figure 3.7). Although in the majority of the clones, mutant FUS showed diffuse distribution in the cytoplasm, in ΔNLS2_het and ΔNLS11_het clones, spontaneously assembled small FUS granules (FGs) could be seen (Figure 3.6 inset). No FUS immunoreactivity was detected in the FUS KO clone.

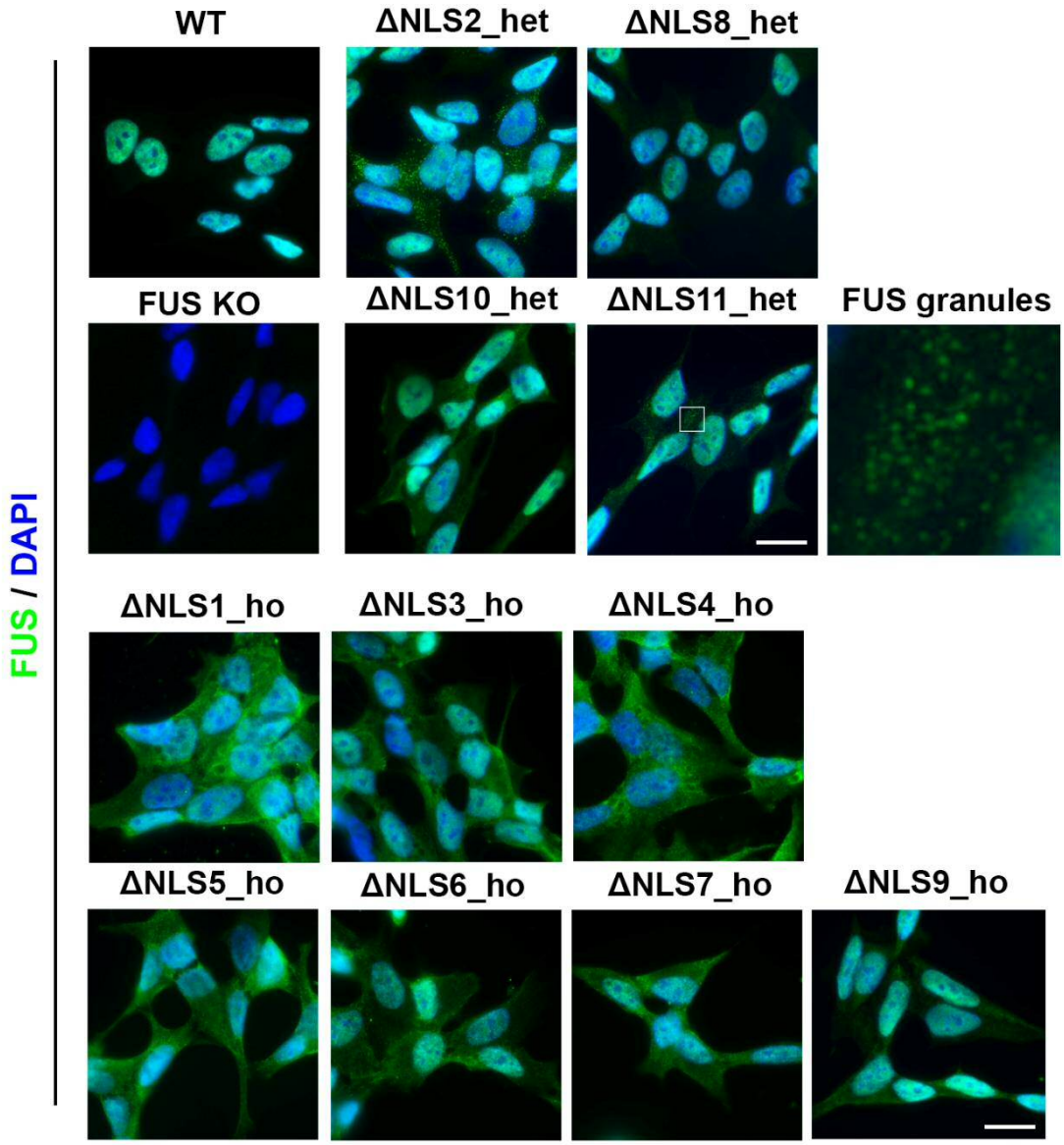

Figure 3.6 FUS immunostaining in FUS mutant clones.

ΔNLS_het clones show mild to moderate degree of FUS cytoplasmic mislocalisation, and ΔNLS_ho clones exhibit severe FUS redistribution. Two ΔNLS_het clones, ΔNLS2 and ΔNLS11, developed spontaneous cytoplasmic FUS granules (FGs). No FUS immunoreactivity was detectable in the FUS KO clone. FUS was visualised using an antibody against N-terminus of the protein. Scale bar is 10 μm.

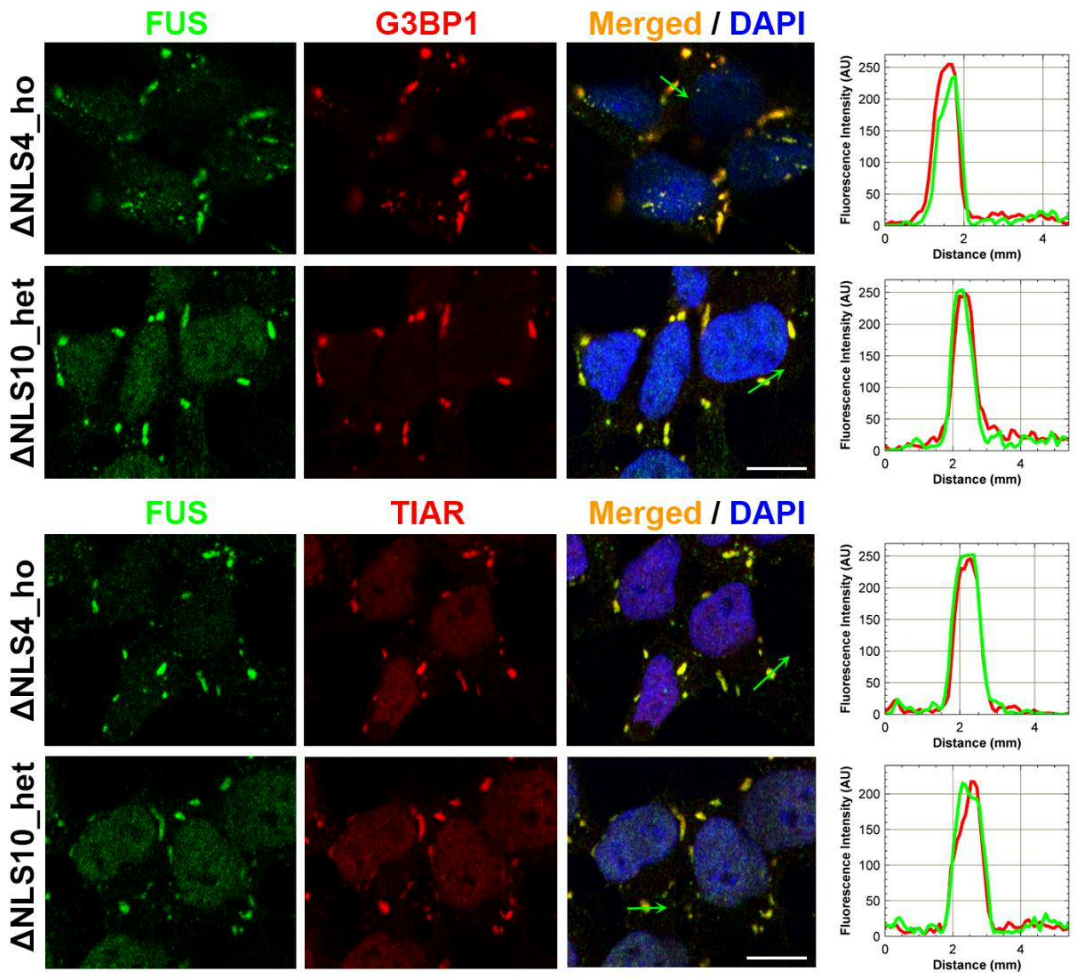

Figure 3.7 Cytoplasmically mislocalised FUS protein is recruited into stress granules formed under oxidative stress.

Confocal microscope images showing colocalisation of cytoplasmic FUS and SG marker proteins, G3BP1 and TIAR, in cells treated with sodium arsenite for 1 h. FUS was visualised with an antibody against N-terminus of the protein. Profile plots generated along the green arrows in merged images show almost complete colocalisation of FUS and SG proteins. Scale bars are 10 μm.

3.2.4. FUS mRNA expression

Two pairs of primers were designed to measure total FUS and WT FUS mRNA expression level in the clones by qPCR (Figure 3.8A). In the majority of ΔNLS clones, both heterozygotes and homozygotes, total FUS expression was increased by ~1.5-fold compared to WT cells. Since *FUS* expression is subject to autoregulation (Zhou *et al.* 2013), this increase is presumably resulted from FUS autoregulation to make up for the nuclear deficiency caused by protein mislocalisation. However, there were exceptions – ΔNLS8_het, ΔNLS7_ho and ΔNLS9_ho clones displayed slightly lower FUS mRNA levels, possibly because modified mRNAs in these clones might have shorter half-lives due to certain sequences within them (Figure 3.8B, left). When measuring the levels of WT FUS mRNA only, the result was in agreement with total FUS mRNA levels. Heterozygotes only have one copy of WT gene, hence they should produce half the amount of WT FUS mRNA compared to that in WT cells; whereas homozygotes clones should produce no WT FUS mRNA since they do not possess WT alleles. However, as described above, many alleles still carry the intermediate fragment after gene modification, and the retained fragment has the WT FUS primer-binding site. Figure 3.8C summarises data of the clones that have the intermediate fragment, and it explains the unusually high levels of 'WT' FUS mRNA in ΔNLS10_het, ΔNLS3_ho and ΔNLS5_ho clones (Figure 3.8B, right). Residual amount of FUS mRNA was still detectable in FUS KO clone despite the absence of detectable FUS protein (Figure 3.6, Figure 3.9).

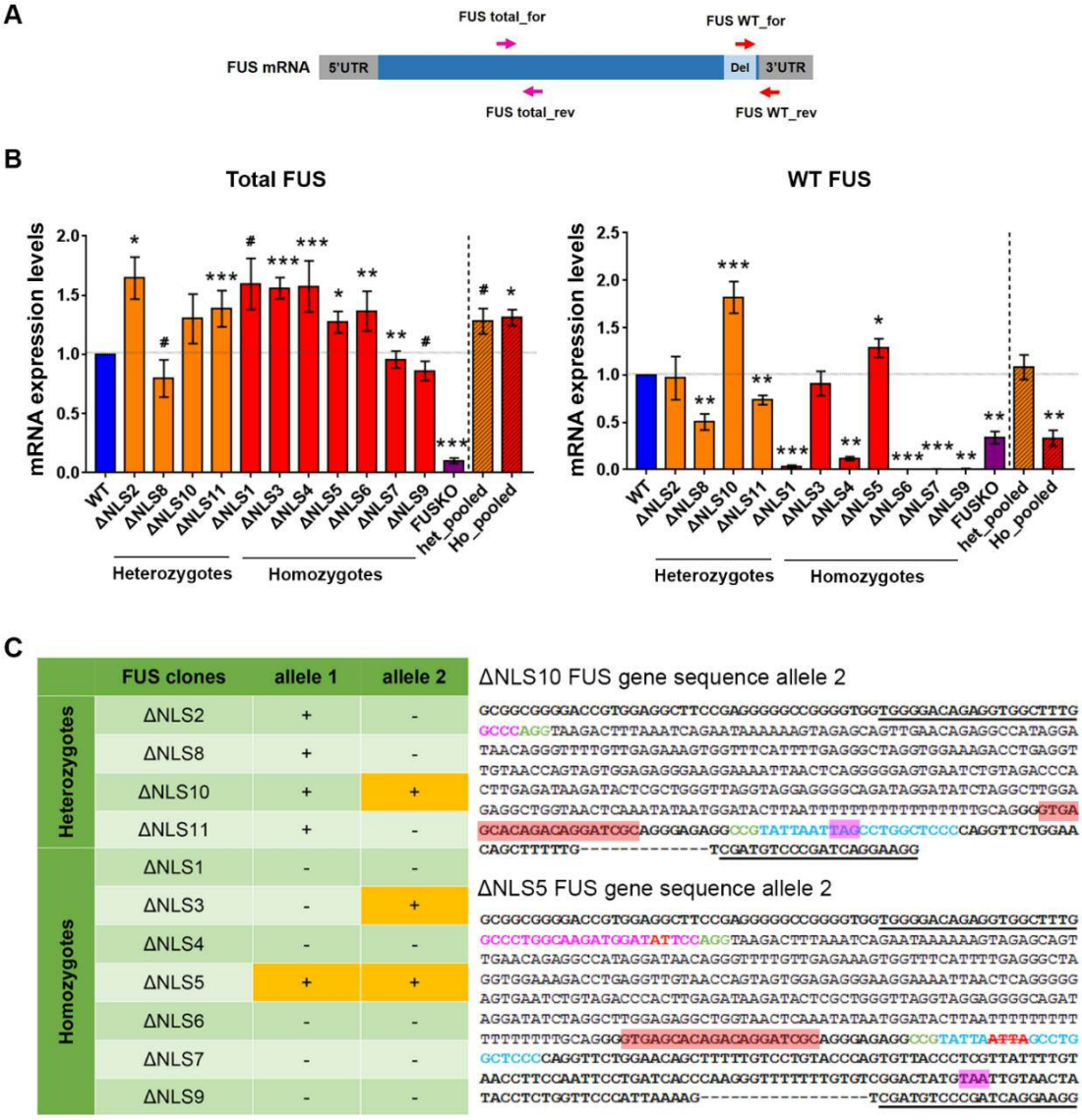

	FUS clones	allele 1	allele 2
Heterozygotes	ΔNLS2	+	-
	ΔNLS8	+	-
	ΔNLS10	+	+
	ΔNLS11	+	-
Homozygotes	ΔNLS1	-	-
	ΔNLS3	-	+
	ΔNLS4	-	-
	ΔNLS5	+	+
	ΔNLS6	-	-
	ΔNLS7	-	-
	ΔNLS9	-	-

ΔNLS10 FUS gene sequence allele 2

GCGGCGGGGACCGTGGAGGCTTCCGAGGGGGCCGGGGTGGTGGGGACAGAGGTGGCTTTG
GCCCAGGTAAGACTTTAAATCAGAATAAAAAAGTAGAGCAGTTGAACAGAGGCCATAGGA
TAACAGGGTTTTGTTGAGAAAGTGGTTTCATTTTGAGGGCTAGGTGGAAAGACCTGAGGT
TGTAACCAGTAGTGGAGAGGGAAGGAAAATTAACTCAGGGGGAGTGAATCTGTAGACCCA
CTTGAGATAAGATACTCGCTGGGTTAGGTAGGAGGGGCAGATAGGATATCTAGGCTTGGA
GAGGCTGGTAACTCAAATATAATGGATACTTAATTTTTTTTTTTTTTTTGCAGGGTGA
GCACAGACAGGATCGCAGGGAGAGGCCGTATTAATTAGCCTGGCTCCCCAGGTTCTGGAA
CAGCTTTTTG----------TCGATGTCCCGATCAGGAAGG

ΔNLS5 FUS gene sequence allele 2

GCGGCGGGGACCGTGGAGGCTTCCGAGGGGGCCGGGGTGGTGGGGACAGAGGTGGCTTTG
GCCCTGGCAAGATGGATATTCCAGGTAAGACTTTAAATCAGAATAAAAAAGTAGAGCAGT
TGAACAGAGGCCATAGGATAACAGGGTTTTGTTGAGAAAGTGGTTTCATTTTGAGGGCTA
GGTGGAAAGACCTGAGGTTGTAACCAGTAGTGGAGAGGGAAGGAAAATTAACTCAGGGGG
AGTGAATCTGTAGACCCACTTGAGATAAGATACTCGCTGGGTTAGGTAGGAGGGGCAGAT
AGGATATCTAGGCTTGGAGAGGCTGGTAACTCAAATATAATGGATACTTAATTTTTTTTT
TTTTTTTTGCAGGGGTGAGCACAGACAGGATCGCAGGGAGAGGCCGTATTAATTAGCCTG
GCTCCCCAGGTTCTGGAACAGCTTTTTGTCCTGTACCCAGTGTTACCCTCGTTATTTTGT
AACCTTCCAATTCCTGATCACCCAAGGGTTTTTTTGTGTCGGACTATGTAATTGTAACTA
TACCTCTGGTTCCCATTAAAAG----------TCGATGTCCCGATCAGGAAGG

Figure 3.8 Total FUS and WT FUS mRNA levels in FUS clones measured by qPCR.

A) FUS transcript, position of deletion (del) and primer locations. (not drawn to scale; 'for' and 'rev' stand for forward and reverse primer, respectively) **B)** qPCR results for total FUS (left) and WT FUS (right) mRNA expression in clones. Bars representing ΔNLS_het and ΔNLS_ho clones are orange and red, respectively. N ≥ 4 for each clone. Data pooled from all ΔNLS_het or ΔNLS_ho clones (bars filled with diagonal pattern) are also shown. Mann-Whitney U test is used. $^{\#}p<0.01$, *p < 0.05, **p < 0.01, ***p < 0.001. **C)** A table summarises the presence of FUS WT forward primer-binding sequence in all ΔNLS clones. Alleles which possess the sequence are marked with '+'. Genetically modified alleles that still carry the WT primer binding sequence are highlighted in yellow. FUS mRNA sequences of ΔNLS10 and ΔNLS5 retaining the WT primer binding sequence (highlighted in red on the sequence). Upstream and downstream CRISPR/Cas9 target sequences are in pink and blue. PAM sequences

are in green. Indel mutations at the cleavage sites are in red letters (insertion) or in red letters with a strikethrough (deletion). Pre-mature stop codons are highlighted in pink.

3.2.5. FUS protein expression

A panel of antibodies recognising different parts of FUS protein were used to measure FUS protein expression levels and protein sizes by western blot. FUS (full, Proteintech) recognises the whole protein; FUS (NT, Abcam) recognises the first 50 amino acids on the N-terminus; FUS (mid, Santa Cruz) recognises aa. 370 -467 in the middle and FUS (CT, Bethyl) recognises the last 27 amino acids on the C-terminus. In this analysis, ΔNLS1_ho clone showed two separate bands, in line with the predicted protein sizes – 512 aa. and 545 aa (Figure 3.9A). The separation was not obvious in ΔNLS2_het clone where the size difference between the two protein products (WT protein and mutant protein with a tail) is small (526 aa. and 528 aa.)(Figure 3.9A). FUS CT antibody, which recognises the NLS domain of FUS protein, showed no immunoreactivity in ΔNLS1_ho clone, where both alleles produce FUS proteins with disrupted NLS. In ΔNLS2_het clone, FUS CT detected half of the amount of WT FUS protein (Figure 3.9A). In FUS KO cells, neither the full size FUS nor the truncated form of FUS (~ 55 KDa, assuming the modified mRNA with a pre-mature stop codon is somehow translated) were detectable (Figure 3.9A).

It has been noticed that ΔNLS_het clones often displayed mild FUS redistribution, even though half of FUS protein produced by the clones is mutated. In contrast, ΔNLS_ho clones displayed severe FUS mislocalisation, with the boundaries of the nuclei sometimes undetectable (Figure 3.9B). The extent of FUS cytoplasmic mislocalisation was quantified by measuring FUS protein levels in the cytoplasmic fraction and total lysates. The cytoplasmic/total FUS ratio was about 8 times higher in ΔNLS_ho clones than in ΔNLS_het clones (Figure 3.9C), which was different from the predicted two-fold increase. The finding suggests that the presence of non-mutated, nuclear localised FUS partially protects mutant FUS from mislocalisation to the cytoplasm.

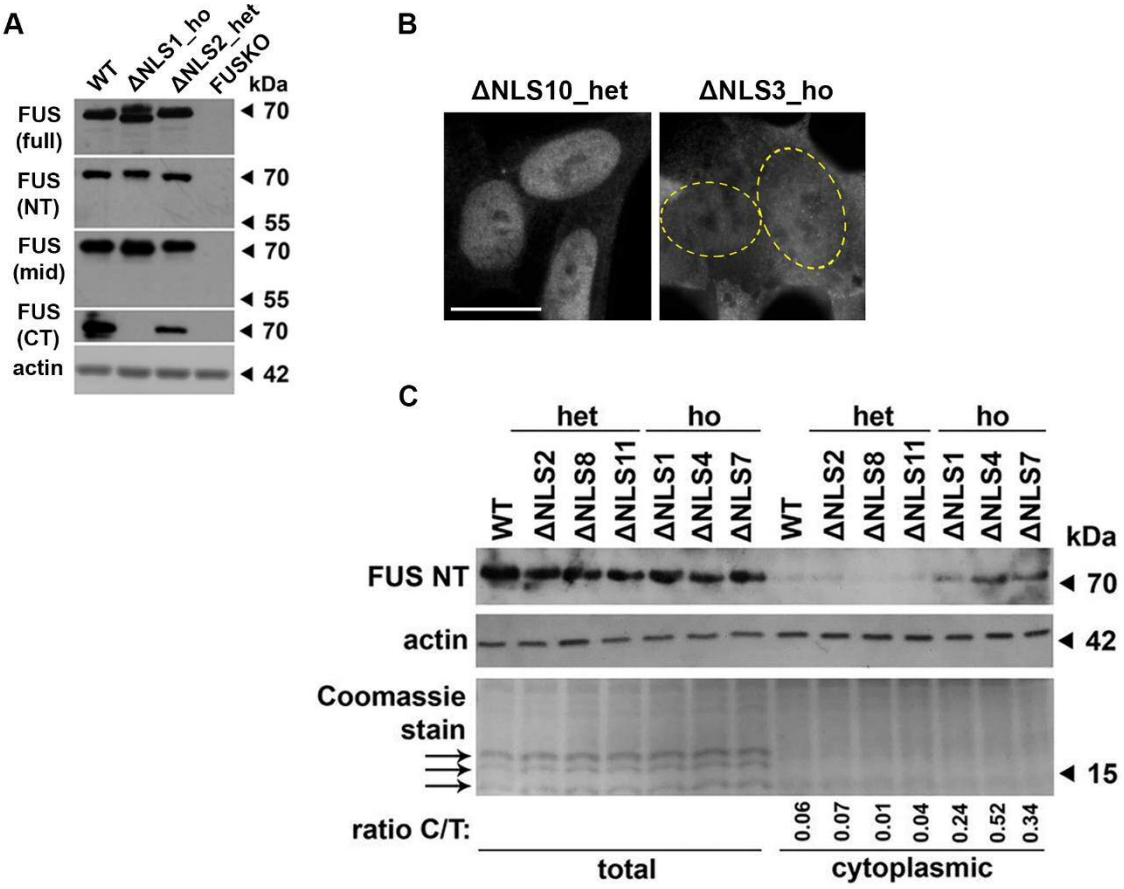

Figure 3.9 FUS protein expression levels of FUS clones measured by western blot.

A) A panel of FUS antibodies recognising different parts of FUS protein are used to detect FUS proteins. Neither WT FUS (70 KDa) nor a possible truncated form (55 KDa) is detectable in FUS KO clone using any of the antibodies. FUS (full) antibody is raised against the whole protein, whereas FUS (NT) recognises aa.1-50, FUS (CT) recognises aa.500-526, and FUS (mid) recognises aa.370-467 of FUS protein. Actin is measured as a control for equal loading. **B)** FUS distribution in representative ΔNLS_het and ΔNLS_ho clones. Nuclei border in ΔNLS_ho cells is indicated with a dashed line. Scale bar is 10 μm. **C)** FUS levels in total lysates and cytoplasmic fraction from WT and ΔNLS clones. Ratio C/T, ratio cytoplasmic to total FUS levels. Small proteins absent from the cytoplasmic fraction (arrows) may correspond to histones.

3.2.6. Characterisation of cytoplasmic granules formed by endogenous mutant FUS

Overexpressed cytoplasmic FUS protein is known to spontaneously form small granules when the protein accumulates to a certain amount in the cytoplasm (Shelkovnikova *et al.* 2014a). These granules (exogenous FGs, exoFGs hereafter), are about 150-200 nm in size and require RNA for their structural integrity. It was unknown whether mutant FUS protein expressed at the endogenous level, as in ΔNLS clones from the current study, could nucleate such FGs (endogenous FGs, endoFGs hereafter) under basal conditions. I found that their formation is indeed possible in some ΔNLS clones (Figure 3.6, Figure 3.10). The morphology of endoFGs formed in ΔNLS2_het and ΔNLS11_het clones was examined using a confocal microscope. These endoFGs were roughly spherical in shape, with the diameter ranging between 200 and 300 nm. They were evenly distributed throughout the cytoplasm without obvious clustering (Figure 3.10A) and were negative for core SG proteins G3BP1 or TIAR (Figure 3.10B, C).

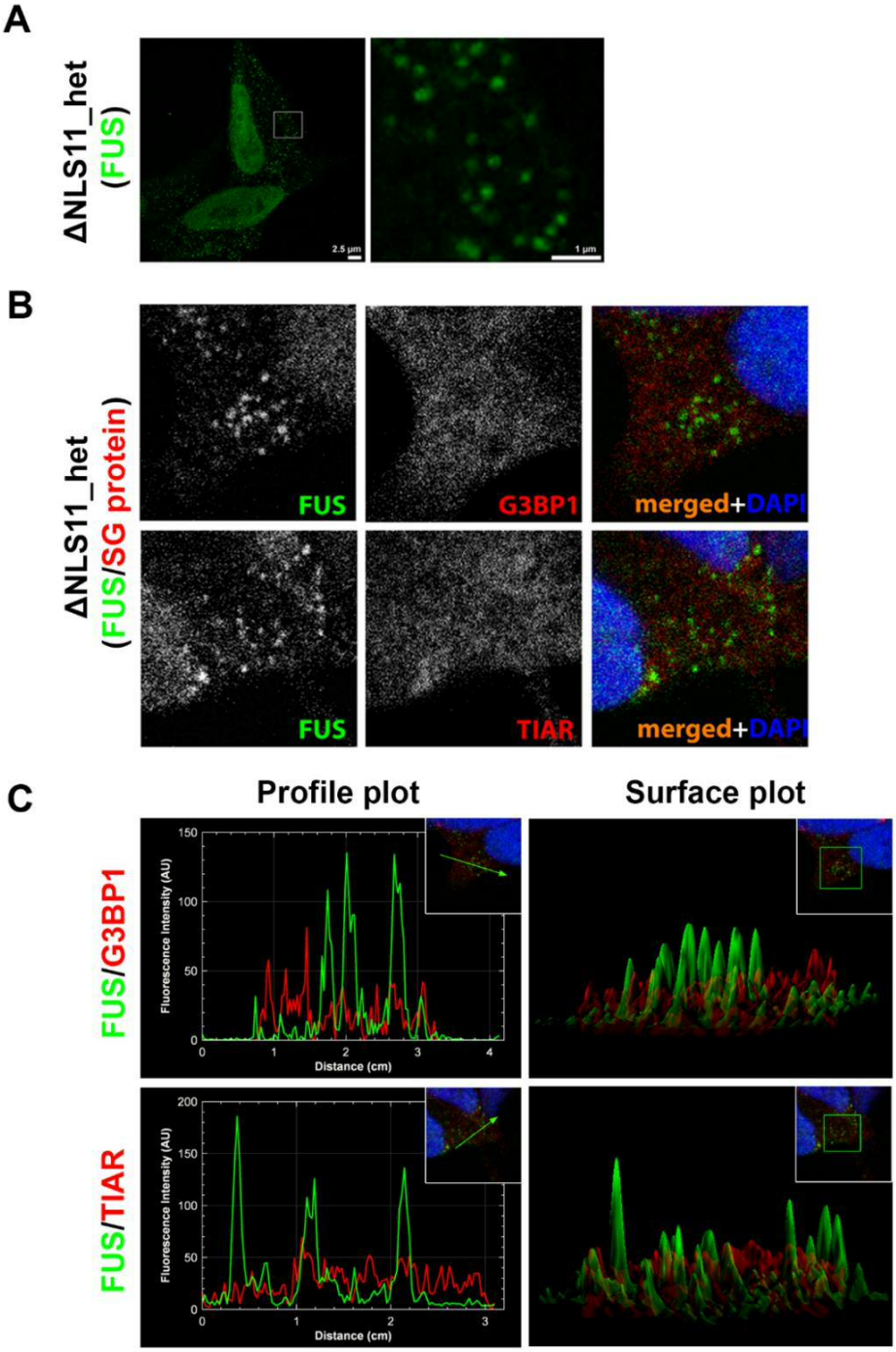

Figure 3.10 FUS granules (endoFGs) in ΔNLS clones are negative for stress granule markers.

A) Confocal microscopy images of endoFGs in ΔNLS11_het clone visualised using FUS N-terminus antibody. On the right, is the enlarged image of the inset. **B)** Single optical sections of confocal images of endoFGs showing that they do not colocalise with either G3BP1 or TIAR. **C)** Profile plots and surface plots are generated from the confocal images in B. Both plots confirm non-overlapping signal distribution between FUS and SG proteins.

RNA has been suggested to be essential for the integrity of exoFGs and similar structures containing FUS, such as transport granules (Kanai *et al.* 2004, Shelkovnikova *et al.* 2014a). I tested whether endoFGs are also sensitive to RNA depletion. Indeed, when ΔNLS11_het cells were exposed to the global transcription inhibitor actinomycin D for 18 h, endoFGs disassembled into smaller particles (Figure 3.11A) as evidenced by the increased granule numbers and significantly decreased average sizes (Figure 3.11B). No further changes were observed in granule numbers and sizes upon prolonged transcription inhibition (Figure 3.11A, B).

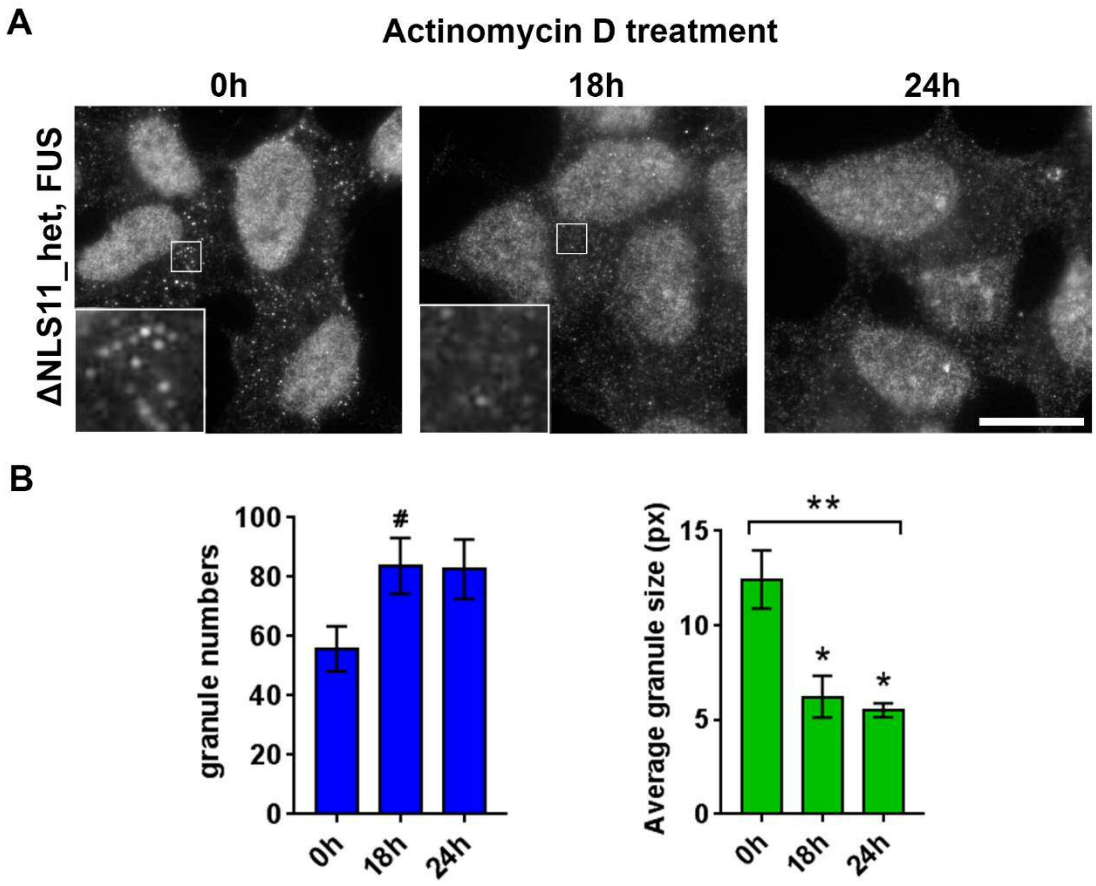

Figure 3.11 RNA is required for the integrity of endoFGs.

A) Immunostaining of endoFG-containing ΔNLS11_het clone treated with actinomycin D for the indicated period of time using FUS antibody detecting middle region of FUS. A representative region of each image is enlarged. Scale bar is 10 μm. **B)** EndoFG numbers and their average sizes are quantified for each time point using Analyze Particles function of image J (6~8 cells). Kruskal-Wallis test and Dunn's multiple comparison tests are used. #p=0.1, *p<0.05, **p=0.001.

3.2.7. Differentiation of FUS clones into neuron-like cells

Next, SH-SY5Y clones with the endogenous *FUS* gene modified were differentiated into neuron-like cells using retinoic acid and brain-derived neurotrophic factor (BDNF). All clones were shown to express high levels of beta III tubulin, the post-mitotic neuron marker, and display neuron-like morphology, with a small, round cell body and, long processes (Figure 3.12). This result suggested that targeted modification of the *FUS* gene and subsequent single-cell cloning process did not affect their capability to differentiate. Differentiated ΔNLS cells still preserved original FUS subcellular localisation pattern, and ΔNLS2_het clone still had FGs in the cytoplasm after differentiation.

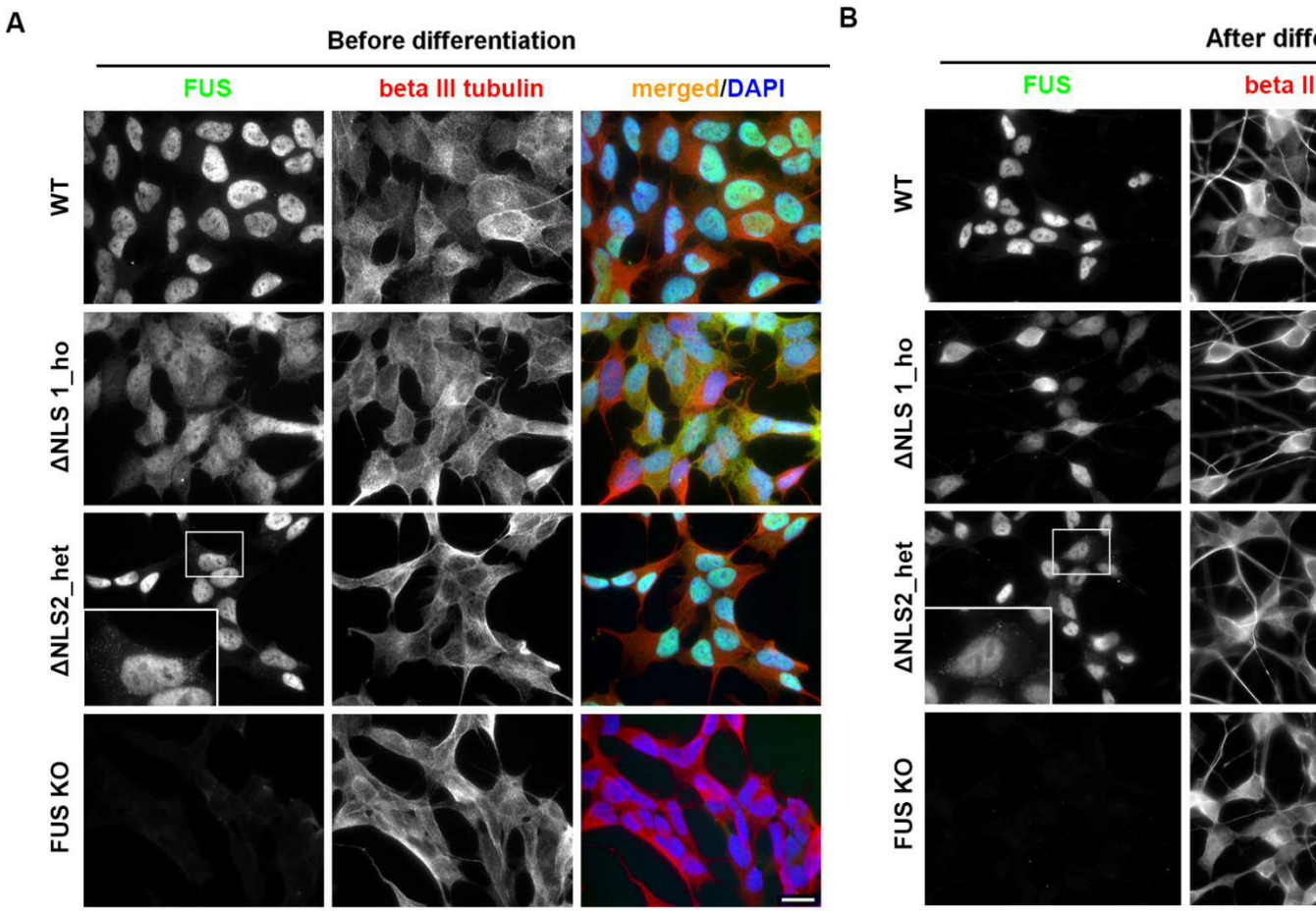

Figure 3.12 FUS clones can be differentiated into neuron-like cells.

A) Co-staining for FUS and beta III tubulin of FUS clones before (A) and after (B) differentiation. Scale bars a

3.3. Discussion

Cellular models established by overexpression of mutant FUS have been widely used to address many questions regarding the roles of mutant FUS protein in the development of FUSopathy. However, the reliability of these models is sometimes questioned because protein overexpression *per se* can trigger many undesirable effects. For example, protein overexpression causes resource overload within the cell by monopolising cellular machinery and molecules required for protein synthesis and turnover. Furthermore, overexpression of regulatory proteins can cause promiscuous interaction and abnormal pathway modulation (Moriya 2015). Indeed, it has been proven that overexpression of otherwise benign proteins is sufficient to cause detrimental effects on cellular functions and growth (Makanae *et al.* 2013, Tomala and Korona 2013). Therefore, cellular models expressing endogenous levels of mutant FUS protein will be extremely valuable for studying FUSopathy in a more physiological context.

Here I successfully established a panel of single cell-derived stable clones expressing physiological levels of mutant FUS protein lacking NLS (ΔNLS) as well as a clone that is devoid of FUS expression (FUS KO), by directly modifying *FUS* gene in human neuroblastoma SH-SY5Y cells using CRISPR/Cas9 gene editing. Primary characterisation of the clones has allowed the establishment of the *FUS* gene editing outcomes including changes in gene sequence, expression levels and subcellular localisation of mutant proteins. As I have expressed Cas9 in the cells without a repair template, DSBs created were repaired through the NHEJ DNA repair pathway, which often introduces small indels at the repair sites (Lieber 2010, Hsu *et al.* 2014). This error-prone nature of NHEJ has been exploited to create the FUS KO clone, where a single nucleotide was inserted at the repair site, inducing mRNA decay due to the ORF frameshift. However, when it comes to the precise deletion of the region encoding the NLS, repair errors become disadvantageous, as in nearly half of the alleles sequenced, highly heterogeneous indels result in mutant proteins with C-terminal peptide “tails” that vary in length and sequence. Other, more advanced and sophisticated versions of CRISPR/Cas9 gene editing system are required to guarantee a

more precise and efficient modification of the *FUS* gene in the future studies. A host of strategies have been developed to improve editing precision and efficiency over the past few years, and this will be discussed in detail in the general discussion chapter.

FUS protein is known to regulate its own expression levels by controlling alternative splicing of its pre-mRNA (Zhou *et al.* 2013). Exon 7 of *FUS* gene is subjected to alternative splicing: FUS mRNA with exon 7 skipped undergoes NMD while mRNA containing exon 7 produces normal protein. FUS protein overexpression represses exon 7 splicing, thereby downregulating total FUS protein levels and vice versa. In light of this, decreased nuclear FUS protein levels in ΔNLS clones due to FUS cytoplasmic mislocalisation could alleviate the suppressive effect of FUS protein on exon 7 splicing, resulting in FUS upregulation. Indeed, the majority of ΔNLS clones exhibited elevated total FUS mRNA levels. In regard to the decreased mRNA levels in some ΔNLS clones, I speculate that certain sequence elements present in mutant FUS transcripts in these clones might be responsible for their compromised stability (Guhaniyogi and Brewer 2001, Hollams *et al.* 2002). It is surprising that a small amount of FUS mRNA was still detectable in FUS KO cells, although no FUS protein was detectable either in immunostaining or in western blot using antibodies against different domains of the protein. Probably, these mRNAs are not yet fully degraded residual transcripts that are not capable of being translated.

Mutant FUS proteins with the NLS sequence deleted or replaced by cryptic sequences display cytoplasmic mislocalisation, and they are recruited into SGs assembled under oxidative stress, which is consistent with previous reports (Dormann *et al.* 2010, Gal *et al.* 2011, Ito *et al.* 2011a, Kino *et al.* 2011). As only one copy of the *FUS* gene is edited in the heterozygous clones, one would expect that about half of the protein would be redistributed to cytoplasm. However, a very mild mislocalisation of FUS is observed in heterozygous clones, with most FUS protein remaining in the nucleus, suggesting that a putative, less potent NLS signal(s) might be present in the unmodified region of FUS. This possibility has also been discussed by others (Dormann *et al.* 2010). In addition, although FUS mislocalisation was more

pronounced in the homozygous clones than heterozygous ones, the difference, however, was not proportional. It seems that WT FUS may help retain mutant FUS within the nucleus. It has been proposed that the degree of cytoplasmic export of shuttling proteins is determined primarily by their intranuclear interactions (Schmidt-Zachmann *et al.* 1993). FUS is known to self-interact through low-complexity prion-like domain on its N-terminus (Monahan *et al.* 2017). Therefore, I reason that higher local concentration of FUS in the nuclei of heterozygous cells facilitated the retention of mutant FUS proteins in the nucleus, thereby alleviating their cytoplasmic accumulation. My finding is consistent with the observations from post-mortem studies of ALS-FUS cases (which are nearly all heterozygous for FUS mutation) where affected neurons with cytoplasmic FUS inclusions still have considerable amount of FUS in the nucleus (Kwiatkowski *et al.* 2009, Vance *et al.* 2009, Rademakers *et al.* 2010).

To the best of my knowledge, this study is the first to report the capability of endogenous mutant FUS to spontaneously assemble into stable granules in the cytoplasm. This is very important for understanding the mechanisms underlying the formation of pathological inclusions in the degenerating motor neurons in ALS-FUS patients. There is an ongoing debate on the initial structure that might give rise to the pathological inclusions. SGs, being the most extensively studied cytoplasmic RNP granules that contain FUS, are considered to be the foci where pathological FUS aggregates emerge. It is proposed that SGs that fail to disassemble are the precursors for pathological inclusions, as supported by the findings where incorporation of ALS-associated mutant proteins into SGs reduces their dynamics (Dewey *et al.* 2011, Boeynaems *et al.* 2017, Zhang *et al.* 2018c). In the case of FUS mutations, while some reported persistent SGs in mutant FUS expressing cells (Acosta *et al.* 2014), others found accelerated SG disassembly after removal of stress (Baron *et al.* 2013). Another hypothesis states that pathological inclusions may arise from FUS aggregates, a stress-induced cytoplasmic structure nucleated from spontaneously assembled FGs (Shelkovnikova *et al.* 2014a). Observations leading to this hypothesis were based on cellular models overexpressing mutant FUS, therefore it was not clear whether endogenous mutant FUS could nucleate such granules under

basal conditions. My results indicate that even endogenous levels of mutant FUS in cells with one *FUS* gene copy modified can drive formation of such granules. Further studies into the behaviour of these granules under stress conditions will shed light on the possible mechanisms underlying the formation of pathological FUS inclusions.

In conclusion, cellular models expressing endogenous levels of mutant FUS protein have been successfully generated by targeted modification of the *FUS* gene, and the modified proteins mislocalise to the cytoplasm and even form spontaneous granules in some clones, making these clones valuable FUSopathy models.

Chapter 4. Paraspeckles and ALS-FUS

4.1. Overview

Cytoplasmic mislocalisation of FUS protein and formation of FUS-positive inclusions in the neurons and glial cells of spinal cord is the histopathological hallmark of ALS-FUS (Kwiatkowski *et al.* 2009, Vance *et al.* 2009, Hewitt *et al.* 2010). However, significant FUS mislocalisation is rare among ALS-FUS cases, and even in these cases, only a subset of neurons display dramatic FUS mislocalisation (Hewitt *et al.* 2010, Mackenzie *et al.* 2010b, King *et al.* 2015). This suggests that mutant FUS in the nucleus can exert toxic functions that can drive pathological changes sufficient to cause the disease. Indeed, mutant FUS proteins showing only mild cytoplasmic redistribution, such as R521G(H), are proven to be detrimental *in vitro* and *in vivo* models (Qiu *et al.* 2014, Rulten *et al.* 2014, Sephton *et al.* 2014, Wang *et al.* 2018a). In addition, ALS-associated FUS mutations outside the NLS-coding region have been identified (Ticozzi *et al.* 2009), and corresponding mutant FUS can also cause pathological cellular phenotypes (Nomura *et al.* 2014, Patel *et al.* 2015). Finally, in mouse models of FUSopathy, mutant FUS is capable of causing neurodegeneration in the absence of cytoplasmic FUS aggregation and even without significant mislocalisation, indicating that FUS nuclear gain of function is an important disease mechanism (Devoy *et al.* 2017, Lopez-Erauskin *et al.* 2018). Our understanding of the cytoplasmic gain of function of mutant FUS has improved significantly during the past decade, however, less is known about its nuclear toxic functions.

Multiple lines of evidence support the strong association between paraspeckles and ALS pathogenesis – many ALS-associated mutations affect paraspeckle proteins, and human spinal motor neurons, which normally lack paraspeckles, develop paraspeckles in ALS patients (discussed in Chapter 1). FUS is an essential paraspeckle protein since its depletion eliminates paraspeckles (Naganuma *et al.* 2012, Shelkovnikova *et al.* 2014b). However, little is known regarding whether and how the paraspeckles are affected in the presence of mutant FUS protein in ALS-FUS. Since NEAT1 levels are sensitive to intracellular FUS levels (Shelkovnikova et al. 2014b), cellular models based on FUS protein overexpression have limited value in studying the effect of mutant FUS protein on paraspeckles. FUS ΔNLS clones

expressing mutant FUS proteins at endogenous levels can provide an excellent platform for investigating paraspeckle dysregulation in ALS-FUS. This chapter aims to investigate pathological impact of mutant FUS on paraspeckles using FUS ΔNLS clones.

4.2. Results

4.2.1. Excessive paraspeckle formation in ΔNLS_het clones

Three homozygous (ΔNLS1_ho, ΔNLS4_ho and ΔNLS7_ho), three heterozygous (ΔNLS2_het, ΔNLS8_het, ΔNLS 11_het) clones and FUS KO clone were included in this study. RNA-FISH was performed using a probe recognising the 3' region of NEAT1_2 on the clones. As predicted, paraspeckles were hardly detectable in FUS KO clone (Figure 4.1A). ΔNLS_ho clones showed a similar phenotype, although some cells still had residual paraspeckles, and this is consistent with the significant cytoplasmic mislocalisation of FUS in these clones (Figure 4.1A, arrowheads). FUS is known to contribute to the structural integrity of paraspeckles by holding together the individual NEAT1 RNP complexes (Yasuda *et al.* 2013). In agreement with this, numerous small NEAT1-positive particles, likely corresponding to the NEAT1 RNP complexes – the "primary units" of paraspeckles, were detected in FUS KO and ΔNLS_ho cells (Figure 4.1A, bottom panel insets). What surprised me, however, was the significantly enhanced paraspeckle formation in ΔNLS_het clones, which was further confirmed by paraspeckle quantification (Figure 4.1 and 4.2). In fact, the paraspeckle numbers in this analysis may be an underestimation since paraspeckles often exist as clusters, which were counted as single foci, particularly in ΔNLS_het cells (Figure 4.1A, arrows). Total NEAT1-positive area per nucleus was also quantified, which showed a two-fold increase in ΔNLS_het cells (Figure 4.2). According to the current definition, paraspeckles are structures composed of both NEAT1_2 and an essential protein component (Naganuma *et al.* 2012). Therefore, cells were double-labelled using NEAT1_2 RNA-FISH in combination with NONO immunostaining, which

confirmed the colocalisation of NONO with NEAT1_2-positive foci in ΔNLS_het clones (Figure 4.1B).

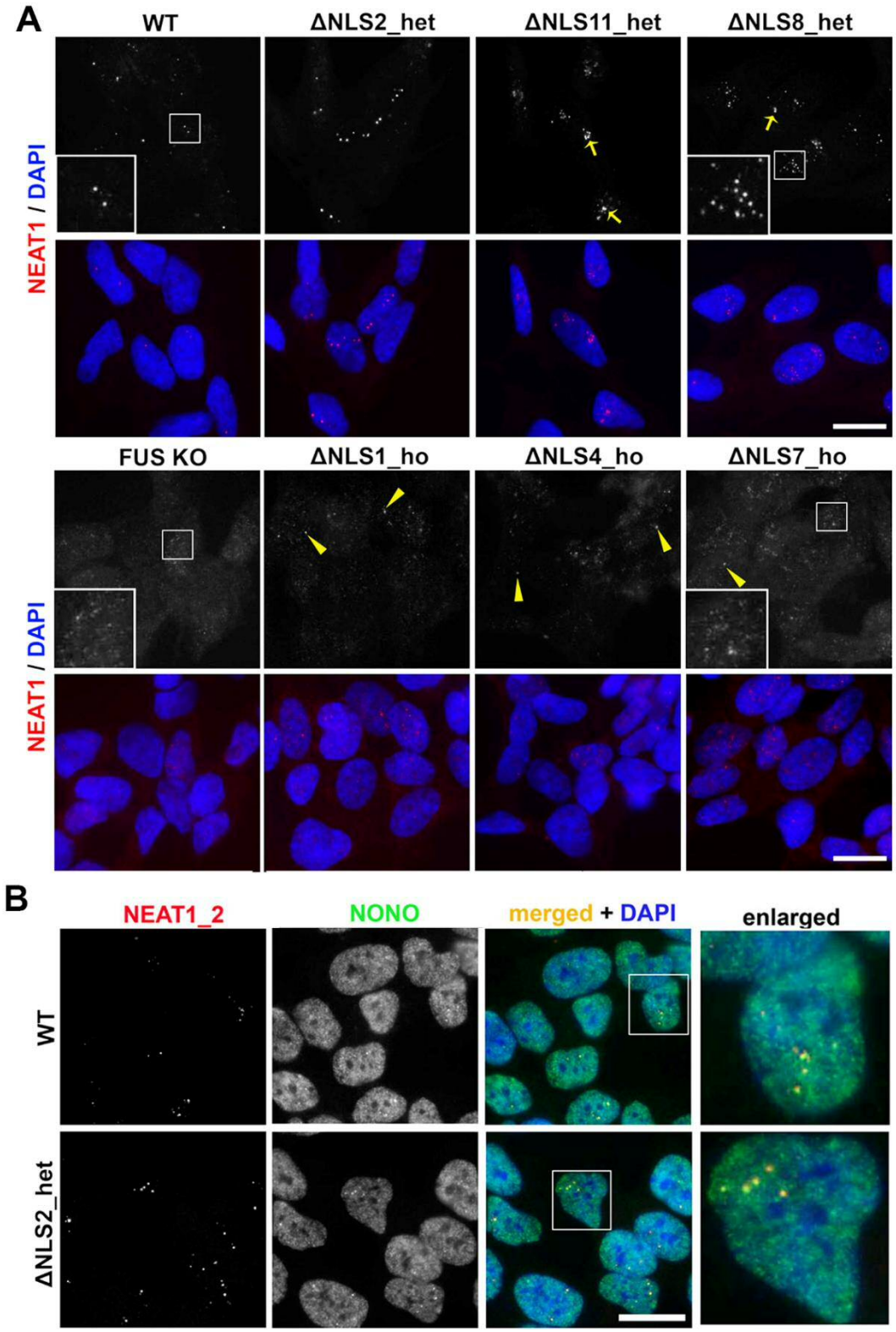

Figure 4.1 Augmented paraspeckle assembly in ΔNLS_het clones.

A) RNA-FISH using NEAT1 probe reveals increased number of paraspeckles in ΔNLS_het clones, whereas ΔNLS_ho clones and FUS KO clone were almost devoid

of paraspeckles. Yellow arrows point to clusters of paraspeckles in ΔNLS_het clones; yellow arrowheads indicate residual paraspeckles in ΔNLS_ho clones. Insets in upper panel (WT cells and ΔNLS_het clones) show paraspeckles; Insets in lower panel (FUS Ko and ΔNLS_ho clones) show paraspeckle primary units. **B)** A core paraspeckle protein NONO colocalises to NEAT1_2 in paraspeckles of ΔNLS_het clones. Scale bars are 10 μm.

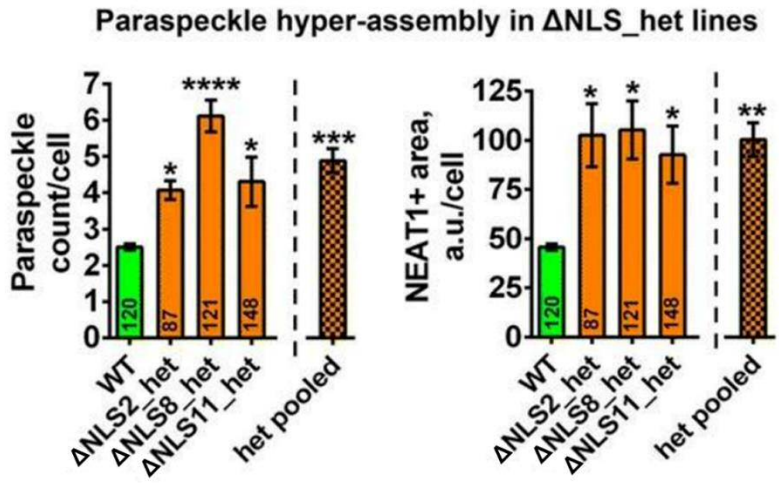

Figure 4.2 Quantification of paraspeckles in ΔNLS_het clones.
The number of paraspeckles and NEAT1-positive area per cell are quantified for ΔNLS_het clones. Total cell numbers analysed are indicated within each bar. One-way ANOVA with Holm-Sidak test is used. *p < 0.05, **p < 0.01, ***p < 0.001, ****p < 0.0001.

4.2.2. NEAT1 isoforms are upregulated in ΔNLS clones

Since paraspeckle formation depends on NEAT1_2, augmented paraspeckle assembly in ΔNLS_het clones is very likely resulted from NEAT1_2 upregulation. NEAT1_2 transcripts are known to be “semi-extractable” (Chujo *et al.* 2017), therefore, a heating step was introduced during RNA purification using QIAzol for the accurate measurement of NEAT1_2 levels. As expected, qPCR showed upregulation of NEAT1_2 in ΔNLS_het clones; however, similar upregulation was also observed in ΔNLS_ho clones (Figure 4.3A). Adenosine deaminase RNA specific B2 (ADARB2) is one of the genes negatively regulated by NEAT1 (Hirose *et al.* 2014). As predicted, ADARB2 levels were dramatically downregulated in ΔNLS clones as measured by RNA-Seq and qPCR, and NEAT1 knockdown was able to limit its downregulation (Figure 4.3B).

Interestingly, NEAT1 levels in FUS KO clone, which lacks paraspeckles, were normal (Figure 4.3A), suggesting that elevated NEAT1 level is not caused by compensatory upregulation triggered by paraspeckle disruption, but is more likely resulted from the presence of mutant FUS.

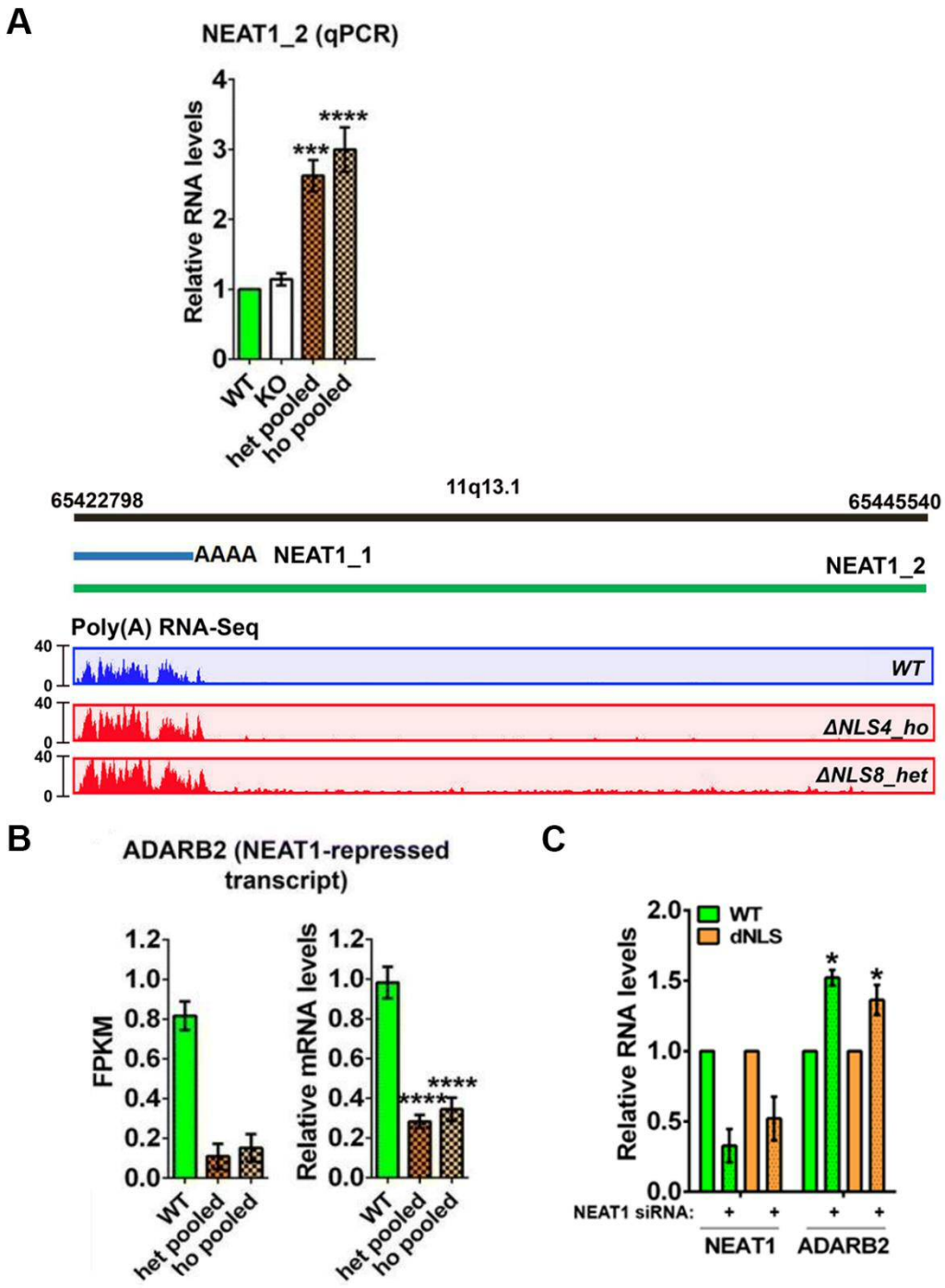

Figure 4.3 NEAT1 is upregulated in ΔNLS clones.

A) NEAT1_2 levels are measured by qPCR. N = 4 for each clone; one-way ANOVA; ***p < 0.001, ****p < 0.0001. Representative tracks for poly(A)-captured RNA-Seq analysis of *NEAT1* gene in ΔNLS8_het and ΔNLS4_ho clones are also shown. Higher peaks within first 1/5 region on the left correspond to reads from both NEAT1 isoforms and much lower peaks across the rest of the region correspond to NEAT1_2 reads. Due to much lower abundance of NEAT1_2 relative to NEAT1_1, NEAT1_2 peaks in WT cells are almost absent in the graph. **B)** *ADARB2*, a gene supressed by

NEAT1, is downregulated in ΔNLS clones as measured by RNA-Seq and qPCR. N = 3 for each line; one-way ANOVA with Dunnett's test; ****p < 0.0001. **C)** Knockdown of NEAT1 (both isoforms) upregulates ADARB2 in WT and ΔNLS cells. Cells were analysed 48 h after siRNA transfection. N=3; Mann-Whitney U test; *p<0.05. For all quantifications, data from three heterozygous (ΔNLS2_het, ΔNLS8_het and ΔNLS11_het) and three homozygous (ΔNLS1_ho, ΔNLS4_ho and ΔNLS7_ho) clones are pooled.

Increased level of NEAT1_2 could be explained by increased expression of SFPQ and NONO. These two proteins are essential paraspeckle components, and their binding to NEAT1_2 is known to stabilise the transcript, therefore, increase its steady-state levels (Naganuma *et al.* 2012). However, their expression levels and distribution did not differ significantly between WT and ΔNLS clones (Figure 4.4) suggesting a different mechanism of NEAT1 upregulation.

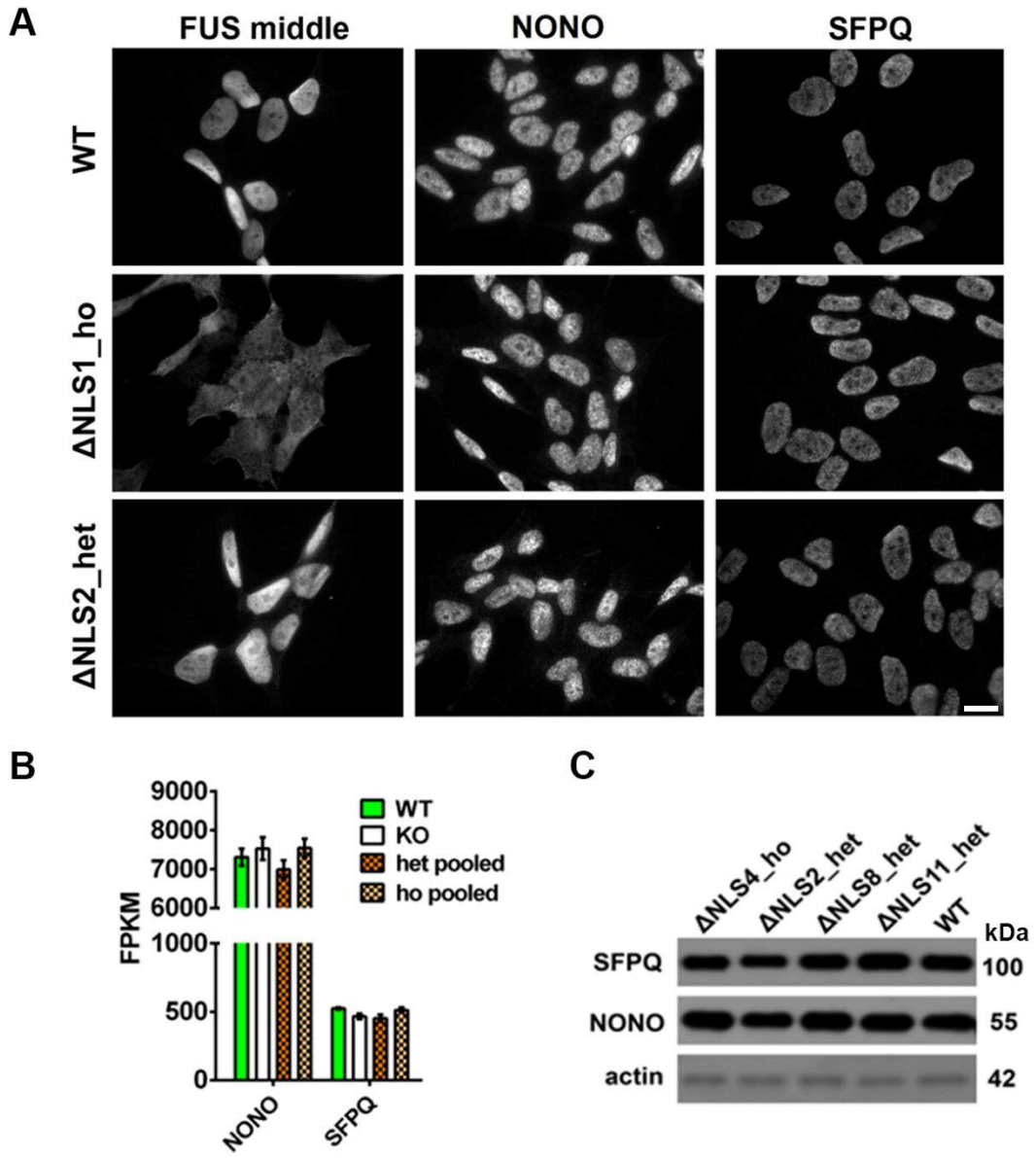

Figure 4.4 Distribution as well as mRNA and protein expression levels of core paraspeckle proteins are not significantly affected in ΔNLS clones.

A) Representative images of ΔNLS clones immunostained for FUS, NONO and SFPQ are shown. Scale bar is 10 μm. **B)** mRNA levels of NONO and SFPQ are measured by RNA-Seq and the corresponding fragments per kilobase of transcript per million mapped reads (FPKM) values are shown. Data from three heterozygous (ΔNLS2_het, ΔNLS8_het and ΔNLS11_het) and three homozygous (ΔNLS1_ho, ΔNLS4_ho and ΔNLS7_ho) clones are pooled. N=3. **C)** Protein expression levels of SFPQ and NONO are measured by western blot.

4.2.3. Overexpression of normal or mutant FUS restores paraspeckles in ΔNLS_ho and FUS KO cells

Although FUS does not stabilise NEAT1_2, it is required for paraspeckle maturation downstream of NEAT1_2 synthesis (Naganuma *et al.* 2012, West *et al.* 2016). I asked whether expressing exogenous mutant FUS would rebuild paraspeckles in FUS KO and ΔNLS_ho cells. Green fluorescent protein (GFP)-tagged FUS WT, ALS-linked FUS R524T and R518K (predominantly nuclear), and ΔNLS (predominantly cytoplasmic) (Shelkovnikova, Robinson et al. 2014) mutants were expressed in the cells. Overexpression of all the above FUS variants resulted in the appearance of bright NEAT1-positive foci in the majority of transfected FUS KO and ΔNLS1_ho cells (Figure 4.5A,B), and this was accompanied by the disappearance of paraspeckle precursors (Figure 4.5B, inset). All FUS variants showed the similar capability of paraspeckle nucleation (Figure 4.5C), despite the fact that in the cells expressing GFP-tagged ΔNLS, nuclear levels of ectopic protein were much lower than in cells expressing other variants (Figure 4.5A). This suggests that nuclear mutant FUS, when its level exceeds a certain threshold, is able to form and maintain visible paraspeckles.

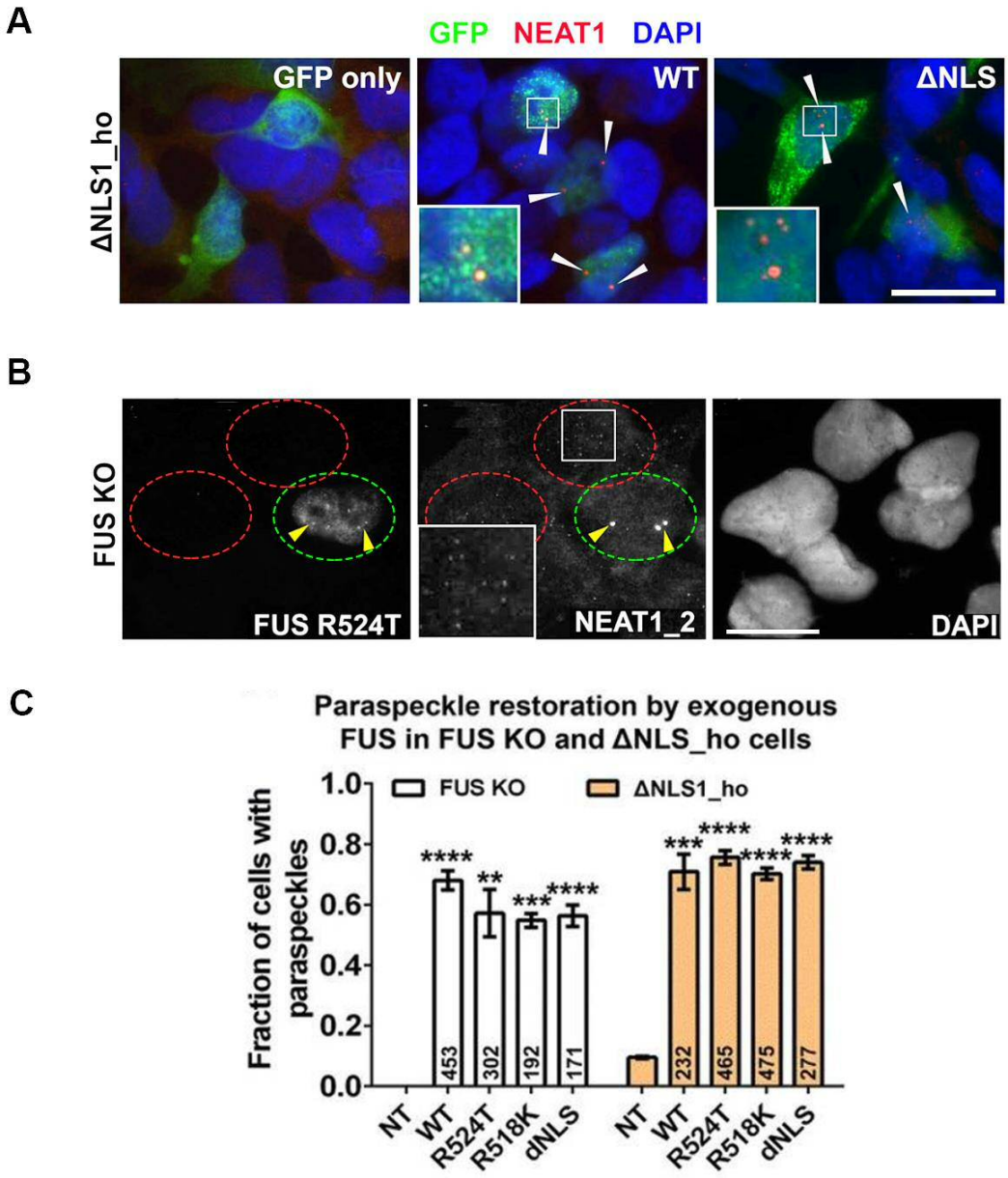

Figure 4.5 Overexpression of FUS or its mutants restores paraspeckles in FUS KO and ΔNLS_ho cells.

A) Expressing GFP-tagged WT FUS or FUS ΔNLS in ΔNLS1_ho cells restores paraspeckls as revealed by NEAT1 RNA-FISH. ΔNLS1_ho cells expressing GFP is included as a negative control. **B)** Restoration of paraspeckles in FUS-deficient cells results in the disappearance of paraspeckle precursors (inset). Transfected and non-transfected cells are highlighted with green and red circles, respectively. Note the presence of the precursors in non-transfected cells (inset). In both A and B, arrowheads point to mature paraspeckles. Scale bars are 10 μm. **C)** Efficient restoration of paraspeckles by overexpression or either normal or mutant FUS. Fractions of cells with one or more paraspeckles among transfected ΔNLS1_ho and

FUS KO cells are quantified. Numbers of cells analysed are indicated within each bar. One-way ANOVA with Holm-Sidak test; **p < 0.01, ***p < 0.001, ****p < 0.0001.

4.2.4. Interactions between FUS and core paraspeckle components are decreased in ΔNLS clones

Although nuclear FUS levels in ΔNLS_het clones are sufficient for the assembly of visible paraspeckles, it is unclear whether these structures differ from normal paraspeckles in terms of structural integrity and functionality. During paraspeckle formation, NONO and SFPQ heterodimers bind to NEAT1_2 to form paraspeckle precursors, which are subsequently held together by FUS (West *et al.* 2016). I measured FUS interaction with SFPQ and NONO using proximity ligation assay (PLA), which revealed significantly decreased interaction of FUS with both proteins within the nuclei of ΔNLS_het and ΔNLS_ho clones (Figure 4.6).

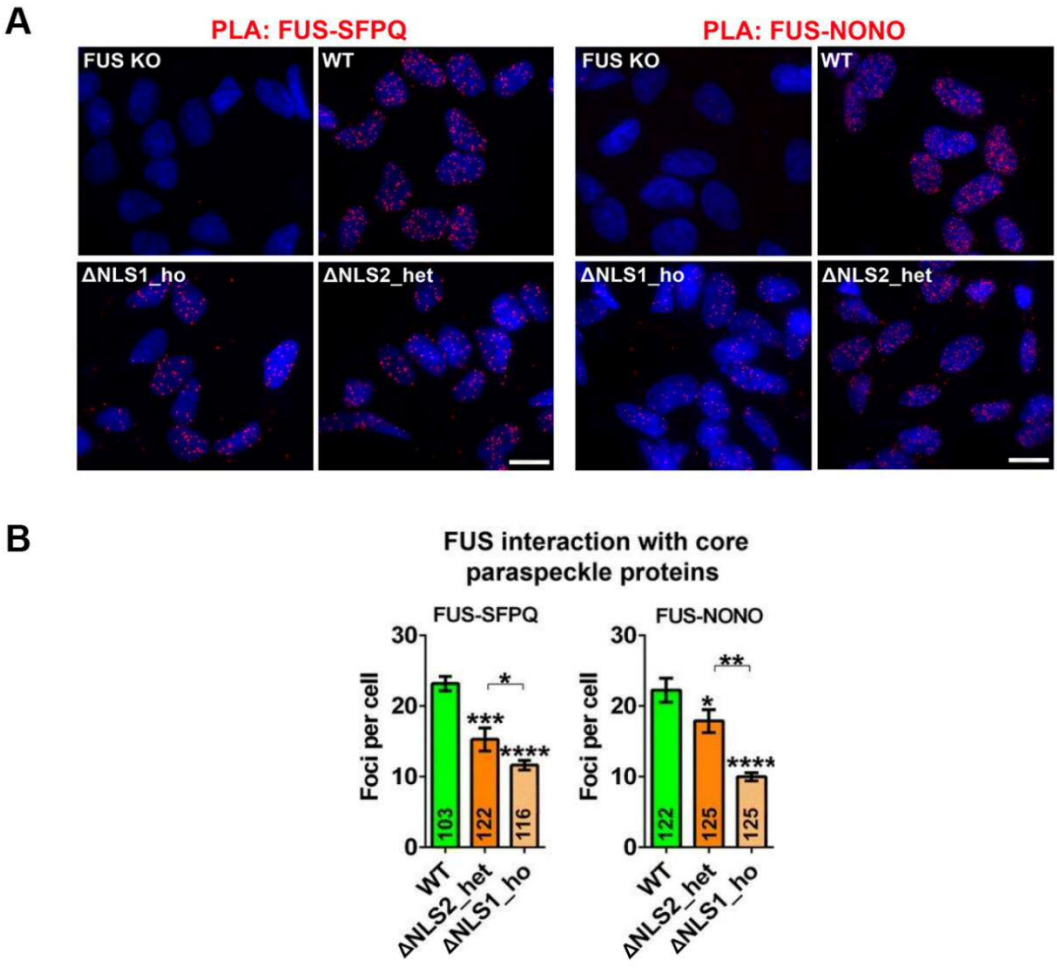

Figure 4.6 The interaction of FUS with SFPQ and NONO is reduced in ΔNLS clones.

A) Proximity ligation assay (PLA) was performed to measure the interaction between FUS and SFPQ or NONO in a heterozygous and a homozygous clone. FUS KO cells were included as a negative control. Representative images are shown. Scale bars are 10 μm. **B)** Number of interactions are quantified from the PLA images. Numbers of cells analysed are indicated within each bar. One-way ANOVA with Holm-Sidak test; *p < 0.05, **p < 0.01, ***p < 0.001, ****p < 0.0001.

Weakened interaction of FUS with SFPQ and NONO indicates that its interaction with NEAT1_2 might also be affected. It is known that interaction between FUS and NEAT1_2 renders NEAT1_2 difficult to extract using standard Trizol-based RNA extraction method unless an additional heating step is introduced (Chujo *et al.* 2017). Therefore, I hypothesised that NEAT1_2 should be extracted more efficiently if the interaction between FUS and NEAT1_2 becomes weaker due to the mutation. To assess the interaction between FUS and NEAT1_2, NEAT1_2 levels were compared between two RNA samples prepared with or without heating step during the QIAzol RNA purification process. In WT cells, the extractability of NEAT1_2 increased ~ 3.5-fold with heating, while the extractability of another lncRNA, Metastasis Associated Lung Adenocarcinoma Transcript 1 (MALAT1), was not affected (Figure 4.7). In FUS KO cells, which lack paraspeckles, NEAT1_2 was almost fully extractable as the ratio of heated/non-heated was close to 1. Similarly, ΔNLS_ho clones that do not form visible paraspeckles also exhibited significantly increased NEAT1_2 extractability. Importantly, ΔNLS_het clones, which show enhanced paraspeckle formation, also showed significantly elevated NEAT1_2 extractability, albeit to a lesser extent than ΔNLS_ho or FUS KO cells (Figure 4.7).

Therefore, mutant FUS showed compromised interaction with core paraspeckle components – NEAT1_2, SFPQ and NONO, compared to WT FUS.

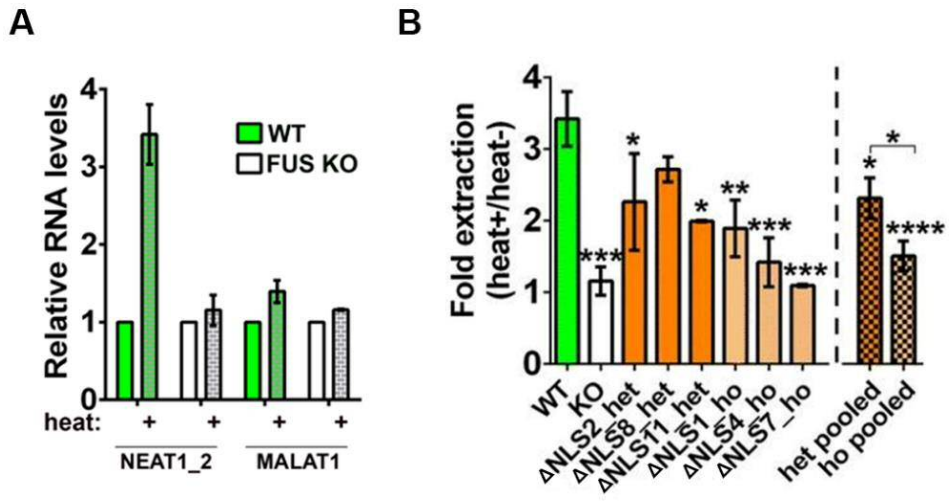

Figure 4.7 Increased extractability of NEAT1_2 in the ΔNLS clones indicates reduced binding of FUS to NEAT1_2.

A) NEAT1_2 but not MALAT1 is semi-extractable in WT neuroblastoma cells. **B)** Increased NEAT1_2 semi-extractability in ΔNLS clones. Note that near-complete NEAT1_2 extraction is achieved in FUS KO cells (fold extraction ~ 1). N = 3 per clone; One-way ANOVA; *p < 0.05, **p < 0.01, ***p < 0.001, ****p < 0.0001. In A and B, NEAT1_2 extractability is measured by comparing its levels in heated versus non-heated QIAzol-lysed samples ("fold extraction") by qPCR.

4.2.5. NEAT1_1 accumulates in the nucleoplasm outside paraspeckles in ΔNLS clones

FUS CLIP-Seq studies have reported that FUS protein preferentially binds to NEAT1_1 since the read density was highest at the 5' region of NEAT1 (Lagier-Tourenne *et al.* 2012). This finding raises the possibility that NEAT1_1 is recruited into the paraspeckles via its interaction with FUS during the higher-order assembly of paraspeckles, and the deficiency of mutant FUS in paraspeckles assembly would lead to insufficient NEAT1_1 recruitment. It has been shown that *NEAT1* gene products are highly enriched (~10-fold) in chromatin-bound fraction (Werner and Ruthenburg 2015), suggesting that paraspeckles can be co-pelleted with chromatin during cell fractionation. I obtained a soluble nuclear extract (SNE) from ΔNLS clones and WT cells and prepared cDNAs using oligo(dT) primer to amplify only NEAT1_1 which is

polyadenylated, but excluding NEAT1_2 that do not have poly(A) tails. Indeed, NEAT1_1 levels in SNE were significantly higher in ΔNLS clones compared to WT cells as measured by non-saturated PCR and qPCR (Figure 4.8A), indicating decreased recruitment and retention of NEAT1_1 within paraspeckles in the cells expressing mutant FUS.

I speculated that under stressful conditions, which normally trigger paraspeckle hyper-assembly/enlargement, the functional deficiencies of mutant FUS in maintaining paraspeckle structure might become more apparent. To test this, I stimulated cells with poly(I:C), a synthetic viral mimic that has been reported to increase NEAT1 levels and enhance paraspeckle formation (Imamura *et al.* 2014). A significant proportion of poly(I:C)-stimulated cells in ΔNLS_het clones displayed a diffuse NEAT1 signal, which was in contrast to the signal located only in well-defined paraspeckles in all WT cells (Figure 4.8B,C). This suggests that stress-induced paraspeckle formation is indeed impaired in cells expressing mutant FUS. A similar observation was made in the cells treated with proteasome inhibitor MG132, another paraspeckle-inducing stressor (Hirose *et al.* 2014) (Figure 4.8D).

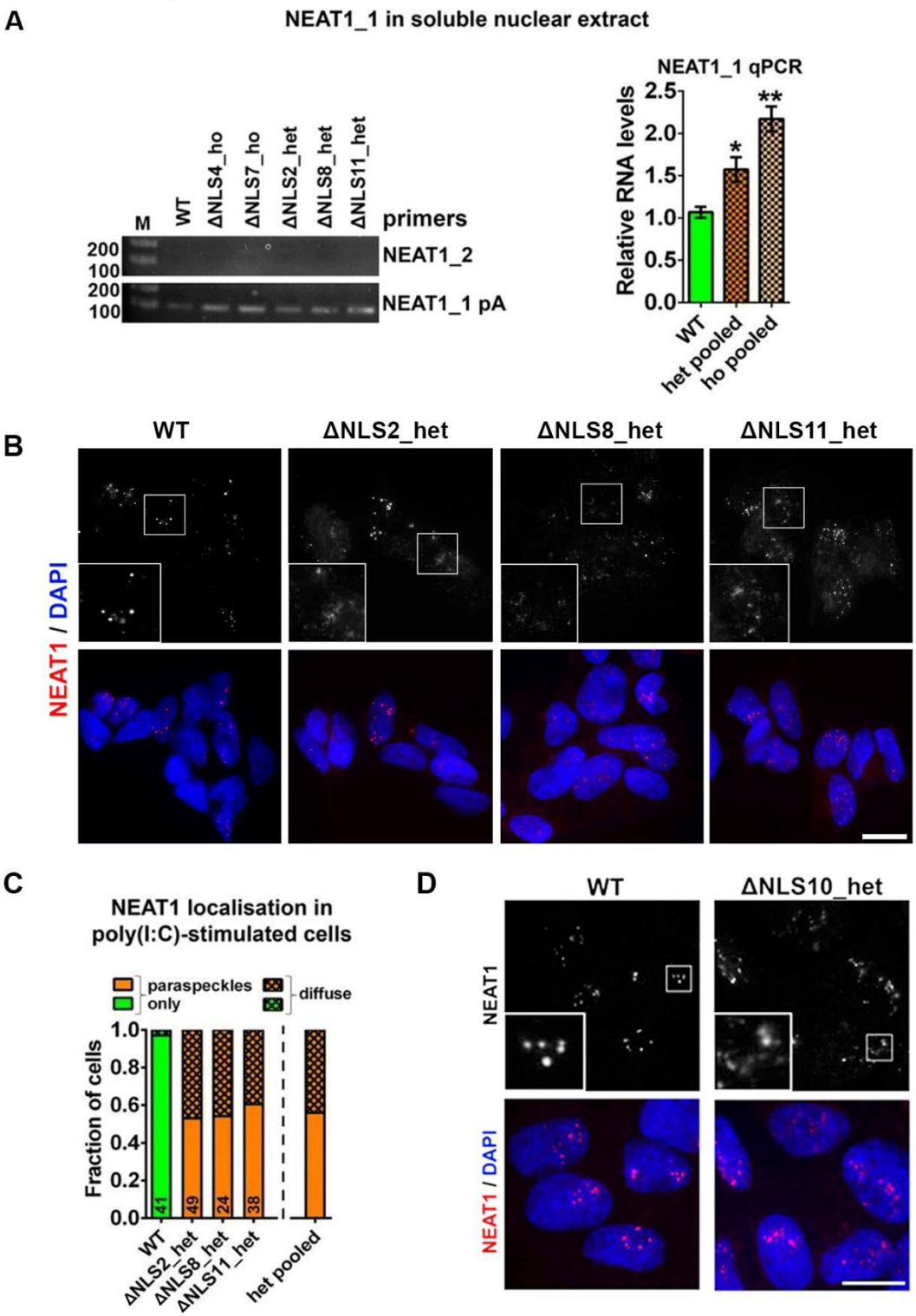

Figure 4.8 NEAT1_1 accumulates in soluble nuclear extract (SNE) in ΔNLS clones, and cellular stress enhances non-paraspeckle NEAT1_1 accumulation.

A) Non-saturated PCR (26 cycles) (left) and qPCR (right) results show increased NEAT1_1 levels in SNEs of ΔNLS clones compared to WT cells. A primer pair located immediately upstream NEAT1_1 polyA-tail is used to quantify NEAT1_1 in cDNA prepared from polyadenylated RNA. Note that this primer pair does not detect

NEAT1_2 which is not polyadenylated. One-way ANOVA with Holm-Sidak test; *p < 0.05, **p < 0.01. N=3. **B)** RNA-FISH with total NEAT1 probe shows diffuse NEAT1 distribution in poly(I:C)-transfected ΔNLS_het clones. Cells were analysed 8 h post-transfection. Representative images are shown. **C)** Proportion of cells showing diffuse NEAT1 signal is quantified in ΔNLS_het clones transfected with poly(I:C). Numbers of cells analysed are indicated within each bar. **D)** MG132 treatment, another paraspeckle-inducing stress, causes diffuse NEAT1 distribution in a ΔNLS_het clone. Representative images are shown. Scale bars are 10 μm.

4.2.6. miRNA biogenesis regulated by paraspeckles is impaired in ΔNLS clones

The compromised structural integrity of paraspeckles in ΔNLS clones suggests that their functions might also be affected. One of the established paraspeckle functions is the regulation of miRNA biogenesis. It has been reported that paraspeckles modulate pri-miR-17~92 transcript processing by enhancing Microprocessor activity (Jiang *et al.* 2017). I measured miRNA levels produced form this miRNA precursor, and found that all six miRNAs are significantly decreased in homozygous ΔNLS clones. In addition, some miRNA are also decreased in heterozygous ΔNLS clones (Figure 4.9). This suggests compromised functionality of paraspeckles in the cells expressing mutant FUS.

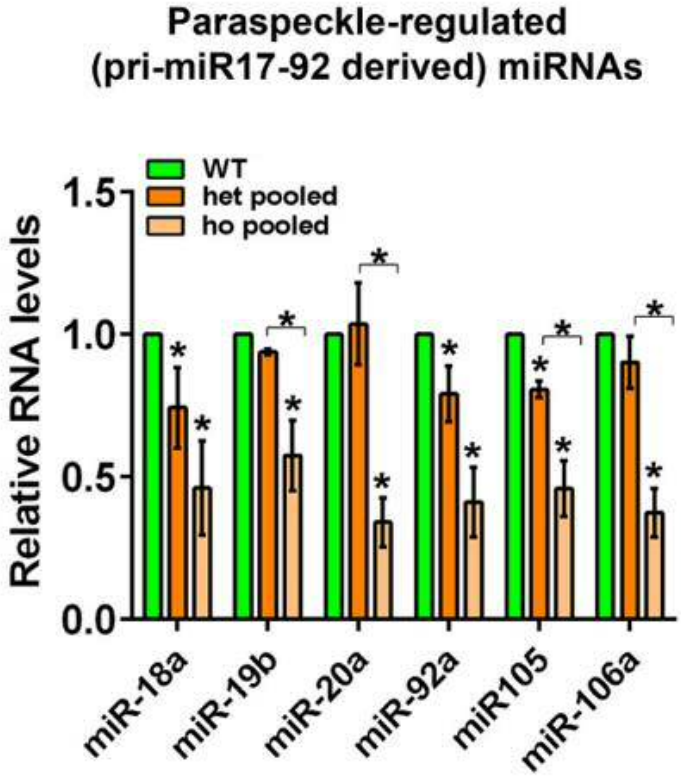

Figure 4.9 Paraspeckle-regulated miRNAs are decreased in ΔNLS clones.

Levels of six mature miRNAs generated from pri-miR17~92 are measured by qPCR. Data from three heterozygous clones (ΔNLS2_het, ΔNLS8_het and ΔNLS11_het) and three homozygous clones (ΔNLS1_ho, ΔNLS4_ho and ΔNLS7_ho) are pooled. Mann-Whitney U test, *$p < 0.05$. N=3.

4.2.7. ALS-FUS patient fibroblasts display enhanced paraspeckles assembly and decreased NEAT1_1 sequestration capability

I asked whether my findings in ΔNLS clones could be corroborated in another cellular system, human fibroblasts. Fibroblasts have a large nucleus with numerous paraspeckles, making them a well-suited system for paraspeckle studies. Fibroblasts derived from a patient with FUS P525L mutation, which impairs NLS of FUS protein, displayed only mild FUS cytoplasmic mislocalisation (Figure 4.10A). Consistent with the findings in ΔNLS clones, paraspeckle numbers and NEAT1-positive area are increased ~ 2-fold in the fibroblasts expressing mutant FUS compared to control fibroblasts (Figure 4.10B).

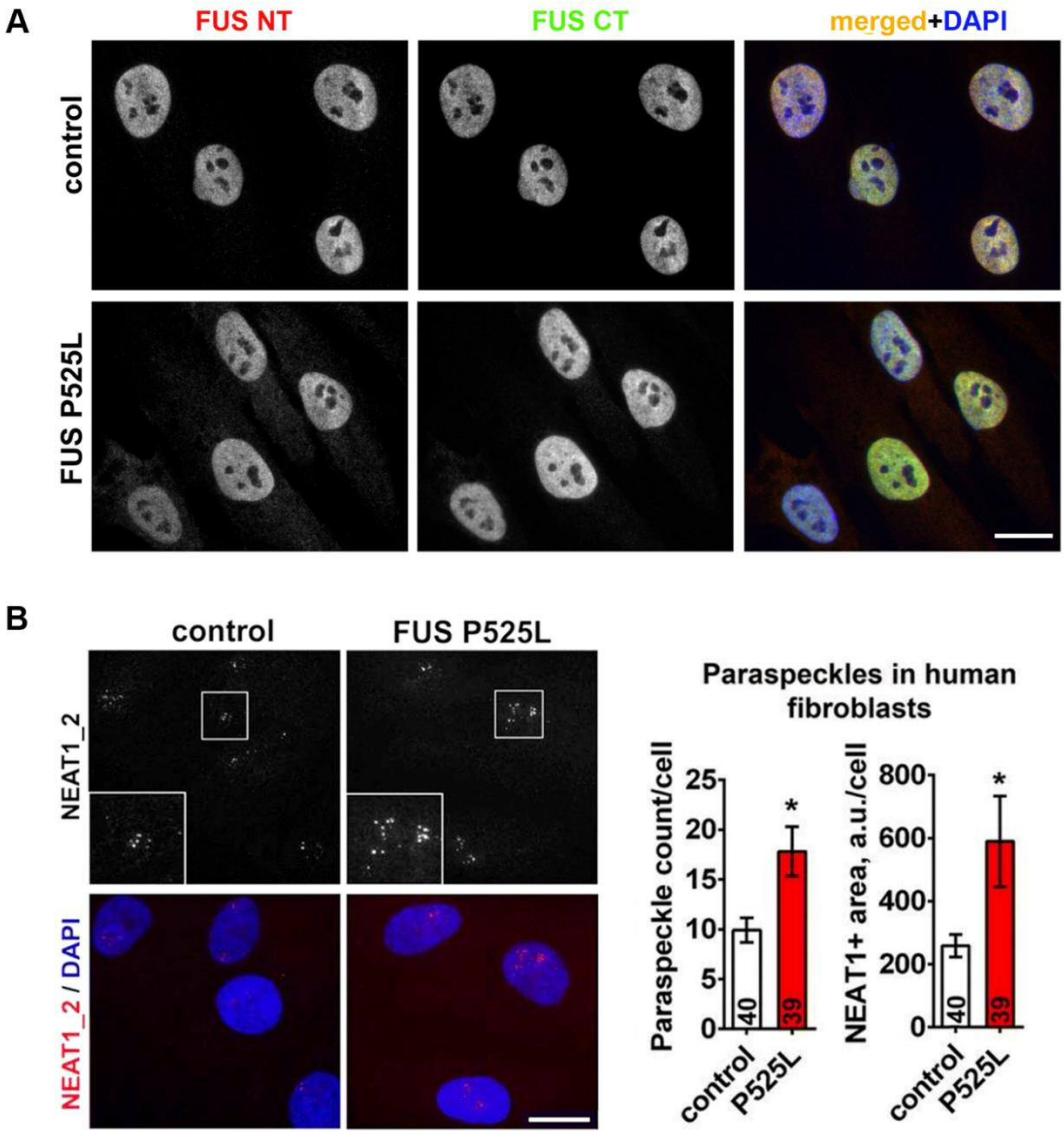

Figure 4.10 Accumulation of NEAT1 and augmented paraspeckle assembly is found in patient fibroblasts bearing FUS mutation.

A) FUS is predominantly nuclear in human fibroblasts obtained from an ALS patient carrying FUS P525L mutation. **B)** RNA-FISH using NEAT1_2 probe shows augmented paraspeckle assembly in FUS P525L human fibroblasts. The number of paraspeckles and NEAT1-positive area per cell are quantified. Numbers of cells analysed are indicated within each bar. Mann-Whitney U-test; *p < 0.05. Scale bars are 10 μm.

Although the morphology of paraspeckles in the FUS P525 cells appeared normal when detected by NEAT1_2 RNA-FISH (Figure 4.10B), NEAT1 signal was observed outside paraspeckles in these cells using the probe detecting

both NEAT1 isoforms (5’ segment of NEAT1) (Figure 4.11A, left). Since NEAT1_2 FISH did not produce a diffuse signal, the observed diffuse non-paraspeckle NEAT1 corresponds to NEAT1_1. Interestingly, the area of diffuse NEAT1_1 signal largely overlapped with nuclear speckles, as detected by polyA+RNA (Figure 4.11B). A similar pattern of NEAT1_1 distribution, termed ‘microspeckle’, has been reported recently in the cells lacking NEAT1_2/paraspeckles (Li *et al.* 2017). In an independent fibroblast line expressing FUS P525L, obtained from the same individual before the disease onset, total NEAT1 probe detected the same paraspeckle abnormalities (Figure 4.11A, right). These findings are consistent with the NEAT1_1 accumulation in the nucleoplasm of ΔNLS clones (Figure 4.8) and further confirm that ALS-linked FUS mutations compromise the ability of FUS protein to recruit NEAT1_1 into paraspeckles.

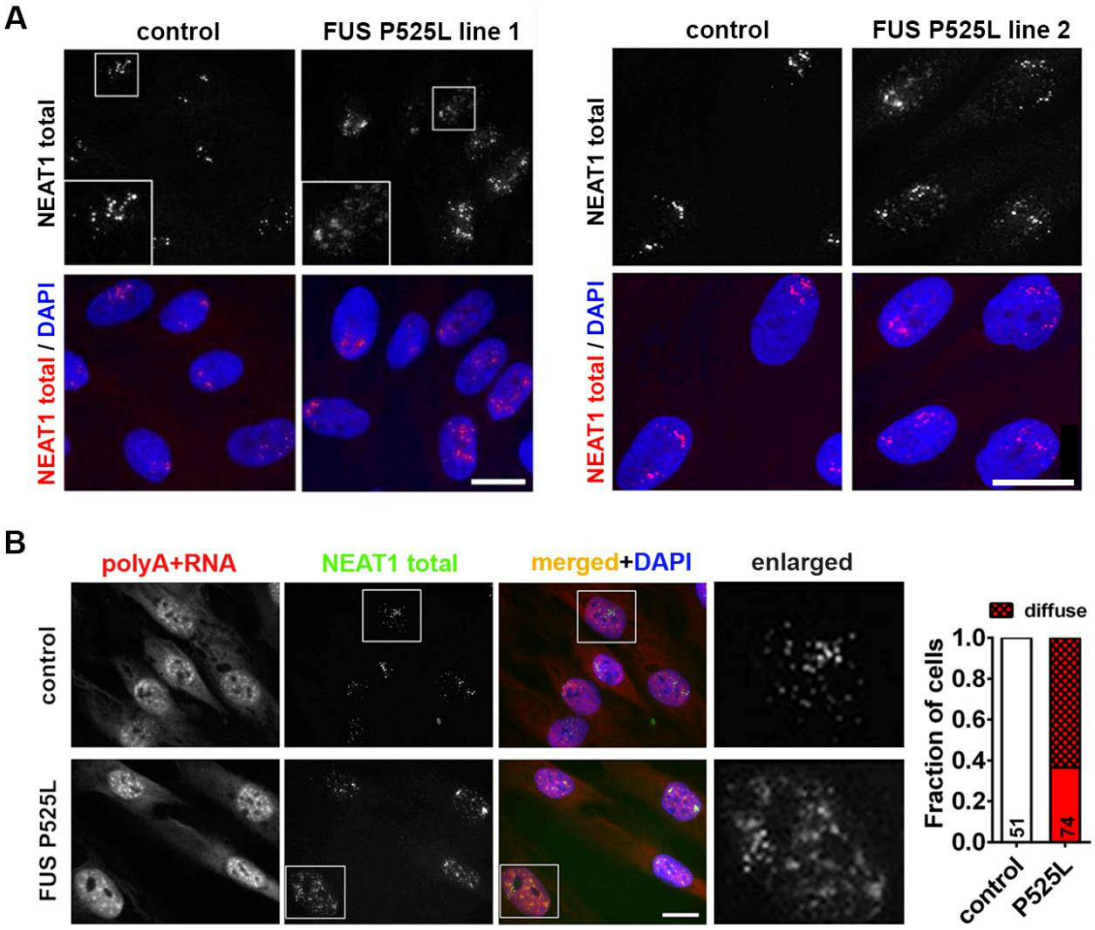

Figure 4.11 Localisation of NEAT1_1 outside paraspeckles in patient fibroblasts bearing FUS mutation.

A) RNA-FISH using a probe recognising total NEAT1 shows diffuse, non-paraspeckle distribution of NEAT1 in two independent lines of FUS P525L fibroblasts. **B)** RNA-FISH using a probe detecting total NEAT1 together with a probe detecting polyA+ RNA reveals that NEAT1_1 is abnormally localised to nuclear speckles in FUS P525L fibroblasts. Fraction of cells with speckle-localised NEAT1 is quantified. Numbers of cells analysed are indicated within bars. Scale bars are 10 µm.

4.2.8. Paraspeckles are formed in spinal motor neurons and glial cells of ALS-FUS patients

De novo paraspeckle assembly is one of the pathological characteristics of spinal motor neurons and glial cells in sALS and fALS with TDP-43 pathology (Nishimoto *et al.* 2013, Shelkovnikova *et al.* 2018). We performed NEAT1 RNA-FISH on human spinal cord sections of ALS-FUS patients to examine paraspeckle formation. Three ALS-FUS cases characterised by early disease onset and predominantly spinal motor neuron degeneration, clinically and histopathologically representing the majority of ALS-FUS cases, were included in the analysis (Table 4.1). sALS cases served as a positive control. Paraspeckles were detected in all three ALS-FUS cases, being present in on average ~27% of spinal neurons examined (Figure 4.12A), and this is comparable with what has been observed in sALS and other fALS cases (Shelkovnikova *et al.* 2018). Paraspeckles were also detected in glial cells (Figure 4.12A). This result was also confirmed using RNAscope® ISH with NEAT1_2 probe (Figure 4.12B). Therefore, augmented paraspeckle assembly in spinal cord cells is a shared pathological phenotype in the majority of ALS cases including ALS-FUS.

In conclusion, the presence of mutant FUS in the nucleus causes NEAT1 accumulation and augmented paraspeckle assembly. However, these paraspeckles are structurally and functionally impaired due to weakened interaction of mutant FUS protein with core paraspeckle proteins and NEAT1_2. This in turn leads to abnormal accumulation of NEAT1_1 in the nucleoplasm outside of paraspeckles, which might have adverse effects on normal cellular functions.

Table 4.1 Characteristics of ALS-FUS cases used in the study

Patient No	Sex	Age at onset	Mutation	FUS pathology in spinal cord	References
1	M	33	p.R521C	FUS-positive GCI	Vance et al., 200
2	F	35	p.R521C	FUS-positive NCI and GCI	King et al., 2015
3	F	35	p.R521H	FUS-positive NCI and GCI	

*GCI – glial cytoplasmic inclusions

*NCI – neuronal cytoplasmic inclusions

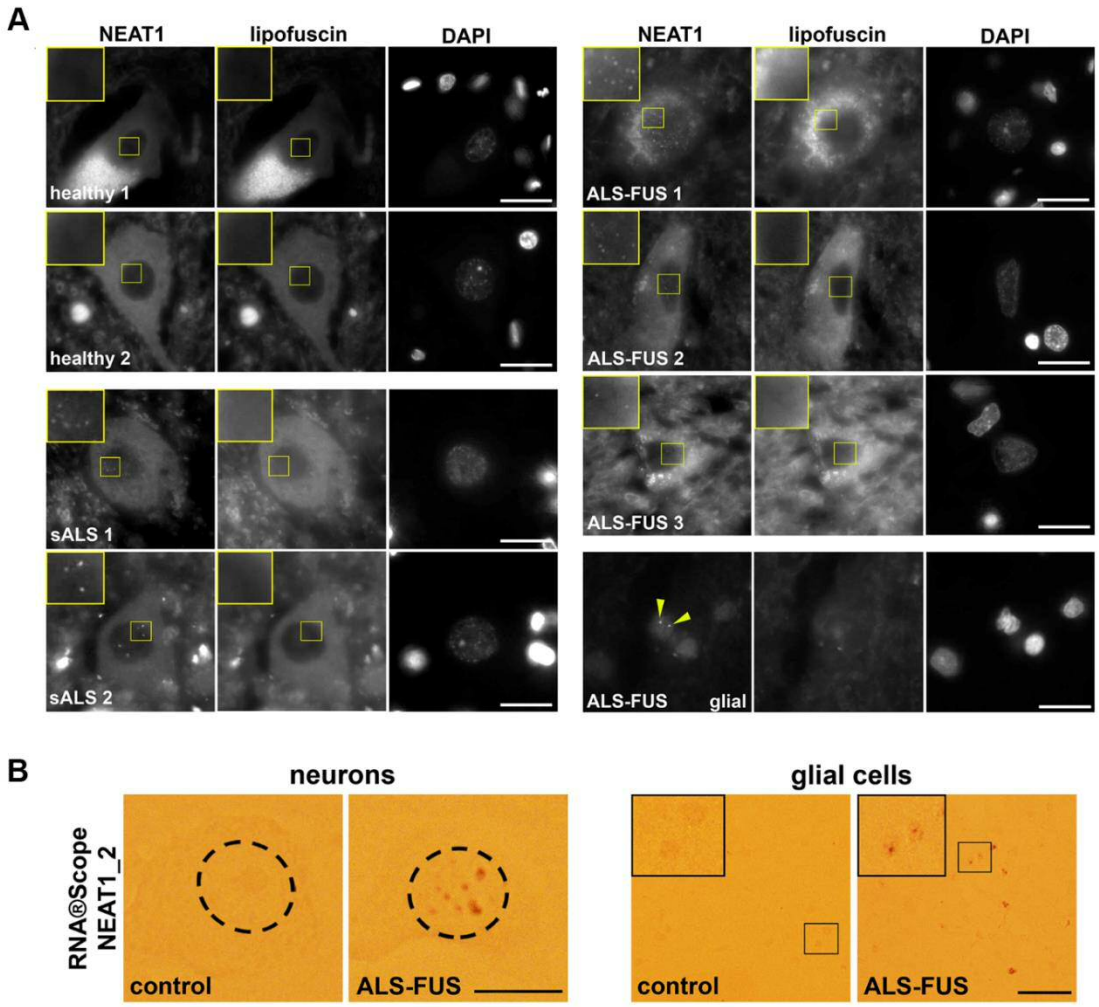

Figure 4.12 Accumulation of paraspeckles in spinal neurons and glial cells in ALS-FUS.

A) Paraspeckle formation in spinal neurons and glia of ALS-FUS and sALS patients is visualised using RNA-FISH with a probe recognising total NEAT1. Images are taken in the orange (NEAT1) and green (Lipofuscin) channels to distinguish between specific NEAT1 signal and non-specific autofluorescence from lipofuscin. Arrowheads indicate paraspeckles in a glial cell. Scale bars are 10 µm. **B)** Representative images of paraspeckles in spinal neurons (left panels) and glial cells (right panels) in an ALS-FUS patient visualised with RNAscope® ISH using NEAT1_2 probe. Neuronal nuclei are circled. Scale bars are 10 µm (left panels) and 50 µm (right panels). This dataset is generated by Dr. Tatyana Shelkovnikova.

4.3. Discussion

In this study, by analysing FUS ΔNLS clones, I have demonstrated upregulation of both NEAT1 isoforms in the presence of endogenous levels of mutant FUS protein. Since nuclear FUS is an important protein component required for the formation of higher order structure of paraspeckles (Yasuda et al. 2013), homozygous FUS ΔNLS clones did not form paraspeckles regardless of upregulated NEAT1_2. In contrast, in heterozygous FUS ΔNLS clones, where sufficient level of mutant FUS is present in the nucleus, hyper-assembly of paraspeckles was observed due to elevated NEAT1_2. Nevertheless, the paraspeckles formed in heterozygous clones were defective in both structure and function, which is caused by decreased interaction between mutant FUS protein and core paraspeckle proteins. Hyper-assembly of structurally impaired paraspeckles was also confirmed in fibroblasts derived from ALS-FUS patients, and enhanced paraspeckle formation was also observed in the spinal cord of ALS-FUS patients. This study provides further evidence for the enhanced paraspeckle formation in spinal motor neurons and glial cells in ALS with different aetiology, even in the cases with the essential structural component of paraspeckles – FUS is mutated.

Apart from paraspeckle abnormalities, other potential toxic effects of mutant FUS in the nucleus have also been suggested by others. Nuclear mutant FUS (FUS R514G) contributes to the loss of nuclear Gems, through its increased binding to survival motor neuron (SMN) protein – an essential protein component of Gems (Yamazaki *et al.* 2012, Sun *et al.* 2015). Although the exact function of nuclear Gems is not clear, it is generally believed that they might participate in snRNP maturation, and snRNP is crucial for the formation of spliceosomes, whose malformation is detrimental for RNA splicing process (Zhang *et al.* 2008, Lotti *et al.* 2012). Moreover, FUS is known to participate in DNA damage response by direct interaction with histone deacetylase 1 (HDAC1), and mutant FUS (FUS R521C) binds to WT FUS to form a stable complex thereby interfering with normal FUS-HDAC1 interaction (Wang *et al.* 2013, Qiu *et al.* 2014). In addition, FUS regulates target gene expression through its direct interaction with single-stranded DNA response elements present in their promoter regions (Tan *et al.* 2012), therefore nuclear mutant

FUS could affect this interaction resulting in altered target gene expression, although there is no direct evidence to support this hypothesis yet. Taken together, nuclear gain-of-function of mutant FUS may play more important roles in the development of FUSopathy than previously appreciated.

NEAT1 expression level is known to increase in response to several environmental stimuli, such as viral infection and proteasomal inhibition. However, the molecular mechanism that upregulates the basal NEAT1 level is largely unknown. Certain paraspeckle proteins, such as SFPQ and NONO, are known to stabilise NEAT1_2 transcripts (Hirose and Nakagawa 2012), therefore accumulation of these proteins can result in NEAT1_2 upregulation. However, I could not detect significant upregulation of SFPQ and NONO in FUS ΔNLS clones, indicating that other regulatory mechanisms must be involved. Furthermore, according to unpublished data obtained in our laboratory, transcriptomic analysis of FUS ΔNLS clones did not highlight any cellular pathways, dysregulation of which might explain the upregulation of NEAT1. It is possible that slight alterations of multiple pathways caused by FUS mutations exert synergetic effect ultimately resulting in NEAT1 upregulation. In addition, due to the relatively low read coverage of my transcriptomic analysis (~ 20 M reads/sample), changes of low-abundance transcripts that have impacts on NEAT1 expression might have been overlooked. Further studies are required to decipher the underlying mechanisms of NEAT1 upregulation in the cells expressing mutant FUS protein.

An immediate consequence of disrupted paraspeckle integrity in the cells expressing mutant FUS is the increased release of free NEAT1_1 transcripts to the nucleoplasm. As one of the most abundant lncRNAs in human cells (Gibb *et al.* 2011, Li *et al.* 2017), NEAT1_1 likely has its own paraspeckle-independent functions. For example, NEAT1_1 increases its target gene expression by directly interacting with histone H3 of chromatin, thereby promoting chromatin active state (Chakravarty *et al.* 2014, West *et al.* 2014). Therefore, it is highly likely that the accumulation of free NEAT1_1 in the nucleoplasm will alter the expression levels of multiple genes, causing widespread changes in cellular pathways. Recently, researchers reported that

in human cells where NEAT1_2 is specifically knocked out, NEAT1_1 appeared as numerous nuclear foci (microspeckles) that are distinct from paraspeckles. They are found throughout the nucleus and a subset of them colocalise with splicing speckles (Li *et al.* 2017). In addition, NEAT1_1 has been shown to interact with the p53 pathway (Adriaens *et al.* 2016, Mello *et al.* 2017) and directly modulate neuronal excitability (Barry *et al.* 2017). The latter study is particularly interesting as elevated neuronal excitability is a well-known phenomenon in ALS (Bae *et al.* 2013). Yet there is still a long way to go before we could answer how exactly NEAT1_1 function and how the accumulated NEAT1_1 contributes to the ALS-FUS.

ADARB2, which encodes a subtype of RNA-editing enzymes that may play a regulatory role in A-to-I RNA editing (Bass 2002), is found to be significantly downregulated in FUS ΔNLS clones. ADARB2 is found sequestered in the pathological nuclear foci of C9orf72 RNA in the motor neurons of ALS-C9 patients (Donnelly *et al.* 2013), suggesting loss of ADARB2 function in this subset of ALS, although the functional consequences of this pathological changes are not known yet. The results obtained in the current study, together with above report, suggest that ADARB2 depletion might constitute a converging mechanism of ALS-FUS and ALS-C9.

One of the well-established paraspeckle functions is the nuclear retention of A-to-I hyper-edited RNAs (Zhang and Carmichael 2001, Prasanth *et al.* 2005, Chen and Carmichael 2009). Nuclear retention of hyper-edited RNA is considered beneficial for the robust response to environmental stresses, as these RNAs can be rapidly released to the cytoplasm and produce proteins required for cell survival (Prasanth *et al.* 2005). A large number of mammalian transcripts are believed to be regulated in a similar manner (Chen *et al.* 2008, Faulkner *et al.* 2009). How the dysregulation of paraspeckles in ALS-FUS affects nuclear retention of hyper-edited RNA as well as the stress response will be an interesting aspect of FUSopathy to study.

Modulation of miRNA biogenesis is a recently identified function of paraspeckles, where NEAT1 and SFPQ-NONO heterodimer bind to a large number of pri-miRNAs and attract the Microprocessor complex to globally enhance miRNA biogenesis (Jiang *et al.* 2017). Consistently, in FUS ΔNLS

clones, mature miRNA produced from pri-miR-17~92 transcript are significantly decreased. Expression of more than 20-30% of all human protein-coding genes are fine-tuned by miRNAs-induced silencing (Lewis *et al.* 2005), and altered miRNA expression in the CNS is a well-known pathomechanism of ALS. As paraspeckles seem to influence miRNA expression on a global scale, presumably, overall miRNA levels are downregulated in these cells. Therefore, disrupted paraspeckle integrity due to the presence of mutant FUS could possibly contribute to the pathogenesis of ALS through miRNA dysregulation.

In conclusion, my study reports loss and gain of nuclear function for mutant FUS and their possible contribution to ALS-FUS pathogenesis.

Chapter 5. Antiviral immune response, stress granules and ALS-FUS

5.1. Overview

A multi-step model has been proposed to explain the formation of insoluble FUS aggregates in FUSopathy (Droppelmann *et al.* 2014, Shelkovnikova *et al.* 2014a). Although FUS readily aggregates *in vitro*, it has proven difficult to achieve its aggregation *in vivo*, especially in mammals. Rodent models expressing human FUS bearing ALS-associated point mutations do not develop FUS-positive inclusions in affected neurons (Huang *et al.* 2011, Scekic-Zahirovic *et al.* 2016, Sharma *et al.* 2016, Devoy *et al.* 2017, Lopez-Erauskin *et al.* 2018). Our group has previously demonstrated that in order to achieve FUS aggregation in the CNS of murine models, highly aggregate-prone artificial FUS variants lacking both major RNA-binding domains and NLS have to be used (Shelkovnikova *et al.* 2013a, Robinson *et al.* 2015). Therefore, it is conceivable that an additional trigger is needed to promote robust FUS aggregation and inclusion formation in human diseases.

As discussed in Chapter 1, ALS-associated mutant FUS is known to have a strong affinity to SGs (Bosco *et al.* 2010, Dormann *et al.* 2010), cytoplasmic RNP granules heavily implicated in ALS pathogenesis. In addition to being recruited into SGs formed under stress conditions, overexpressed mutant FUS can also form spontaneous cytoplasmic RNP granules that sequester SG marker proteins, and it has been proposed that various cytoplasmic FUS assemblies, when persist, may become the precursors of the pathological FUS inclusions found in ALS-FUS neurons (Kino *et al.* 2011, Shelkovnikova *et al.* 2014a). Conspicuously, FUS-positive inclusions in ALS-FUS are also positive for SG markers (Dormann *et al.* 2010). However, the nature of the stressor(s) that could induce the prolonged presence of FUS assemblies and thereby act as the trigger for FUSopathy still remains elusive. I sought to identify a possible environmental stimulus that can provoke persistent FUS aggregation using ΔNLS clones.

5.2. Results

5.2.1. Poly(I:C) transfection triggers formation of persistent stress granules in WT SH-SY5Y cells

A panel of known triggers of SG assembly that induce neurodegeneration-relevant stresses, including oxidative stress (sodium arsenite, SA), ER stress (dithiothreitol, DTT) and proteasome inhibition (MG132) were tested for their ability to promote persistent SG formation in WT SH-SY5Y cells. I also included a combination of puromycin and the HSP70 inhibitor pifithrin-μ that is reported to cause SG formation by a simultaneous accumulation of misfolded proteins and polysome dissociation (Bounedjah *et al.* 2014). Viral infection is also a potent trigger of SG formation, therefore I also tested poly(I:C), the viral dsRNA mimic. It has been proposed that multiple SG assembly-disassembly cycles caused by repetitive stresses might result in the appearance of persistent SGs (Wolozin 2012). Since SA, DTT and MG132 are reversible stressors, I was able to examine the effect of repetitive stresses. The timeline of treatment for each stressor is shown in Figure 5.1. SGs were visualised by G3BP1 staining.

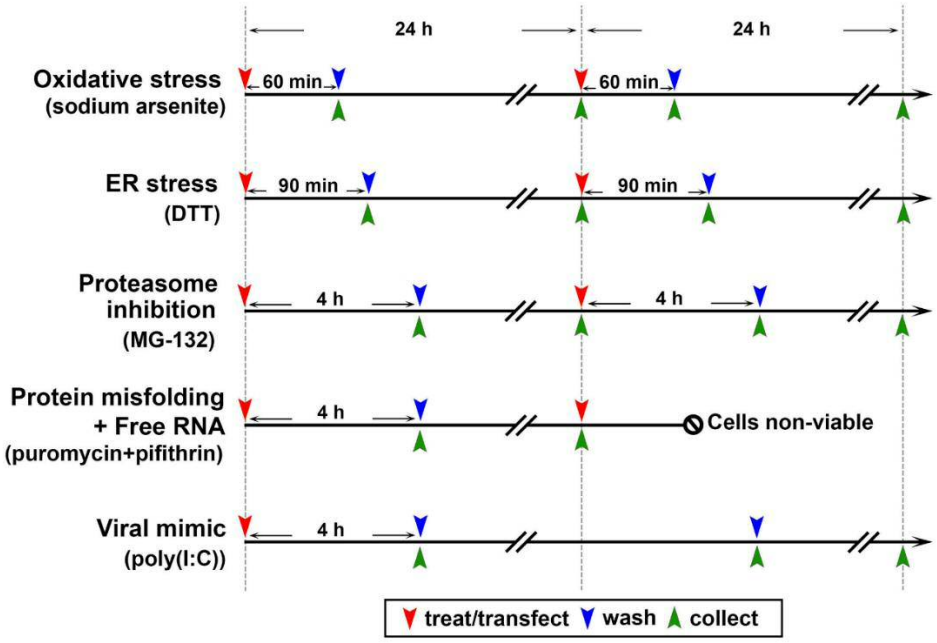

Figure 5.1 Timelines of SG persistence experiments.

Red arrowheads indicate treatment or transfection. Blue arrowheads indicate wash-off. Green arrowheads indicate cell fixation.

SA, DTT, MG132, pifithrin-μ/puromycin and poly(I:C) induced SGs in 100%, 95.3±1.8%, 34.7±2.3%, 30.0±3.6% and 52.4±3.0% cells, respectively (Figure 5.2). Two consecutive treatments with SA, DTT and MG132, separated by a 24 h recovery period, did not increase the proportion of cells containing SGs following the second treatments (Figure 5.2). The viral infection was the only stressor capable of inducing prolonged SG presence among all the stressors tested. SGs were detectable in 47.6±3.5% and 27.7±4.0% the cells transfected with poly(I:C) at 24 h and 48 h post-transfection, respectively, but not in cells subjected to any other stressors (Figure 5.2). Interestingly, viral infection has been claimed to be a risk factor for ALS (Celeste and Miller 2018, Kury *et al.* 2018, Xue *et al.* 2018a), and an increasing number of viruses have been found to interact with the SG pathway (Protter and Parker 2016, McCormick and Khaperskyy 2017). Therefore, I decided to further investigate this SG-inducing stress.

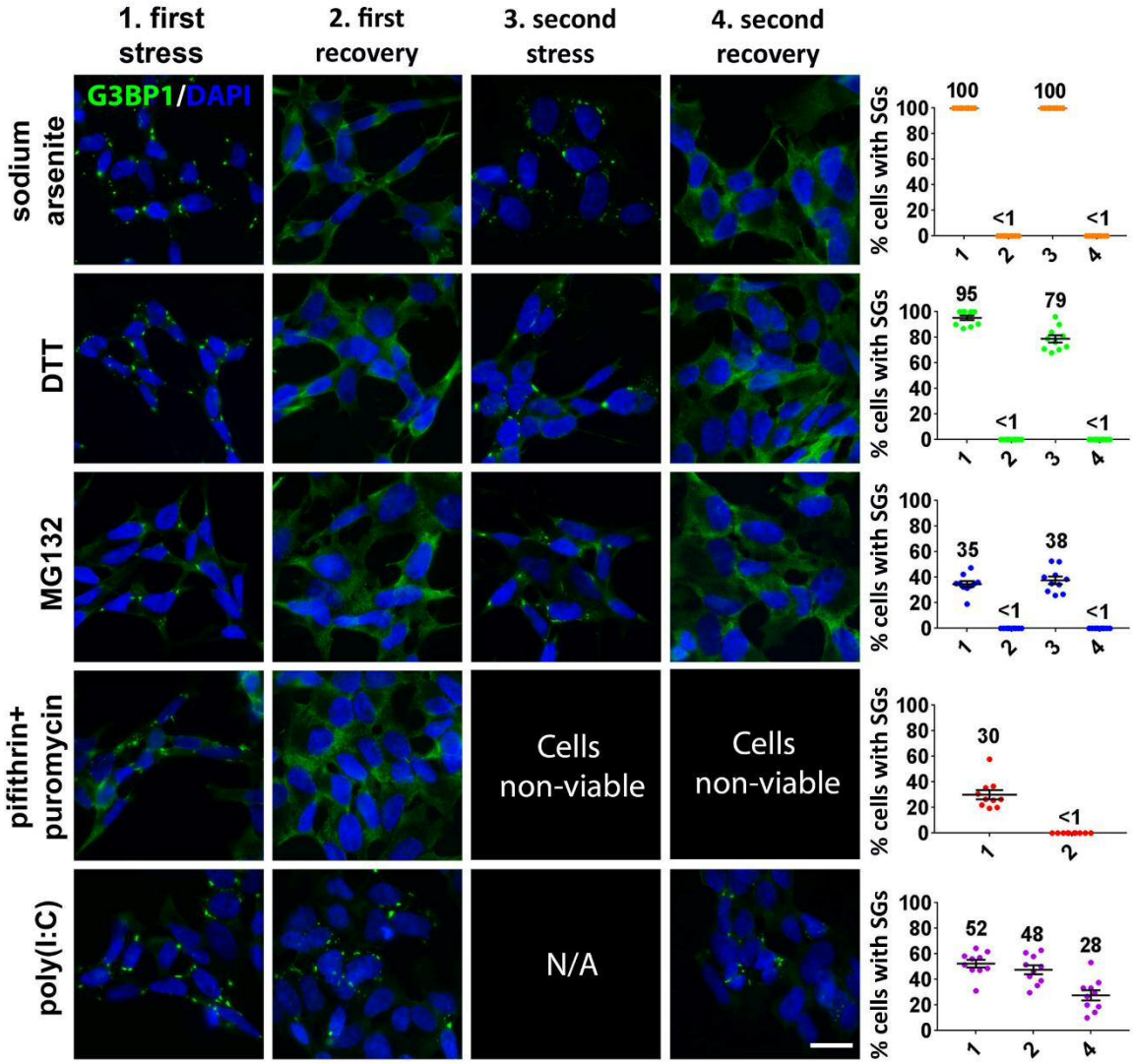

Figure 5.2 A viral dsRNA mimic triggers formation of persistent stress granules.

Representative images and quantification of SG-containing cells after stress and recovery. Scatter plots show percentage of SG-containing cells at each time-point. X-axis labelling 1 ~ 4 correspond to 1st stress, 1st recovery, 2nd stress, 2nd recovery, respectively. Between 250 and 300 cells were analysed per time point for each stressor. Scale bar is 10 μm.

5.2.2. Cytoplasmic mutant FUS is recruited into the poly(I:C)-induced stress granules

Although several stresses, including oxidative stress, proteasome inhibition, heat shock and osmotic stress, are known to promote the assembly of FUS-positive SGs in cells expressing mutant FUS protein (Dormann *et al.* 2010,

Sama *et al.* 2013, Shelkovnikova *et al.* 2014a, Mateju *et al.* 2017), mutant FUS incorporation into dsRNA-induced SGs has not been reported. First, I showed that overexpressed GFP-tagged FUS R522G and ΔNLS were readily recruited into SGs induced by poly(I:C) transfection (Figure 5.3A). Next, I transfected ΔNLS clones with poly(I:C) and found that endogenous mutant FUS was also readily recruited into poly(I:C)-induced SGs (Figure 5.3B). In WT cells FUS was absent from SGs induced by poly(I:C) (Figure 5.3B). Furthermore, significantly more cells contained SGs at 2 h and 4 h post-transfection in ΔNLS_het clones as compared to WT cells, and even after 24 h, ΔNLS_het clones still had more cells containing SGs (Figure 5.3C). In contrast, there was no difference in the numbers of SG-containing cells between ΔNLS_het and WT cells during the recovery from SA stress (Figure 5.3C).

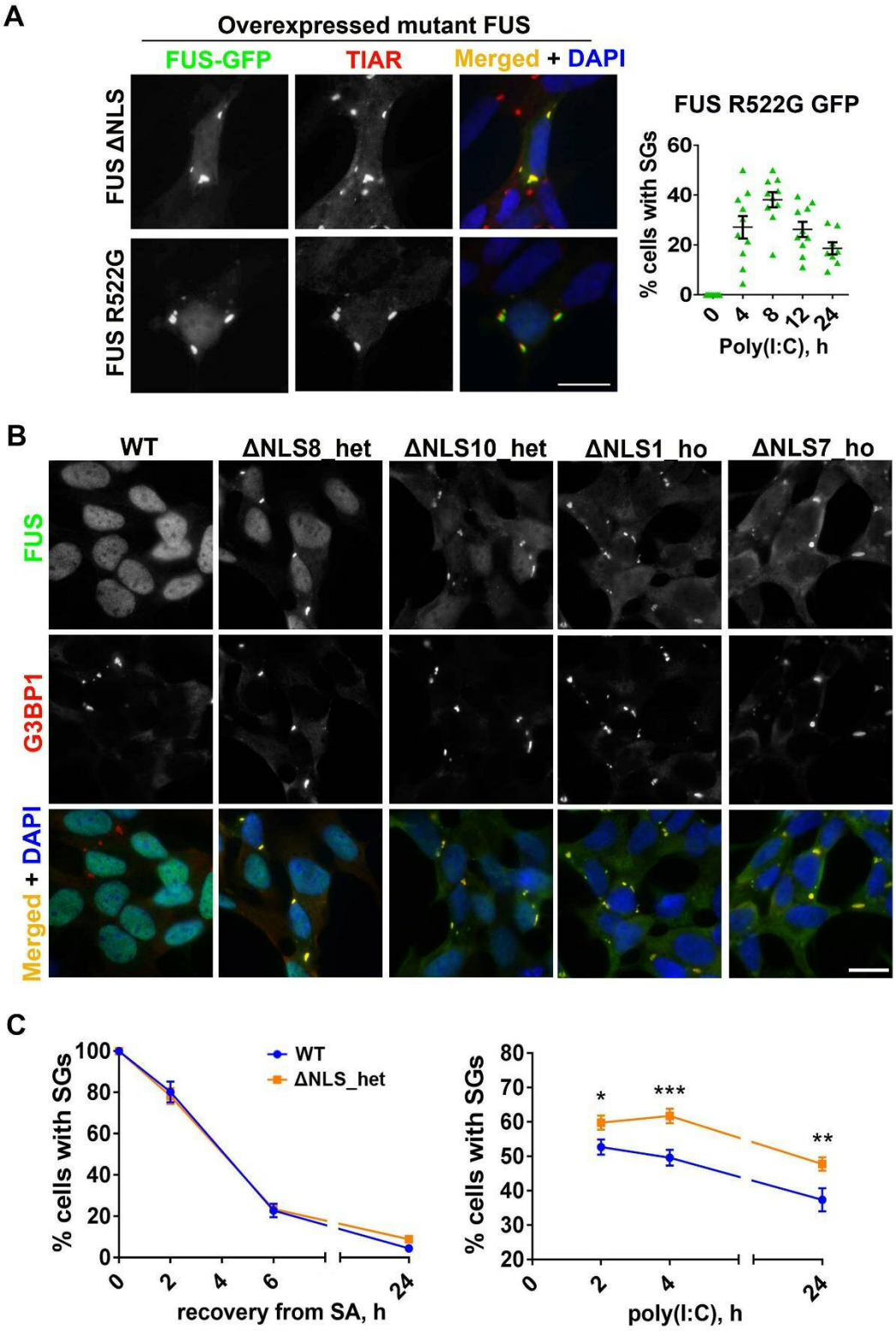

Figure 5.3 Mutant FUS is recruited to poly(I:C)-induced stress granules.

A) WT SH-SY5Y cells overexpressing GFP-tagged FUS protein lacking NLS (FUSΔNLS) or carrying ALS-associated point mutation (FUS R522G) were transfected by poly(I:C). Representative image of cells 4 h post-transfection is shown. Proportion of cells containing SGs among GFP-FUS R522G-expressing cells were

quantified over 24 h period after poly(I:C) transfection. ≥100 cells were analysed per clone/time-point. **B)** Endogenous mutant FUS is recruited to poly(I:C)-induced SGs in ΔNLS clones. Representative images of 4 h after poly(I:C) transfection are shown. **C)** Poly(I:C), but not sodium arsenite (SA), causes persisting SGs in ΔNLS_het clones. For quantification, data from two heterozygous clones (ΔNLS8_het and ΔNLS10_het) are pooled. Cells were treated with SA for 1 h, washed and analysed during recovery. ≥500 cells were analysed per clone/time-point; Student's t-test; *p<0.05; **p<0.01; ***p<0.001. Scale bars are10 µm.

5.2.3. Poly(I:C) induces morphologically distinct stress granules

I noticed that poly(I:C)-stimulated cells usually developed large, few-per-cell SGs, while cells treated with other stressors formed multiple small- or medium-sized SGs. The proportion of cells containing 1, 2 or >2 SGs per cell among all SG-positive cells, as well as mean SG sizes, were quantified in ΔNLS clones transfected with poly(I:C) for 6 h or treated with SA for 1.5 h. Indeed, quantification showed that poly(I:C)-transfected ΔNLS cells contained 1-2 large SGs per cell, as compared to SA-treated cells which developed smaller and more abundant SGs (Figure 5.4A), as confirmed by quantification (Figure 5.4B). Strikingly, in ΔNLS_ho cells, poly(I:C)-induced large SGs were able to sequester a substantial amount of FUS, causing its significant depletion from the nucleus (Figure 5.4C).

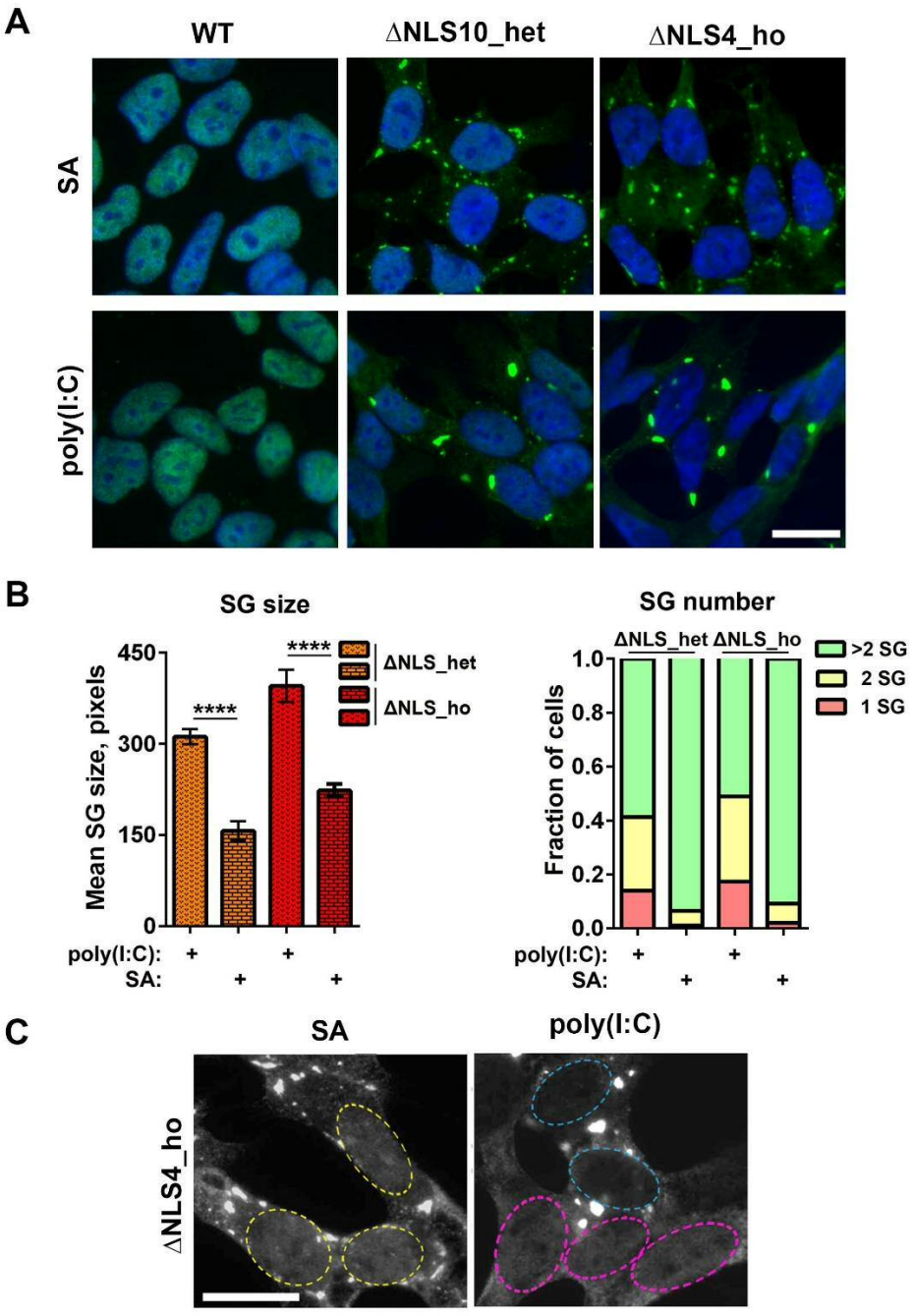

Figure 5.4 Stress granules induced by poly(I:C) are morphologically distinct from stress granules induced by sodium arsenite.

A) Representative images showing SGs induced by SA and poly(I:C) in ΔNLS clones visualised using a FUS antibody. **B)** SG sizes and proportion of cells containing 1, 2 and >2 SGs are quantified in FUSΔNLS cells transfected with poly(I:C). 250~400 cells were analysed for SG size and 90~150 cells were analysed for SG number. **C)** Poly(I:C)-induced SGs in ΔNLS_ho clone sequester significant amount of FUS protein causing its near-complete clearance from the nucleus. Nuclei of SA-treated cells are delineated with yellow circles. Nuclei of poly(I:C)-transfected and non-transfected cells are delineated with blue and pink circles, respectively. Cells were

analysed 6 h after poly(I:C) transfection and 1.5 h after SA treatment. Scale bars are 10 μm.

5.2.4. Preformed cytoplasmic FUS granules coalesce into persistent FUS aggregates in response to poly(I:C) stimulation

It has been demonstrated that exogenously expressed mutant FUS can form cytoplasmic FGs spontaneously in a fraction of unstressed cells (Kino *et al.* 2011, Shelkovnikova *et al.* 2014a). The presence of cytoplasmic FGs in some of my ΔNLS clones (ΔNLS2_het and ΔNLS11_het) proves that mutant FUS expressed at endogenous level can also support the assembly of FGs. Similar to exoFGs formed by overexpressed mutant FUS, the endoFGs in ΔNLS clones were negative for SG markers (shown in Chapter 3, Figure 3.10).

In the cells treated with SA, exoFGs coalesce into large FUS aggregates (exoFAs hereafter), which sequester SG proteins (Shelkovnikova *et al.* 2014a). I found that poly(I:C) was also able to trigger the formation of FAs in cells containing endoFGs (Figure 5.5) and exoFGs (Figure 5.6). These FAs formed by endoFG coalescence, termed endoFAs, were morphologically distinct from FUS-containing SGs formed in endoFG-negative ΔNLS clones. Although endoFAs were capable of recruiting core SG proteins G3BP1 and TIAR, their distribution within the structure was different from FUS-containing SGs. In FAs, the immunofluorescent signal of G3BP1 and TIAR was intermingled with FUS signal, showing a “patchy” pattern, whereas in FUS-containing SGs, G3BP1, TIAR and FUS were distributed homogenously throughout the structure (Figure 5.5A,B). Similar to FUS-positive SGs, poly(I:C)-induced endoFAs also persisted in ΔNLS_het cells, being present in 45.6±2.1% of cells 24 h post-transfection (Figure 5.5C).

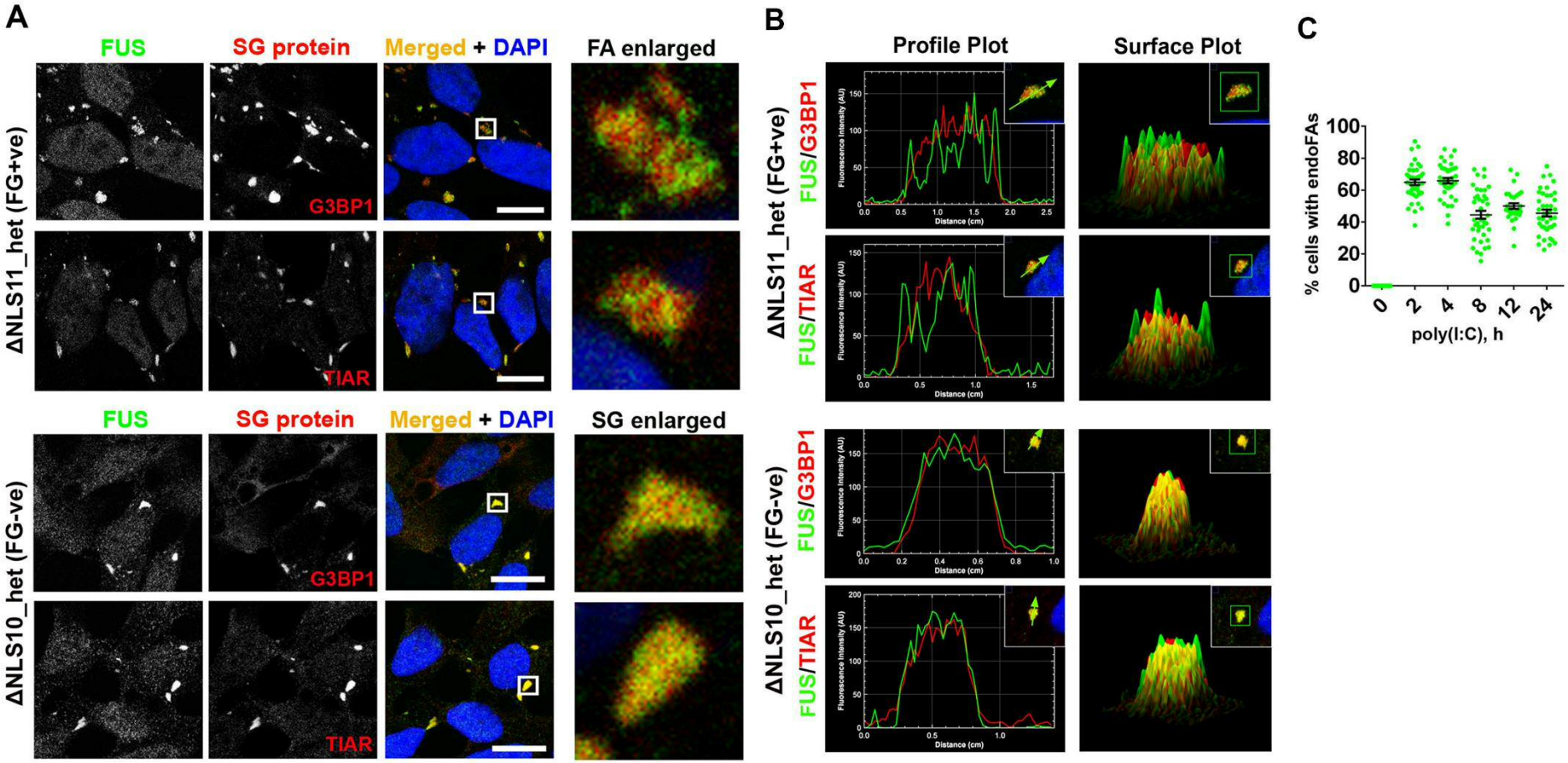
A
FUS
SG protein
Merged + DAPI
FA enlarged
ΔNLS11_het (FG+ve)
G3BP1
TIAR
FUS
SG protein
Merged + DAPI
SG enlarged
ΔNLS10_het (FG-ve)
G3BP1
TIAR
B
Profile Plot
Surface Plot
ΔNLS11_het (FG+ve)
FUS/G3BP1
FUS/TIAR
ΔNLS10_het (FG-ve)
FUS/G3BP1
FUS/TIAR
Fluorescence Intensity (AU)
Distance (cm)
C
% cells with endoFAs
poly(I:C), h

Figure 5.5 Mimicking viral infection promotes formation of persistent cytoplasmic FAs in ΔNLS clones containing FGs.

A) In endogenous FUS aggregates (endoFAs) induced by poly(I:C) transfection, fluorescent signals of SG proteins G3BP1 and TIAR do not completely overlap with that of mutant FUS. However, in FUS-containing SGs formed in ΔNLS10_het clone, these signals are more homogeneous and overlap. Representative confocal images are shown; scale bars are 10 μm. **B)** Profile plots and surface profiles of endoFAs and FUS-containing SGs are shown. **C)** Cells containing endoFAs in ΔNLS11_het clone transfected with poly(I:C) are quantified over a 24. ≥500 cells were analysed per clone/time-point.

In order to study the dynamics of FA formation induced by poly(I:C), I recorded the assembly of exoFAs in SH-SY5Y cells containing exoFGs formed by GFP-tagged FUS R522G, using confocal live imaging. Preformed exoFGs assembled into exoFAs promptly after poly(I:C) stimulation, and multiple small FAs grew by fusion, eventually forming one large aggregate per cell, and such cells stayed viable for at least 12 h of recording period (Figure 5.6).

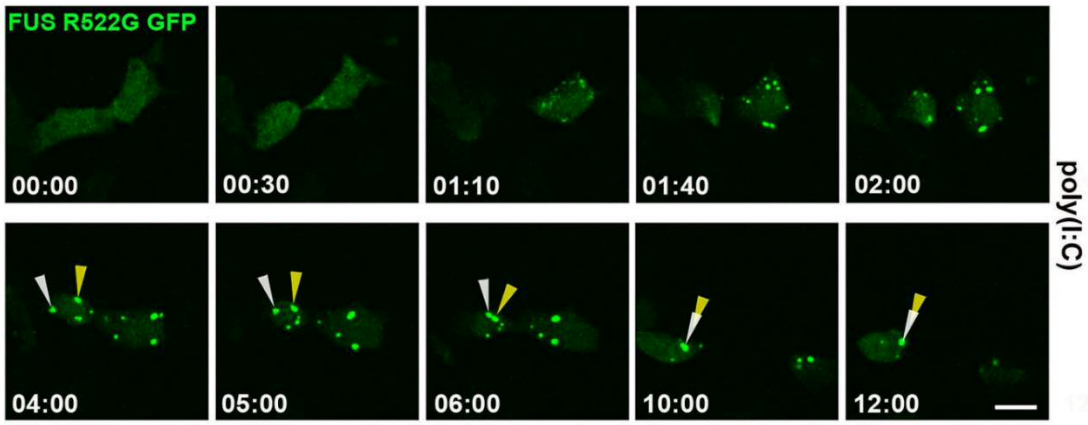

Figure 5.6 Poly(I:C) induces persistent FAs in cells containing exogenous FGs (exoFGs).

Cells were transfected with a plasmid expressing FUS R522G GFP 24 h before poly(I:C) transfection. Immediately after poly(I:C) transfection, two cells with preformed exoFGs were followed up for 12 h using confocal live imaging. Arrowheads indicate two aggregates that eventually fuse to form one large aggregate. Scale bar is 10 μm.

5.2.5. Poly(I:C)-induced mutant FUS assemblies sequester nucleocytoplasmic transport factors and the autophagy receptor optineurin

Aggregates composed of mutant FUS have been shown to trap other proteins, such as P body and paraspeckle components and SMN complex factors, resulting in their loss of function (Groen *et al.* 2013, Shelkovnikova *et al.* 2014a, Shelkovnikova *et al.* 2014b). Optineurin, an autophagy receptor protein encoded by ALS-associated *OPTN* gene, plays important regulatory functions in critical cellular processes on the crossroads of autophagy and anti-viral immunity (Ryan and Tumbarello 2018). Previously, optineurin has been found in the FUS-positive inclusions in ALS-FUS post-mortem tissue (Ito *et al.* 2011b). I found that optineurin was a component of poly(I:C)-induced SGs (Figure 5.7A) in WT SH-SY5Y cells, and significantly more optineurin was recruited into the FUS-containing SGs formed in ΔNLS clones compared to those in WT cells (Figure 5.7B). Furthermore, optineurin was also detected in the exoFAs formed by GFP-tagged FUS R522G under basal conditions (Figure 5.7C).

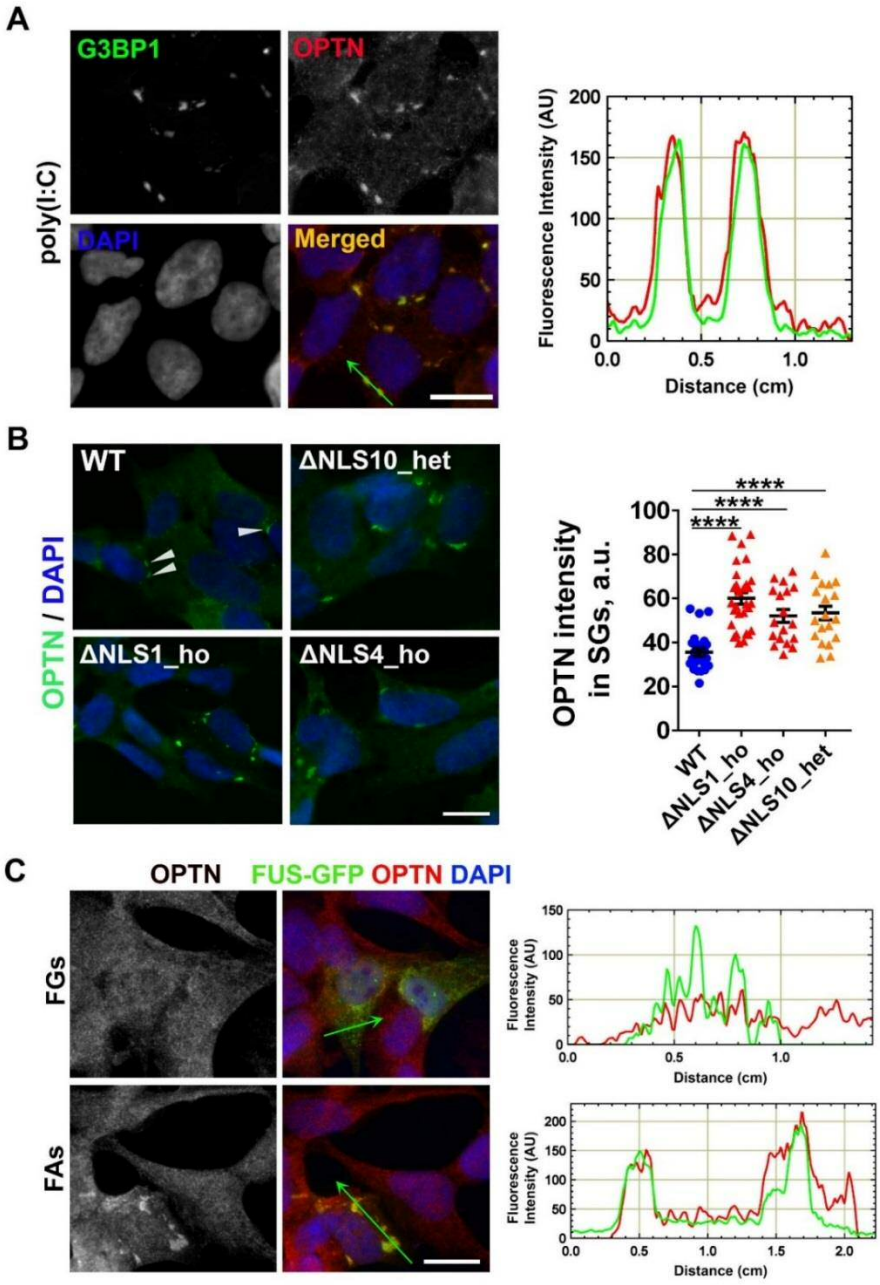

Figure 5.7 Optineurin is recruited to stress granules induced by poly(I:C) and exoFAs under basal conditions.

A) Poly(I:C)-induced SGs in WT SH-SY5Y cells contain optineurin. **B)** Poly(I:C)-induced SGs containing mutant FUS protein sequester more optineurin compared to FUS-negative SGs. Arrowheads indicate SGs containing optineurin in WT cells. Cells were analysed 24 h post-transfection. Optineurin intensity in SGs is quantified (≥30 cells). ****p<0.0001. **C)** Under basal conditions, FAs formed by overexpressed FUS R522G GFP also sequester optineurin. Profile plots are generated along the green arrows in merged images. Scale bars are 10 μm.

Recently, impaired nucleocytoplasmic transport has been suggested as one of the pathomechanisms contributing to ALS pathogenesis (Boeynaems *et al.* 2016). Several nucleocytoplasmic transport factors have been found sequestered into SGs, including transportin 1 (TNPO1), the major receptor for FUS nuclear import (Zhang *et al.* 2018a). I examined whether mutant FUS-containing cytoplasmic assemblies induced by poly(I:C) also sequester transport factors. Proteins located at the inner ring of nuclear pore complex (NPC) - TNPO1 and Karyopherin Alpha 2 (KNPA2), as well as factors at the outer ring of NPC – nucleoporins Nup98 and Nup107, were examined in the poly(I:C)-transfected ΔNLS clones. Indeed, TNPO1, KNPA2, and Nup107 were found to be enriched in poly(I:C)-induced SGs and endoFAs (Figure 5.8).

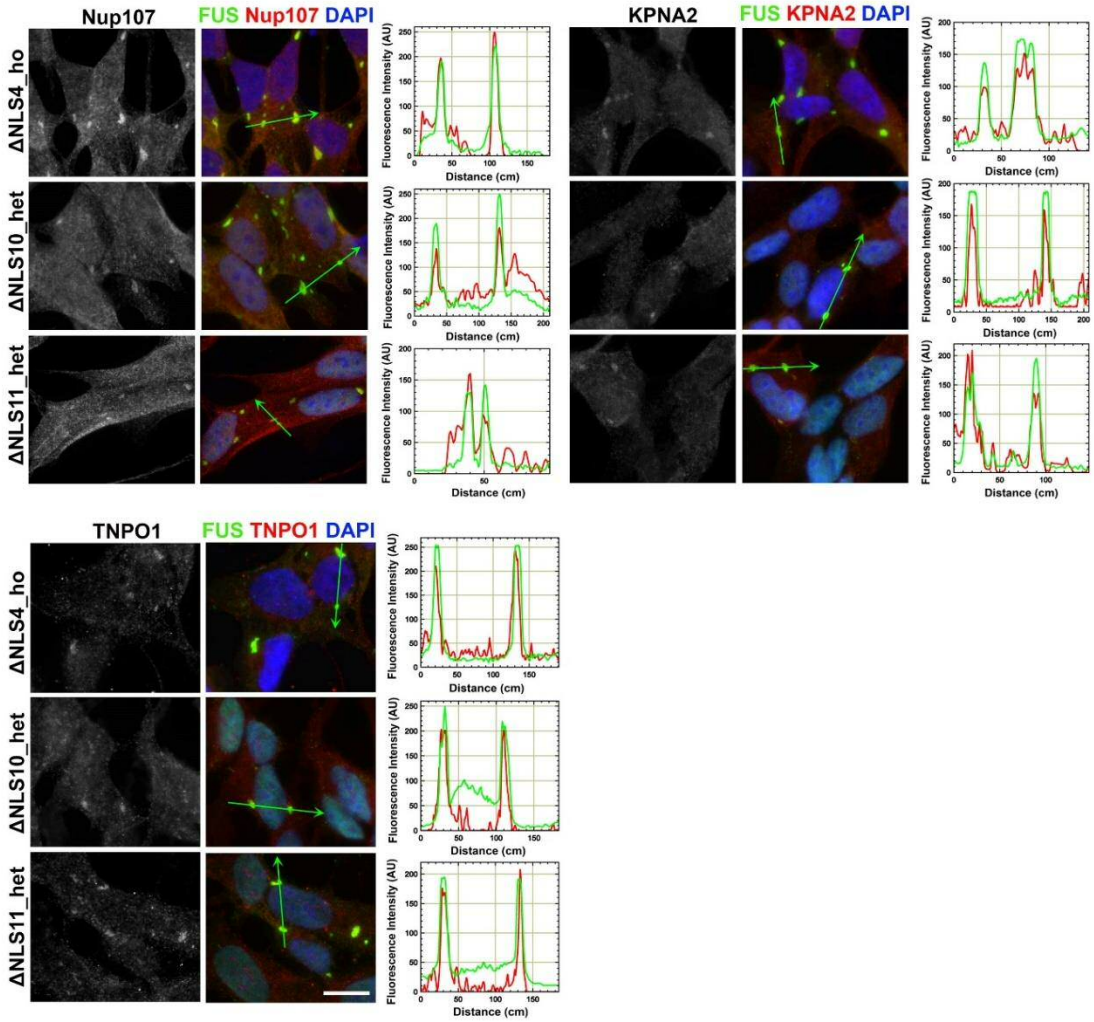

Figure 5.8 Nucleocytoplasmic transport factors Nup107, KPNA2 and TNPO1 are recruited to mutant FUS-containing cytoplasmic assemblies in poly(I:C)-transfected ΔNLS cells.

Cells were analysed 6 h post-transfection. Profile plots are generated along the green arrows in merged images. Scale bar is10 μm.

5.2.6. Cells expressing mutant FUS are hypersensitive to dsRNA toxicity

I asked whether the presence of mutant FUS renders cells more sensitive to dsRNA exposure. Indeed, upon poly(I:C) transfection, significantly more cells underwent apoptosis, as visualised by cleaved caspase 3 (CC3) immunostaining, at least in ΔNLS_ho clones compared to WT cells (Figure 5.9A). The pro-apoptotic factor C/EBP homologous protein (CHOP) is also upregulated in ΔNLS clones (Figure 5.9B). Differences in survival were assessed by the number of CC3-positive cells between fibroblasts bearing FUS P525L mutation and control fibroblasts. CC3 immunostaining at 8 h post-transfection showed significantly more cells undergoing apoptosis in the FUS P525L fibroblast cultures suggesting that mutant fibroblasts show increased susceptibility to poly(I:C)-induced cell death (Figure 5.9C). I concluded that cells expressing mutant FUS are less competent in handling the dsRNA-induced toxicity.

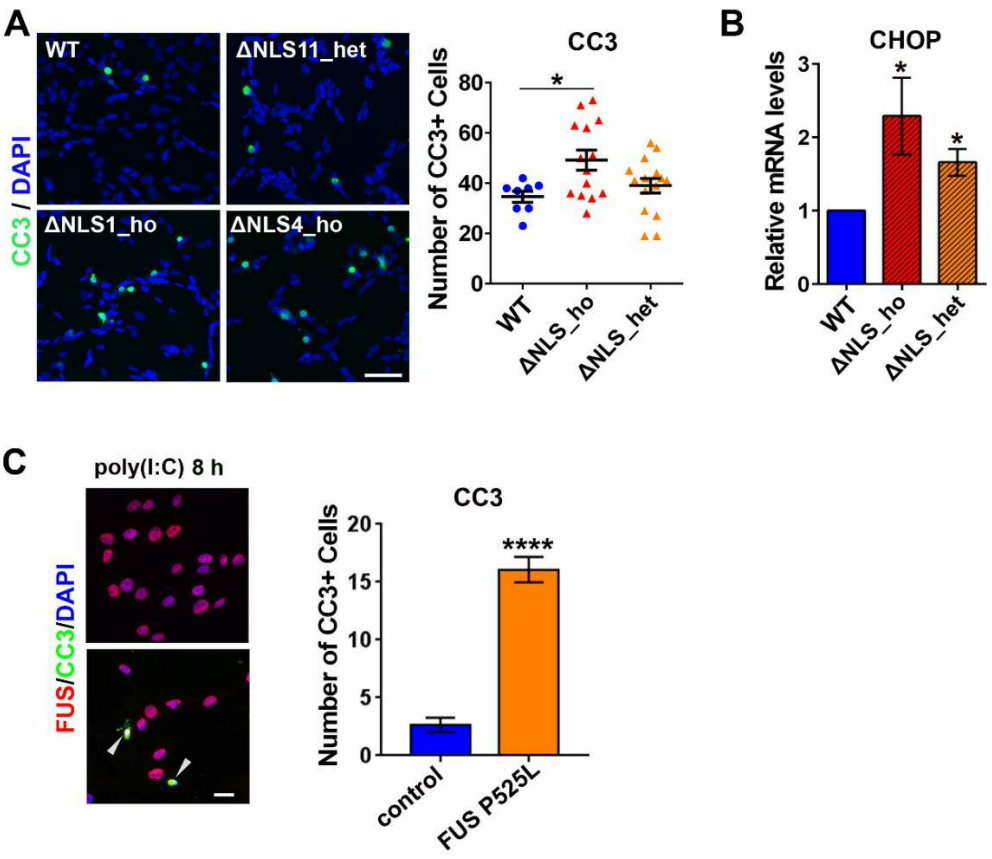

Figure 5.9 Cells expressing mutant FUS protein are hypersensitive to dsRNA toxicity.

A) More cells in ΔNLS_ho clone are positive for cleaved caspase 3 (CC3) upon poly(I:C) transfection. Representative images are shown. For quantification, data from two homozygous (ΔNLS1_ho and ΔNLS4_ho) and two heterozygous (ΔNLS10_het and ΔNLS11_het) clones are pooled. Cells were analysed 24 h post-transfection. For each clone, ≥7 fields of view (x20 magnification) were analysed. Mann-Whitney U-test; *p<0.05. Scale bar is 50 μm. **B)** Pro-apoptotic factor CHOP is upregulated in ΔNLS clones compared to WT cells after poly(I:C) transfection. Cells were analysed at 24 h post-transfection. Data from three homozygous (ΔNLS1_ho, ΔNLS4_ho and ΔNLS7_ho) and three heterozygous (ΔNLS2_het, ΔNLS10_het and ΔNLS11_het) clones are pooled (N=3 for each clone). Mann-Whitney U-test; *p<0.05. **C)** Fibroblasts derived from an ALS patient carrying FUS P525L mutation are more sensitive to poly(I:C) toxicity compared to the fibroblasts from a healthy individual. CC3-positive cells are quantified at 8 h post-transfection. For control and patient fibroblasts, 9 and 12 fields of view (x20 magnification) were included into analysis, respectively. Arrowheads indicate CC3-positive cells. Student's t-test; ****-p<0.0001. Scale bar, 10 μm.

5.2.7. Type I interferon stimulates accumulation of normal and mutant FUS protein

Previously, FUS was identified as a strong negative regulator of antiviral gene expression (Amit *et al.* 2009). Thus, it is plausible that cells may demand more FUS protein during the antiviral response. Indeed, in WT SH-SY5Y cells, FUS mRNA was upregulated upon poly(I:C) transfection as measured by qPCR (Figure 5.10A). Type I interferons (IFNs) are the principal drivers of gene expression changes in response to dsRNA. Therefore, I examined whether the FUS mRNA upregulation observed after poly(I:C) stimulation is downstream of IFN signalling. IFNbeta is the main type I IFN induced by poly(I:C) in SH-SY5Y cells (Shelkovnikova *et al.* 2018). As predicted, treatment of cells using IFNbeta resulted in a significant increase in FUS mRNA levels, an effect that peaked at 4 h post-treatment and declined over time (Figure 5.10B). More pronounced FUS mRNA increase was achieved by IFNbeta treatment than by poly(I:C) transfection, consistent with <100% transfection efficiency and hence IFN induction only in a fraction of cells in poly(I:C)-stimulated cultures. In line with mRNA increase, FUS protein also accumulated in IFNbeta-treated cells in a time-dependent manner. IFN-alpha/beta receptor alpha chain (IFNAR1) degradation was observed following IFNbeta treatment, which was consistent with the well-established notion that IFNARs undergo degradation upon activation by ligands (de Weerd and Nguyen 2012) (Figure 5.10C).

Next, I tested whether IFNbeta could exert a similar effect on mutant FUS. Like in WT cells, FUS protein levels increased in ΔNLS clones when measured after 24 h IFNbeta treatment (Figure 5.10D). Strikingly, both normal and mutant FUS proteins continued to accumulate 24 h after IFNbeta withdrawal from the medium (Figure 5.10E). The subcellular localisation of FUS protein in ΔNLS clones remained unaffected (Figure 5.10F).

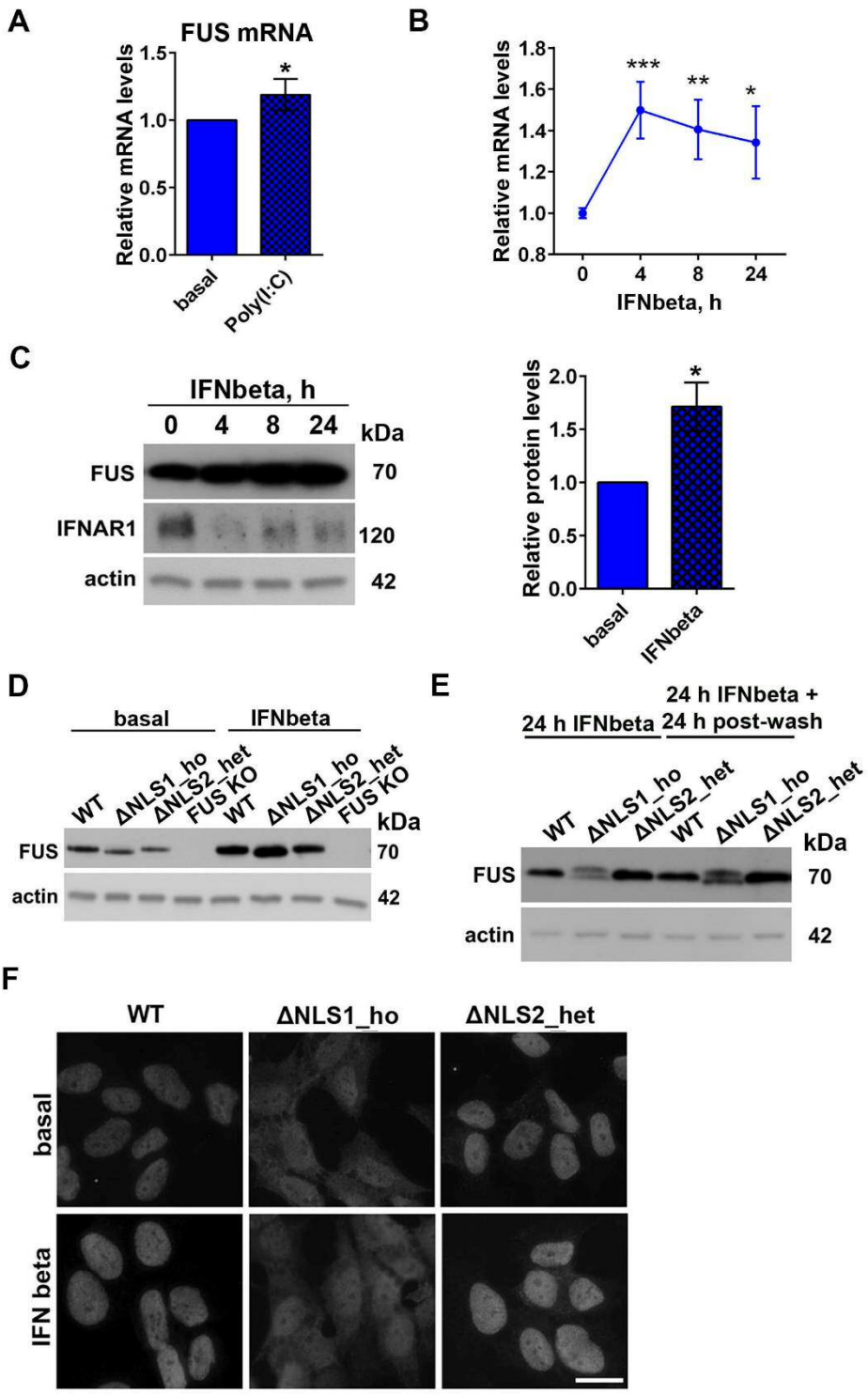

Figure 5.10 IFNbeta treatment causes accumulation of both WT and mutant FUS protein.

A) Poly(I:C) transfection causes upregulation of FUS mRNA levels in WT SH-SY5Y cells. Cells were analysed at 24 h post-transfection. N=4, *p<0.05. **B)** IFNbeta stimulation alone increases FUS mRNA level in WT SH-SY5Y cells. N=4-5. *p<0.05; **p<0.01; ***p<0.001. **C)** FUS protein accumulates upon IFNbeta treatment in a time-

dependent manner in WT SH-SY5Y cells. Representative western blot and quantification are shown. N=3, *p<0.05. IFNAR1 ligand-dependent degradation is shown as the readout of receptor activation. **D)** IFNbeta treatment also causes accumulation of mutant FUS proteins in ΔNLS cells. FUS KO clone was included as a negative control. Cells were analysed after 24 h treatment. **E)** FUS protein continues to accumulate after the removal of IFNbeta from culture media in both WT cells and ΔNLS clones. Cells were treated with IFN beta for 24 h, washed and analysed after another 24 h. Of note, the different appearances of the FUS protein bands of ΔNLS1_ho clone in panel D and E can be explained by the different gel used for western blot (Pre-cast gradient gel was used in panel D whereas house-made SDS-PAGE gel was used in panel E). **F)** Subcellular localisation of WT and mutant FUS protein does not change upon IFNbeta treatment.

Of note, the levels of FUS protein did not increase in poly(I:C)-transfected cells despite mRNA upregulation (Figure 5.11A). Puromycin labelling of nascent proteins revealed significantly reduced protein translation in poly(I:C)-transfected cells, but not in the cells treated with IFNbeta. This finding could explain the discrepancy between FUS mRNA and protein levels in poly(I:C)-stimulated cells (Figure 5.11B).

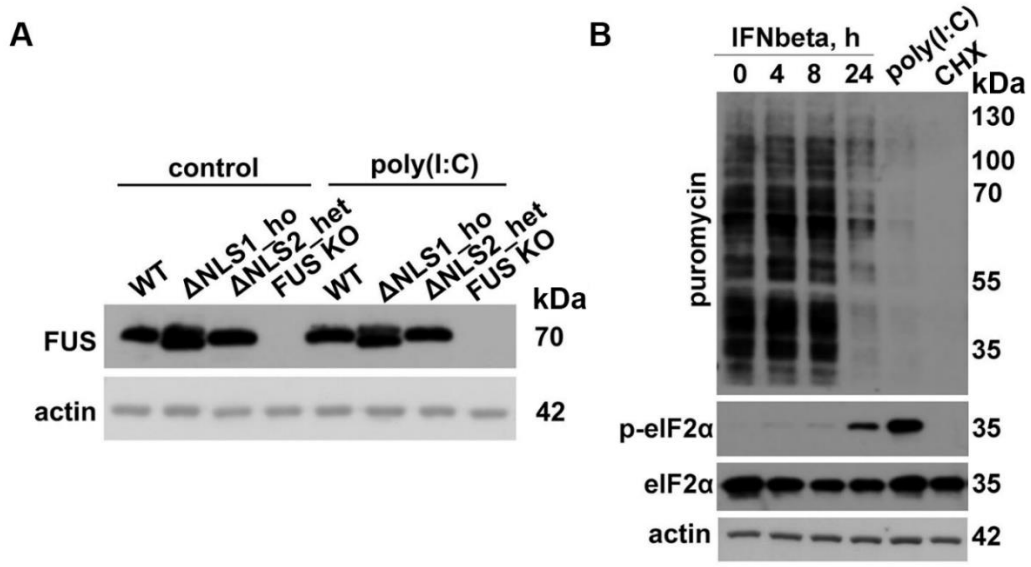

Figure 5.11 Poly(I:C) transfection does not cause FUS protein accumulation due to impaired protein translation.

A) FUS proteins do not accumulate upon poly(I:C) transfection in WT or FUSΔNLS cells. Cells were analysed at 24 h post-transfection. **B)** Poly(I:C) transfection

significantly impairs protein translation due to eIF2α phosphorylation as revealed by puromycin labelling of nascent proteins. IFNbeta treatment did not affect protein translation up to 8 h of treatment. Cells collected at 8 h after poly(I:C) transfection, and at indicated time-points for IFNbeta treatment. Protein synthesis inhibitor cycloheximide (CHX) treatment was carried out as a negative control.

5.2.8. IFNbeta induces FUS mRNA accumulation by increasing its stability

In IFNbeta-treated cells, FUS mRNA can be increased either through a transcriptional upregulation or due to its increased stability.

qPCR quantification revealed that the levels of FUS pre-mRNA did not increase upon IFNbeta stimulation (Figure 5.12A). Furthermore, transcription inhibition by actinomycin D or 5,6-dichloro-1-beta-D-ribofuranosylbenzimidazole (DRB) did not prevent FUS mRNA upregulation (Figure 5.12B). IFNbeta signalling is mainly mediated by the transcription factor signal transducer and activator of transcription 1 (STAT1), and *FUS* gene is known to possess a STAT1-binding site in the promoter region. However, STAT1 knockdown by siRNA did not affect FUS mRNA upregulation in response to IFNbeta (Figure 5.12C). Taken together, these findings suggest that transcriptional mechanism is unlikely involved in the IFNbeta-induced FUS mRNA upregulation.

Since the stability of mRNAs is mainly regulated by polyadenylation, I performed poly(A) tail-length assay (PAT) to compare the poly(A) tail length of FUS mRNA before and after IFNbeta treatment. IFNbeta exposure indeed shifted the intensity of PCR product smear towards longer poly(A) tails (Figure 5.12D), indicating the presence of more stable FUS mRNA in the cells treated with IFNbeta.

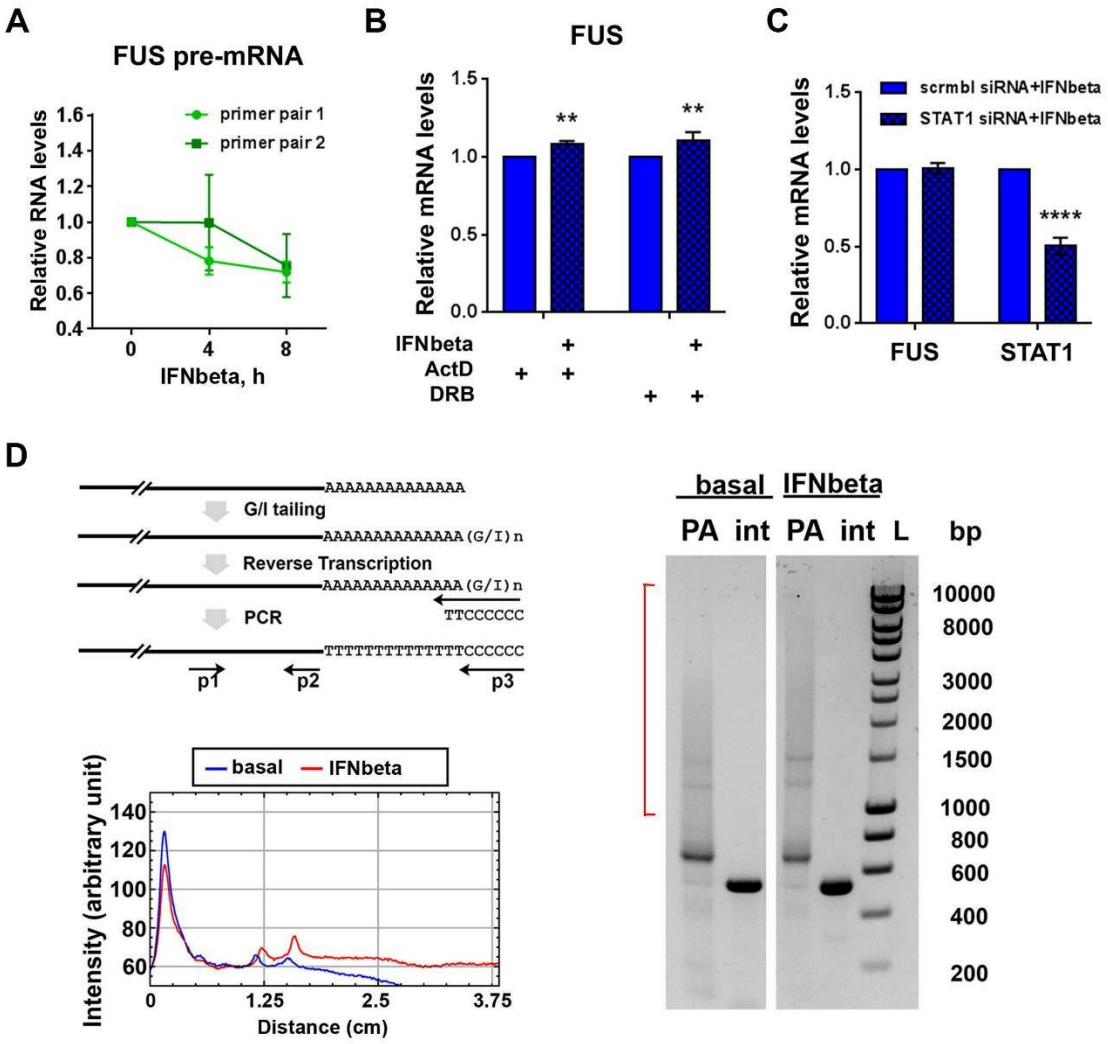

Figure 5.12 IFNbeta induces FUS mRNA accumulation by increasing its stability.

A) FUS pre-mRNA does not increase after IFNbeta treatment in WT SH-SY5Y cells. Intron sequences of FUS gene have been amplified using two pairs of primers from cDNA samples prepared from total RNA. N=3. **B)** Transcriptional inhibition using actinomycin D or DRB does not prevent FUS mRNA upregulation on IFNbeta treatment. Actinomycin D or DRB were added to the cells 1 h before IFNbeta treatment and FUS mRNA levels were measured at 4 h post-treatment of IFNbeta. Mann-Whitney U-test; **p<0.01; N=4. **C)** FUS mRNA upregulation after IFNbeta treatment is not dependent on STAT1. Cells were transfected with siRNAs 48 h before IFNbeta treatment, and FUS mRNA levels were measured 4 h post-treatment. Mann-Whitney U-test; ****p<0.0001; N=4. **D)** Poly(A) tail-length (PAT) assay revealed that FUS mRNA species with longer poly(A)-tails accumulate in cells treated with IFNbeta. Diagram on the left shows the principle behind PAT assay. p1 and p2 are FUS-specific primers. p3 is a universal reverse primer provided in the kit. 'PA' stands

for poly(A) tail (amplified using p1 and p2) and ‘int’ stands for the internal FUS fragment (amplified using P1 and p3). Gel electrophoresis image shows increased intensity of the smear corresponding to the longer poly(A) tails in IFNbeta treated PA lane (indicated with red square brackets). Profile plot is generated for PA lanes. Samples are collected at 8h after IFNbeta treatment.

5.2.9. IFN receptor IFNAR1 is highly expressed in spinal motor neurons and is downregulated in ALS-FUS

Type I IFNs modulate adaptive immune responses in many tissues and organs including CNS (Paul *et al.* 2007), and both neurons and glia express IFNs and their receptors (Chhatbar *et al.* 2018). Consistently, we also detected a high level of interferon-alpha/beta receptor alpha chain (IFNAR1), one of the IFN receptor subunits, specifically in ventral horn neurons of the human spinal cord (Figure 5.13A). Further, we found that the spinal cord of two ALS-FUS patients displayed a dramatic decrease in IFNAR1 levels (Figure 5.13B). Since IFNAR1 is known to undergo ligand-dependent degradation during viral infection (de Weerd and Nguyen 2012), this observation raises the possibility of sustained antiviral signalling activation in the CNS of ALS-FUS patients.

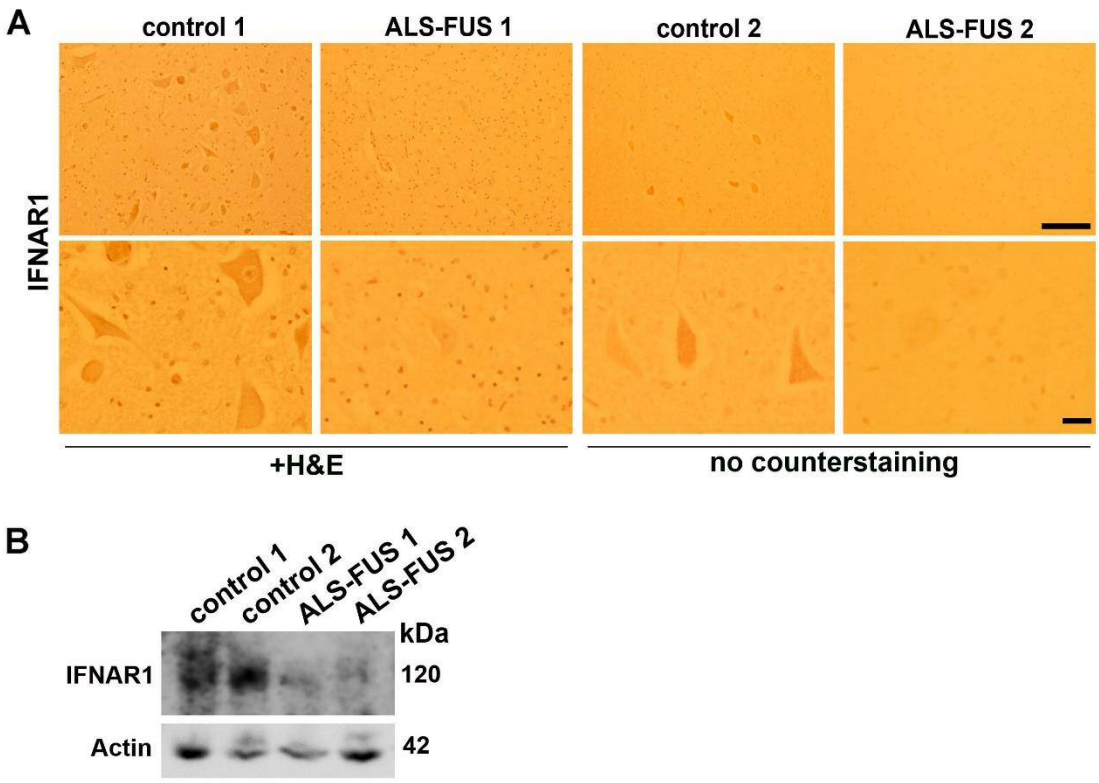

Figure 5.13 IFNAR1 is highly expressed in spinal motor neurons and is downregulated in ALS-FUS.

A) IFNAR1 immunohistochemistry (control 1 and ALS-FUS 1 is counterstained with H&E) in the spinal cord sections from control and ALS-FUS patients. Scale bars are 50 and 10 µm in upper and lower panels, respectively. **B)** IFNAR1 levels are decreased in the spinal cord tissue of ALS-FUS patients as revealed by western blot. This dataset is produced by Dr. Tatyana Shelkovnikova.

5.3. Discussion

Although dramatic cytoplasmic FUS accumulation and large FUS-immunopositive inclusions that fill up the entire cytosolic space are the most prominent pathological features of ALS-FUS (Deng *et al.* 2010), even overexpression of ALS-causing mutant FUS in the rodent CNS is not sufficient to cause apparent FUS deposition and proteinopathy (Huang *et al.* 2011, Scekic-Zahirovic *et al.* 2016, Sharma *et al.* 2016, Devoy *et al.* 2017, Lopez-Erauskin *et al.* 2018).

Based on the results of the current study, I suggest a model (schematically depicted in Figure 5.14) where a viral infection that induces dsRNA response can trigger FUSopathy. Initially, nuclear import defects caused by ALS-causing mutations act as the “first hit” to relocalise FUS proteins to the cytoplasm, where they build up and possibly form FGs. Antiviral immune response serves as the “second hit” and leads to the formation of large persisting FUS-positive assemblies. These aggregates further exacerbate the proteinopathy by impairing nuclear import and aggrephagy through sequestration of nucleocytoplasmic transport factors and the autophagy receptor optineurin, respectively. In addition, IFNs produced during antiviral immune response promote accumulation of FUS protein, which also aggravates the condition. When these persistent cytoplasmic assemblies encounter a (yet unknown) “third hit”, they further transform to form stable aggregates that mark the onset of FUSopathy. This model is consistent with the recently proposed “multi-step model” for ALS development, where intrinsic and extrinsic risk factors are both required to initiate the pathological process in the individuals bearing genetic predisposition (Al-Chalabi *et al.* 2014). Consistent with the proposed role for environmental factors, others also reported that although gene mutations do decrease the number of steps required for the disease onset, 2 or 3 more steps would still be necessary (Chio *et al.* 2018).

The nature of the “third hit”, which triggers the formation of insoluble inclusions, still remains unclear. However, based on the facts that binding of specific target RNA protects FUS from irreversible aggregation (Shelkovnikova *et al.* 2014a, Maharana *et al.* 2018), and that viral infection often causes attenuated host gene expression and RNase L-mediated cleavage of cellular RNAs (Abernathy

and Glaunsinger 2015), I speculate that viral manipulation of the cellular RNA levels might contribute to the process, at least partly.

Here the term “FUS-containing cytoplasmic assemblies” is used to refer to the two different types of cytoplasmic structures: SGs containing FUS protein and FAs composed of spontaneous FGs. The ability of mutant FUS to form FGs under basal conditions and subsequently transform them into FAs under stress has been demonstrated in many cellular models including cultured neurons (Kino *et al.* 2011, Shelkovnikova *et al.* 2014a, Japtok *et al.* 2015), although whether it indeed occurs in human disease is unknown. Regardless of their relative contributions towards the onset of FUSopathy, in my current study, I demonstrate that antiviral immune response can trigger the formation and persistence of both types of FUS assemblies.

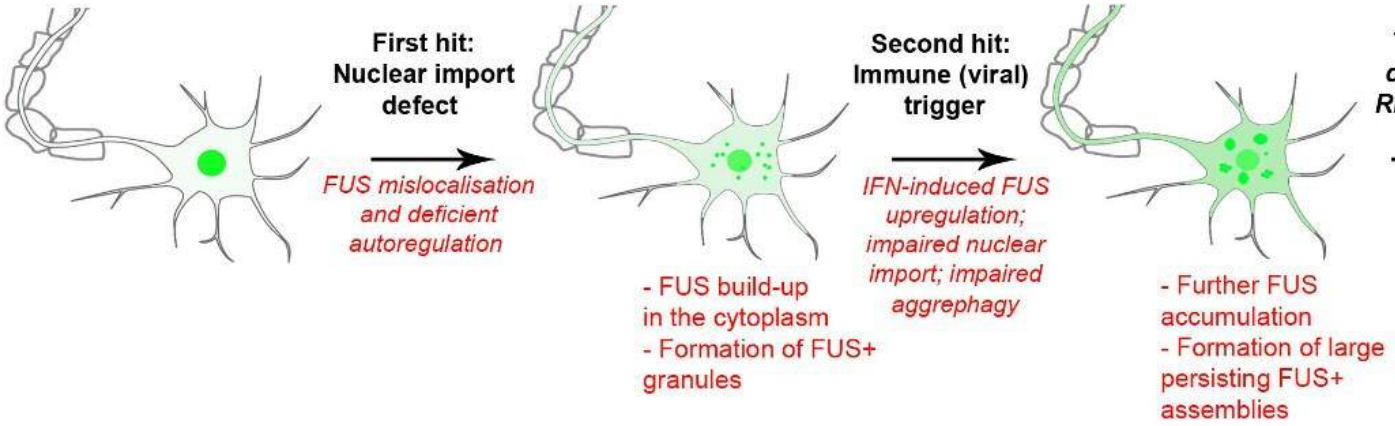

Figure 5.14 FUSopathy triggered by antiviral immune response.

Other neurodegeneration-associated stresses, such as oxidative stress, ER stress and proteasomal dysfunction, can also trigger the assembly of cytoplasmic assemblies containing FUS in cultured cells including neurons (Ederle and Dormann 2017). However, these assemblies are unstable, and therefore they easily disassemble when the stress is resolved. Moreover, the above stresses are acute stresses, which could kill the cells within several hours, if not resolved. In this regard, viral infection is principally distinct from these stresses, because it leads to long-lasting SGs while maintaining cell survival. SG oscillation, which is the regular cycles of SG assembly and disassembly, is the unique feature of SGs induced by viruses, which ensures host cell survival while establishing chronic infection (Ruggieri *et al.* 2012). Therefore, viral infection may initiate FUSopathy in neurons while keeping these cells alive for a period of time long enough to allow FUS inclusion formation.

Compromised autophagy is a well-known mechanism underlying excessive protein deposition in ALS (Weishaupt *et al.* 2016). Previously, optineurin has been identified in the pathological inclusions in motor neurons of ALS-FUS patients (Ito *et al.* 2011b). Furthermore, it has been reported that mutant FUS can impede the autophagic protein clearance thereby contributing to FUSopathy development (Ryu *et al.* 2014, Soo *et al.* 2015). Autophagy plays important roles during antiviral response including viral replication control (Shelly *et al.* 2009). Therefore, many viruses have evolved to adopt various strategies to inhibit the autophagy pathway of host cells (Lee and Iwasaki 2008). My finding that optineurin is sequestered into FUS-positive assemblies suggests an additional mechanism of autophagy dysfunction in the cells expressing mutant FUS.

I believe that type I IFN is the only treatment known so far that causes FUS protein accumulation. Apart from viral infection, type I IFN can also be induced by other immune stimuli, however, sustained IFN expression is only seen during antiviral response (Amit *et al.* 2009). Decreased IFNAR1 level in the ventral horn neurons of ALS-FUS patients suggests that there exists a sustained activation of antiviral signalling in the CNS of ALS-FUS patients. Interestingly, viral infection is known to induce paraspeckle assembly (Imamura *et al.* 2014), and paraspeckle hyper-assembly is a pathological feature of ALS including

ALS-FUS (Nishimoto *et al.* 2013, Shelkovnikova *et al.* 2018, An *et al.* 2019). Therefore, paraspeckle signalling activation in the ALS spinal cord provides another piece of evidence supporting activated antiviral signalling in these tissues.

The model proposed here is also applicable to other FUSopathies that usually do not involve *FUS* gene mutation, such as FTLD-FUS cases. In these cases, normal FUS protein is relocalised to the cytoplasm due to its impaired nuclear transport caused by yet unknown reasons, and viral infection can be one of them. Viruses are known to hijack the components NPCs to facilitate the trafficking of viral proteins, thereby causing NPC dysfunction (Le Sage and Mouland 2013). For example, enterovirus and cardiovirus can change NPC composition resulting in the cytoplasmic relocalisation of some nuclear proteins, whereas enterovirous can induce degradation of nucleoporins Nup62, Nup98 and Nup 153 (Hindley *et al.* 2007). Therefore, viral infection itself and the secondary sequestration of NPC components into the virus-induced cytoplasmic FUS assemblies could together contribute to the compromised nucleocytoplasmic transport in FUSopathy.

In conclusion, my study lays the groundwork for further investigations into the roles the antiviral immune response plays during FUSopathy development. Further studies are needed to examine whether viral infection in other model systems, such as motor neurons derived from ALS-FUS patients and transgenic mouse models, is sufficient to trigger the formation of FUS inclusions and expedite the disease.

Chapter 6. Analysis of FUS truncation mutations

6.1. Overview

Most of ALS-causing FUS mutations are missense mutations, however, other types of mutations, such as indels, duplications, splicing site point mutations, have also been reported in rare fALS cases (Deng *et al.* 2014a). These mutations disturb the original open reading frame (ORF) of FUS downstream of the mutation site, leading to a complete disruption of downstream protein sequence, and a C-terminal "tail" of novel, frameshift peptide replaces the disrupted region. It has been reported repeatedly that patients bearing *FUS* frameshift mutations display a more aggressive ALS phenotype, which is characterised by early disease onset, rapid progression and shorter life expectancy, compared to patients carrying missense mutations. For example, among individuals with FUS frameshift mutations, the majority develop muscle weakness in their teens or 20s and die within 1-2 years after disease onset (DeJesus-Hernandez *et al.* 2010, Yan *et al.* 2010, Yamashita *et al.* 2012, Waibel *et al.* 2013). The youngest patient reported to date developed the first symptoms as early as at the age of 12.5 years and survived for only 18 months (Yan *et al.* 2010). *In vitro* studies found that FUS proteins with truncation mutations show more pronounced mislocalisation as compared to missense mutations (DeJesus-Hernandez *et al.* 2010, Yamashita *et al.* 2012). While it is clear that C-terminal truncations lead to deletion of FUS NLS and sometimes affect other functional domains of the protein (RGG domains), it still remains to be established whether the C-terminal peptide "tail" may confer additional pathological characteristics to the truncated proteins.

To address these questions, I constructed a panel of plasmids expressing N-terminally FLAG-tagged truncated FUS proteins with or without frameshift peptide "tails" (described in Chapter 2). I sought to compare their subcellular distribution and aggregation by expressing these constructs in SH-SY5Y cells and mouse hippocampal neurons.

6.2. Results

Firstly, I reviewed the existing literature to collect information of all reported truncation mutations in the *FUS* gene (Table 6.1). I found information on 12 different frameshift mutations, with the majority being deletion mutations. Mutant protein products in all these cases were predicted to have a C-terminal truncation and a stretch of frameshift peptide at the C-terminus, with the lengths of the "tail" varying between 7 and 54 aa. Certain peptide sequences appeared as the result of more than one type of *FUS* gene mutations (Table 6.1), and these common sequences (VSTDRIAGRGRIN, GVVGTEVALALARWIPGVSTDRIAGRGRIN, WLWPWQDGFQG and SMSRSGR) were chosen for the study (Table 6.2). FUS ORFs with the corresponding truncation with or without the "tail" were inserted into pFLAG-CMV-4 vector to express the proteins as N-terminal FLAG tag fusions.

Table 6.1 A summary of FUS frameshift mutations reported

Gene mutation	Mutant protein	Mutation type	Predicted C-terminal frameshift peptide sequence	Age of onset	References
g.10747A>G; IVS13-2A>G	p.G466VfsX14	splicing mutation	VSTDRIAGRGRIN*	20	DeJesus-Hernandez, M., et al. (2010)
c.1432_1478del GGCTATGATCGAGGC GGCTACCGGGGCCG CGGCGGGGACCGTG GAGG	p.G478LfsX23	deletion	LPRGPGWWGQRWLWPWQDGFQG*	21, 26	Waibel, S., et al. (2013)
c.1419_1420insGT	p.G474VfsX56	insertion	VVAEEAMIEAATGAAAGTVEASEGAGVVGTEVAL ALARWIPGVSTDRIAGRGRIN*	26	Hara, M., et al. (2012)
c.1449_1488del CTACCGGGGCCGCG GCGGGGACCGTGGA GGCTTCCGAGGG	p.Y484AfsX32	deletion	AGVVGTEVALALARWIPGVSTDRIAGRGRIN*	N/A	Yan, J., et al. (2010)
c. 1475delG	p.G492EfsX37	deletion	EASEGAGVVGTEVALALARWIPGVSTDRIAGRGR IN*	17	Yamashita, S., et al. (2012)
c.1483delC	p.R495EfsX34	deletion	EGAGVVGTEVALALARWIPGVSTDRIAGRGRIN*	23, 72	Yan, J., et al. (2010)
c. 1484delG	p.R495QfsX34	deletion	QGAGVVGTEVALALARWIPGVSTDRIAGRGRIN*	19	Belzil, V. V., et al. (2012)

c.1485delA	p.G497AfsX32	deletion	AGVVGTEVALALARWIPGVSTDRIAGRGRIN*	12.5	Yan, J., et al. (2010)
c.1506dupA	p.D502EfsX15	duplication	EQRWLWPWQDGFQG*	49	Belzil, V. V., et al. (2011)
c.1509_1510delAG	p.G504WfsX12	deletion	WLWPWQDGFQG*	15, 23, 33	Kent, L., et al. (2014)
c.1527insTGGC	p.K510WfsX8	insertion	WQDGFQG*	23, 46	Yan, J., et al. (2010)
c.1542-2A>C	p.G515SfsX8	splicing mutation	SMSRSGR*	N/A	Belzil, V. V., et al. (2010)
c.1554_1557delACAG	p.Q519IfsX9	deletion	IAGRGRIN*	18	Bäumer, D., et al. (2010)

Table 6.2 FUS constructs expressing truncated FUS with/without "tails"

Construct	Truncated FUS	C-terminal frameshift peptide sequence
FUS466	FUS 1-466	none
FUS466fs	FUS 1-466	VSTDRIAGRGRIN
FUS491	FUS 1-491	none
FUS491tail	FUS 1-491	GVVGTEVALALARWIPGVSTDRIAGRGRIN
FUS503	FUS 1-503	none
FUS503tail	FUS 1-503	WLWPWQDGFQG
FUS513	FUS 1-513	none
FUS514tail	FUS 1-514	SMSRSGR

* FUS466 and FUS513 were already available in the lab.

* C-terminal "tail" sequences are labelled with the same colour code as in table 6.1.

Each of the constructs was transiently expressed in WT SH-SY5Y cells and subsequently in 5 days *in vitro* (DIV5) mouse hippocampal neurons. Microscopic analysis revealed that the same types of intracellular FUS distribution (diffuse, small granules and large aggregates) are formed in cells transfected with constructs expressing truncated FUS variants with or without the "tail", either in SH-SY5Y cells or in the neurons (Figure 6.1 and 6.2).

Although this preliminary experiment did not reveal dramatic differences in FUS aggregation between truncated FUS proteins with or without a "tail", more comprehensive studies are required in the future, which might highlight interesting aspects of FUSopathy caused by truncation mutations. This will be discussed in Chapter 7.

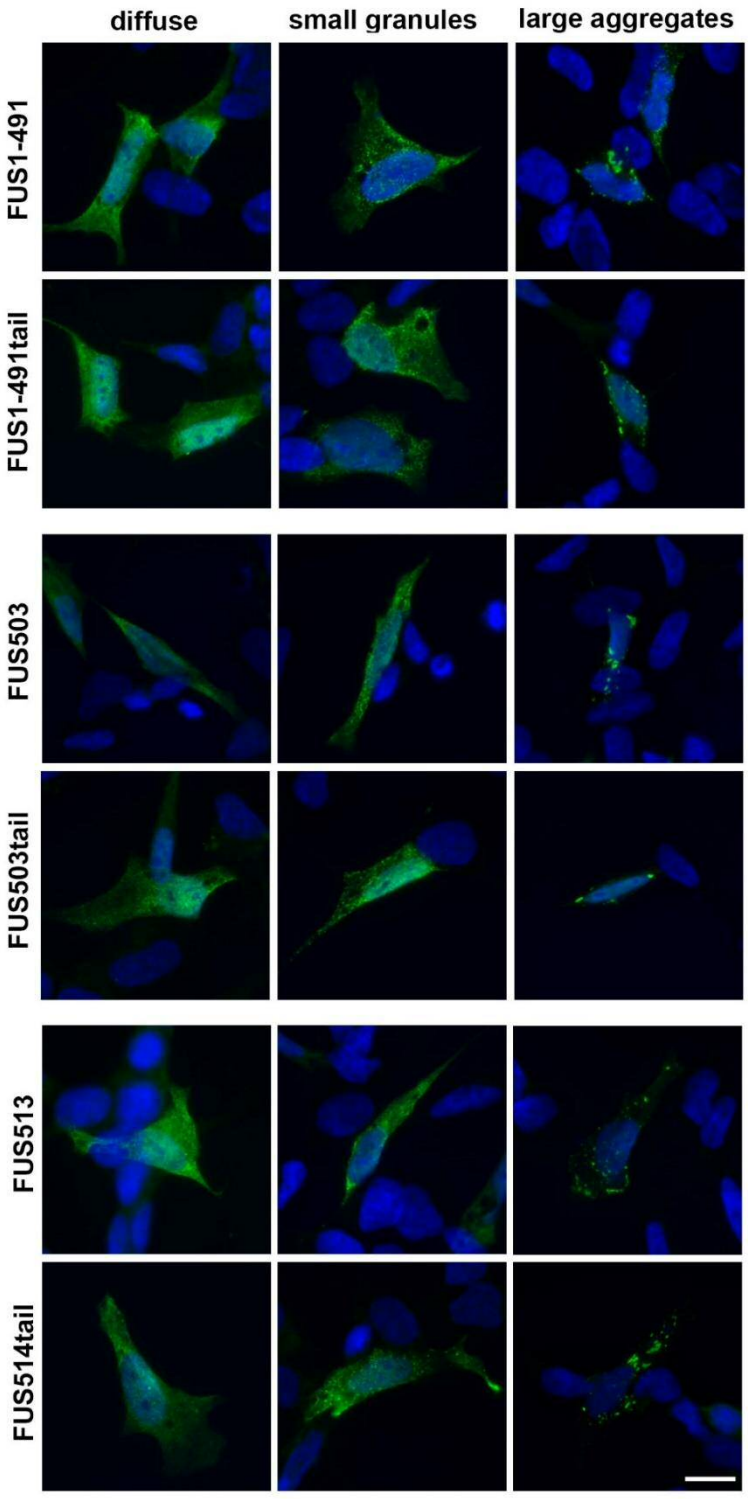

Figure 6.1 Expression of truncated FUS proteins in WT SH-SY5Y cells.

No obvious difference in granule formation and protein aggregation between proteins with or without a C-terminal “tail” was observed. Proteins are N-terminally labelled with FLAG. Cells are stained with an anti-FLAG antibody 24 h post-transfection. Representative images are shown. Scale bar is 10 μm.

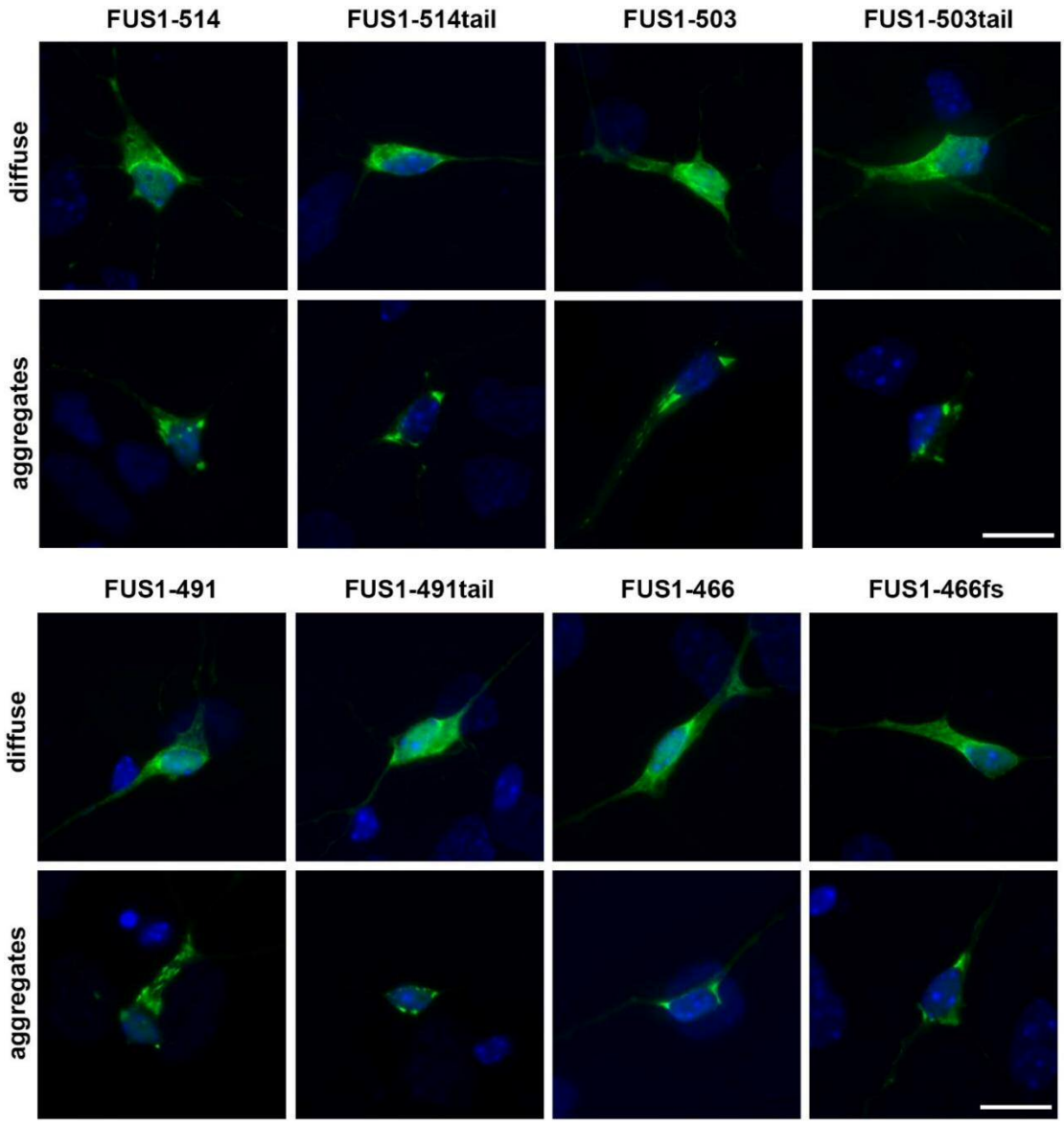

Figure 6.2 Truncated FUS proteins expressed in the mouse hippocampal neurons display similar aggregation propensity.

Proteins are N-terminally labelled with FLAG. Cells are stained with an anti-FLAG antibody 24 h post-transfection. Representative images are shown. Scale bar is 10 μm.

6.3. Discussion

In this part of the project, I sought to investigate whether a stretch of frameshift peptide on the C-terminus of FUS protein caused by frameshift mutations has additional contribution to the aggregate formation, independent of the truncation itseft. Of note, among the “tails” tested, there is a “tail” with exactly the same amino acid sequence (VSTDRIAGRGRIN) as found in ΔNLS10_het clone. By microscopic observation of two cellular models overexpressing mutant FUS (with or without a “tail”), I could not detect obvious differences in protein aggregation between truncated FUS protein and truncated FUS protein with any of the “tails”.

The degree of cytoplasmic mislocalisation of FUS is suggested to be positively correlated to the disease severity (Dormann *et al.* 2010). FUS P525L and R522H mutations, which show the strongest degree of mislocalisation, are found in the patients with very early disease onset - 24 and 28.5 years, respectively (Chio *et al.* 2009, Kwiatkowski *et al.* 2009). Mutant FUS proteins encoded by the *FUS* gene bearing frameshift mutations showed more pronounced cytoplasmic redistribution compared to the missense mutations (DeJesus-Hernandez *et al.* 2010, Yamashita *et al.* 2012, Kent *et al.* 2014). While it is clear that the increased cytoplasmic FUS levels caused by almost complete disruption of NLS is one of the mechanisms behind the increased toxicity of the truncated FUS protein, the role of the *de novo* peptide “tails” in truncated proteins remained uncertain.

In the current study, I did not find dramatic differences in the pattern of subcellular distribution and aggregation between proteins with and without C-terminal “tail”. However, I cannot exclude that subtle changes might still be present.

In conclusion, the exceptionally aggressive clinical manifestations observed among the patients carrying frameshift FUS mutations are very likely caused by the dramatic cytoplasmic mislocalisation due to the complete NLS loss of function, and the presence of C-terminal “tails” dose not further aggravate FUS aggregation. However, the possibility that the “tails” might perturb other

cellular pathways by promiscuous interaction with other proteins cannot be excluded, which requires further investigation.

Chapter 7. Final discussion and perspectives

7.1. Overview

A decade has passed since the link between *FUS* gene and ALS was first established, and data from hundreds of reports published since then have greatly improved our understanding of the molecular mechanisms underlying ALS-FUS. Ubiquitin-positive, TDP-43-negative cytoplasmic inclusions containing FUS protein are a pathological hallmark of affected neurons and glia in ALS-FUS (Kwiatkowski *et al.* 2009, Vance *et al.* 2009). ALS-associated mutations in *FUS* gene cause mislocalisation of the encoded protein to the cytoplasm by disrupting its NLS, and the degree of mislocalisation is correlated with the age of disease onset (Dormann *et al.* 2010, Ito *et al.* 2011a). Despite recent insights, there are still a number of important outstanding questions: how does mutant FUS exert its toxicity in the neurons and glial cells? Is cytoplasmic gain of function or rather nuclear loss/gain of function the main mechanism in the molecular pathogenesis of ALS? How do the pathological inclusions form? Does an external stress trigger FUSopathy and if so, what is the nature of the stress?

Modification of the endogenous *FUS* gene has made it possible to study the pathogenic behaviour of ALS-associated mutant FUS in a more (patho)physiological setting. Using a panel of single cell-derived SH-SY5Y sub-clones with *FUS* gene modifications, I have identified two molecular mechanisms that may underlie ALS-FUS, namely, hyper-assembly of structurally and functionally abnormal paraspeckles and antiviral immune response. Hereafter, I will discuss broader implications of my findings and how FUSopathy modelling can be improved in the future.

7.2. Modeling FUSopathy

Cellular models expressing endogenous mutant FUS protein provide a reliable platform for researchers to study cellular and molecular mechanisms leading to FUSopathy. These models can either be established from cells obtained from individuals bearing *FUS* gene mutation or be generated through gene modification in cultured cells.

Human iPSCs derived from fibroblasts of FUS mutation carriers are highly instrumental in the study of pathological behaviour of FUS proteins by modelling exact genetic background. In addition, they can be differentiated into disease-relevant cell types, such as spinal motor neurons, to recapitulate the microenvironment. In order to achieve adequate power to attribute certain cellular phenotypes to disease development, multiple independent iPSC lines are required. However, since FUS mutations account for only about 5% of total fALS cases, and fALS cases account only 10% of total ALS cases, this resource is not readily available for most laboratories. Furthermore, the acquisition of human fibroblasts, their reprogramming into iPSCs and subsequent characterisation and maintenance is an expensive, time-consuming, and technically challenging process, which until recently greatly hampered their widespread application. There also exists a flexibility issue, since patient-derived iPSCs can only model specific point mutations, they are not suitable for some research purposes such as functional dissection of the protein domains.

Targeted gene modification by the CRISPR/Cas9 is an extremely versatile approach to obtain cellular models of FUSopathy. It can not only be used to model exact ALS-causing *FUS* gene point mutations but also be used to modify or delete any part of the gene in a variety of cell types. Recently, a number of groups have reported FUS cellular models generated by this method. Naumann and his colleagues used CRISPR/Cas9 to establish iPSCs expressing FUSP525L tagged with C-terminal GFP based on an iPSC line obtained from an ALS patient carrying FUS R521C mutation. That was achieved by correcting the original mutation and introducing a new c.1574C>T mutation together with C-terminal GFP sequence. The authors reported that impaired DNA damage response, that exacerbated FUS cytoplasmic mislocalisation and resulted in distal axonal pathology, is an early pathological event upstream of FUS aggregation (Naumann *et al.* 2018). Marrone et al. also generated reporter iPSC lines expressing FUS P525L with C-terminal GFP to study SG dynamics. They found that SGs were more numerous and larger in mutant FUS-expressing iPSCs compared to isogenic WT lines, and enhancing autophagy ameliorated the phenotype (Marrone *et al.* 2018).

Our cellular models are different from above-mentioned models in three ways. First of all, instead of iPSCs, I opted for the human neuroblastoma SH-SY5Y cell line, whose manipulation is more cost-effective and less labour-intensive. It allowed us to achieve the desired results quickly with less cost. Secondly, rather than modelling just one specific disease mutation, e.g. FUS P525L, I deleted the entire NLS domain, which harbours the majority of ALS-associated FUS mutations, in order to put my cellular models on the more severe end of the ALS-FUS spectrum. In addition, this approach also significantly increased gene editing efficiency, since it relied on the removal of a target fragment during DNA repair through the highly efficient NHEJ mechanism, rather than through a less-efficient homology directed repair (HDR) mechanism which also requires a donor template to guide the creation of a point mutation (Cong *et al.* 2013). Finally, I minimized the introduction of non-physiological elements in my clones, such as fluorescent tags or selection markers, to avoid any background effects that might be caused by these elements. Overall, the strategy I used to generate FUSΔNLS clones represents an easily accessible, fast and cost-effective way of creating reliable cellular models expressing endogenous mutant FUS protein.

However, due to the error-prone nature of NHEJ DNA repair pathway caused frameshift mutations in about half of the sequenced alleles, resulting in a stretch of amino acid “tail” on the C-terminus of FUS protein. The apparent solution to achieve error-free *FUS* gene editing is to simultaneously introduce a repair template to guide DNA repair through the HDR pathway (Ran *et al.* 2013). However, as HDR is relatively rare compared to the predominant NHEJ in mammalian cells, widespread application of this method is hampered by low efficiency (Cong *et al.* 2013, Canver *et al.* 2014). Several strategies have been suggested to increase HDR rate and inhibit NHEJ to improve the editing efficiency (Paquet *et al.* 2016, Aird *et al.* 2018), including the application of NHEJ pathway inhibitors or covalent tethering of DNA repair template to the gRNA-Cas9 complex. Recently, the research focus has begun to shift towards improving the repair accuracy of the NHEJ pathway (Guo *et al.* 2018, Shen *et al.* 2018). For example, a machine learning model is used to accurately predict the spectrum of genotypic products at a target site of interest, enabling template-free genome editing with higher precision (Shen *et*

al. 2018). Therefore, modification of the *FUS* gene with greatly improved efficiency and accuracy will be achievable in future studies.

Another concern about gene modification is the “off-target” effect, i.e. the undesirable editing activities of CRISPR/Cas9 at the genomic foci outside the intended targeting site. Several strategies have been developed to tackle the problem. Modification of gRNAs, such as 5' end truncated or chemically modified gRNAs, can decrease the recognition of mismatched targets (Pattanayak *et al.* 2013, Fu *et al.* 2014, Doench *et al.* 2016, Cromwell *et al.* 2018, Listgarten *et al.* 2018). In addition, genetically engineered Cas9 variants can be used to improve editing specificity (Ran *et al.* 2013, Guilinger *et al.* 2014, Kleinstiver *et al.* 2016, Chen *et al.* 2017). Double nickase strategy, which exploits a mutant form of Cas9 that only cleaves single strand of DNA, is the most well-known example (Ran *et al.* 2013, Shen *et al.* 2014a), where only the specific sites containing two very close target sites can be cleaved by two nickases to create a DSB. Recently, a range of high-fidelity Cas9 nuclease variants have been developed, which are proven to dramatically reduce off-target effects, such as pCas9-HF1 (Kleinstiver *et al.* 2016), eSpCas9 (Slaymaker *et al.* 2016) and HypaCas9 (Chen *et al.* 2017). Although off-target modifications cannot be completely eliminated, clonality issues can be bypassed by using a heterogeneous population of edited cells obtained, for instance, by fluorescence-activated cell sorting (FACS). I believe that synergistic use of the above-mentioned strategies will significantly improve the specificity in the future attempts to modify the *FUS* gene.

7.3. Paraspeckles in ALS pathology

Post-mitotic neurons are naturally devoid of paraspeckles due to low NEAT1_2 levels (Nakagawa *et al.* 2011), however, at the early stage of ALS, paraspeckles become detectable in the motor neurons and glial cells (Nishimoto *et al.* 2013). Enhanced paraspeckle assembly is not only evident in sALS spinal cord, but could also be identified in fALS cases with various genetic background, namely ALS-C9 and ALS-TDP43 (Shelkovnikova *et al.* 2018). In Chapter 4, I also reported paraspeckle hyper-assembly in ALS-FUS

spinal cord, further supporting the notion that *de novo* paraspeckle assembly is one of the pathological hallmarks of spinal cord motor neurons in ALS. What is the physiological or pathological significance of this change? Is it protective against neuronal death or detrimental for neuronal survival? Can we modulate the disease course by manipulating NEAT1_2 levels and paraspeckle formation?

NEAT1_2 expression and paraspeckle assembly show a strict tissue-specific distribution *in vivo*: they are restricted to the surface epithelial cells of the gastrointestinal tract, which are exposed to harsh environmental conditions and undergo active renewal (Nakagawa *et al.* 2011), suggesting that paraspeckles might be required for stress response. In line with this assumption, NEAT1 was initially found increased in the mice brain infected with Japanese encephalitis virus (Saha *et al.* 2006). Furthermore, in *in vitro* cellular models, paraspeckles are dramatically enlarged upon exposure to various stresses, including proteasome inhibition and viral infection. Therefore, in ALS motor neurons, NEAT1 expression and paraspeckle assembly are likely enhanced in response to internal or external stressful conditions, such as disrupted cellular homeostasis (e.g. collapse of proteostasis) or environmental stimuli (e.g. neuroinflammation).

Paraspeckles are known to participate in the maintenance of cellular homeostasis in the stressful environment by sequestering transcription factors (Hirose *et al.* 2014, Imamura *et al.* 2014, Ma *et al.* 2017) and a specific subgroup of RNA molecules (Chen and Carmichael 2009, Hu *et al.* 2015). For example, paraspeckle formation as a part of antiviral response facilitates antiviral gene expression, such as *IL8, CCL5* and retinoic acid-inducible gene I (*RIG-I)*, by relocating SFPQ from the promoter region to paraspeckles thereby ameliorating its inhibitory effect on the antiviral genes (Imamura *et al.* 2014, Ma *et al.* 2017), and depletion of NEAT1_2 delayed innate immune response and accelerated viral replication in mice infected with Hantaan virus (Ma *et al.* 2017). Moreover, mouse embryonic fibroblasts (MEF) prepared from NEAT1 KO mice showed a dramatically decreased survival rate during proteasomal stress, indicating antiapoptotic roles of paraspeckles (Hirose *et al.* 2014). In addition, paraspeckle formation stimulated by p53 activation

prevented the accumulation of DNA damage in the cells under oncogenic stress (Adriaens *et al.* 2016). Hence, it is plausible that paraspeckle assembly in ALS neurons is a protective measure to maintain cellular homeostasis and promote neuronal survival. Indeed, in cellular models of TDP-43 proteinopathy, paraspeckle hyper-assembly is proven to be beneficial for cell survival as disruption of them resulted in increased cytotoxicity (Shelkovnikova *et al.* 2018).

In ALS-FUS neurons, despite the increased NEAT1 level, this safety mechanism is significantly impaired since paraspeckles no longer maintain normal structure and function due to the presence of mutant FUS. In addition, increased release of free NEAT1_1 into the nucleoplasm further exacerbates the condition. Making things even worse, the core paraspeckle protein NONO is found trapped in the cytoplasmic and nuclear FUS inclusions, which also diminishes paraspeckle integrity by decreasing the nuclear pool of NONO (Shelkovnikova *et al.* 2014b). Perhaps, inadequate protective response due to the impaired paraspeckle assembly could explain why ALS-FUS usually shows an extremely aggressive disease course compared to sALS and other forms of fALS cases (Shang and Huang 2016).

Although much work still needs to be done, once we have sufficient knowledge about the functional significance of paraspeckles and NEAT1 levels during ALS development, we can possibly modulate disease course by manipulating NEAT1 levels and paraspeckle assembly. Antisense oligonucleotides (ASOs), which are being tested as a candidate therapeutic approach for monogenic forms of neurodegenerative diseases, can also be used to modulate NEAT1 levels. However, it should be noted that an unconventional mechanism of ASOs action has been reported for NEAT1, where phosphorothioate (PS)-modified ASOs formed paraspeckle-like structures recruiting multiple paraspeckle proteins, which eventually led to rapid degradation of NEAT1 (Shen *et al.* 2014b). Moreover, it is also reported that widely used 2'F modified PS-ASOs induced degradation of NONO and SFPQ thereby downregulating NEAT1 levels (Shen *et al.* 2015). Therefore, careful design of ASOs is essential for their therapeutic applications. Since no clinically applicable chemical compounds which can regulate NEAT1 levels

are known, it will be of great value developing a cell-based assay to screen chemical compound libraries to identify potential modulators of NEAT1 in the future.

The strong association between NEAT1/paraspeckles and ALS is gaining more credence, although we have just started to paint the picture of their distribution, regulation and functions in the CNS and their changes during the disease. In order to fully appreciate the spectrum of effects of NEAT1/paraspeckles in ALS, there are a number of important knowledge gaps we need to fill in: 1) cell-specific pattern of NEAT1 expression and regulation in CNS, and whether this pattern can be recapitulated in cultured cells *in vitro*; 2) molecular and cellular functions of NEAT1 in normal neurons and other cells in the CNS; 3) mechanisms leading to NEAT1 upregulation and paraspeckle assembly and neuroprotection in motor neurons in ALS; 4) differential roles of the two NEAT1 isoforms during ALS development. *In vivo* and *in vitro* models lacking total NEAT1 or NEAT1_2 expression will be extremely instrumental in experimental studies aiming to answer these questions. Although no obvious neurological abnormalities have been reported in total NEAT1 KO mouse model (Nakagawa *et al.* 2011), thorough scrutiny of the neurons isolated from these mice should reveal the neuro-specific roles of NEAT1.

7.4. Viral infection and ALS

I have demonstrated in Chapter 5 that the antiviral immune response triggers and aggravates FUSopathy by promoting FUS assembly persistence and FUS protein accumulation. In addition, possible impairment in aggrephagy and nucleocytoplasmic transport could also contribute to FUSopathy development. Here I will further discuss the link between viral infection and ALS to outline possible future directions of these studies.

7.4.1. Evidence supporting the connection between viral infection and ALS

Since decades ago, there has been accumulating epidemiological and clinical evidence suggesting the link between ALS and viral infection (Celeste and Miller 2018). Early on, it has been reported that individuals who have a history of poliomyelitis showed an increased risk of developing MND later in their lives (Martyn *et al.* 1988). In addition, a large scale, multi-centre case control study reported a higher rate of enterovirus RNA detection in the cerebrospinal fluid (CSF) among ALS patients (Vandenberghe *et al.* 2010), which showed no seasonal pattern, indicating a persistent enteroviral infection. Interestingly, several common cellular and molecular phenotypes have been found between enteroviral infection and ALS (Ravits 2005, Vandenberghe *et al.* 2010). It has been reported that coxsackievirus B3 (CVB3) infection in HeLa cells results in cytoplasmic mislocalisation and cleavage of TDP-43, the most common pathological hallmark of ALS, via the action of CVB3-encoded proteinase (Fung *et al.* 2015). Enterovirus infection in the murine CNS resulted in cellular pathologies that are typically found in ALS including cytoplasmic inclusions containing TDP-43 (Xue *et al.* 2018b, Masaki *et al.* 2019). Notably, during the life cycle of enteroviruses, a dsRNA intermediate is formed, which is capable of triggering SG assembly (Lloyd 2016).

Retroviral infection might also be involved in ALS. Patients infected with human immunodeficiency virus (HIV) or human T cell leukemia virus -1 (HTLV-I) sometimes develop neurological conditions clinically resembling ALS (Alfahad and Nath 2013). Furthermore, human endogenous retrovirus (HERV) reactivation from the human genome has been recently associated with ALS (Brutting *et al.* 2017). About 8% of the human genome is composed of HERV sequences that are transcriptionally silent (Jern and Coffin 2008). However, certain viral infections, such as HIV and Epstein Barr virus, or hypoxia could reactivate them (Nellaker *et al.* 2006, Kewitz and Staege 2013). Expression of HERV-K, the biologically most active HERV family, is significantly upregulated in the brain of ALS patients (Douville *et al.* 2011). Intriguingly, mutant TDP-43, but not WT TDP-43, is shown to promote the accumulation and aggregation of HERV-K viral protein (Manghera *et al.* 2016), and expression of HERV-K

protein in human neurons or in the murine CNS caused neurotoxicity and selective motor neuron loss (Li *et al.* 2015).

I speculate that viral infections (or reactivation of HERV by various environmental stimuli) and subsequent immune response could trigger the disease onset by further dysregulating cellular pathways that are already perturbed by ALS-causing mutations. My study is the first to demonstrate the mechanism by which antiviral response may initiate and exacerbate the disease in the cells bearing a *FUS* gene mutation.

7.4.2. Stress granules during antiviral response

In Chapter 5, I have demonstrated that poly(I:C)-induced SGs persist in the cells, which may contribute to the insoluble cytoplasmic inclusion formation in ALS by holding together proteins harbouring prion-like domains. Here I will discuss other features of virus-induced SGs that might shed light on the link between viral infection and ALS pathology.

Piotrowska et al. reported long-lasting presence of SGs over the course of infection in poliovirus-infected cells, where the SGs were composed of TIA-1 and mRNA, but lacked G3BP1 (Piotrowska *et al.* 2010). Later, a follow-up study demonstrated that these TIA-1-containing SGs became devoid of mRNAs and other SG marker proteins, transforming to protein aggregates at the later stage of infection (White and Lloyd 2011). These studies demonstrated that cytoplasmic RNP assemblies induced by viruses can transform into protein aggregates, through the depletion of protein and RNA components, over the prolonged infection. Interestingly, recruitment of mutant FUS into SGs has been demonstrated to be protective against irreversible aggregate formation (Shelkovnikova *et al.* 2013b), and RNA depletion has been proposed to be the critical step triggering the transition of reversible FUS assemblies into pathological aggregates (Shelkovnikova *et al.* 2014a). Therefore, the transformable feature of virus-induced SGs into protein aggregates reinforces the link between viral infection and the onset of FUSopathy.

Another intriguing finding regarding the effect of viral infection on SGs is that virus-infected cells show impaired SG assembly when exposed to additional stressful conditions. For example, cells infected with herpes simplex virus 2 (HSV-2) failed to assemble SGs in response to SA-induced oxidative stress (Finnen *et al.* 2012, Finnen *et al.* 2014), and such impairment is ascribed to the virion host shutoff protein (VHS), which acts downstream of eIF2α phosphorylation (Finnen *et al.* 2014). SGs are central hubs for stress response and innate immunity, and cells with impaired SG assembly show decreased survival in stressful conditions (Anderson and Kedersha 2009b). These findings suggest that viral infection can render neurons incapable of managing cellular stresses, which will be extremely detrimental to neurons already expressing ALS-causative mutant proteins such as FUS.

Of note, during a genuine viral infection (as opposed to poly(I:C) stimulation), the intracellular environment is much more complicated due to the expression of viral genes. Moreover, each virus affects SGs and related cellular signalling very differently in distinct cell types. Therefore, it will be very interesting to study SG dynamics in motor neurons of mice infected with certain neurotropic viruses that are associated with ALS.

7.4.3. Virus-induced pathological changes associated with ALS

In addition to persistent SGs, I have also found that nucleocytoplasmic transport and autophagy changes occur in mutant FUS-expressing cells subjected to a viral trigger. Other ALS-associated cellular abnormalities have also been reported in virus-infected cells by other groups.

Many ALS mutations affect RBPs, as has been discussed earlier. Viruses rely heavily on host cell proteins for their replication, and many nuclear RBPs are found hijacked and detained in the cytoplasm by viruses. In cells infected with Enterovirus A71, the ALS-associated protein hnRNPA1 is found to be mislocalised to the cytoplasm, where it facilitates translation of viral proteins (Tolbert *et al.* 2017). Most interestingly, cytoplasmic translocation and cleavage of TDP-43, which is mediated by viral proteases, was reported in the

CVB3-infected cells (Fung *et al.* 2015). The cleaved TDP-43 N-terminal fragment compromised the function of WT TDP-43 resulting in abnormal alternative splicing of cystic fibrosis transmembrane conductance (CFTC) regulator gene. A similar finding was also reported very recently in the CNS of mice infected with Theiler's murine encephalomyelitis virus (TMEV). In these mice, TDP-43 was found mislocalised and aggregated in the affected neurons and glia, and *in vitro* study revealed abnormal splicing events in infected cells (Masaki *et al.* 2019). Not only viral components, but host antiviral immune reaction itself is known to trigger RBP translocation. For instance, TNF-α and IFN-γ cause the mislocalisation of TDP-43 and hnRNPA1, respectively (Correia *et al.* 2015, Salapa *et al.* 2018). Therefore, altered localisation and function of RBPs, coupled with viral modification of SGs, collectively contribute to the dysregulation of RNA homeostasis.

Attenuated clearance of misfolded proteins is one of the well-known mechanisms causing proteinaceous inclusion formation and neuronal death in ALS. In Chapter 5, I have demonstrated that the autophagy receptor optineurin was sequestered into dsRNA-induced cytoplasmic FUS assemblies, which could potentially subvert efficient clearance of misfolded proteins. In addition, many viruses exploit and/or modify the components of the protein quality control system for their own benefit. The autophagy adapter protein Sequestosome-1/p62, encoded by an ALS-associated gene *SQSTM1*, is also found cleaved by a viral protease of CVB3, leading to the functional loss of p62 and disruption of selective autophagy (Shi *et al.* 2013). Furthermore, the C-terminal cleavage product of p62 can compete with the uncleaved, functional form of the protein, further jeopardising autophagy (Shi *et al.* 2014). This is consistent with earlier studies that reported abnormal accumulation and aggregation of misfolded proteins in the cells infected with the CVB3 virus (Gao *et al.* 2008, Si *et al.* 2008). Although limited evidence is available to directly support the link between virus-induced disruption of the protein degradation process and ALS, UPS and autophagy are among the most affected cellular machineries hijacked by viruses, supported by hundreds of reports (reviewed in (Luo 2016)). Likewise, many viruses are known to cause ER stress by utilizing ER membrane for viral replication (Jheng *et al.* 2014), or by overwhelming host cell protein translation and folding machinery

(Zhang and Wang 2012). Hence, viral infection can be particularly detrimental to the neurons with perturbed proteostasis due to ALS-associated mutations.

Chronic neuroinflammation is a common histopathological feature of ALS, and activation of microglia and astrocytes has been suggested to be the underlying cause (Robertson *et al.* 2001). Apart from direct damage to neurons, viruses could also cause immune-mediated injury by stimulating pro-inflammatory cytokine release and activating glial cells. For example, in the CNS of mice infected with CVB3, a rapid release of chemokines, cytokines, and type I IFNs was observed, which remained upregulated for weeks post-infection (Feuer *et al.* 2009). Consistently, the levels of IL-6 and IL-1beta are found upregulated in the CSF and serum of patients infected with enterovirus 71 in CNS (Lin *et al.* 2003). Moreover, positron emission tomography imaging of HIV-1 infected patients revealed microglia activation even in the absence of neurological symptoms (Garvey *et al.* 2014). Activation of immune response is undoubtedly beneficial for the nervous system to fight against viral infection. However, dysregulation of the complicated network or persistent inflammation and glial cell activation can be deleterious for neuronal survival, which is particularly true in individuals with mutations in the genes encoding proteins participating in immune signalling, such as TBK1 and optineurin (Oakes *et al.* 2017, Slowicka and van Loo 2018).

In conclusion, an increasing number of studies suggest that viral infection, enteroviruses and retroviruses in particular, may act as a potential trigger for ALS onset and progression. Future studies should focus on finding direct evidence of viral infection in patients-derived samples. Histopathological analysis of infection-related proteins in the CNS of ALS patients might provide important clues. Meta-analysis of existing epidemiological data can also highlight previously unknown links between viral infections and ALS.

7.5. Frameshift mutations in ALS

In Chapter 7, I attempted to address possible effects of C-terminal peptide “tails” introduced by frameshift *FUS* mutations. Although these “tails” did not visibly change the distribution and aggregation patterns of truncated FUS, it is

still possible that they could confer toxicity by altering other features of FUS protein, for example the pattern of its post-translational modifications.

Post-translation modifications, such as phosphorylation and methylation, are known to affect FUS protein subcellular localisation and functions. For example, phosphorylation of FUS protein on the N-terminus triggered its cytoplasmic translocation (Deng *et al.* 2014b), and phosphorylation of C-terminal tyrosine residue inhibited its nuclear import (Darovic *et al.* 2015). Additionally, methylation of FUS protein is required for the toxic function of ALS-associated mutant FUS protein (Tradewell *et al.* 2012). Certain amino acids are the target of post-translational modifications - serines (S), threonines (T) and tyrosines (Y) are often targeted by phosphorylation, while arginines (R) are usually subject to methylation (Brautigan 1995, Bedford and Clarke 2009). Intriguingly, C-terminal “tails” caused by frameshift mutations are enriched in such modification target sites, such as SMSRSGR (caused by G515SfsX8 mutation), VSTDRIAGRGRIN (caused by G466VfsX14 and some other mutations). As an important regulatory mechanism, post-translational modifications not only alter protein conformation and localisation but also change the nature and strength of protein-protein interaction, thereby affecting various cellular pathways (Fronz *et al.* 2011, Nishi *et al.* 2011). Therefore, investigating whether the C-terminal “tails” are post-translationally modified will provide us with clues about the properties conferred by these “tails”.

Apart from post-translational modifications, the presence of an extra chain of amino acids itself could result in changes in protein behaviours through changing protein conformation, which might in turn promote promiscuous protein interactions or interfere with normal FUS protein functions, which include transcription, splicing, DNA damage repair, miRNA biogenesis, mRNA transport, among others (Deng *et al.* 2014a). In addition, C-terminal “tails” can also affect protein turnover, as protein stability is in part determined by protein sequence and structure (Martin-Perez and Villen 2017). Environmental stresses, such as oxidative stress and heat shock, are known to trigger protein aggregation by causing unfolding of bulk cellular proteins or by irreversible protein modifications (Parsell *et al.* 1994, Stadtman and Levine 2000). Hence,

it is would be helpful to compare the aggregation of mutant FUS proteins with or without “tails” under various stress conditions.

7.6. Concluding remarks

In the past decade, we have begun to appreciate the extraordinarily complicated mechanisms that underlie ALS. The global incidence of ALS is on the rise, especially in developing nations, due to the improved diagnosis and prolonged lifespan. It is estimated that the global number of ALS patients will increase globally by 69% by the year 2040 (Arthur *et al.* 2016). ALS greatly limits autonomy of patients and severely affects their quality of life. Furthermore, it causes substantial economic burden to their families and societies due to their early retirement, absolute dependence on caregiving and increased demand of orthopaedic devices (Lopez-Bastida *et al.* 2009). Since the FDA approval of the first ALS drug Riluzole in 1995, over 60 molecules have been tested as potential ALS drugs in more than 50 clinical trials worldwide (Petrov *et al.* 2017). These chemical compounds represent a wide range of broadly defined mechanisms of action including anti-glutamatergic, anti-oxidative, anti-inflammatory and neuroprotective, among others. Among them, only one drug, a potent free radical scavenger Edaravone, has demonstrated clinical efficacy and has been approved by FDA as the second drug for ALS treatment (Bhandari *et al.* 2018). Even though Riluzole and Edaravone can moderately improve some clinical manifestations of the disease and patients’ quality of life for a limited period of time, they cannot prevent or stop the disease progression. Therefore, therapeutic developments in the ALS field are still very limited, and more relevant disease model systems and further mechanistic studies are desperately needed.

Abernathy, E. and B. Glaunsinger (2015). "Emerging roles for RNA degradation in viral replication and antiviral defense." Virology **479-480**: 600-608.

Acosta, J. R., C. Goldsbury, C. Winnick, A. P. Badrock, S. T. Fraser, A. S. Laird, T. E. Hall, E. K. Don, J. A. Fifita, I. P. Blair, G. A. Nicholson and N. J. Cole (2014). "Mutant human FUS Is ubiquitously mislocalized and generates persistent stress granules in primary cultured transgenic zebrafish cells." PLoS One **9**(6): e90572.

Adriaens, C., L. Standaert, J. Barra, M. Latil, A. Verfaillie, P. Kalev, B. Boeckx, P. W. Wijnhoven, E. Radaelli, W. Vermi, E. Leucci, G. Lapouge, B. Beck, J. van den Oord, S. Nakagawa, T. Hirose, A. A. Sablina, D. Lambrechts, S. Aerts, C. Blanpain and J. C. Marine (2016). "p53 induces formation of NEAT1 lncRNA-containing paraspeckles that modulate replication stress response and chemosensitivity." Nat Med **22**(8): 861-868.

Aird, E. J., K. N. Lovendahl, A. St Martin, R. S. Harris and W. R. Gordon (2018). "Increasing Cas9-mediated homology-directed repair efficiency through covalent tethering of DNA repair template." Commun Biol **1**: 54.

Al-Chalabi, A., P. M. Andersen, P. Nilsson, B. Chioza, J. L. Andersson, C. Russ, C. E. Shaw, J. F. Powell and P. N. Leigh (1999). "Deletions of the heavy neurofilament subunit tail in amyotrophic lateral sclerosis." Hum Mol Genet **8**(2): 157-164.

Al-Chalabi, A., A. Calvo, A. Chio, S. Colville, C. M. Ellis, O. Hardiman, M. Heverin, R. S. Howard, M. H. B. Huisman, N. Keren, P. N. Leigh, L. Mazzini, G. Mora, R. W. Orrell, J. Rooney, K. M. Scott, W. J. Scotton, M. Seelen, C. E. Shaw, K. S. Sidle, R. Swingler, M. Tsuda, J. H. Veldink, A. E. Visser, L. H. van den Berg and N. Pearce (2014). "Analysis of amyotrophic lateral sclerosis as a multistep process: a population-based modelling study." Lancet Neurol **13**(11): 1108-1113.

Al-Saif, A., F. Al-Mohanna and S. Bohlega (2011). "A mutation in sigma-1 receptor causes juvenile amyotrophic lateral sclerosis." Ann Neurol **70**(6): 913-919.

Alami, N. H., R. B. Smith, M. A. Carrasco, L. A. Williams, C. S. Winborn, S. S. W. Han, E. Kiskinis, B. Winborn, B. D. Freibaum, A. Kanagaraj, A. J. Clare, N. M. Badders, B. Bilican, E. Chaum, S. Chandran, C. E. Shaw, K. C. Eggan, T. Maniatis and J. P. Taylor (2014). "Axonal transport of TDP-43 mRNA granules is impaired by ALS-causing mutations." Neuron **81**(3): 536-543.

Alfahad, T. B. and A. Nath (2013). "Update on HIV-associated neurocognitive disorders." Curr Neurol Neurosci Rep **13**(10): 387.

Amit, I., M. Garber, N. Chevrier, A. P. Leite, Y. Donner, T. Eisenhaure, M. Guttman, J. K. Grenier, W. Li, O. Zuk, L. A. Schubert, B. Birditt, T. Shay, A. Goren, X. Zhang, Z. Smith, R. Deering, R. C. McDonald, M. Cabili, B. E. Bernstein, J. L. Rinn, A. Meissner, D. E. Root, N. Hacohen and A. Regev (2009). "Unbiased reconstruction

of a mammalian transcriptional network mediating pathogen responses." Science **326**(5950): 257-263.

An, H., L. Skelt, A. Notaro, J. R. Highley, A. H. Fox, V. La Bella, V. L. Buchman and T. A. Shelkovnikova (2019). "ALS-linked FUS mutations confer loss and gain of function in the nucleus by promoting excessive formation of dysfunctional paraspeckles." Acta Neuropathol Commun **7**(1): 7.

Andersen, J. S., C. E. Lyon, A. H. Fox, A. K. Leung, Y. W. Lam, H. Steen, M. Mann and A. I. Lamond (2002). "Directed proteomic analysis of the human nucleolus." Curr Biol **12**(1): 1-11.

Andersen, P. M. and A. Al-Chalabi (2011). "Clinical genetics of amyotrophic lateral sclerosis: what do we really know?" Nat Rev Neurol **7**(11): 603-615.

Anderson, P. and N. Kedersha (2008). "Stress granules: the Tao of RNA triage." Trends Biochem Sci **33**(3): 141-150.

Anderson, P. and N. Kedersha (2009a). "RNA granules: post-transcriptional and epigenetic modulators of gene expression." Nat Rev Mol Cell Biol **10**(6): 430-436.

Anderson, P. and N. Kedersha (2009b). "Stress granules." Curr Biol **19**(10): R397-398.

Arthur, K. C., A. Calvo, T. R. Price, J. T. Geiger, A. Chio and B. J. Traynor (2016). "Projected increase in amyotrophic lateral sclerosis from 2015 to 2040." Nat Commun **7**: 12408.

Ash, P. E., K. F. Bieniek, T. F. Gendron, T. Caulfield, W. L. Lin, M. Dejesus-Hernandez, M. M. van Blitterswijk, K. Jansen-West, J. W. Paul, 3rd, R. Rademakers, K. B. Boylan, D. W. Dickson and L. Petrucelli (2013). "Unconventional translation of C9ORF72 GGGGCC expansion generates insoluble polypeptides specific to c9FTD/ALS." Neuron **77**(4): 639-646.

Aulas, A., S. Stabile and C. Vande Velde (2012). "Endogenous TDP-43, but not FUS, contributes to stress granule assembly via G3BP." Mol Neurodegener **7**: 54.

Aulas, A. and C. Vande Velde (2015). "Alterations in stress granule dynamics driven by TDP-43 and FUS: a link to pathological inclusions in ALS?" Front Cell Neurosci **9**: 423.

Ayala, Y. M., P. Zago, A. D'Ambrogio, Y. F. Xu, L. Petrucelli, E. Buratti and F. E. Baralle (2008). "Structural determinants of the cellular localization and shuttling of TDP-43." J Cell Sci **121**(Pt 22): 3778-3785.

Bae, J. S., N. G. Simon, P. Menon, S. Vucic and M. C. Kiernan (2013). "The puzzling case of hyperexcitability in amyotrophic lateral sclerosis." J Clin Neurol **9**(2): 65-74.

Baldwin, K. R., V. K. Godena, V. L. Hewitt and A. J. Whitworth (2016). "Axonal transport defects are a common phenotype in Drosophila models of ALS." Hum Mol Genet **25**(12): 2378-2392.

Balendra, R. and A. M. Isaacs (2018). "C9orf72-mediated ALS and FTD: multiple pathways to disease." Nat Rev Neurol **14**(9): 544-558.

Banerjee, A., K. E. Vest, G. K. Pavlath and A. H. Corbett (2017). "Nuclear poly(A) binding protein 1 (PABPN1) and Matrin3 interact in muscle cells and regulate RNA processing." Nucleic Acids Res **45**(18): 10706-10725.

Bannwarth, S., S. Ait-El-Mkadem, A. Chaussenot, E. C. Genin, S. Lacas-Gervais, K. Fragaki, L. Berg-Alonso, Y. Kageyama, V. Serre, D. G. Moore, A. Verschueren, C. Rouzier, I. Le Ber, G. Auge, C. Cochaud, F. Lespinasse, K. N'Guyen, A. de Septenville, A. Brice, P. Yu-Wai-Man, H. Sesaki, J. Pouget and V. Paquis-Flucklinger (2014). "A mitochondrial origin for frontotemporal dementia and amyotrophic lateral sclerosis through CHCHD10 involvement." Brain **137**(Pt 8): 2329-2345.

Barmada, S. J., S. Ju, A. Arjun, A. Batarse, H. C. Archbold, D. Peisach, X. Li, Y. Zhang, E. M. Tank, H. Qiu, E. J. Huang, D. Ringe, G. A. Petsko and S. Finkbeiner (2015). "Amelioration of toxicity in neuronal models of amyotrophic lateral sclerosis by hUPF1." Proc Natl Acad Sci U S A **112**(25): 7821-7826.

Barmada, S. J., G. Skibinski, E. Korb, E. J. Rao, J. Y. Wu and S. Finkbeiner (2010). "Cytoplasmic mislocalization of TDP-43 is toxic to neurons and enhanced by a mutation associated with familial amyotrophic lateral sclerosis." J Neurosci **30**(2): 639-649.

Baron, D. M., L. J. Kaushansky, C. L. Ward, R. R. Sama, R. J. Chian, K. J. Boggio, A. J. Quaresma, J. A. Nickerson and D. A. Bosco (2013). "Amyotrophic lateral sclerosis-linked FUS/TLS alters stress granule assembly and dynamics." Mol Neurodegener **8**: 30.

Barry, G., J. A. Briggs, D. W. Hwang, S. P. Nayler, P. R. Fortuna, N. Jonkhout, F. Dachet, J. L. Maag, P. Mestdagh, E. M. Singh, L. Avesson, D. C. Kaczorowski, E. Ozturk, N. C. Jones, I. Vetter, L. Arriola-Martinez, J. Hu, G. R. Franco, V. M. Warn, A. Gong, M. E. Dinger, F. Rigo, L. Lipovich, M. J. Morris, T. J. O'Brien, D. S. Lee, J. A. Loeb, S. Blackshaw, J. S. Mattick and E. J. Wolvetang (2017). "The long non-coding RNA NEAT1 is responsive to neuronal activity and is associated with hyperexcitability states." Sci Rep **7**: 40127.

Bass, B. L. (2002). "RNA editing by adenosine deaminases that act on RNA." Annu Rev Biochem **71**: 817-846.

Basso, M., G. Samengo, G. Nardo, T. Massignan, G. D'Alessandro, S. Tartari, L. Cantoni, M. Marino, C. Cheroni, S. De Biasi, M. T. Giordana, M. J. Strong, A. G. Estevez, M. Salmona, C. Bendotti and V. Bonetto (2009). "Characterization of detergent-insoluble proteins in ALS indicates a causal link between nitrative stress and aggregation in pathogenesis." PLoS One **4**(12): e8130.

Bedford, M. T. and S. G. Clarke (2009). "Protein arginine methylation in mammals: who, what, and why." Mol Cell **33**(1): 1-13.

Belzil, V. V., P. O. Bauer, M. Prudencio, T. F. Gendron, C. T. Stetler, I. K. Yan, L. Pregent, L. Daughrity, M. C. Baker, R. Rademakers, K. Boylan, T. C. Patel, D. W. Dickson and L. Petrucelli (2013). "Reduced C9orf72 gene expression in c9FTD/ALS is caused by histone trimethylation, an epigenetic event detectable in blood." Acta Neuropathol **126**(6): 895-905.

Bhandari, R., A. Kuhad and A. Kuhad (2018). "Edaravone: a new hope for deadly amyotrophic lateral sclerosis." Drugs Today (Barc) **54**(6): 349-360.

Bilsland, L. G., E. Sahai, G. Kelly, M. Golding, L. Greensmith and G. Schiavo (2010). "Deficits in axonal transport precede ALS symptoms in vivo." Proc Natl Acad Sci U S A **107**(47): 20523-20528.

Blokhuis, A. M., E. J. Groen, M. Koppers, L. H. van den Berg and R. J. Pasterkamp (2013). "Protein aggregation in amyotrophic lateral sclerosis." Acta Neuropathol **125**(6): 777-794.

Bluthgen, N., M. van Bentum, B. Merz, D. Kuhl and G. Hermey (2017). "Profiling the MAPK/ERK dependent and independent activity regulated transcriptional programs in the murine hippocampus in vivo." Sci Rep **7**: 45101.

Boeynaems, S., E. Bogaert, D. Kovacs, A. Konijnenberg, E. Timmerman, A. Volkov, M. Guharoy, M. De Decker, T. Jaspers, V. H. Ryan, A. M. Janke, P. Baatsen, T. Vercruysse, R. M. Kolaitis, D. Daelemans, J. P. Taylor, N. Kedersha, P. Anderson, F. Impens, F. Sobott, J. Schymkowitz, F. Rousseau, N. L. Fawzi, W. Robberecht, P. Van Damme, P. Tompa and L. Van Den Bosch (2017). "Phase Separation of C9orf72 Dipeptide Repeats Perturbs Stress Granule Dynamics." Mol Cell **65**(6): 1044-1055 e1045.

Boeynaems, S., E. Bogaert, E. Michiels, I. Gijselinck, A. Sieben, A. Jovicic, G. De Baets, W. Scheveneels, J. Steyaert, I. Cuijt, K. J. Verstrepen, P. Callaerts, F. Rousseau, J. Schymkowitz, M. Cruts, C. Van Broeckhoven, P. Van Damme, A. D. Gitler, W. Robberecht and L. Van Den Bosch (2016). "Drosophila screen connects nuclear transport genes to DPR pathology in c9ALS/FTD." Sci Rep **6**: 20877.

Bosco, D. A., N. Lemay, H. K. Ko, H. Zhou, C. Burke, T. J. Kwiatkowski, Jr., P. Sapp, D. McKenna-Yasek, R. H. Brown, Jr. and L. J. Hayward (2010). "Mutant FUS proteins that cause amyotrophic lateral sclerosis incorporate into stress granules." Hum Mol Genet **19**(21): 4160-4175.

Bose, J. K., C. C. Huang and C. K. Shen (2011). "Regulation of autophagy by neuropathological protein TDP-43." J Biol Chem **286**(52): 44441-44448.

Bottini, S., N. Hamouda-Tekaya, R. Mategot, L. E. Zaragosi, S. Audebert, S. Pisano, V. Grandjean, C. Mauduit, M. Benahmed, P. Barbry, E. Repetto and M.

Trabucchi (2017). "Post-transcriptional gene silencing mediated by microRNAs is controlled by nucleoplasmic Sfpq." Nat Commun **8**(1): 1189.

Bounedjah, O., B. Desforges, T. D. Wu, C. Pioche-Durieu, S. Marco, L. Hamon, P. A. Curmi, J. L. Guerquin-Kern, O. Pietrement and D. Pastre (2014). "Free mRNA in excess upon polysome dissociation is a scaffold for protein multimerization to form stress granules." Nucleic Acids Res **42**(13): 8678-8691.

Brautigan, D. L. (1995). "Flicking the switches: phosphorylation of serine/threonine protein phosphatases." Semin Cancer Biol **6**(4): 211-217.

Brengues, M., D. Teixeira and R. Parker (2005). "Movement of eukaryotic mRNAs between polysomes and cytoplasmic processing bodies." Science **310**(5747): 486-489.

Brown, J. A., M. L. Valenstein, T. A. Yario, K. T. Tycowski and J. A. Steitz (2012). "Formation of triple-helical structures by the 3'-end sequences of MALAT1 and MENbeta noncoding RNAs." Proc Natl Acad Sci U S A **109**(47): 19202-19207.

Brutting, C., A. Emmer, M. E. Kornhuber and M. S. Staege (2017). "Cooccurrences of Putative Endogenous Retrovirus-Associated Diseases." Biomed Res Int **2017**: 7973165.

Buchan, J. R., R. M. Kolaitis, J. P. Taylor and R. Parker (2013). "Eukaryotic stress granules are cleared by autophagy and Cdc48/VCP function." Cell **153**(7): 1461-1474.

Buchan, J. R. and R. Parker (2009). "Eukaryotic stress granules: the ins and outs of translation." Mol Cell **36**(6): 932-941.

Buratti, E. and F. E. Baralle (2012). "TDP-43: gumming up neurons through protein-protein and protein-RNA interactions." Trends Biochem Sci **37**(6): 237-247.

Canver, M. C., D. E. Bauer, A. Dass, Y. Y. Yien, J. Chung, T. Masuda, T. Maeda, B. H. Paw and S. H. Orkin (2014). "Characterization of genomic deletion efficiency mediated by clustered regularly interspaced short palindromic repeats (CRISPR)/Cas9 nuclease system in mammalian cells." J Biol Chem **289**(31): 21312-21324.

Celeste, D. B. and M. S. Miller (2018). "Reviewing the evidence for viruses as environmental risk factors for ALS: A new perspective." Cytokine **108**: 173-178.

Chakravarty, D., A. Sboner, S. S. Nair, E. Giannopoulou, R. Li, S. Hennig, J. M. Mosquera, J. Pauwels, K. Park, M. Kossai, T. Y. MacDonald, J. Fontugne, N. Erho, I. A. Vergara, M. Ghadessi, E. Davicioni, R. B. Jenkins, N. Palanisamy, Z. Chen, S. Nakagawa, T. Hirose, N. H. Bander, H. Beltran, A. H. Fox, O. Elemento and M. A. Rubin (2014). "The oestrogen receptor alpha-regulated lncRNA NEAT1 is a critical modulator of prostate cancer." Nat Commun **5**: 5383.

Chang, J. R., M. Ghafouri, R. Mukerjee, A. Bagashev, T. Chabrashvili and B. E. Sawaya (2012). "Role of p53 in neurodegenerative diseases." Neurodegener Dis **9**(2): 68-80.

Chen, B., M. Retzlaff, T. Roos and J. Frydman (2011). "Cellular strategies of protein quality control." Cold Spring Harb Perspect Biol **3**(8): a004374.

Chen, H. J., J. C. Mitchell, S. Novoselov, J. Miller, A. L. Nishimura, E. L. Scotter, C. A. Vance, M. E. Cheetham and C. E. Shaw (2016). "The heat shock response plays an important role in TDP-43 clearance: evidence for dysfunction in amyotrophic lateral sclerosis." Brain **139**(Pt 5): 1417-1432.

Chen, L. L. and G. G. Carmichael (2009). "Altered nuclear retention of mRNAs containing inverted repeats in human embryonic stem cells: functional role of a nuclear noncoding RNA." Mol Cell **35**(4): 467-478.

Chen, L. L., J. N. DeCerbo and G. G. Carmichael (2008). "Alu element-mediated gene silencing." EMBO J **27**(12): 1694-1705.

Chen, W., Y. Zhang, W. S. Yeo, T. Bae and Q. Ji (2017). "Rapid and Efficient Genome Editing in Staphylococcus aureus by Using an Engineered CRISPR/Cas9 System." J Am Chem Soc **139**(10): 3790-3795.

Chen, Y. Z., C. L. Bennett, H. M. Huynh, I. P. Blair, I. Puls, J. Irobi, I. Dierick, A. Abel, M. L. Kennerson, B. A. Rabin, G. A. Nicholson, M. Auer-Grumbach, K. Wagner, P. De Jonghe, J. W. Griffin, K. H. Fischbeck, V. Timmerman, D. R. Cornblath and P. F. Chance (2004). "DNA/RNA helicase gene mutations in a form of juvenile amyotrophic lateral sclerosis (ALS4)." Am J Hum Genet **74**(6): 1128-1135.

Chesi, A., B. T. Staahl, A. Jovicic, J. Couthouis, M. Fasolino, A. R. Raphael, T. Yamazaki, L. Elias, M. Polak, C. Kelly, K. L. Williams, J. A. Fifita, N. J. Maragakis, G. A. Nicholson, O. D. King, R. Reed, G. R. Crabtree, I. P. Blair, J. D. Glass and A. D. Gitler (2013). "Exome sequencing to identify de novo mutations in sporadic ALS trios." Nat Neurosci **16**(7): 851-855.

Chhatbar, C., C. N. Detje, E. Grabski, K. Borst, J. Spanier, L. Ghita, D. A. Elliott, M. J. C. Jordao, N. Mueller, J. Sutton, C. K. Prajeeth, V. Gudi, M. A. Klein, M. Prinz, F. Bradke, M. Stangel and U. Kalinke (2018). "Type I Interferon Receptor Signaling of Neurons and Astrocytes Regulates Microglia Activation during Viral Encephalitis." Cell Rep **25**(1): 118-129 e114.

Chia, R., A. Chio and B. J. Traynor (2018). "Novel genes associated with amyotrophic lateral sclerosis: diagnostic and clinical implications." Lancet Neurol **17**(1): 94-102.

Chio, A., L. Mazzini, S. D'Alfonso, L. Corrado, A. Canosa, C. Moglia, U. Manera, E. Bersano, M. Brunetti, M. Barberis, J. H. Veldink, L. H. van den Berg, N. Pearce, W. Sproviero, R. McLaughlin, A. Vajda, O. Hardiman, J. Rooney, G. Mora, A. Calvo and

A. Al-Chalabi (2018). "The multistep hypothesis of ALS revisited: The role of genetic mutations." Neurology **91**(7): e635-e642.

Chio, A., G. Restagno, M. Brunetti, I. Ossola, A. Calvo, G. Mora, M. Sabatelli, M. R. Monsurro, S. Battistini, J. Mandrioli, F. Salvi, R. Spataro, J. Schymick, B. J. Traynor, V. La Bella and I. Consortium (2009). "Two Italian kindreds with familial amyotrophic lateral sclerosis due to FUS mutation." Neurobiol Aging **30**(8): 1272-1275.

Choudhry, H., A. Albukhari, M. Morotti, S. Haider, D. Moralli, J. Smythies, J. Schodel, C. M. Green, C. Camps, F. Buffa, P. Ratcliffe, J. Ragoussis, A. L. Harris and D. R. Mole (2015). "Tumor hypoxia induces nuclear paraspeckle formation through HIF-2alpha dependent transcriptional activation of NEAT1 leading to cancer cell survival." Oncogene **34**(34): 4482-4490.

Chow, C. Y., J. E. Landers, S. K. Bergren, P. C. Sapp, A. E. Grant, J. M. Jones, L. Everett, G. M. Lenk, D. M. McKenna-Yasek, L. S. Weisman, D. Figlewicz, R. H. Brown and M. H. Meisler (2009). "Deleterious variants of FIG4, a phosphoinositide phosphatase, in patients with ALS." Am J Hum Genet **84**(1): 85-88.

Chujo, T., T. Yamazaki, T. Kawaguchi, S. Kurosaka, T. Takumi, S. Nakagawa and T. Hirose (2017). "Unusual semi-extractability as a hallmark of nuclear body-associated architectural noncoding RNAs." EMBO J **36**(10): 1447-1462.

Cirulli, E. T., B. N. Lasseigne, S. Petrovski, P. C. Sapp, P. A. Dion, C. S. Leblond, J. Couthouis, Y. F. Lu, Q. Wang, B. J. Krueger, Z. Ren, J. Keebler, Y. Han, S. E. Levy, B. E. Boone, J. R. Wimbish, L. L. Waite, A. L. Jones, J. P. Carulli, A. G. Day-Williams, J. F. Staropoli, W. W. Xin, A. Chesi, A. R. Raphael, D. McKenna-Yasek, J. Cady, J. M. Vianney de Jong, K. P. Kenna, B. N. Smith, S. Topp, J. Miller, A. Gkazi, F. S. Consortium, A. Al-Chalabi, L. H. van den Berg, J. Veldink, V. Silani, N. Ticozzi, C. E. Shaw, R. H. Baloh, S. Appel, E. Simpson, C. Lagier-Tourenne, S. M. Pulst, S. Gibson, J. Q. Trojanowski, L. Elman, L. McCluskey, M. Grossman, N. A. Shneider, W. K. Chung, J. M. Ravits, J. D. Glass, K. B. Sims, V. M. Van Deerlin, T. Maniatis, S. D. Hayes, A. Ordureau, S. Swarup, J. Landers, F. Baas, A. S. Allen, R. S. Bedlack, J. W. Harper, A. D. Gitler, G. A. Rouleau, R. Brown, M. B. Harms, G. M. Cooper, T. Harris, R. M. Myers and D. B. Goldstein (2015). "Exome sequencing in amyotrophic lateral sclerosis identifies risk genes and pathways." Science **347**(6229): 1436-1441.

Clemson, C. M., J. N. Hutchinson, S. A. Sara, A. W. Ensminger, A. H. Fox, A. Chess and J. B. Lawrence (2009). "An architectural role for a nuclear noncoding RNA: NEAT1 RNA is essential for the structure of paraspeckles." Mol Cell **33**(6): 717-726.

Cloutier, F., A. Marrero, C. O'Connell and P. Morin, Jr. (2015). "MicroRNAs as potential circulating biomarkers for amyotrophic lateral sclerosis." J Mol Neurosci **56**(1): 102-112.

Cong, L., F. A. Ran, D. Cox, S. Lin, R. Barretto, N. Habib, P. D. Hsu, X. Wu, W. Jiang, L. A. Marraffini and F. Zhang (2013). "Multiplex genome engineering using CRISPR/Cas systems." Science **339**(6121): 819-823.

Cooper-Knock, J., P. J. Shaw and J. Kirby (2014). "The widening spectrum of C9ORF72-related disease; genotype/phenotype correlations and potential modifiers of clinical phenotype." Acta Neuropathol **127**(3): 333-345.

Corrado, L., R. Del Bo, B. Castellotti, A. Ratti, C. Cereda, S. Penco, G. Soraru, Y. Carlomagno, S. Ghezzi, V. Pensato, C. Colombrita, S. Gagliardi, L. Cozzi, V. Orsetti, M. Mancuso, G. Siciliano, L. Mazzini, G. P. Comi, C. Gellera, M. Ceroni, S. D'Alfonso and V. Silani (2010). "Mutations of FUS gene in sporadic amyotrophic lateral sclerosis." J Med Genet **47**(3): 190-194.

Correia, A. S., P. Patel, K. Dutta and J. P. Julien (2015). "Inflammation Induces TDP-43 Mislocalization and Aggregation." PLoS One **10**(10): e0140248.

Couthouis, J., M. P. Hart, R. Erion, O. D. King, Z. Diaz, T. Nakaya, F. Ibrahim, H. J. Kim, J. Mojsilovic-Petrovic, S. Panossian, C. E. Kim, E. C. Frackelton, J. A. Solski, K. L. Williams, D. Clay-Falcone, L. Elman, L. McCluskey, R. Greene, H. Hakonarson, R. G. Kalb, V. M. Lee, J. Q. Trojanowski, G. A. Nicholson, I. P. Blair, N. M. Bonini, V. M. Van Deerlin, Z. Mourelatos, J. Shorter and A. D. Gitler (2012). "Evaluating the role of the FUS/TLS-related gene EWSR1 in amyotrophic lateral sclerosis." Hum Mol Genet **21**(13): 2899-2911.

Couthouis, J., M. P. Hart, J. Shorter, M. DeJesus-Hernandez, R. Erion, R. Oristano, A. X. Liu, D. Ramos, N. Jethava, D. Hosangadi, J. Epstein, A. Chiang, Z. Diaz, T. Nakaya, F. Ibrahim, H. J. Kim, J. A. Solski, K. L. Williams, J. Mojsilovic-Petrovic, C. Ingre, K. Boylan, N. R. Graff-Radford, D. W. Dickson, D. Clay-Falcone, L. Elman, L. McCluskey, R. Greene, R. G. Kalb, V. M. Lee, J. Q. Trojanowski, A. Ludolph, W. Robberecht, P. M. Andersen, G. A. Nicholson, I. P. Blair, O. D. King, N. M. Bonini, V. Van Deerlin, R. Rademakers, Z. Mourelatos and A. D. Gitler (2011). "A yeast functional screen predicts new candidate ALS disease genes." Proc Natl Acad Sci U S A **108**(52): 20881-20890.

Cromwell, C. R., K. Sung, J. Park, A. R. Krysler, J. Jovel, S. K. Kim and B. P. Hubbard (2018). "Incorporation of bridged nucleic acids into CRISPR RNAs improves Cas9 endonuclease specificity." Nat Commun **9**(1): 1448.

Crozat, A., P. Aman, N. Mandahl and D. Ron (1993). "Fusion of CHOP to a novel RNA-binding protein in human myxoid liposarcoma." Nature **363**(6430): 640-644.

Cui, R., M. Tuo, P. Li and C. Zhou (2018). "Association between TBK1 mutations and risk of amyotrophic lateral sclerosis/frontotemporal dementia spectrum: a meta-analysis." Neurol Sci **39**(5): 811-820.

Daigle, J. G., N. A. Lanson, Jr., R. B. Smith, I. Casci, A. Maltare, J. Monaghan, C. D. Nichols, D. Kryndushkin, F. Shewmaker and U. B. Pandey (2013). "RNA-binding ability of FUS regulates neurodegeneration, cytoplasmic mislocalization and incorporation into stress granules associated with FUS carrying ALS-linked mutations." Hum Mol Genet **22**(6): 1193-1205.

Darovic, S., S. Prpar Mihevc, V. Zupunski, G. Guncar, M. Stalekar, Y. B. Lee, C. E. Shaw and B. Rogelj (2015). "Phosphorylation of C-terminal tyrosine residue 526 in FUS impairs its nuclear import." J Cell Sci **128**(22): 4151-4159.

De Santis, R., L. Santini, A. Colantoni, G. Peruzzi, V. de Turris, V. Alfano, I. Bozzoni and A. Rosa (2017). "FUS Mutant Human Motoneurons Display Altered Transcriptome and microRNA Pathways with Implications for ALS Pathogenesis." Stem Cell Reports **9**(5): 1450-1462.

De Vos, K. J., A. L. Chapman, M. E. Tennant, C. Manser, E. L. Tudor, K. F. Lau, J. Brownlees, S. Ackerley, P. J. Shaw, D. M. McLoughlin, C. E. Shaw, P. N. Leigh, C. C. J. Miller and A. J. Grierson (2007). "Familial amyotrophic lateral sclerosis-linked SOD1 mutants perturb fast axonal transport to reduce axonal mitochondria content." Hum Mol Genet **16**(22): 2720-2728.

de Weerd, N. A. and T. Nguyen (2012). "The interferons and their receptors--distribution and regulation." Immunol Cell Biol **90**(5): 483-491.

DeJesus-Hernandez, M., J. Kocerha, N. Finch, R. Crook, M. Baker, P. Desaro, A. Johnston, N. Rutherford, A. Wojtas, K. Kennelly, Z. K. Wszolek, N. Graff-Radford, K. Boylan and R. Rademakers (2010). "De novo truncating FUS gene mutation as a cause of sporadic amyotrophic lateral sclerosis." Hum Mutat **31**(5): E1377-1389.

DeJesus-Hernandez, M., I. R. Mackenzie, B. F. Boeve, A. L. Boxer, M. Baker, N. J. Rutherford, A. M. Nicholson, N. A. Finch, H. Flynn, J. Adamson, N. Kouri, A. Wojtas, P. Sengdy, G. Y. Hsiung, A. Karydas, W. W. Seeley, K. A. Josephs, G. Coppola, D. H. Geschwind, Z. K. Wszolek, H. Feldman, D. S. Knopman, R. C. Petersen, B. L. Miller, D. W. Dickson, K. B. Boylan, N. R. Graff-Radford and R. Rademakers (2011). "Expanded GGGGCC hexanucleotide repeat in noncoding region of C9ORF72 causes chromosome 9p-linked FTD and ALS." Neuron **72**(2): 245-256.

Deng, H., K. Gao and J. Jankovic (2014a). "The role of FUS gene variants in neurodegenerative diseases." Nat Rev Neurol **10**(6): 337-348.

Deng, H. X., W. Chen, S. T. Hong, K. M. Boycott, G. H. Gorrie, N. Siddique, Y. Yang, F. Fecto, Y. Shi, H. Zhai, H. Jiang, M. Hirano, E. Rampersaud, G. H. Jansen, S. Donkervoort, E. H. Bigio, B. R. Brooks, K. Ajroud, R. L. Sufit, J. L. Haines, E. Mugnaini, M. A. Pericak-Vance and T. Siddique (2011). "Mutations in UBQLN2 cause dominant X-linked juvenile and adult-onset ALS and ALS/dementia." Nature **477**(7363): 211-215.

Deng, H. X., H. Zhai, E. H. Bigio, J. Yan, F. Fecto, K. Ajroud, M. Mishra, S. Ajroud-Driss, S. Heller, R. Sufit, N. Siddique, E. Mugnaini and T. Siddique (2010). "FUS-immunoreactive inclusions are a common feature in sporadic and non-SOD1 familial amyotrophic lateral sclerosis." Ann Neurol **67**(6): 739-748.

Deng, Q., C. J. Holler, G. Taylor, K. F. Hudson, W. Watkins, M. Gearing, D. Ito, M. E. Murray, D. W. Dickson, N. T. Seyfried and T. Kukar (2014b). "FUS is phosphorylated by DNA-PK and accumulates in the cytoplasm after DNA damage." J Neurosci **34**(23): 7802-7813.

Devoy, A., B. Kalmar, M. Stewart, H. Park, B. Burke, S. J. Noy, Y. Redhead, J. Humphrey, K. Lo, J. Jaeger, A. Mejia Maza, P. Sivakumar, C. Bertolin, G. Soraru, V. Plagnol, L. Greensmith, A. Acevedo Arozena, A. M. Isaacs, B. Davies, P. Fratta and E. M. C. Fisher (2017). "Humanized mutant FUS drives progressive motor neuron degeneration without aggregation in 'FUSDelta14' knockin mice." Brain **140**(11): 2797-2805.

Dewey, C. M., B. Cenik, C. F. Sephton, D. R. Dries, P. Mayer, 3rd, S. K. Good, B. A. Johnson, J. Herz and G. Yu (2011). "TDP-43 is directed to stress granules by sorbitol, a novel physiological osmotic and oxidative stressor." Mol Cell Biol **31**(5): 1098-1108.

Doench, J. G., N. Fusi, M. Sullender, M. Hegde, E. W. Vaimberg, K. F. Donovan, I. Smith, Z. Tothova, C. Wilen, R. Orchard, H. W. Virgin, J. Listgarten and D. E. Root (2016). "Optimized sgRNA design to maximize activity and minimize off-target effects of CRISPR-Cas9." Nat Biotechnol **34**(2): 184-191.

Donnelly, C. J., P. W. Zhang, J. T. Pham, A. R. Haeusler, N. A. Mistry, S. Vidensky, E. L. Daley, E. M. Poth, B. Hoover, D. M. Fines, N. Maragakis, P. J. Tienari, L. Petrucelli, B. J. Traynor, J. Wang, F. Rigo, C. F. Bennett, S. Blackshaw, R. Sattler and J. D. Rothstein (2013). "RNA toxicity from the ALS/FTD C9ORF72 expansion is mitigated by antisense intervention." Neuron **80**(2): 415-428.

Dormann, D., T. Madl, C. F. Valori, E. Bentmann, S. Tahirovic, C. Abou-Ajram, E. Kremmer, O. Ansorge, I. R. Mackenzie, M. Neumann and C. Haass (2012). "Arginine methylation next to the PY-NLS modulates Transportin binding and nuclear import of FUS." EMBO J **31**(22): 4258-4275.

Dormann, D., R. Rodde, D. Edbauer, E. Bentmann, I. Fischer, A. Hruscha, M. E. Than, I. R. Mackenzie, A. Capell, B. Schmid, M. Neumann and C. Haass (2010). "ALS-associated fused in sarcoma (FUS) mutations disrupt Transportin-mediated nuclear import." EMBO J **29**(16): 2841-2857.

Douville, R., J. Liu, J. Rothstein and A. Nath (2011). "Identification of active loci of a human endogenous retrovirus in neurons of patients with amyotrophic lateral sclerosis." Ann Neurol **69**(1): 141-151.

Droppelmann, C. A., D. Campos-Melo, M. Ishtiaq, K. Volkening and M. J. Strong (2014). "RNA metabolism in ALS: when normal processes become pathological." Amyotroph Lateral Scler Frontotemporal Degener **15**(5-6): 321-336.

Ederle, H. and D. Dormann (2017). "TDP-43 and FUS en route from the nucleus to the cytoplasm." FEBS Lett **591**(11): 1489-1507.

Elden, A. C., H. J. Kim, M. P. Hart, A. S. Chen-Plotkin, B. S. Johnson, X. Fang, M. Armakola, F. Geser, R. Greene, M. M. Lu, A. Padmanabhan, D. Clay-Falcone, L. McCluskey, L. Elman, D. Juhr, P. J. Gruber, U. Rub, G. Auburger, J. Q. Trojanowski, V. M. Lee, V. M. Van Deerlin, N. M. Bonini and A. D. Gitler (2010). "Ataxin-2

intermediate-length polyglutamine expansions are associated with increased risk for ALS." Nature **466**(7310): 1069-1075.

Emde, A., C. Eitan, L. L. Liou, R. T. Libby, N. Rivkin, I. Magen, I. Reichenstein, H. Oppenheim, R. Eilam, A. Silvestroni, B. Alajajian, I. Z. Ben-Dov, J. Aebischer, A. Savidor, Y. Levin, R. Sons, S. M. Hammond, J. M. Ravits, T. Moller and E. Hornstein (2015). "Dysregulated miRNA biogenesis downstream of cellular stress and ALS-causing mutations: a new mechanism for ALS." EMBO J **34**(21): 2633-2651.

Emde, A. and E. Hornstein (2014). "miRNAs at the interface of cellular stress and disease." EMBO J **33**(13): 1428-1437.

Fallini, C., G. J. Bassell and W. Rossoll (2012). "The ALS disease protein TDP-43 is actively transported in motor neuron axons and regulates axon outgrowth." Hum Mol Genet **21**(16): 3703-3718.

Farg, M. A., V. Sundaramoorthy, J. M. Sultana, S. Yang, R. A. Atkinson, V. Levina, M. A. Halloran, P. A. Gleeson, I. P. Blair, K. Y. Soo, A. E. King and J. D. Atkin (2014). "C9ORF72, implicated in amytrophic lateral sclerosis and frontotemporal dementia, regulates endosomal trafficking." Hum Mol Genet **23**(13): 3579-3595.

Faulkner, G. J., Y. Kimura, C. O. Daub, S. Wani, C. Plessy, K. M. Irvine, K. Schroder, N. Cloonan, A. L. Steptoe, T. Lassmann, K. Waki, N. Hornig, T. Arakawa, H. Takahashi, J. Kawai, A. R. Forrest, H. Suzuki, Y. Hayashizaki, D. A. Hume, V. Orlando, S. M. Grimmond and P. Carninci (2009). "The regulated retrotransposon transcriptome of mammalian cells." Nat Genet **41**(5): 563-571.

Fecto, F., J. Yan, S. P. Vemula, E. Liu, Y. Yang, W. Chen, J. G. Zheng, Y. Shi, N. Siddique, H. Arrat, S. Donkervoort, S. Ajroud-Driss, R. L. Sufit, S. L. Heller, H. X. Deng and T. Siddique (2011). "SQSTM1 mutations in familial and sporadic amyotrophic lateral sclerosis." Arch Neurol **68**(11): 1440-1446.

Feuer, R., C. M. Ruller, N. An, J. M. Tabor-Godwin, R. E. Rhoades, S. Maciejewski, R. R. Pagarigan, C. T. Cornell, S. J. Crocker, W. B. Kiosses, N. Pham-Mitchell, I. L. Campbell and J. L. Whitton (2009). "Viral persistence and chronic immunopathology in the adult central nervous system following Coxsackievirus infection during the neonatal period." J Virol **83**(18): 9356-9369.

Finnen, R. L., T. J. Hay, B. Dauber, J. R. Smiley and B. W. Banfield (2014). "The herpes simplex virus 2 virion-associated ribonuclease vhs interferes with stress granule formation." J Virol **88**(21): 12727-12739.

Finnen, R. L., K. R. Pangka and B. W. Banfield (2012). "Herpes simplex virus 2 infection impacts stress granule accumulation." J Virol **86**(15): 8119-8130.

Fischer, L. R., D. G. Culver, P. Tennant, A. A. Davis, M. Wang, A. Castellano-Sanchez, J. Khan, M. A. Polak and J. D. Glass (2004). "Amyotrophic lateral sclerosis is a distal axonopathy: evidence in mice and man." Exp Neurol **185**(2): 232-240.

Forman, M. S., J. Q. Trojanowski and V. M. Lee (2004). "Neurodegenerative diseases: a decade of discoveries paves the way for therapeutic breakthroughs." Nat Med **10**(10): 1055-1063.

Fox, A. H., Y. W. Lam, A. K. Leung, C. E. Lyon, J. Andersen, M. Mann and A. I. Lamond (2002). "Paraspeckles: a novel nuclear domain." Curr Biol **12**(1): 13-25.

Fox, A. H. and A. I. Lamond (2010). "Paraspeckles." Cold Spring Harb Perspect Biol **2**(7): a000687.

Fox, A. H., S. Nakagawa, T. Hirose and C. S. Bond (2018). "Paraspeckles: Where Long Noncoding RNA Meets Phase Separation." Trends Biochem Sci **43**(2): 124-135.

Fratta, P., P. Sivakumar, J. Humphrey, K. Lo, T. Ricketts, H. Oliveira, J. M. Brito-Armas, B. Kalmar, A. Ule, Y. Yu, N. Birsa, C. Bodo, T. Collins, A. E. Conicella, A. Mejia Maza, A. Marrero-Gagliardi, M. Stewart, J. Mianne, S. Corrochano, W. Emmett, G. Codner, M. Groves, R. Fukumura, Y. Gondo, M. Lythgoe, E. Pauws, E. Peskett, P. Stanier, L. Teboul, M. Hallegger, A. Calvo, A. Chio, A. M. Isaacs, N. L. Fawzi, E. Wang, D. E. Housman, F. Baralle, L. Greensmith, E. Buratti, V. Plagnol, E. M. Fisher and A. Acevedo-Arozena (2018). "Mice with endogenous TDP-43 mutations exhibit gain of splicing function and characteristics of amyotrophic lateral sclerosis." EMBO J **37**(11).

Freischmidt, A., T. Wieland, B. Richter, W. Ruf, V. Schaeffer, K. Muller, N. Marroquin, F. Nordin, A. Hubers, P. Weydt, S. Pinto, R. Press, S. Millecamps, N. Molko, E. Bernard, C. Desnuelle, M. H. Soriani, J. Dorst, E. Graf, U. Nordstrom, M. S. Feiler, S. Putz, T. M. Boeckers, T. Meyer, A. S. Winkler, J. Winkelman, M. de Carvalho, D. R. Thal, M. Otto, T. Brannstrom, A. E. Volk, P. Kursula, K. M. Danzer, P. Lichtner, I. Dikic, T. Meitinger, A. C. Ludolph, T. M. Strom, P. M. Andersen and J. H. Weishaupt (2015). "Haploinsufficiency of TBK1 causes familial ALS and fronto-temporal dementia." Nat Neurosci **18**(5): 631-636.

Fronz, K., S. Guttinger, K. Burkert, U. Kuhn, N. Stohr, A. Schierhorn and E. Wahle (2011). "Arginine methylation of the nuclear poly(a) binding protein weakens the interaction with its nuclear import receptor, transportin." J Biol Chem **286**(38): 32986-32994.

Fu, Y., J. D. Sander, D. Reyon, V. M. Cascio and J. K. Joung (2014). "Improving CRISPR-Cas nuclease specificity using truncated guide RNAs." Nat Biotechnol **32**(3): 279-284.

Fujii, R., S. Okabe, T. Urushido, K. Inoue, A. Yoshimura, T. Tachibana, T. Nishikawa, G. G. Hicks and T. Takumi (2005). "The RNA binding protein TLS is translocated to dendritic spines by mGluR5 activation and regulates spine morphology." Curr Biol **15**(6): 587-593.

Fung, G., J. Shi, H. Deng, J. Hou, C. Wang, A. Hong, J. Zhang, W. Jia and H. Luo (2015). "Cytoplasmic translocation, aggregation, and cleavage of TDP-43 by enteroviral proteases modulate viral pathogenesis." Cell Death Differ **22**(12): 2087-2097.

Gal, J., J. Zhang, D. M. Kwinter, J. Zhai, H. Jia, J. Jia and H. Zhu (2011). "Nuclear localization sequence of FUS and induction of stress granules by ALS mutants." Neurobiol Aging **32**(12): 2323 e2327-2340.

Ganesan, S., G. Rohde, K. Eckermann, K. Sroka, M. K. Schaefer, C. P. Dohm, P. Kermer, G. Haase, F. Wouters, M. Bahr and J. H. Weishaupt (2008). "Mutant SOD1 detoxification mechanisms in intact single cells." Cell Death Differ **15**(2): 312-321.

Gao, G., J. Zhang, X. Si, J. Wong, C. Cheung, B. McManus and H. Luo (2008). "Proteasome inhibition attenuates coxsackievirus-induced myocardial damage in mice." Am J Physiol Heart Circ Physiol **295**(1): H401-408.

Garvey, L. J., N. Pavese, M. Politis, A. Ramlackhansingh, D. J. Brooks, S. D. Taylor-Robinson and A. Winston (2014). "Increased microglia activation in neurologically asymptomatic HIV-infected patients receiving effective ART." AIDS **28**(1): 67-72.

Gendron, T. F., K. F. Bieniek, Y. J. Zhang, K. Jansen-West, P. E. Ash, T. Caulfield, L. Daughrity, J. H. Dunmore, M. Castanedes-Casey, J. Chew, D. M. Cosio, M. van Blitterswijk, W. C. Lee, R. Rademakers, K. B. Boylan, D. W. Dickson and L. Petrucelli (2013). "Antisense transcripts of the expanded C9ORF72 hexanucleotide repeat form nuclear RNA foci and undergo repeat-associated non-ATG translation in c9FTD/ALS." Acta Neuropathol **126**(6): 829-844.

Gibb, E. A., E. A. Vucic, K. S. Enfield, G. L. Stewart, K. M. Lonergan, J. Y. Kennett, D. D. Becker-Santos, C. E. MacAulay, S. Lam, C. J. Brown and W. L. Lam (2011). "Human cancer long non-coding RNA transcriptomes." PLoS One **6**(10): e25915.

Gilks, N., N. Kedersha, M. Ayodele, L. Shen, G. Stoecklin, L. M. Dember and P. Anderson (2004). "Stress granule assembly is mediated by prion-like aggregation of TIA-1." Mol Biol Cell **15**(12): 5383-5398.

Gitcho, M. A., R. H. Baloh, S. Chakraverty, K. Mayo, J. B. Norton, D. Levitch, K. J. Hatanpaa, C. L. White, 3rd, E. H. Bigio, R. Caselli, M. Baker, M. T. Al-Lozi, J. C. Morris, A. Pestronk, R. Rademakers, A. M. Goate and N. J. Cairns (2008). "TDP-43 A315T mutation in familial motor neuron disease." Ann Neurol **63**(4): 535-538.

Greenway, M. J., P. M. Andersen, C. Russ, S. Ennis, S. Cashman, C. Donaghy, V. Patterson, R. Swingler, D. Kieran, J. Prehn, K. E. Morrison, A. Green, K. R. Acharya, R. H. Brown, Jr. and O. Hardiman (2006). "ANG mutations segregate with familial and 'sporadic' amyotrophic lateral sclerosis." Nat Genet **38**(4): 411-413.

Gregory, R. I., K. P. Yan, G. Amuthan, T. Chendrimada, B. Doratotaj, N. Cooch and R. Shiekhattar (2004). "The Microprocessor complex mediates the genesis of microRNAs." Nature **432**(7014): 235-240.

Groen, E. J., K. Fumoto, A. M. Blokhuis, J. Engelen-Lee, Y. Zhou, D. M. van den Heuvel, M. Koppers, F. van Diggelen, J. van Heest, J. A. Demmers, J. Kirby, P. J.

Shaw, E. Aronica, W. G. Spliet, J. H. Veldink, L. H. van den Berg and R. J. Pasterkamp (2013). "ALS-associated mutations in FUS disrupt the axonal distribution and function of SMN." Hum Mol Genet **22**(18): 3690-3704.

Gromicho, M., M. Oliveira Santos, A. Pinto, A. Pronto-Laborinho and M. De Carvalho (2017). "Young-onset rapidly progressive ALS associated with heterozygous FUS mutation." Amyotroph Lateral Scler Frontotemporal Degener **18**(5-6): 451-453.

Gros-Louis, F., R. Lariviere, G. Gowing, S. Laurent, W. Camu, J. P. Bouchard, V. Meininger, G. A. Rouleau and J. P. Julien (2004). "A frameshift deletion in peripherin gene associated with amyotrophic lateral sclerosis." J Biol Chem **279**(44): 45951-45956.

Guhaniyogi, J. and G. Brewer (2001). "Regulation of mRNA stability in mammalian cells." Gene **265**(1-2): 11-23.

Guilinger, J. P., D. B. Thompson and D. R. Liu (2014). "Fusion of catalytically inactive Cas9 to FokI nuclease improves the specificity of genome modification." Nat Biotechnol **32**(6): 577-582.

Guo, T., Y. L. Feng, J. J. Xiao, Q. Liu, X. N. Sun, J. F. Xiang, N. Kong, S. C. Liu, G. Q. Chen, Y. Wang, M. M. Dong, Z. Cai, H. Lin, X. J. Cai and A. Y. Xie (2018). "Harnessing accurate non-homologous end joining for efficient precise deletion in CRISPR/Cas9-mediated genome editing." Genome Biol **19**(1): 170.

Guru, S. C., S. E. Olufemi, P. Manickam, C. Cummings, L. M. Gieser, B. L. Pike, M. L. Bittner, Y. Jiang, A. C. Chinault, N. J. Nowak, A. Brzozowska, J. S. Crabtree, Y. Wang, B. A. Roe, J. M. Weisemann, M. S. Boguski, S. K. Agarwal, A. L. Burns, A. M. Spiegel, S. J. Marx, W. L. Flejter, P. J. de Jong, F. S. Collins and S. C. Chandrasekharappa (1997). "A 2.8-Mb clone contig of the multiple endocrine neoplasia type 1 (MEN1) region at 11q13." Genomics **42**(3): 436-445.

Hadano, S., C. K. Hand, H. Osuga, Y. Yanagisawa, A. Otomo, R. S. Devon, N. Miyamoto, J. Showguchi-Miyata, Y. Okada, R. Singaraja, D. A. Figlewicz, T. Kwiatkowski, B. A. Hosler, T. Sagie, J. Skaug, J. Nasir, R. H. Brown, Jr., S. W. Scherer, G. A. Rouleau, M. R. Hayden and J. E. Ikeda (2001). "A gene encoding a putative GTPase regulator is mutated in familial amyotrophic lateral sclerosis 2." Nat Genet **29**(2): 166-173.

Haramati, S., E. Chapnik, Y. Sztainberg, R. Eilam, R. Zwang, N. Gershoni, E. McGlinn, P. W. Heiser, A. M. Wills, I. Wirguin, L. L. Rubin, H. Misawa, C. J. Tabin, R. Brown, Jr., A. Chen and E. Hornstein (2010). "miRNA malfunction causes spinal motor neuron disease." Proc Natl Acad Sci U S A **107**(29): 13111-13116.

Hardiman, O., A. Al-Chalabi, A. Chio, E. M. Corr, G. Logroscino, W. Robberecht, P. J. Shaw, Z. Simmons and L. H. van den Berg (2017). "Amyotrophic lateral sclerosis." Nat Rev Dis Primers **3**: 17071.

Hennig, S., G. Kong, T. Mannen, A. Sadowska, S. Kobelke, A. Blythe, G. J. Knott, K. S. Iyer, D. Ho, E. A. Newcombe, K. Hosoki, N. Goshima, T. Kawaguchi, D. Hatters, L. Trinkle-Mulcahy, T. Hirose, C. S. Bond and A. H. Fox (2015). "Prion-like domains in RNA binding proteins are essential for building subnuclear paraspeckles." J Cell Biol **210**(4): 529-539.

Heo, J. M., A. Ordureau, J. A. Paulo, J. Rinehart and J. W. Harper (2015). "The PINK1-PARKIN Mitochondrial Ubiquitylation Pathway Drives a Program of OPTN/NDP52 Recruitment and TBK1 Activation to Promote Mitophagy." Mol Cell **60**(1): 7-20.

Hewitt, C., J. Kirby, J. R. Highley, J. A. Hartley, R. Hibberd, H. C. Hollinger, T. L. Williams, P. G. Ince, C. J. McDermott and P. J. Shaw (2010). "Novel FUS/TLS mutations and pathology in familial and sporadic amyotrophic lateral sclerosis." Arch Neurol **67**(4): 455-461.

Hicks, G. G., N. Singh, A. Nashabi, S. Mai, G. Bozek, L. Klewes, D. Arapovic, E. K. White, M. J. Koury, E. M. Oltz, L. Van Kaer and H. E. Ruley (2000). "Fus deficiency in mice results in defective B-lymphocyte development and activation, high levels of chromosomal instability and perinatal death." Nat Genet **24**(2): 175-179.

Hindley, C. E., F. J. Lawrence and D. A. Matthews (2007). "A role for transportin in the nuclear import of adenovirus core proteins and DNA." Traffic **8**(10): 1313-1322.

Hirokawa, N. (2006). "mRNA transport in dendrites: RNA granules, motors, and tracks." J Neurosci **26**(27): 7139-7142.

Hirose, T. and S. Nakagawa (2012). "Paraspeckles: possible nuclear hubs by the RNA for the RNA." Biomol Concepts **3**(5): 415-428.

Hirose, T., G. Virnicchi, A. Tanigawa, T. Naganuma, R. Li, H. Kimura, T. Yokoi, S. Nakagawa, M. Benard, A. H. Fox and G. Pierron (2014). "NEAT1 long noncoding RNA regulates transcription via protein sequestration within subnuclear bodies." Mol Biol Cell **25**(1): 169-183.

Hollams, E. M., K. M. Giles, A. M. Thomson and P. J. Leedman (2002). "MRNA stability and the control of gene expression: implications for human disease." Neurochem Res **27**(10): 957-980.

Holt, C. E. and E. M. Schuman (2013). "The central dogma decentralized: new perspectives on RNA function and local translation in neurons." Neuron **80**(3): 648-657.

Hsu, P. D., E. S. Lander and F. Zhang (2014). "Development and applications of CRISPR-Cas9 for genome engineering." Cell **157**(6): 1262-1278.

Hu, S. B., J. F. Xiang, X. Li, Y. Xu, W. Xue, M. Huang, C. C. Wong, C. A. Sagum, M. T. Bedford, L. Yang, D. Cheng and L. L. Chen (2015). "Protein arginine

methyltransferase CARM1 attenuates the paraspeckle-mediated nuclear retention of mRNAs containing IRAlus." Genes Dev **29**(6): 630-645.

Huang, C., H. Zhou, J. Tong, H. Chen, Y. J. Liu, D. Wang, X. Wei and X. G. Xia (2011). "FUS transgenic rats develop the phenotypes of amyotrophic lateral sclerosis and frontotemporal lobar degeneration." PLoS Genet **7**(3): e1002011.

Hutchinson, J. N., A. W. Ensminger, C. M. Clemson, C. R. Lynch, J. B. Lawrence and A. Chess (2007). "A screen for nuclear transcripts identifies two linked noncoding RNAs associated with SC35 splicing domains." BMC Genomics **8**: 39.

Iko, Y., T. S. Kodama, N. Kasai, T. Oyama, E. H. Morita, T. Muto, M. Okumura, R. Fujii, T. Takumi, S. Tate and K. Morikawa (2004). "Domain architectures and characterization of an RNA-binding protein, TLS." J Biol Chem **279**(43): 44834-44840.

Imamura, K., N. Imamachi, G. Akizuki, M. Kumakura, A. Kawaguchi, K. Nagata, A. Kato, Y. Kawaguchi, H. Sato, M. Yoneda, C. Kai, T. Yada, Y. Suzuki, T. Yamada, T. Ozawa, K. Kaneki, T. Inoue, M. Kobayashi, T. Kodama, Y. Wada, K. Sekimizu and N. Akimitsu (2014). "Long noncoding RNA NEAT1-dependent SFPQ relocation from promoter region to paraspeckle mediates IL8 expression upon immune stimuli." Mol Cell **53**(3): 393-406.

Ishiguro, A., N. Kimura, Y. Watanabe, S. Watanabe and A. Ishihama (2016). "TDP-43 binds and transports G-quadruplex-containing mRNAs into neurites for local translation." Genes Cells **21**(5): 466-481.

Ishihara, T., Y. Ariizumi, A. Shiga, T. Kato, C. F. Tan, T. Sato, Y. Miki, M. Yokoo, T. Fujino, A. Koyama, A. Yokoseki, M. Nishizawa, A. Kakita, H. Takahashi and O. Onodera (2013). "Decreased number of Gemini of coiled bodies and U12 snRNA level in amyotrophic lateral sclerosis." Hum Mol Genet **22**(20): 4136-4147.

Ito, D., M. Seki, Y. Tsunoda, H. Uchiyama and N. Suzuki (2011a). "Nuclear transport impairment of amyotrophic lateral sclerosis-linked mutations in FUS/TLS." Ann Neurol **69**(1): 152-162.

Ito, H., K. Fujita, M. Nakamura, R. Wate, S. Kaneko, S. Sasaki, K. Yamane, N. Suzuki, M. Aoki, N. Shibata, S. Togashi, A. Kawata, Y. Mochizuki, T. Mizutani, H. Maruyama, A. Hirano, R. Takahashi, H. Kawakami and H. Kusaka (2011b). "Optineurin is co-localized with FUS in basophilic inclusions of ALS with FUS mutation and in basophilic inclusion body disease." Acta Neuropathol **121**(4): 555-557.

Jaarsma, D., E. D. Haasdijk, J. A. Grashorn, R. Hawkins, W. van Duijn, H. W. Verspaget, J. London and J. C. Holstege (2000). "Human Cu/Zn superoxide dismutase (SOD1) overexpression in mice causes mitochondrial vacuolization, axonal degeneration, and premature motoneuron death and accelerates motoneuron disease in mice expressing a familial amyotrophic lateral sclerosis mutant SOD1." Neurobiol Dis **7**(6 Pt B): 623-643.

Jackson, K. L., R. D. Dayton, E. A. Orchard, S. Ju, D. Ringe, G. A. Petsko, L. E. Maquat and R. L. Klein (2015). "Preservation of forelimb function by UPF1 gene therapy in a rat model of TDP-43-induced motor paralysis." Gene Ther **22**(1): 20-28.

Jain, S. and R. Parker (2013). "The discovery and analysis of P Bodies." Adv Exp Med Biol **768**: 23-43.

Jain, S., J. R. Wheeler, R. W. Walters, A. Agrawal, A. Barsic and R. Parker (2016). "ATPase-Modulated Stress Granules Contain a Diverse Proteome and Substructure." Cell **164**(3): 487-498.

Japtok, J., X. Lojewski, M. Naumann, M. Klingenstein, P. Reinhardt, J. Sterneckert, S. Putz, M. Demestre, T. M. Boeckers, A. C. Ludolph, S. Liebau, A. Storch and A. Hermann (2015). "Stepwise acquirement of hallmark neuropathology in FUS-ALS iPSC models depends on mutation type and neuronal aging." Neurobiol Dis **82**: 420-429.

Jern, P. and J. M. Coffin (2008). "Effects of retroviruses on host genome function." Annu Rev Genet **42**: 709-732.

Jheng, J. R., J. Y. Ho and J. T. Horng (2014). "ER stress, autophagy, and RNA viruses." Front Microbiol **5**: 388.

Jiang, L., C. Shao, Q. J. Wu, G. Chen, J. Zhou, B. Yang, H. Li, L. T. Gou, Y. Zhang, Y. Wang, G. W. Yeo, Y. Zhou and X. D. Fu (2017). "NEAT1 scaffolds RNA-binding proteins and the Microprocessor to globally enhance pri-miRNA processing." Nat Struct Mol Biol **24**(10): 816-824.

Johnson, B. S., D. Snead, J. J. Lee, J. M. McCaffery, J. Shorter and A. D. Gitler (2009). "TDP-43 is intrinsically aggregation-prone, and amyotrophic lateral sclerosis-linked mutations accelerate aggregation and increase toxicity." J Biol Chem **284**(30): 20329-20339.

Johnson, J. O., J. Mandrioli, M. Benatar, Y. Abramzon, V. M. Van Deerlin, J. Q. Trojanowski, J. R. Gibbs, M. Brunetti, S. Gronka, J. Wuu, J. Ding, L. McCluskey, M. Martinez-Lage, D. Falcone, D. G. Hernandez, S. Arepalli, S. Chong, J. C. Schymick, J. Rothstein, F. Landi, Y. D. Wang, A. Calvo, G. Mora, M. Sabatelli, M. R. Monsurro, S. Battistini, F. Salvi, R. Spataro, P. Sola, G. Borghero, I. Consortium, G. Galassi, S. W. Scholz, J. P. Taylor, G. Restagno, A. Chio and B. J. Traynor (2010). "Exome sequencing reveals VCP mutations as a cause of familial ALS." Neuron **68**(5): 857-864.

Johnson, J. O., E. P. Pioro, A. Boehringer, R. Chia, H. Feit, A. E. Renton, H. A. Pliner, Y. Abramzon, G. Marangi, B. J. Winborn, J. R. Gibbs, M. A. Nalls, S. Morgan, M. Shoai, J. Hardy, A. Pittman, R. W. Orrell, A. Malaspina, K. C. Sidle, P. Fratta, M. B. Harms, R. H. Baloh, A. Pestronk, C. C. Weihl, E. Rogaeva, L. Zinman, V. E. Drory, G. Borghero, G. Mora, A. Calvo, J. D. Rothstein, Italsgen, C. Drepper, M. Sendtner, A. B. Singleton, J. P. Taylor, M. R. Cookson, G. Restagno, M. Sabatelli, R. Bowser,

A. Chio and B. J. Traynor (2014). "Mutations in the Matrin 3 gene cause familial amyotrophic lateral sclerosis." Nat Neurosci **17**(5): 664-666.

Kabashi, E., P. N. Valdmanis, P. Dion, D. Spiegelman, B. J. McConkey, C. Vande Velde, J. P. Bouchard, L. Lacomblez, K. Pochigaeva, F. Salachas, P. F. Pradat, W. Camu, V. Meininger, N. Dupre and G. A. Rouleau (2008). "TARDBP mutations in individuals with sporadic and familial amyotrophic lateral sclerosis." Nat Genet **40**(5): 572-574.

Kamelgarn, M., J. Chen, L. Kuang, A. Arenas, J. Zhai, H. Zhu and J. Gal (2016). "Proteomic analysis of FUS interacting proteins provides insights into FUS function and its role in ALS." Biochim Biophys Acta **1862**(10): 2004-2014.

Kamelgarn, M., J. Chen, L. Kuang, H. Jin, E. J. Kasarskis and H. Zhu (2018). "ALS mutations of FUS suppress protein translation and disrupt the regulation of nonsense-mediated decay." Proc Natl Acad Sci U S A **115**(51): E11904-E11913.

Kanai, Y., N. Dohmae and N. Hirokawa (2004). "Kinesin transports RNA: isolation and characterization of an RNA-transporting granule." Neuron **43**(4): 513-525.

Kaneb, H. M., A. W. Folkmann, V. V. Belzil, L. E. Jao, C. S. Leblond, S. L. Girard, H. Daoud, A. Noreau, D. Rochefort, P. Hince, A. Szuto, A. Levert, S. Vidal, C. Andre-Guimont, W. Camu, J. P. Bouchard, N. Dupre, G. A. Rouleau, S. R. Wente and P. A. Dion (2015). "Deleterious mutations in the essential mRNA metabolism factor, hGle1, in amyotrophic lateral sclerosis." Hum Mol Genet **24**(5): 1363-1373.

Karch, C. M., N. Wen, C. C. Fan, J. S. Yokoyama, N. Kouri, O. A. Ross, G. Hoglinger, U. Muller, R. Ferrari, J. Hardy, G. D. Schellenberg, P. M. Sleiman, P. Momeni, C. P. Hess, B. L. Miller, M. Sharma, V. Van Deerlin, O. B. Smeland, O. A. Andreassen, A. M. Dale, R. S. Desikan, I. C. f. F. D. P. S. P. G. C. International Frontotemporal Dementia -Genomics Consortium and C. International Parkinson's Disease Genomics (2018). "Selective Genetic Overlap Between Amyotrophic Lateral Sclerosis and Diseases of the Frontotemporal Dementia Spectrum." JAMA Neurol **75**(7): 860-875.

Kawahara, Y. and A. Mieda-Sato (2012). "TDP-43 promotes microRNA biogenesis as a component of the Drosha and Dicer complexes." Proc Natl Acad Sci U S A **109**(9): 3347-3352.

Kedersha, N. and P. Anderson (2002). "Stress granules: sites of mRNA triage that regulate mRNA stability and translatability." Biochem Soc Trans **30**(Pt 6): 963-969.

Kedersha, N., M. R. Cho, W. Li, P. W. Yacono, S. Chen, N. Gilks, D. E. Golan and P. Anderson (2000). "Dynamic shuttling of TIA-1 accompanies the recruitment of mRNA to mammalian stress granules." J Cell Biol **151**(6): 1257-1268.

Kedersha, N., P. Ivanov and P. Anderson (2013). "Stress granules and cell signaling: more than just a passing phase?" Trends Biochem Sci **38**(10): 494-506.

Kedersha, N., M. D. Panas, C. A. Achorn, S. Lyons, S. Tisdale, T. Hickman, M. Thomas, J. Lieberman, G. M. McInerney, P. Ivanov and P. Anderson (2016). "G3BP-Caprin1-USP10 complexes mediate stress granule condensation and associate with 40S subunits." J Cell Biol **212**(7): 845-860.

Kedersha, N., G. Stoecklin, M. Ayodele, P. Yacono, J. Lykke-Andersen, M. J. Fritzler, D. Scheuner, R. J. Kaufman, D. E. Golan and P. Anderson (2005). "Stress granules and processing bodies are dynamically linked sites of mRNP remodeling." J Cell Biol **169**(6): 871-884.

Kedersha, N. L., M. Gupta, W. Li, I. Miller and P. Anderson (1999). "RNA-binding proteins TIA-1 and TIAR link the phosphorylation of eIF-2 alpha to the assembly of mammalian stress granules." J Cell Biol **147**(7): 1431-1442.

Kenna, K. P., P. T. van Doormaal, A. M. Dekker, N. Ticozzi, B. J. Kenna, F. P. Diekstra, W. van Rheenen, K. R. van Eijk, A. R. Jones, P. Keagle, A. Shatunov, W. Sproviero, B. N. Smith, M. A. van Es, S. D. Topp, A. Kenna, J. W. Miller, C. Fallini, C. Tiloca, R. L. McLaughlin, C. Vance, C. Troakes, C. Colombrita, G. Mora, A. Calvo, F. Verde, S. Al-Sarraj, A. King, D. Calini, J. de Belleroche, F. Baas, A. J. van der Kooi, M. de Visser, A. L. Ten Asbroek, P. C. Sapp, D. McKenna-Yasek, M. Polak, S. Asress, J. L. Munoz-Blanco, T. M. Strom, T. Meitinger, K. E. Morrison, S. Consortium, G. Lauria, K. L. Williams, P. N. Leigh, G. A. Nicholson, I. P. Blair, C. S. Leblond, P. A. Dion, G. A. Rouleau, H. Pall, P. J. Shaw, M. R. Turner, K. Talbot, F. Taroni, K. B. Boylan, M. Van Blitterswijk, R. Rademakers, J. Esteban-Perez, A. Garcia-Redondo, P. Van Damme, W. Robberecht, A. Chio, C. Gellera, C. Drepper, M. Sendtner, A. Ratti, J. D. Glass, J. S. Mora, N. A. Basak, O. Hardiman, A. C. Ludolph, P. M. Andersen, J. H. Weishaupt, R. H. Brown, Jr., A. Al-Chalabi, V. Silani, C. E. Shaw, L. H. van den Berg, J. H. Veldink and J. E. Landers (2016). "NEK1 variants confer susceptibility to amyotrophic lateral sclerosis." Nat Genet **48**(9): 1037-1042.

Kent, L., T. N. Vizard, B. N. Smith, S. D. Topp, C. Vance, A. Gkazi, J. Miller, C. E. Shaw and K. Talbot (2014). "Autosomal dominant inheritance of rapidly progressive amyotrophic lateral sclerosis due to a truncation mutation in the fused in sarcoma (FUS) gene." Amyotroph Lateral Scler Frontotemporal Degener **15**(7-8): 557-562.

Kewitz, S. and M. S. Staege (2013). "Expression and Regulation of the Endogenous Retrovirus 3 in Hodgkin's Lymphoma Cells." Front Oncol **3**: 179.

Kim, H. J., N. C. Kim, Y. D. Wang, E. A. Scarborough, J. Moore, Z. Diaz, K. S. MacLea, B. Freibaum, S. Li, A. Molliex, A. P. Kanagaraj, R. Carter, K. B. Boylan, A. M. Wojtas, R. Rademakers, J. L. Pinkus, S. A. Greenberg, J. Q. Trojanowski, B. J. Traynor, B. N. Smith, S. Topp, A. S. Gkazi, J. Miller, C. E. Shaw, M. Kottlors, J. Kirschner, A. Pestronk, Y. R. Li, A. F. Ford, A. D. Gitler, M. Benatar, O. D. King, V. E. Kimonis, E. D. Ross, C. C. Weihl, J. Shorter and J. P. Taylor (2013). "Mutations in prion-like domains in hnRNPA2B1 and hnRNPA1 cause multisystem proteinopathy and ALS." Nature **495**(7442): 467-473.

Kim, W. J., S. H. Back, V. Kim, I. Ryu and S. K. Jang (2005). "Sequestration of TRAF2 into stress granules interrupts tumor necrosis factor signaling under stress conditions." Mol Cell Biol **25**(6): 2450-2462.

King, A., S. Maekawa, I. Bodi, C. Troakes and S. Al-Sarraj (2011). "Ubiquitinated, p62 immunopositive cerebellar cortical neuronal inclusions are evident across the spectrum of TDP-43 proteinopathies but are only rarely additionally immunopositive for phosphorylation-dependent TDP-43." Neuropathology **31**(3): 239-249.

King, A., C. Troakes, B. Smith, M. Nolan, O. Curran, C. Vance, C. E. Shaw and S. Al-Sarraj (2015). "ALS-FUS pathology revisited: singleton FUS mutations and an unusual case with both a FUS and TARDBP mutation." Acta Neuropathol Commun **3**: 62.

Kino, Y., C. Washizu, E. Aquilanti, M. Okuno, M. Kurosawa, M. Yamada, H. Doi and N. Nukina (2011). "Intracellular localization and splicing regulation of FUS/TLS are variably affected by amyotrophic lateral sclerosis-linked mutations." Nucleic Acids Res **39**(7): 2781-2798.

Kleinstiver, B. P., V. Pattanayak, M. S. Prew, S. Q. Tsai, N. T. Nguyen, Z. Zheng and J. K. Joung (2016). "High-fidelity CRISPR-Cas9 nucleases with no detectable genome-wide off-target effects." Nature **529**(7587): 490-495.

Klim, J. R., L. A. Williams, F. Limone, I. Guerra San Juan, B. N. Davis-Dusenbery, D. A. Mordes, A. Burberry, M. J. Steinbaugh, K. K. Gamage, R. Kirchner, R. Moccia, S. H. Cassel, K. Chen, B. J. Wainger, C. J. Woolf and K. Eggan (2019). "ALS-implicated protein TDP-43 sustains levels of STMN2, a mediator of motor neuron growth and repair." Nat Neurosci **22**(2): 167-179.

Kukharsky, M. S., A. Quintiero, T. Matsumoto, K. Matsukawa, H. An, T. Hashimoto, T. Iwatsubo, V. L. Buchman and T. A. Shelkovnikova (2015). "Calcium-responsive transactivator (CREST) protein shares a set of structural and functional traits with other proteins associated with amyotrophic lateral sclerosis." Mol Neurodegener **10**: 20.

Kuroda, M., J. Sok, L. Webb, H. Baechtold, F. Urano, Y. Yin, P. Chung, D. G. de Rooij, A. Akhmedov, T. Ashley and D. Ron (2000). "Male sterility and enhanced radiation sensitivity in TLS(-/-) mice." EMBO J **19**(3): 453-462.

Kury, P., A. Nath, A. Creange, A. Dolei, P. Marche, J. Gold, G. Giovannoni, H. P. Hartung and H. Perron (2018). "Human Endogenous Retroviruses in Neurological Diseases." Trends Mol Med **24**(4): 379-394.

Kwiatkowski, T. J., Jr., D. A. Bosco, A. L. Leclerc, E. Tamrazian, C. R. Vanderburg, C. Russ, A. Davis, J. Gilchrist, E. J. Kasarskis, T. Munsat, P. Valdmanis, G. A. Rouleau, B. A. Hosler, P. Cortelli, P. J. de Jong, Y. Yoshinaga, J. L. Haines, M. A. Pericak-Vance, J. Yan, N. Ticozzi, T. Siddique, D. McKenna-Yasek, P. C. Sapp, H. R. Horvitz, J. E. Landers and R. H. Brown, Jr. (2009). "Mutations in the FUS/TLS gene on chromosome 16 cause familial amyotrophic lateral sclerosis." Science **323**(5918): 1205-1208.

Lagier-Tourenne, C. and D. W. Cleveland (2009). "Rethinking ALS: the FUS about TDP-43." Cell **136**(6): 1001-1004.

Lagier-Tourenne, C., M. Polymenidou, K. R. Hutt, A. Q. Vu, M. Baughn, S. C. Huelga, K. M. Clutario, S. C. Ling, T. Y. Liang, C. Mazur, E. Wancewicz, A. S. Kim, A. Watt, S. Freier, G. G. Hicks, J. P. Donohue, L. Shiue, C. F. Bennett, J. Ravits, D. W. Cleveland and G. W. Yeo (2012). "Divergent roles of ALS-linked proteins FUS/TLS and TDP-43 intersect in processing long pre-mRNAs." Nat Neurosci **15**(11): 1488-1497.

Lattante, S., G. A. Rouleau and E. Kabashi (2013). "TARDBP and FUS mutations associated with amyotrophic lateral sclerosis: summary and update." Hum Mutat **34**(6): 812-826.

Le Sage, V. and A. J. Mouland (2013). "Viral subversion of the nuclear pore complex." Viruses **5**(8): 2019-2042.

Leblond, C. S., Z. Gan-Or, D. Spiegelman, S. B. Laurent, A. Szuto, A. Hodgkinson, A. Dionne-Laporte, P. Provencher, M. de Carvalho, S. Orru, D. Brunet, J. P. Bouchard, P. Awadalla, N. Dupre, P. A. Dion and G. A. Rouleau (2016). "Replication study of MATR3 in familial and sporadic amyotrophic lateral sclerosis." Neurobiol Aging **37**: 209 e217-209 e221.

Lee, H. K. and A. Iwasaki (2008). "Autophagy and antiviral immunity." Curr Opin Immunol **20**(1): 23-29.

Lee, Y. B., H. J. Chen, J. N. Peres, J. Gomez-Deza, J. Attig, M. Stalekar, C. Troakes, A. L. Nishimura, E. L. Scotter, C. Vance, Y. Adachi, V. Sardone, J. W. Miller, B. N. Smith, J. M. Gallo, J. Ule, F. Hirth, B. Rogelj, C. Houart and C. E. Shaw (2013). "Hexanucleotide repeats in ALS/FTD form length-dependent RNA foci, sequester RNA binding proteins, and are neurotoxic." Cell Rep **5**(5): 1178-1186.

Lellahi, S. M., I. A. Rosenlund, A. Hedberg, L. T. Kiaer, I. Mikkola, E. Knutsen and M. Perander (2018). "The long noncoding RNA NEAT1 and nuclear paraspeckles are up-regulated by the transcription factor HSF1 in the heat shock response." J Biol Chem **293**(49): 18965-18976.

Leung, A. K., J. M. Calabrese and P. A. Sharp (2006). "Quantitative analysis of Argonaute protein reveals microRNA-dependent localization to stress granules." Proc Natl Acad Sci U S A **103**(48): 18125-18130.

Lewis, B. P., C. B. Burge and D. P. Bartel (2005). "Conserved seed pairing, often flanked by adenosines, indicates that thousands of human genes are microRNA targets." Cell **120**(1): 15-20.

Li, R., A. R. Harvey, S. I. Hodgetts and A. H. Fox (2017). "Functional dissection of NEAT1 using genome editing reveals substantial localization of the NEAT1_1 isoform outside paraspeckles." RNA **23**(6): 872-881.

Li, W., M. H. Lee, L. Henderson, R. Tyagi, M. Bachani, J. Steiner, E. Campanac, D. A. Hoffman, G. von Geldern, K. Johnson, D. Maric, H. D. Morris, M. Lentz, K. Pak,

A. Mammen, L. Ostrow, J. Rothstein and A. Nath (2015). "Human endogenous retrovirus-K contributes to motor neuron disease." Sci Transl Med **7**(307): 307ra153.

Li, Y. R., O. D. King, J. Shorter and A. D. Gitler (2013). "Stress granules as crucibles of ALS pathogenesis." J Cell Biol **201**(3): 361-372.

Lieber, M. R. (2010). "The mechanism of double-strand DNA break repair by the nonhomologous DNA end-joining pathway." Annu Rev Biochem **79**: 181-211.

Ligon, L. A., B. H. LaMonte, K. E. Wallace, N. Weber, R. G. Kalb and E. L. Holzbaur (2005). "Mutant superoxide dismutase disrupts cytoplasmic dynein in motor neurons." Neuroreport **16**(6): 533-536.

Lin, T. Y., S. H. Hsia, Y. C. Huang, C. T. Wu and L. Y. Chang (2003). "Proinflammatory cytokine reactions in enterovirus 71 infections of the central nervous system." Clin Infect Dis **36**(3): 269-274.

Lin, W. L. and D. W. Dickson (2008). "Ultrastructural localization of TDP-43 in filamentous neuronal inclusions in various neurodegenerative diseases." Acta Neuropathol **116**(2): 205-213.

Lin, Y., B. F. Schmidt, M. P. Bruchez and C. J. McManus (2018). "Structural analyses of NEAT1 lncRNAs suggest long-range RNA interactions that may contribute to paraspeckle architecture." Nucleic Acids Res **46**(7): 3742-3752.

Ling, S. C., C. P. Albuquerque, J. S. Han, C. Lagier-Tourenne, S. Tokunaga, H. Zhou and D. W. Cleveland (2010). "ALS-associated mutations in TDP-43 increase its stability and promote TDP-43 complexes with FUS/TLS." Proc Natl Acad Sci U S A **107**(30): 13318-13323.

Ling, S. C., M. Polymenidou and D. W. Cleveland (2013). "Converging mechanisms in ALS and FTD: disrupted RNA and protein homeostasis." Neuron **79**(3): 416-438.

Lipovich, L., F. Dachet, J. Cai, S. Bagla, K. Balan, H. Jia and J. A. Loeb (2012). "Activity-dependent human brain coding/noncoding gene regulatory networks." Genetics **192**(3): 1133-1148.

Listgarten, J., M. Weinstein, B. P. Kleinstiver, A. A. Sousa, J. K. Joung, J. Crawford, K. Gao, L. Hoang, M. Elibol, J. G. Doench and N. Fusi (2018). "Prediction of off-target activities for the end-to-end design of CRISPR guide RNAs." Nat Biomed Eng **2**(1): 38-47.

Liu-Yesucevitz, L., A. Bilgutay, Y. J. Zhang, T. Vanderweyde, A. Citro, T. Mehta, N. Zaarur, A. McKee, R. Bowser, M. Sherman, L. Petrucelli and B. Wolozin (2010). "Tar DNA binding protein-43 (TDP-43) associates with stress granules: analysis of cultured cells and pathological brain tissue." PLoS One **5**(10): e13250.

Liu, Q., S. Shu, R. R. Wang, F. Liu, B. Cui, X. N. Guo, C. X. Lu, X. G. Li, M. S. Liu, B. Peng, L. Y. Cui and X. Zhang (2016). "Whole-exome sequencing identifies a missense mutation in hnRNPA1 in a family with flail arm ALS." Neurology **87**(17): 1763-1769.

Lloyd, R. E. (2016). "Enterovirus Control of Translation and RNA Granule Stress Responses." Viruses **8**(4): 93.

Lopez-Bastida, J., L. Perestelo-Perez, F. Monton-Alvarez, P. Serrano-Aguilar and J. L. Alfonso-Sanchez (2009). "Social economic costs and health-related quality of life in patients with amyotrophic lateral sclerosis in Spain." Amyotroph Lateral Scler **10**(4): 237-243.

Lopez-Erauskin, J., T. Tadokoro, M. W. Baughn, B. Myers, M. McAlonis-Downes, C. Chillon-Marinas, J. N. Asiaban, J. Artates, A. T. Bui, A. P. Vetto, S. K. Lee, A. V. Le, Y. Sun, M. Jambeau, J. Boubaker, D. Swing, J. Qiu, G. G. Hicks, Z. Ouyang, X. D. Fu, L. Tessarollo, S. C. Ling, P. A. Parone, C. E. Shaw, M. Marsala, C. Lagier-Tourenne, D. W. Cleveland and S. Da Cruz (2018). "ALS/FTD-Linked Mutation in FUS Suppresses Intra-axonal Protein Synthesis and Drives Disease Without Nuclear Loss-of-Function of FUS." Neuron **100**(4): 816-830 e817.

Loschi, M., C. C. Leishman, N. Berardone and G. L. Boccaccio (2009). "Dynein and kinesin regulate stress-granule and P-body dynamics." J Cell Sci **122**(Pt 21): 3973-3982.

Lotti, F., W. L. Imlach, L. Saieva, E. S. Beck, T. Hao le, D. K. Li, W. Jiao, G. Z. Mentis, C. E. Beattie, B. D. McCabe and L. Pellizzoni (2012). "An SMN-dependent U12 splicing event essential for motor circuit function." Cell **151**(2): 440-454.

Luo, H. (2016). "Interplay between the virus and the ubiquitin-proteasome system: molecular mechanism of viral pathogenesis." Curr Opin Virol **17**: 1-10.

Ma, H., P. Han, W. Ye, H. Chen, X. Zheng, L. Cheng, L. Zhang, L. Yu, X. Wu, Z. Xu, Y. Lei and F. Zhang (2017). "The Long Noncoding RNA NEAT1 Exerts Antihantaviral Effects by Acting as Positive Feedback for RIG-I Signaling." J Virol **91**(9).

Mackenzie, I. R., O. Ansorge, M. Strong, J. Bilbao, L. Zinman, L. C. Ang, M. Baker, H. Stewart, A. Eisen, R. Rademakers and M. Neumann (2011). "Pathological heterogeneity in amyotrophic lateral sclerosis with FUS mutations: two distinct patterns correlating with disease severity and mutation." Acta Neuropathol **122**(1): 87-98.

Mackenzie, I. R., M. Neumann, E. H. Bigio, N. J. Cairns, I. Alafuzoff, J. Kril, G. G. Kovacs, B. Ghetti, G. Halliday, I. E. Holm, P. G. Ince, W. Kamphorst, T. Revesz, A. J. Rozemuller, S. Kumar-Singh, H. Akiyama, A. Baborie, S. Spina, D. W. Dickson, J. Q. Trojanowski and D. M. Mann (2010a). "Nomenclature and nosology for neuropathologic subtypes of frontotemporal lobar degeneration: an update." Acta Neuropathol **119**(1): 1-4.

Mackenzie, I. R., R. Rademakers and M. Neumann (2010b). "TDP-43 and FUS in amyotrophic lateral sclerosis and frontotemporal dementia." Lancet Neurol **9**(10): 995-1007.

Magrane, J., C. Cortez, W. B. Gan and G. Manfredi (2014). "Abnormal mitochondrial transport and morphology are common pathological denominators in SOD1 and TDP43 ALS mouse models." Hum Mol Genet **23**(6): 1413-1424.

Maharana, S., J. Wang, D. K. Papadopoulos, D. Richter, A. Pozniakovsky, I. Poser, M. Bickle, S. Rizk, J. Guillen-Boixet, T. M. Franzmann, M. Jahnel, L. Marrone, Y. T. Chang, J. Sterneckert, P. Tomancak, A. A. Hyman and S. Alberti (2018). "RNA buffers the phase separation behavior of prion-like RNA binding proteins." Science **360**(6391): 918-921.

Makanae, K., R. Kintaka, T. Makino, H. Kitano and H. Moriya (2013). "Identification of dosage-sensitive genes in Saccharomyces cerevisiae using the genetic tug-of-war method." Genome Res **23**(2): 300-311.

Manghera, M., J. Ferguson-Parry and R. N. Douville (2016). "TDP-43 regulates endogenous retrovirus-K viral protein accumulation." Neurobiol Dis **94**: 226-236.

Manjaly, Z. R., K. M. Scott, K. Abhinav, L. Wijesekera, J. Ganesalingam, L. H. Goldstein, A. Janssen, A. Dougherty, E. Willey, B. R. Stanton, M. R. Turner, M. A. Ampong, M. Sakel, R. W. Orrell, R. Howard, C. E. Shaw, P. N. Leigh and A. Al-Chalabi (2010). "The sex ratio in amyotrophic lateral sclerosis: A population based study." Amyotroph Lateral Scler **11**(5): 439-442.

Mao, Y. S., H. Sunwoo, B. Zhang and D. L. Spector (2011). "Direct visualization of the co-transcriptional assembly of a nuclear body by noncoding RNAs." Nat Cell Biol **13**(1): 95-101.

Marin, B., F. Boumediene, G. Logroscino, P. Couratier, M. C. Babron, A. L. Leutenegger, M. Copetti, P. M. Preux and E. Beghi (2017). "Variation in worldwide incidence of amyotrophic lateral sclerosis: a meta-analysis." Int J Epidemiol **46**(1): 57-74.

Marrone, L., I. Poser, I. Casci, J. Japtok, P. Reinhardt, A. Janosch, C. Andree, H. O. Lee, C. Moebius, E. Koerner, L. Reinhardt, M. E. Cicardi, K. Hackmann, B. Klink, A. Poletti, S. Alberti, M. Bickle, A. Hermann, U. B. Pandey, A. A. Hyman and J. L. Sterneckert (2018). "Isogenic FUS-eGFP iPSC Reporter Lines Enable Quantification of FUS Stress Granule Pathology that Is Rescued by Drugs Inducing Autophagy." Stem Cell Reports **10**(2): 375-389.

Martin-Perez, M. and J. Villen (2017). "Determinants and Regulation of Protein Turnover in Yeast." Cell Syst **5**(3): 283-294 e285.

Martin, L. J. (2000). "p53 is abnormally elevated and active in the CNS of patients with amyotrophic lateral sclerosis." Neurobiol Dis **7**(6 Pt B): 613-622.

Martyn, C. N., D. J. Barker and C. Osmond (1988). "Motoneuron disease and past poliomyelitis." Lancet **2**(8626-8627): 1485.

Maruyama, H., H. Morino, H. Ito, Y. Izumi, H. Kato, Y. Watanabe, Y. Kinoshita, M. Kamada, H. Nodera, H. Suzuki, O. Komure, S. Matsuura, K. Kobatake, N. Morimoto, K. Abe, N. Suzuki, M. Aoki, A. Kawata, T. Hirai, T. Kato, K. Ogasawara, A. Hirano, T. Takumi, H. Kusaka, K. Hagiwara, R. Kaji and H. Kawakami (2010). "Mutations of optineurin in amyotrophic lateral sclerosis." Nature **465**(7295): 223-226.

Masaki, K., Y. Sonobe, G. Ghadge, P. Pytel and R. P. Roos (2019). "TDP-43 proteinopathy in Theiler's murine encephalomyelitis virus infection." PLoS Pathog **15**(2): e1007574.

Mastrocola, A. S., S. H. Kim, A. T. Trinh, L. A. Rodenkirch and R. S. Tibbetts (2013). "The RNA-binding protein fused in sarcoma (FUS) functions downstream of poly(ADP-ribose) polymerase (PARP) in response to DNA damage." J Biol Chem **288**(34): 24731-24741.

Mateju, D., T. M. Franzmann, A. Patel, A. Kopach, E. E. Boczek, S. Maharana, H. O. Lee, S. Carra, A. A. Hyman and S. Alberti (2017). "An aberrant phase transition of stress granules triggered by misfolded protein and prevented by chaperone function." EMBO J **36**(12): 1669-1687.

McCormick, C. and D. A. Khaperskyy (2017). "Translation inhibition and stress granules in the antiviral immune response." Nat Rev Immunol **17**(10): 647-660.

McDonald, K. K., A. Aulas, L. Destroismaisons, S. Pickles, E. Beleac, W. Camu, G. A. Rouleau and C. Vande Velde (2011). "TAR DNA-binding protein 43 (TDP-43) regulates stress granule dynamics via differential regulation of G3BP and TIA-1." Hum Mol Genet **20**(7): 1400-1410.

Mello, S. S., C. Sinow, N. Raj, P. K. Mazur, K. Bieging-Rolett, D. K. Broz, J. F. C. Imam, H. Vogel, L. D. Wood, J. Sage, T. Hirose, S. Nakagawa, J. Rinn and L. D. Attardi (2017). "Neat1 is a p53-inducible lincRNA essential for transformation suppression." Genes Dev **31**(11): 1095-1108.

Mercer, T. R., I. A. Qureshi, S. Gokhan, M. E. Dinger, G. Li, J. S. Mattick and M. F. Mehler (2010). "Long noncoding RNAs in neuronal-glial fate specification and oligodendrocyte lineage maturation." BMC Neurosci **11**: 14.

Meyer, T., A. Schwan, J. S. Dullinger, J. Brocke, K. T. Hoffmann, C. H. Nolte, A. Hopt, U. Kopp, P. Andersen, J. T. Epplen and P. Linke (2005). "Early-onset ALS with long-term survival associated with spastin gene mutation." Neurology **65**(1): 141-143.

Mitchell, J., P. Paul, H. J. Chen, A. Morris, M. Payling, M. Falchi, J. Habgood, S. Panoutsou, S. Winkler, V. Tisato, A. Hajitou, B. Smith, C. Vance, C. Shaw, N. D. Mazarakis and J. de Belleroche (2010). "Familial amyotrophic lateral sclerosis is

associated with a mutation in D-amino acid oxidase." Proc Natl Acad Sci U S A **107**(16): 7556-7561.

Mitchell, J. D. and G. D. Borasio (2007). "Amyotrophic lateral sclerosis." Lancet **369**(9578): 2031-2041.

Mizielinska, S., T. Lashley, F. E. Norona, E. L. Clayton, C. E. Ridler, P. Fratta and A. M. Isaacs (2013). "C9orf72 frontotemporal lobar degeneration is characterised by frequent neuronal sense and antisense RNA foci." Acta Neuropathol **126**(6): 845-857.

Monahan, Z., V. H. Ryan, A. M. Janke, K. A. Burke, S. N. Rhoads, G. H. Zerze, R. O'Meally, G. L. Dignon, A. E. Conicella, W. Zheng, R. B. Best, R. N. Cole, J. Mittal, F. Shewmaker and N. L. Fawzi (2017). "Phosphorylation of the FUS low-complexity domain disrupts phase separation, aggregation, and toxicity." EMBO J **36**(20): 2951-2967.

Morchikh, M., A. Cribier, R. Raffel, S. Amraoui, J. Cau, D. Severac, E. Dubois, O. Schwartz, Y. Bennasser and M. Benkirane (2017). "HEXIM1 and NEAT1 Long Non-coding RNA Form a Multi-subunit Complex that Regulates DNA-Mediated Innate Immune Response." Mol Cell **67**(3): 387-399 e385.

Mori, K., T. Arzberger, F. A. Grasser, I. Gijselinck, S. May, K. Rentzsch, S. M. Weng, M. H. Schludi, J. van der Zee, M. Cruts, C. Van Broeckhoven, E. Kremmer, H. A. Kretzschmar, C. Haass and D. Edbauer (2013a). "Bidirectional transcripts of the expanded C9orf72 hexanucleotide repeat are translated into aggregating dipeptide repeat proteins." Acta Neuropathol **126**(6): 881-893.

Mori, K., S. M. Weng, T. Arzberger, S. May, K. Rentzsch, E. Kremmer, B. Schmid, H. A. Kretzschmar, M. Cruts, C. Van Broeckhoven, C. Haass and D. Edbauer (2013b). "The C9orf72 GGGGCC repeat is translated into aggregating dipeptide-repeat proteins in FTLD/ALS." Science **339**(6125): 1335-1338.

Mori, M. A., P. Raghavan, T. Thomou, J. Boucher, S. Robida-Stubbs, Y. Macotela, S. J. Russell, J. L. Kirkland, T. K. Blackwell and C. R. Kahn (2012). "Role of microRNA processing in adipose tissue in stress defense and longevity." Cell Metab **16**(3): 336-347.

Morimoto, R. I. and A. M. Cuervo (2009). "Protein homeostasis and aging: taking care of proteins from the cradle to the grave." J Gerontol A Biol Sci Med Sci **64**(2): 167-170.

Moriya, H. (2015). "Quantitative nature of overexpression experiments." Mol Biol Cell **26**(22): 3932-3939.

Morlando, M., S. Dini Modigliani, G. Torrelli, A. Rosa, V. Di Carlo, E. Caffarelli and I. Bozzoni (2012). "FUS stimulates microRNA biogenesis by facilitating co-transcriptional Drosha recruitment." EMBO J **31**(24): 4502-4510.

Moscat, J. and M. T. Diaz-Meco (2012). "p62: a versatile multitasker takes on cancer." Trends Biochem Sci **37**(6): 230-236.

Naganuma, T., S. Nakagawa, A. Tanigawa, Y. F. Sasaki, N. Goshima and T. Hirose (2012). "Alternative 3'-end processing of long noncoding RNA initiates construction of nuclear paraspeckles." EMBO J **31**(20): 4020-4034.

Nagase, M., Y. Yamamoto, Y. Miyazaki and H. Yoshino (2016). "Increased oxidative stress in patients with amyotrophic lateral sclerosis and the effect of edaravone administration." Redox Rep **21**(3): 104-112.

Nakagawa, S., T. Naganuma, G. Shioi and T. Hirose (2011). "Paraspeckles are subpopulation-specific nuclear bodies that are not essential in mice." J Cell Biol **193**(1): 31-39.

Naumann, M., A. Pal, A. Goswami, X. Lojewski, J. Japtok, A. Vehlow, M. Naujock, R. Gunther, M. Jin, N. Stanslowsky, P. Reinhardt, J. Sterneckert, M. Frickenhaus, F. Pan-Montojo, E. Storkebaum, I. Poser, A. Freischmidt, J. H. Weishaupt, K. Holzmann, D. Troost, A. C. Ludolph, T. M. Boeckers, S. Liebau, S. Petri, N. Cordes, A. A. Hyman, F. Wegner, S. W. Grill, J. Weis, A. Storch and A. Hermann (2018). "Impaired DNA damage response signaling by FUS-NLS mutations leads to neurodegeneration and FUS aggregate formation." Nat Commun **9**(1): 335.

Nellaker, C., Y. Yao, L. Jones-Brando, F. Mallet, R. H. Yolken and H. Karlsson (2006). "Transactivation of elements in the human endogenous retrovirus W family by viral infection." Retrovirology **3**: 44.

Neumann, M., E. Bentmann, D. Dormann, A. Jawaid, M. DeJesus-Hernandez, O. Ansorge, S. Roeber, H. A. Kretzschmar, D. G. Munoz, H. Kusaka, O. Yokota, L. C. Ang, J. Bilbao, R. Rademakers, C. Haass and I. R. Mackenzie (2011). "FET proteins TAF15 and EWS are selective markers that distinguish FTLD with FUS pathology from amyotrophic lateral sclerosis with FUS mutations." Brain **134**(Pt 9): 2595-2609.

Neumann, M., R. Rademakers, S. Roeber, M. Baker, H. A. Kretzschmar and I. R. Mackenzie (2009). "A new subtype of frontotemporal lobar degeneration with FUS pathology." Brain **132**(Pt 11): 2922-2931.

Neumann, M., D. M. Sampathu, L. K. Kwong, A. C. Truax, M. C. Micsenyi, T. T. Chou, J. Bruce, T. Schuck, M. Grossman, C. M. Clark, L. F. McCluskey, B. L. Miller, E. Masliah, I. R. Mackenzie, H. Feldman, W. Feiden, H. A. Kretzschmar, J. Q. Trojanowski and V. M. Lee (2006). "Ubiquitinated TDP-43 in frontotemporal lobar degeneration and amyotrophic lateral sclerosis." Science **314**(5796): 130-133.

Nicolas, A., K. P. Kenna, A. E. Renton, N. Ticozzi, F. Faghri, R. Chia, J. A. Dominov, B. J. Kenna, M. A. Nalls, P. Keagle, A. M. Rivera, W. van Rheenen, N. A. Murphy, J. van Vugt, J. T. Geiger, R. A. Van der Spek, H. A. Pliner, Shankaracharya, B. N. Smith, G. Marangi, S. D. Topp, Y. Abramzon, A. S. Gkazi, J. D. Eicher, A. Kenna, I. Consortium, G. Mora, A. Calvo, L. Mazzini, N. Riva, J. Mandrioli, C. Caponnetto, S. Battistini, P. Volanti, V. La Bella, F. L. Conforti, G. Borghero, S. Messina, I. L. Simone, F. Trojsi, F. Salvi, F. O. Logullo, S. D'Alfonso, L. Corrado, M.

Capasso, L. Ferrucci, A. L. S. C. C. Genomic Translation for, C. A. M. Moreno, S. Kamalakaran, D. B. Goldstein, A. L. S. S. Consortium, A. D. Gitler, T. Harris, R. M. Myers, N. A. Consortium, H. Phatnani, R. L. Musunuri, U. S. Evani, A. Abhyankar, M. C. Zody, A. L. S. F. Answer, J. Kaye, S. Finkbeiner, S. K. Wyman, A. LeNail, L. Lima, E. Fraenkel, C. N. Svendsen, L. M. Thompson, J. E. Van Eyk, J. D. Berry, T. M. Miller, S. J. Kolb, M. Cudkowicz, E. Baxi, A. L. S. Clinical Research in, C. Related Disorders for Therapeutic Development, M. Benatar, J. P. Taylor, E. Rampersaud, G. Wu, J. Wuu, S. Consortium, G. Lauria, F. Verde, I. Fogh, C. Tiloca, G. P. Comi, G. Soraru, C. Cereda, A. L. S. C. French, P. Corcia, H. Laaksovirta, L. Myllykangas, L. Jansson, M. Valori, J. Ealing, H. Hamdalla, S. Rollinson, S. Pickering-Brown, R. W. Orrell, K. C. Sidle, A. Malaspina, J. Hardy, A. B. Singleton, J. O. Johnson, S. Arepalli, P. C. Sapp, D. McKenna-Yasek, M. Polak, S. Asress, S. Al-Sarraj, A. King, C. Troakes, C. Vance, J. de Belleroche, F. Baas, A. Ten Asbroek, J. L. Munoz-Blanco, D. G. Hernandez, J. Ding, J. R. Gibbs, S. W. Scholz, M. K. Floeter, R. H. Campbell, F. Landi, R. Bowser, S. M. Pulst, J. M. Ravits, D. J. L. MacGowan, J. Kirby, E. P. Pioro, R. Pamphlett, J. Broach, G. Gerhard, T. L. Dunckley, C. B. Brady, N. W. Kowall, J. C. Troncoso, I. Le Ber, K. Mouzat, S. Lumbroso, T. D. Heiman-Patterson, F. Kamel, L. Van Den Bosch, R. H. Baloh, T. M. Strom, T. Meitinger, A. Shatunov, K. R. Van Eijk, M. de Carvalho, M. Kooyman, B. Middelkoop, M. Moisse, R. L. McLaughlin, M. A. Van Es, M. Weber, K. B. Boylan, M. Van Blitterswijk, R. Rademakers, K. E. Morrison, A. N. Basak, J. S. Mora, V. E. Drory, P. J. Shaw, M. R. Turner, K. Talbot, O. Hardiman, K. L. Williams, J. A. Fifita, G. A. Nicholson, I. P. Blair, G. A. Rouleau, J. Esteban-Perez, A. Garcia-Redondo, A. Al-Chalabi, E. A. L. S. S. C. Project Min, E. Rogaeva, L. Zinman, L. W. Ostrow, N. J. Maragakis, J. D. Rothstein, Z. Simmons, J. Cooper-Knock, A. Brice, S. A. Goutman, E. L. Feldman, S. B. Gibson, F. Taroni, A. Ratti, C. Gellera, P. Van Damme, W. Robberecht, P. Fratta, M. Sabatelli, C. Lunetta, A. C. Ludolph, P. M. Andersen, J. H. Weishaupt, W. Camu, J. Q. Trojanowski, V. M. Van Deerlin, R. H. Brown, Jr., L. H. van den Berg, J. H. Veldink, M. B. Harms, J. D. Glass, D. J. Stone, P. Tienari, V. Silani, A. Chio, C. E. Shaw, B. J. Traynor and J. E. Landers (2018). "Genome-wide Analyses Identify KIF5A as a Novel ALS Gene." Neuron **97**(6): 1268-1283 e1266.

Nishi, H., K. Hashimoto and A. R. Panchenko (2011). "Phosphorylation in protein-protein binding: effect on stability and function." Structure **19**(12): 1807-1815.

Nishimoto, Y., S. Nakagawa, T. Hirose, H. J. Okano, M. Takao, S. Shibata, S. Suyama, K. Kuwako, T. Imai, S. Murayama, N. Suzuki and H. Okano (2013). "The long non-coding RNA nuclear-enriched abundant transcript 1_2 induces paraspeckle formation in the motor neuron during the early phase of amyotrophic lateral sclerosis." Mol Brain **6**: 31.

Nishimura, A. L., M. Mitne-Neto, H. C. Silva, A. Richieri-Costa, S. Middleton, D. Cascio, F. Kok, J. R. Oliveira, T. Gillingwater, J. Webb, P. Skehel and M. Zatz (2004). "A mutation in the vesicle-trafficking protein VAPB causes late-onset spinal muscular atrophy and amyotrophic lateral sclerosis." Am J Hum Genet **75**(5): 822-831.

Nishitoh, H., H. Kadowaki, A. Nagai, T. Maruyama, T. Yokota, H. Fukutomi, T. Noguchi, A. Matsuzawa, K. Takeda and H. Ichijo (2008). "ALS-linked mutant SOD1 induces ER stress- and ASK1-dependent motor neuron death by targeting Derlin-1." Genes Dev **22**(11): 1451-1464.

Nomura, T., S. Watanabe, K. Kaneko, K. Yamanaka, N. Nukina and Y. Furukawa (2014). "Intranuclear aggregation of mutant FUS/TLS as a molecular pathomechanism of amyotrophic lateral sclerosis." J Biol Chem **289**(2): 1192-1202.

Oakes, J. A., M. C. Davies and M. O. Collins (2017). "TBK1: a new player in ALS linking autophagy and neuroinflammation." Mol Brain **10**(1): 5.

Okamoto, K., Y. Mizuno and Y. Fujita (2008). "Bunina bodies in amyotrophic lateral sclerosis." Neuropathology **28**(2): 109-115.

Onomoto, K., M. Jogi, J. S. Yoo, R. Narita, S. Morimoto, A. Takemura, S. Sambhara, A. Kawaguchi, S. Osari, K. Nagata, T. Matsumiya, H. Namiki, M. Yoneyama and T. Fujita (2012). "Critical role of an antiviral stress granule containing RIG-I and PKR in viral detection and innate immunity." PLoS One **7**(8): e43031.

Orlacchio, A., C. Babalini, A. Borreca, C. Patrono, R. Massa, S. Basaran, R. P. Munhoz, E. A. Rogaeva, P. H. St George-Hyslop, G. Bernardi and T. Kawarai (2010). "SPATACSIN mutations cause autosomal recessive juvenile amyotrophic lateral sclerosis." Brain **133**(Pt 2): 591-598.

Orozco, D. and D. Edbauer (2013). "FUS-mediated alternative splicing in the nervous system: consequences for ALS and FTLD." J Mol Med (Berl) **91**(12): 1343-1354.

Orozco, D., S. Tahirovic, K. Rentzsch, B. M. Schwenk, C. Haass and D. Edbauer (2012). "Loss of fused in sarcoma (FUS) promotes pathological Tau splicing." EMBO Rep **13**(8): 759-764.

Ouyang, H., K. Zhang, K. Fox-Walsh, Y. Yang, C. Zhang, J. Huang, H. Li, Y. Zhou and X. D. Fu (2017). "The RNA binding protein EWS is broadly involved in the regulation of pri-miRNA processing in mammalian cells." Nucleic Acids Res **45**(21): 12481-12495.

Paquet, D., D. Kwart, A. Chen, A. Sproul, S. Jacob, S. Teo, K. M. Olsen, A. Gregg, S. Noggle and M. Tessier-Lavigne (2016). "Efficient introduction of specific homozygous and heterozygous mutations using CRISPR/Cas9." Nature **533**(7601): 125-129.

Parkinson, N., P. G. Ince, M. O. Smith, R. Highley, G. Skibinski, P. M. Andersen, K. E. Morrison, H. S. Pall, O. Hardiman, J. Collinge, P. J. Shaw, E. M. Fisher, M. R. C. P. i. A. Study and F. R. Consortium (2006). "ALS phenotypes with mutations in CHMP2B (charged multivesicular body protein 2B)." Neurology **67**(6): 1074-1077.

Parsell, D. A., A. S. Kowal, M. A. Singer and S. Lindquist (1994). "Protein disaggregation mediated by heat-shock protein Hsp104." Nature **372**(6505): 475-478.

Patel, A., H. O. Lee, L. Jawerth, S. Maharana, M. Jahnel, M. Y. Hein, S. Stoynov, J. Mahamid, S. Saha, T. M. Franzmann, A. Pozniakovski, I. Poser, N. Maghelli, L. A. Royer, M. Weigert, E. W. Myers, S. Grill, D. Drechsel, A. A. Hyman and S. Alberti

(2015). "A Liquid-to-Solid Phase Transition of the ALS Protein FUS Accelerated by Disease Mutation." Cell **162**(5): 1066-1077.

Pattanayak, V., S. Lin, J. P. Guilinger, E. Ma, J. A. Doudna and D. R. Liu (2013). "High-throughput profiling of off-target DNA cleavage reveals RNA-programmed Cas9 nuclease specificity." Nat Biotechnol **31**(9): 839-843.

Paul, S., C. Ricour, C. Sommereyns, F. Sorgeloos and T. Michiels (2007). "Type I interferon response in the central nervous system." Biochimie **89**(6-7): 770-778.

Pederson, T. (2011). "The nucleolus." Cold Spring Harb Perspect Biol **3**(3).

Petrov, D., C. Mansfield, A. Moussy and O. Hermine (2017). "ALS Clinical Trials Review: 20 Years of Failure. Are We Any Closer to Registering a New Treatment?" Front Aging Neurosci **9**: 68.

Phukan, J., M. Elamin, P. Bede, N. Jordan, L. Gallagher, S. Byrne, C. Lynch, N. Pender and O. Hardiman (2012). "The syndrome of cognitive impairment in amyotrophic lateral sclerosis: a population-based study." J Neurol Neurosurg Psychiatry **83**(1): 102-108.

Pilli, M., J. Arko-Mensah, M. Ponpuak, E. Roberts, S. Master, M. A. Mandell, N. Dupont, W. Ornatowski, S. Jiang, S. B. Bradfute, J. A. Bruun, T. E. Hansen, T. Johansen and V. Deretic (2012). "TBK-1 promotes autophagy-mediated antimicrobial defense by controlling autophagosome maturation." Immunity **37**(2): 223-234.

Piotrowska, J., S. J. Hansen, N. Park, K. Jamka, P. Sarnow and K. E. Gustin (2010). "Stable formation of compositionally unique stress granules in virus-infected cells." J Virol **84**(7): 3654-3665.

Polymenidou, M., C. Lagier-Tourenne, K. R. Hutt, S. C. Huelga, J. Moran, T. Y. Liang, S. C. Ling, E. Sun, E. Wancewicz, C. Mazur, H. Kordasiewicz, Y. Sedaghat, J. P. Donohue, L. Shiue, C. F. Bennett, G. W. Yeo and D. W. Cleveland (2011). "Long pre-mRNA depletion and RNA missplicing contribute to neuronal vulnerability from loss of TDP-43." Nat Neurosci **14**(4): 459-468.

Prasanth, K. V., S. G. Prasanth, Z. Xuan, S. Hearn, S. M. Freier, C. F. Bennett, M. Q. Zhang and D. L. Spector (2005). "Regulating gene expression through RNA nuclear retention." Cell **123**(2): 249-263.

Protter, D. S. W. and R. Parker (2016). "Principles and Properties of Stress Granules." Trends Cell Biol **26**(9): 668-679.

Puls, I., C. Jonnakuty, B. H. LaMonte, E. L. Holzbaur, M. Tokito, E. Mann, M. K. Floeter, K. Bidus, D. Drayna, S. J. Oh, R. H. Brown, Jr., C. L. Ludlow and K. H. Fischbeck (2003). "Mutant dynactin in motor neuron disease." Nat Genet **33**(4): 455-456.

Qiu, H., S. Lee, Y. Shang, W. Y. Wang, K. F. Au, S. Kamiya, S. J. Barmada, S. Finkbeiner, H. Lui, C. E. Carlton, A. A. Tang, M. C. Oldham, H. Wang, J. Shorter, A. J. Filiano, E. D. Roberson, W. G. Tourtellotte, B. Chen, L. H. Tsai and E. J. Huang (2014). "ALS-associated mutation FUS-R521C causes DNA damage and RNA splicing defects." J Clin Invest **124**(3): 981-999.

Rabbitts, T. H., A. Forster, R. Larson and P. Nathan (1993). "Fusion of the dominant negative transcription regulator CHOP with a novel gene FUS by translocation t(12;16) in malignant liposarcoma." Nat Genet **4**(2): 175-180.

Rademakers, R., H. Stewart, M. Dejesus-Hernandez, C. Krieger, N. Graff-Radford, M. Fabros, H. Briemberg, N. Cashman, A. Eisen and I. R. Mackenzie (2010). "Fus gene mutations in familial and sporadic amyotrophic lateral sclerosis." Muscle Nerve **42**(2): 170-176.

Radford, R. A., M. Morsch, S. L. Rayner, N. J. Cole, D. L. Pountney and R. S. Chung (2015). "The established and emerging roles of astrocytes and microglia in amyotrophic lateral sclerosis and frontotemporal dementia." Front Cell Neurosci **9**: 414.

Ramaswami, M., J. P. Taylor and R. Parker (2013). "Altered ribostasis: RNA-protein granules in degenerative disorders." Cell **154**(4): 727-736.

Ran, F. A., P. D. Hsu, J. Wright, V. Agarwala, D. A. Scott and F. Zhang (2013). "Genome engineering using the CRISPR-Cas9 system." Nat Protoc **8**(11): 2281-2308.

Ravits, J. (2005). "Sporadic amyotrophic lateral sclerosis: a hypothesis of persistent (non-lytic) enteroviral infection." Amyotroph Lateral Scler Other Motor Neuron Disord **6**(2): 77-87.

Raychaudhuri, S., C. Loew, R. Korner, S. Pinkert, M. Theis, M. Hayer-Hartl, F. Buchholz and F. U. Hartl (2014). "Interplay of acetyltransferase EP300 and the proteasome system in regulating heat shock transcription factor 1." Cell **156**(5): 975-985.

Re, D. B., V. Le Verche, C. Yu, M. W. Amoroso, K. A. Politi, S. Phani, B. Ikiz, L. Hoffmann, M. Koolen, T. Nagata, D. Papadimitriou, P. Nagy, H. Mitsumoto, S. Kariya, H. Wichterle, C. E. Henderson and S. Przedborski (2014). "Necroptosis drives motor neuron death in models of both sporadic and familial ALS." Neuron **81**(5): 1001-1008.

Renton, A. E., A. Chio and B. J. Traynor (2014). "State of play in amyotrophic lateral sclerosis genetics." Nat Neurosci **17**(1): 17-23.

Renton, A. E., E. Majounie, A. Waite, J. Simon-Sanchez, S. Rollinson, J. R. Gibbs, J. C. Schymick, H. Laaksovirta, J. C. van Swieten, L. Myllykangas, H. Kalimo, A. Paetau, Y. Abramzon, A. M. Remes, A. Kaganovich, S. W. Scholz, J. Duckworth, J. Ding, D. W. Harmer, D. G. Hernandez, J. O. Johnson, K. Mok, M. Ryten, D. Trabzuni, R. J. Guerreiro, R. W. Orrell, J. Neal, A. Murray, J. Pearson, I. E. Jansen, D.

Sondervan, H. Seelaar, D. Blake, K. Young, N. Halliwell, J. B. Callister, G. Toulson, A. Richardson, A. Gerhard, J. Snowden, D. Mann, D. Neary, M. A. Nalls, T. Peuralinna, L. Jansson, V. M. Isoviita, A. L. Kaivorinne, M. Holtta-Vuori, E. Ikonen, R. Sulkava, M. Benatar, J. Wuu, A. Chio, G. Restagno, G. Borghero, M. Sabatelli, I. Consortium, D. Heckerman, E. Rogaeva, L. Zinman, J. D. Rothstein, M. Sendtner, C. Drepper, E. E. Eichler, C. Alkan, Z. Abdullaev, S. D. Pack, A. Dutra, E. Pak, J. Hardy, A. Singleton, N. M. Williams, P. Heutink, S. Pickering-Brown, H. R. Morris, P. J. Tienari and B. J. Traynor (2011). "A hexanucleotide repeat expansion in C9ORF72 is the cause of chromosome 9p21-linked ALS-FTD." Neuron **72**(2): 257-268.

Riviere, M., V. Meininger, P. Zeisser and T. Munsat (1998). "An analysis of extended survival in patients with amyotrophic lateral sclerosis treated with riluzole." Arch Neurol **55**(4): 526-528.

Robertson, J., J. M. Beaulieu, M. M. Doroudchi, H. D. Durham, J. P. Julien and W. E. Mushynski (2001). "Apoptotic death of neurons exhibiting peripherin aggregates is mediated by the proinflammatory cytokine tumor necrosis factor-alpha." J Cell Biol **155**(2): 217-226.

Robinson, H. K., A. V. Deykin, E. V. Bronovitsky, R. K. Ovchinnikov, A. A. Ustyugov, T. A. Shelkovnikova, M. S. Kukharsky, T. G. Ermolkevich, I. L. Goldman, E. R. Sadchikova, E. A. Kovrazhkina, S. O. Bachurin, V. L. Buchman and N. N. Ninkina (2015). "Early lethality and neuronal proteinopathy in mice expressing cytoplasm-targeted FUS that lacks the RNA recognition motif." Amyotroph Lateral Scler Frontotemporal Degener **16**(5-6): 402-409.

Romano, M., F. Feiguin and E. Buratti (2016). "TBPH/TDP-43 modulates translation of Drosophila futsch mRNA through an UG-rich sequence within its 5'UTR." Brain Res **1647**: 50-56.

Rosen, D. R., T. Siddique, D. Patterson, D. A. Figlewicz, P. Sapp, A. Hentati, D. Donaldson, J. Goto, J. P. O'Regan, H. X. Deng and et al. (1993). "Mutations in Cu/Zn superoxide dismutase gene are associated with familial amyotrophic lateral sclerosis." Nature **362**(6415): 59-62.

Ruggieri, A., E. Dazert, P. Metz, S. Hofmann, J. P. Bergeest, J. Mazur, P. Bankhead, M. S. Hiet, S. Kallis, G. Alvisi, C. E. Samuel, V. Lohmann, L. Kaderali, K. Rohr, M. Frese, G. Stoecklin and R. Bartenschlager (2012). "Dynamic oscillation of translation and stress granule formation mark the cellular response to virus infection." Cell Host Microbe **12**(1): 71-85.

Rulten, S. L., A. Rotheray, R. L. Green, G. J. Grundy, D. A. Moore, F. Gomez-Herreros, M. Hafezparast and K. W. Caldecott (2014). "PARP-1 dependent recruitment of the amyotrophic lateral sclerosis-associated protein FUS/TLS to sites of oxidative DNA damage." Nucleic Acids Res **42**(1): 307-314.

Russo, A., R. Scardigli, F. La Regina, M. E. Murray, N. Romano, D. W. Dickson, B. Wolozin, A. Cattaneo and M. Ceci (2017). "Increased cytoplasmic TDP-43 reduces global protein synthesis by interacting with RACK1 on polyribosomes." Hum Mol Genet **26**(8): 1407-1418.

Ryan, T. A. and D. A. Tumbarello (2018). "Optineurin: A Coordinator of Membrane-Associated Cargo Trafficking and Autophagy." Front Immunol **9**: 1024.

Ryu, H. H., M. H. Jun, K. J. Min, D. J. Jang, Y. S. Lee, H. K. Kim and J. A. Lee (2014). "Autophagy regulates amyotrophic lateral sclerosis-linked fused in sarcoma-positive stress granules in neurons." Neurobiol Aging **35**(12): 2822-2831.

Saha, S., S. Murthy and P. N. Rangarajan (2006). "Identification and characterization of a virus-inducible non-coding RNA in mouse brain." J Gen Virol **87**(Pt 7): 1991-1995.

Salapa, H. E., C. Johnson, C. Hutchinson, B. F. Popescu and M. C. Levin (2018). "Dysfunctional RNA binding proteins and stress granules in multiple sclerosis." J Neuroimmunol **324**: 149-156.

Sama, R. R., C. L. Ward, L. J. Kaushansky, N. Lemay, S. Ishigaki, F. Urano and D. A. Bosco (2013). "FUS/TLS assembles into stress granules and is a prosurvival factor during hyperosmolar stress." J Cell Physiol **228**(11): 2222-2231.

Sathasivam, S., P. G. Ince and P. J. Shaw (2001). "Apoptosis in amyotrophic lateral sclerosis: a review of the evidence." Neuropathol Appl Neurobiol **27**(4): 257-274.

Saxena, S. and P. Caroni (2011). "Selective neuronal vulnerability in neurodegenerative diseases: from stressor thresholds to degeneration." Neuron **71**(1): 35-48.

Scekic-Zahirovic, J., O. Sendscheid, H. El Oussini, M. Jambeau, Y. Sun, S. Mersmann, M. Wagner, S. Dieterle, J. Sinniger, S. Dirrig-Grosch, K. Drenner, M. C. Birling, J. Qiu, Y. Zhou, H. Li, X. D. Fu, C. Rouaux, T. Shelkovnikova, A. Witting, A. C. Ludolph, F. Kiefer, E. Storkebaum, C. Lagier-Tourenne and L. Dupuis (2016). "Toxic gain of function from mutant FUS protein is crucial to trigger cell autonomous motor neuron loss." EMBO J **35**(10): 1077-1097.

Schmidt-Zachmann, M. S., C. Dargemont, L. C. Kuhn and E. A. Nigg (1993). "Nuclear export of proteins: the role of nuclear retention." Cell **74**(3): 493-504.

Schymick, J. C., Y. Yang, P. M. Andersen, J. P. Vonsattel, M. Greenway, P. Momeni, J. Elder, A. Chio, G. Restagno, W. Robberecht, C. Dahlberg, O. Mukherjee, A. Goate, N. Graff-Radford, R. J. Caselli, M. Hutton, J. Gass, A. Cannon, R. Rademakers, A. B. Singleton, O. Hardiman, J. Rothstein, J. Hardy and B. J. Traynor (2007). "Progranulin mutations and amyotrophic lateral sclerosis or amyotrophic lateral sclerosis-frontotemporal dementia phenotypes." J Neurol Neurosurg Psychiatry **78**(7): 754-756.

Sellier, C., M. L. Campanari, C. Julie Corbier, A. Gaucherot, I. Kolb-Cheynel, M. Oulad-Abdelghani, F. Ruffenach, A. Page, S. Ciura, E. Kabashi and N. Charlet-Berguerand (2016). "Loss of C9ORF72 impairs autophagy and synergizes with polyQ

Ataxin-2 to induce motor neuron dysfunction and cell death." EMBO J **35**(12): 1276-1297.

Senderek, J., S. M. Garvey, M. Krieger, V. Guergueltcheva, A. Urtizberea, A. Roos, M. Elbracht, C. Stendel, I. Tournev, V. Mihailova, H. Feit, J. Tramonte, P. Hedera, K. Crooks, C. Bergmann, S. Rudnik-Schoneborn, K. Zerres, H. Lochmuller, E. Seboun, J. Weis, J. S. Beckmann, M. A. Hauser and C. E. Jackson (2009). "Autosomal-dominant distal myopathy associated with a recurrent missense mutation in the gene encoding the nuclear matrix protein, matrin 3." Am J Hum Genet **84**(4): 511-518.

Sephton, C. F., A. A. Tang, A. Kulkarni, J. West, M. Brooks, J. J. Stubblefield, Y. Liu, M. Q. Zhang, C. B. Green, K. M. Huber, E. J. Huang, J. Herz and G. Yu (2014). "Activity-dependent FUS dysregulation disrupts synaptic homeostasis." Proc Natl Acad Sci U S A **111**(44): E4769-4778.

Shang, Y. and E. J. Huang (2016). "Mechanisms of FUS mutations in familial amyotrophic lateral sclerosis." Brain Res **1647**: 65-78.

Sharma, A., A. K. Lyashchenko, L. Lu, S. E. Nasrabady, M. Elmaleh, M. Mendelsohn, A. Nemes, J. C. Tapia, G. Z. Mentis and N. A. Shneider (2016). "ALS-associated mutant FUS induces selective motor neuron degeneration through toxic gain of function." Nat Commun **7**: 10465.

Shelkovnikova, T. A., M. S. Kukharsky, H. An, P. Dimasi, S. Alexeeva, O. Shabir, P. R. Heath and V. L. Buchman (2018). "Protective paraspeckle hyper-assembly downstream of TDP-43 loss of function in amyotrophic lateral sclerosis." Mol Neurodegener **13**(1): 30.

Shelkovnikova, T. A., O. M. Peters, A. V. Deykin, N. Connor-Robson, H. Robinson, A. A. Ustyugov, S. O. Bachurin, T. G. Ermolkevich, I. L. Goldman, E. R. Sadchikova, E. A. Kovrazhkina, V. I. Skvortsova, S. C. Ling, S. Da Cruz, P. A. Parone, V. L. Buchman and N. N. Ninkina (2013a). "Fused in sarcoma (FUS) protein lacking nuclear localization signal (NLS) and major RNA binding motifs triggers proteinopathy and severe motor phenotype in transgenic mice." J Biol Chem **288**(35): 25266-25274.

Shelkovnikova, T. A., H. K. Robinson, N. Connor-Robson and V. L. Buchman (2013b). "Recruitment into stress granules prevents irreversible aggregation of FUS protein mislocalized to the cytoplasm." Cell Cycle **12**(19): 3194-3202.

Shelkovnikova, T. A., H. K. Robinson, J. A. Southcombe, N. Ninkina and V. L. Buchman (2014a). "Multistep process of FUS aggregation in the cell cytoplasm involves RNA-dependent and RNA-independent mechanisms." Hum Mol Genet **23**(19): 5211-5226.

Shelkovnikova, T. A., H. K. Robinson, C. Troakes, N. Ninkina and V. L. Buchman (2014b). "Compromised paraspeckle formation as a pathogenic factor in FUSopathies." Hum Mol Genet **23**(9): 2298-2312.

Shelly, S., N. Lukinova, S. Bambina, A. Berman and S. Cherry (2009). "Autophagy is an essential component of Drosophila immunity against vesicular stomatitis virus." Immunity **30**(4): 588-598.

Shen, B., W. Zhang, J. Zhang, J. Zhou, J. Wang, L. Chen, L. Wang, A. Hodgkins, V. Iyer, X. Huang and W. C. Skarnes (2014a). "Efficient genome modification by CRISPR-Cas9 nickase with minimal off-target effects." Nat Methods **11**(4): 399-402.

Shen, J., W. Xia, Y. B. Khotskaya, L. Huo, K. Nakanishi, S. O. Lim, Y. Du, Y. Wang, W. C. Chang, C. H. Chen, J. L. Hsu, Y. Wu, Y. C. Lam, B. P. James, X. Liu, C. G. Liu, D. J. Patel and M. C. Hung (2013). "EGFR modulates microRNA maturation in response to hypoxia through phosphorylation of AGO2." Nature **497**(7449): 383-387.

Shen, M. W., M. Arbab, J. Y. Hsu, D. Worstell, S. J. Culbertson, O. Krabbe, C. A. Cassa, D. R. Liu, D. K. Gifford and R. I. Sherwood (2018). "Predictable and precise template-free CRISPR editing of pathogenic variants." Nature **563**(7733): 646-651.

Shen, W., X. H. Liang and S. T. Crooke (2014b). "Phosphorothioate oligonucleotides can displace NEAT1 RNA and form nuclear paraspeckle-like structures." Nucleic Acids Res **42**(13): 8648-8662.

Shen, W., X. H. Liang, H. Sun and S. T. Crooke (2015). "2'-Fluoro-modified phosphorothioate oligonucleotide can cause rapid degradation of P54nrb and PSF." Nucleic Acids Res **43**(9): 4569-4578.

Shi, J., G. Fung, P. Piesik, J. Zhang and H. Luo (2014). "Dominant-negative function of the C-terminal fragments of NBR1 and SQSTM1 generated during enteroviral infection." Cell Death Differ **21**(9): 1432-1441.

Shi, J., J. Wong, P. Piesik, G. Fung, J. Zhang, J. Jagdeo, X. Li, E. Jan and H. Luo (2013). "Cleavage of sequestosome 1/p62 by an enteroviral protease results in disrupted selective autophagy and impaired NFKB signaling." Autophagy **9**(10): 1591-1603.

Si, X., G. Gao, J. Wong, Y. Wang, J. Zhang and H. Luo (2008). "Ubiquitination is required for effective replication of coxsackievirus B3." PLoS One **3**(7): e2585.

Sibilla, C. and A. Bertolotti (2017). "Prion Properties of SOD1 in Amyotrophic Lateral Sclerosis and Potential Therapy." Cold Spring Harb Perspect Biol **9**(10).

Slaymaker, I. M., L. Gao, B. Zetsche, D. A. Scott, W. X. Yan and F. Zhang (2016). "Rationally engineered Cas9 nucleases with improved specificity." Science **351**(6268): 84-88.

Slowicka, K. and G. van Loo (2018). "Optineurin Functions for Optimal Immunity." Front Immunol **9**: 769.

Smith, B. N., N. Ticozzi, C. Fallini, A. S. Gkazi, S. Topp, K. P. Kenna, E. L. Scotter, J. Kost, P. Keagle, J. W. Miller, D. Calini, C. Vance, E. W. Danielson, C. Troakes, C. Tiloca, S. Al-Sarraj, E. A. Lewis, A. King, C. Colombrita, V. Pensato, B. Castellotti, J. de Belleroche, F. Baas, A. L. ten Asbroek, P. C. Sapp, D. McKenna-Yasek, R. L. McLaughlin, M. Polak, S. Asress, J. Esteban-Perez, J. L. Munoz-Blanco, M. Simpson, S. Consortium, W. van Rheenen, F. P. Diekstra, G. Lauria, S. Duga, S. Corti, C. Cereda, L. Corrado, G. Soraru, K. E. Morrison, K. L. Williams, G. A. Nicholson, I. P. Blair, P. A. Dion, C. S. Leblond, G. A. Rouleau, O. Hardiman, J. H. Veldink, L. H. van den Berg, A. Al-Chalabi, H. Pall, P. J. Shaw, M. R. Turner, K. Talbot, F. Taroni, A. Garcia-Redondo, Z. Wu, J. D. Glass, C. Gellera, A. Ratti, R. H. Brown, Jr., V. Silani, C. E. Shaw and J. E. Landers (2014). "Exome-wide rare variant analysis identifies TUBA4A mutations associated with familial ALS." Neuron **84**(2): 324-331.

Son, J. H., J. H. Shim, K. H. Kim, J. Y. Ha and J. Y. Han (2012). "Neuronal autophagy and neurodegenerative diseases." Exp Mol Med **44**(2): 89-98.

Soo, K. Y., J. Sultana, A. E. King, R. Atkinson, S. T. Warraich, V. Sundaramoorthy, I. Blair, M. A. Farg and J. D. Atkin (2015). "ALS-associated mutant FUS inhibits macroautophagy which is restored by overexpression of Rab1." Cell Death Discov **1**: 15030.

Souquere, S., G. Beauclair, F. Harper, A. Fox and G. Pierron (2010). "Highly ordered spatial organization of the structural long noncoding NEAT1 RNAs within paraspeckle nuclear bodies." Mol Biol Cell **21**(22): 4020-4027.

Spector, D. L. (2006). "SnapShot: Cellular bodies." Cell **127**(5): 1071.

Sreedharan, J., I. P. Blair, V. B. Tripathi, X. Hu, C. Vance, B. Rogelj, S. Ackerley, J. C. Durnall, K. L. Williams, E. Buratti, F. Baralle, J. de Belleroche, J. D. Mitchell, P. N. Leigh, A. Al-Chalabi, C. C. Miller, G. Nicholson and C. E. Shaw (2008). "TDP-43 mutations in familial and sporadic amyotrophic lateral sclerosis." Science **319**(5870): 1668-1672.

Stadtman, E. R. and R. L. Levine (2000). "Protein oxidation." Ann N Y Acad Sci **899**: 191-208.

Strong, M. J., K. Volkening, R. Hammond, W. Yang, W. Strong, C. Leystra-Lantz and C. Shoesmith (2007). "TDP43 is a human low molecular weight neurofilament (hNFL) mRNA-binding protein." Mol Cell Neurosci **35**(2): 320-327.

Su, J. H., K. E. Nichol, T. Sitch, P. Sheu, C. Chubb, B. L. Miller, K. J. Tomaselli, R. C. Kim and C. W. Cotman (2000). "DNA damage and activated caspase-3 expression in neurons and astrocytes: evidence for apoptosis in frontotemporal dementia." Exp Neurol **163**(1): 9-19.

Sullivan, P. M., X. Zhou, A. M. Robins, D. H. Paushter, D. Kim, M. B. Smolka and F. Hu (2016). "The ALS/FTLD associated protein C9orf72 associates with SMCR8 and WDR41 to regulate the autophagy-lysosome pathway." Acta Neuropathol Commun **4**(1): 51.

Sun, S., S. C. Ling, J. Qiu, C. P. Albuquerque, Y. Zhou, S. Tokunaga, H. Li, H. Qiu, A. Bui, G. W. Yeo, E. J. Huang, K. Eggan, H. Zhou, X. D. Fu, C. Lagier-Tourenne and D. W. Cleveland (2015). "ALS-causative mutations in FUS/TLS confer gain and loss of function by altered association with SMN and U1-snRNP." Nat Commun **6**: 6171.

Sun, Z., Z. Diaz, X. Fang, M. P. Hart, A. Chesi, J. Shorter and A. D. Gitler (2011). "Molecular determinants and genetic modifiers of aggregation and toxicity for the ALS disease protein FUS/TLS." PLoS Biol **9**(4): e1000614.

Sundaramoorthy, V., J. M. Sultana and J. D. Atkin (2015). "Golgi fragmentation in amyotrophic lateral sclerosis, an overview of possible triggers and consequences." Front Neurosci **9**: 400.

Sunwoo, H., M. E. Dinger, J. E. Wilusz, P. P. Amaral, J. S. Mattick and D. L. Spector (2009). "MEN epsilon/beta nuclear-retained non-coding RNAs are up-regulated upon muscle differentiation and are essential components of paraspeckles." Genome Res **19**(3): 347-359.

Suzuki, K., P. Bose, R. Y. Leong-Quong, D. J. Fujita and K. Riabowol (2010a). "REAP: A two minute cell fractionation method." BMC Res Notes **3**: 294.

Suzuki, N., M. Aoki, H. Warita, M. Kato, H. Mizuno, N. Shimakura, T. Akiyama, H. Furuya, T. Hokonohara, A. Iwaki, S. Togashi, H. Konno and Y. Itoyama (2010b). "FALS with FUS mutation in Japan, with early onset, rapid progress and basophilic inclusion." J Hum Genet **55**(4): 252-254.

Tada, M., H. Doi, S. Koyano, S. Kubota, R. Fukai, S. Hashiguchi, N. Hayashi, Y. Kawamoto, M. Kunii, K. Tanaka, K. Takahashi, Y. Ogawa, R. Iwata, S. Yamanaka, H. Takeuchi and F. Tanaka (2018). "Matrin 3 Is a Component of Neuronal Cytoplasmic Inclusions of Motor Neurons in Sporadic Amyotrophic Lateral Sclerosis." Am J Pathol **188**(2): 507-514.

Tan, A. Y. and J. L. Manley (2009). "The TET family of proteins: functions and roles in disease." J Mol Cell Biol **1**(2): 82-92.

Tan, A. Y., T. R. Riley, T. Coady, H. J. Bussemaker and J. L. Manley (2012). "TLS/FUS (translocated in liposarcoma/fused in sarcoma) regulates target gene transcription via single-stranded DNA response elements." Proc Natl Acad Sci U S A **109**(16): 6030-6035.

Tank, E. M., C. Figueroa-Romero, L. M. Hinder, K. Bedi, H. C. Archbold, X. Li, K. Weskamp, N. Safren, X. Paez-Colasante, C. Pacut, S. Thumma, M. T. Paulsen, K. Guo, J. Hur, M. Ljungman, E. L. Feldman and S. J. Barmada (2018). "Abnormal RNA stability in amyotrophic lateral sclerosis." Nat Commun **9**(1): 2845.

Taylor, J. P., R. H. Brown, Jr. and D. W. Cleveland (2016). "Decoding ALS: from genes to mechanism." Nature **539**(7628): 197-206.

Therrien, M., P. A. Dion and G. A. Rouleau (2016). "ALS: Recent Developments from Genetics Studies." Curr Neurol Neurosci Rep **16**(6): 59.

Thomas-Jinu, S., P. M. Gordon, T. Fielding, R. Taylor, B. N. Smith, V. Snowden, E. Blanc, C. Vance, S. Topp, C. H. Wong, H. Bielen, K. L. Williams, E. P. McCann, G. A. Nicholson, A. Pan-Vazquez, A. H. Fox, C. S. Bond, W. S. Talbot, I. P. Blair, C. E. Shaw and C. Houart (2017). "Non-nuclear Pool of Splicing Factor SFPQ Regulates Axonal Transcripts Required for Normal Motor Development." Neuron **94**(2): 322-336 e325.

Ticozzi, N., V. Silani, A. L. LeClerc, P. Keagle, C. Gellera, A. Ratti, F. Taroni, T. J. Kwiatkowski, Jr., D. M. McKenna-Yasek, P. C. Sapp, R. H. Brown, Jr. and J. E. Landers (2009). "Analysis of FUS gene mutation in familial amyotrophic lateral sclerosis within an Italian cohort." Neurology **73**(15): 1180-1185.

Ticozzi, N., C. Vance, A. L. Leclerc, P. Keagle, J. D. Glass, D. McKenna-Yasek, P. C. Sapp, V. Silani, D. A. Bosco, C. E. Shaw, R. H. Brown, Jr. and J. E. Landers (2011). "Mutational analysis reveals the FUS homolog TAF15 as a candidate gene for familial amyotrophic lateral sclerosis." Am J Med Genet B Neuropsychiatr Genet **156B**(3): 285-290.

Tolbert, M., C. E. Morgan, M. Pollum, C. E. Crespo-Hernandez, M. L. Li, G. Brewer and B. S. Tolbert (2017). "HnRNP A1 Alters the Structure of a Conserved Enterovirus IRES Domain to Stimulate Viral Translation." J Mol Biol **429**(19): 2841-2858.

Tollervey, J. R., T. Curk, B. Rogelj, M. Briese, M. Cereda, M. Kayikci, J. Konig, T. Hortobagyi, A. L. Nishimura, V. Zupunski, R. Patani, S. Chandran, G. Rot, B. Zupan, C. E. Shaw and J. Ule (2011). "Characterizing the RNA targets and position-dependent splicing regulation by TDP-43." Nat Neurosci **14**(4): 452-458.

Tomala, K. and R. Korona (2013). "Evaluating the fitness cost of protein expression in Saccharomyces cerevisiae." Genome Biol Evol **5**(11): 2051-2060.

Tomkins, J., P. Usher, J. Y. Slade, P. G. Ince, A. Curtis, K. Bushby and P. J. Shaw (1998). "Novel insertion in the KSP region of the neurofilament heavy gene in amyotrophic lateral sclerosis (ALS)." Neuroreport **9**(17): 3967-3970.

Tourriere, H., K. Chebli, L. Zekri, B. Courselaud, J. M. Blanchard, E. Bertrand and J. Tazi (2003). "The RasGAP-associated endoribonuclease G3BP assembles stress granules." J Cell Biol **160**(6): 823-831.

Tradewell, M. L., Z. Yu, M. Tibshirani, M. C. Boulanger, H. D. Durham and S. Richard (2012). "Arginine methylation by PRMT1 regulates nuclear-cytoplasmic localization and toxicity of FUS/TLS harbouring ALS-linked mutations." Hum Mol Genet **21**(1): 136-149.

Troakes, C., T. Hortobagyi, C. Vance, S. Al-Sarraj, B. Rogelj and C. E. Shaw (2013). "Transportin 1 colocalization with Fused in Sarcoma (FUS) inclusions is not characteristic for amyotrophic lateral sclerosis-FUS confirming disrupted nuclear

import of mutant FUS and distinguishing it from frontotemporal lobar degeneration with FUS inclusions." Neuropathol Appl Neurobiol **39**(5): 553-561.

Trotti, D., A. Rolfs, N. C. Danbolt, R. H. Brown, Jr. and M. A. Hediger (1999). "SOD1 mutants linked to amyotrophic lateral sclerosis selectively inactivate a glial glutamate transporter." Nat Neurosci **2**(9): 848.

Tsuiji, H., Y. Iguchi, A. Furuya, A. Kataoka, H. Hatsuta, N. Atsuta, F. Tanaka, Y. Hashizume, H. Akatsu, S. Murayama, G. Sobue and K. Yamanaka (2013). "Spliceosome integrity is defective in the motor neuron diseases ALS and SMA." EMBO Mol Med **5**(2): 221-234.

Tummala, H., C. Jung, A. Tiwari, C. M. Higgins, L. J. Hayward and Z. Xu (2005). "Inhibition of chaperone activity is a shared property of several Cu,Zn-superoxide dismutase mutants that cause amyotrophic lateral sclerosis." J Biol Chem **280**(18): 17725-17731.

Turner, M. R. and M. Swash (2015). "The expanding syndrome of amyotrophic lateral sclerosis: a clinical and molecular odyssey." J Neurol Neurosurg Psychiatry **86**(6): 667-673.

Urushitani, M., T. Sato, H. Bamba, Y. Hisa and I. Tooyama (2010). "Synergistic effect between proteasome and autophagosome in the clearance of polyubiquitinated TDP-43." J Neurosci Res **88**(4): 784-797.

Van Langenhove, T., J. van der Zee, K. Sleegers, S. Engelborghs, R. Vandenberghe, I. Gijselinck, M. Van den Broeck, M. Mattheijssens, K. Peeters, P. P. De Deyn, M. Cruts and C. Van Broeckhoven (2010). "Genetic contribution of FUS to frontotemporal lobar degeneration." Neurology **74**(5): 366-371.

Vance, C., B. Rogelj, T. Hortobagyi, K. J. De Vos, A. L. Nishimura, J. Sreedharan, X. Hu, B. Smith, D. Ruddy, P. Wright, J. Ganesalingam, K. L. Williams, V. Tripathi, S. Al-Saraj, A. Al-Chalabi, P. N. Leigh, I. P. Blair, G. Nicholson, J. de Belleroche, J. M. Gallo, C. C. Miller and C. E. Shaw (2009). "Mutations in FUS, an RNA processing protein, cause familial amyotrophic lateral sclerosis type 6." Science **323**(5918): 1208-1211.

Vande Velde, C., K. K. McDonald, Y. Boukhedimi, M. McAlonis-Downes, C. S. Lobsiger, S. Bel Hadj, A. Zandona, J. P. Julien, S. B. Shah and D. W. Cleveland (2011). "Misfolded SOD1 associated with motor neuron mitochondria alters mitochondrial shape and distribution prior to clinical onset." PLoS One **6**(7): e22031.

Vandenberghe, N., N. Leveque, P. Corcia, V. Brunaud-Danel, E. Salort-Campana, G. Besson, C. Tranchant, P. Clavelou, F. Beaulieux, R. Ecochard, C. Vial, E. Broussolle and B. Lina (2010). "Cerebrospinal fluid detection of enterovirus genome in ALS: a study of 242 patients and 354 controls." Amyotroph Lateral Scler **11**(3): 277-282.

Voigt, A., D. Herholz, F. C. Fiesel, K. Kaur, D. Muller, P. Karsten, S. S. Weber, P. J. Kahle, T. Marquardt and J. B. Schulz (2010). "TDP-43-mediated neuron loss in vivo requires RNA-binding activity." PLoS One **5**(8): e12247.

Volk, A. E., J. H. Weishaupt, P. M. Andersen, A. C. Ludolph and C. Kubisch (2018). "Current knowledge and recent insights into the genetic basis of amyotrophic lateral sclerosis." Med Genet **30**(2): 252-258.

Volkening, K., C. Leystra-Lantz, W. Yang, H. Jaffee and M. J. Strong (2009). "Tar DNA binding protein of 43 kDa (TDP-43), 14-3-3 proteins and copper/zinc superoxide dismutase (SOD1) interact to modulate NFL mRNA stability. Implications for altered RNA processing in amyotrophic lateral sclerosis (ALS)." Brain Res **1305**: 168-182.

Volonte, C., S. Apolloni and C. Parisi (2015). "MicroRNAs: newcomers into the ALS picture." CNS Neurol Disord Drug Targets **14**(2): 194-207.

Vucic, S., G. A. Nicholson and M. C. Kiernan (2008). "Cortical hyperexcitability may precede the onset of familial amyotrophic lateral sclerosis." Brain **131**(Pt 6): 1540-1550.

Waibel, S., M. Neumann, A. Rosenbohm, A. Birve, A. E. Volk, J. H. Weishaupt, T. Meyer, U. Muller, P. M. Andersen and A. C. Ludolph (2013). "Truncating mutations in FUS/TLS give rise to a more aggressive ALS-phenotype than missense mutations: a clinico-genetic study in Germany." Eur J Neurol **20**(3): 540-546.

Wang, F., J. Flanagan, N. Su, L. C. Wang, S. Bui, A. Nielson, X. Wu, H. T. Vo, X. J. Ma and Y. Luo (2012). "RNAscope: a novel in situ RNA analysis platform for formalin-fixed, paraffin-embedded tissues." J Mol Diagn **14**(1): 22-29.

Wang, H., W. Guo, J. Mitra, P. M. Hegde, T. Vandoorne, B. J. Eckelmann, S. Mitra, A. E. Tomkinson, L. Van Den Bosch and M. L. Hegde (2018a). "Mutant FUS causes DNA ligation defects to inhibit oxidative damage repair in Amyotrophic Lateral Sclerosis." Nat Commun **9**(1): 3683.

Wang, Q., I. A. Sawyer, M. H. Sung, D. Sturgill, S. P. Shevtsov, G. Pegoraro, O. Hakim, S. Baek, G. L. Hager and M. Dundr (2016). "Cajal bodies are linked to genome conformation." Nat Commun **7**: 10966.

Wang, W. Y., L. Pan, S. C. Su, E. J. Quinn, M. Sasaki, J. C. Jimenez, I. R. Mackenzie, E. J. Huang and L. H. Tsai (2013). "Interaction of FUS and HDAC1 regulates DNA damage response and repair in neurons." Nat Neurosci **16**(10): 1383-1391.

Wang, X., H. Fan, Z. Ying, B. Li, H. Wang and G. Wang (2010). "Degradation of TDP-43 and its pathogenic form by autophagy and the ubiquitin-proteasome system." Neurosci Lett **469**(1): 112-116.

Wang, Y., S. B. Hu, M. R. Wang, R. W. Yao, D. Wu, L. Yang and L. L. Chen (2018b). "Genome-wide screening of NEAT1 regulators reveals cross-regulation between paraspeckles and mitochondria." Nat Cell Biol **20**(10): 1145-1158.

Webster, C. P., E. F. Smith, P. J. Shaw and K. J. De Vos (2017). "Protein Homeostasis in Amyotrophic Lateral Sclerosis: Therapeutic Opportunities?" Front Mol Neurosci **10**: 123.

Weidberg, H. and Z. Elazar (2011). "TBK1 mediates crosstalk between the innate immune response and autophagy." Sci Signal **4**(187): pe39.

Weishaupt, J. H., T. Hyman and I. Dikic (2016). "Common Molecular Pathways in Amyotrophic Lateral Sclerosis and Frontotemporal Dementia." Trends Mol Med **22**(9): 769-783.

Werner, M. S. and A. J. Ruthenburg (2015). "Nuclear Fractionation Reveals Thousands of Chromatin-Tethered Noncoding RNAs Adjacent to Active Genes." Cell Rep **12**(7): 1089-1098.

West, J. A., C. P. Davis, H. Sunwoo, M. D. Simon, R. I. Sadreyev, P. I. Wang, M. Y. Tolstorukov and R. E. Kingston (2014). "The long noncoding RNAs NEAT1 and MALAT1 bind active chromatin sites." Mol Cell **55**(5): 791-802.

West, J. A., M. Mito, S. Kurosaka, T. Takumi, C. Tanegashima, T. Chujo, K. Yanaka, R. E. Kingston, T. Hirose, C. Bond, A. Fox and S. Nakagawa (2016). "Structural, super-resolution microscopy analysis of paraspeckle nuclear body organization." J Cell Biol **214**(7): 817-830.

White, J. P. and R. E. Lloyd (2011). "Poliovirus unlinks TIA1 aggregation and mRNA stress granule formation." J Virol **85**(23): 12442-12454.

White, M. A., E. Kim, A. Duffy, R. Adalbert, B. U. Phillips, O. M. Peters, J. Stephenson, S. Yang, F. Massenzio, Z. Lin, S. Andrews, A. Segonds-Pichon, J. Metterville, L. M. Saksida, R. Mead, R. R. Ribchester, Y. Barhomi, T. Serre, M. P. Coleman, J. R. Fallon, T. J. Bussey, R. H. Brown, Jr. and J. Sreedharan (2018). "TDP-43 gains function due to perturbed autoregulation in a Tardbp knock-in mouse model of ALS-FTD." Nat Neurosci **21**(4): 552-563.

Wild, P., H. Farhan, D. G. McEwan, S. Wagner, V. V. Rogov, N. R. Brady, B. Richter, J. Korac, O. Waidmann, C. Choudhary, V. Dotsch, D. Bumann and I. Dikic (2011). "Phosphorylation of the autophagy receptor optineurin restricts Salmonella growth." Science **333**(6039): 228-233.

Williams, K. L., S. Topp, S. Yang, B. Smith, J. A. Fifita, S. T. Warraich, K. Y. Zhang, N. Farrawell, C. Vance, X. Hu, A. Chesi, C. S. Leblond, A. Lee, S. L. Rayner, V. Sundaramoorthy, C. Dobson-Stone, M. P. Molloy, M. van Blitterswijk, D. W. Dickson, R. C. Petersen, N. R. Graff-Radford, B. F. Boeve, M. E. Murray, C. Pottier, E. Don, C. Winnick, E. P. McCann, A. Hogan, H. Daoud, A. Levert, P. A. Dion, J. Mitsui, H. Ishiura, Y. Takahashi, J. Goto, J. Kost, C. Gellera, A. S. Gkazi, J. Miller, J.

Stockton, W. S. Brooks, K. Boundy, M. Polak, J. L. Munoz-Blanco, J. Esteban-Perez, A. Rabano, O. Hardiman, K. E. Morrison, N. Ticozzi, V. Silani, J. de Belleroche, J. D. Glass, J. B. Kwok, G. J. Guillemin, R. S. Chung, S. Tsuji, R. H. Brown, Jr., A. Garcia-Redondo, R. Rademakers, J. E. Landers, A. D. Gitler, G. A. Rouleau, N. J. Cole, J. J. Yerbury, J. D. Atkin, C. E. Shaw, G. A. Nicholson and I. P. Blair (2016). "CCNF mutations in amyotrophic lateral sclerosis and frontotemporal dementia." Nat Commun **7**: 11253.

Williamson, T. L. and D. W. Cleveland (1999). "Slowing of axonal transport is a very early event in the toxicity of ALS-linked SOD1 mutants to motor neurons." Nat Neurosci **2**(1): 50-56.

Wilson, A. C., B. N. Dugger, D. W. Dickson and D. S. Wang (2011). "TDP-43 in aging and Alzheimer's disease - a review." Int J Clin Exp Pathol **4**(2): 147-155.

Wilusz, J. E., C. K. JnBaptiste, L. Y. Lu, C. D. Kuhn, L. Joshua-Tor and P. A. Sharp (2012). "A triple helix stabilizes the 3' ends of long noncoding RNAs that lack poly(A) tails." Genes Dev **26**(21): 2392-2407.

Wojcik, C., M. Rowicka, A. Kudlicki, D. Nowis, E. McConnell, M. Kujawa and G. N. DeMartino (2006). "Valosin-containing protein (p97) is a regulator of endoplasmic reticulum stress and of the degradation of N-end rule and ubiquitin-fusion degradation pathway substrates in mammalian cells." Mol Biol Cell **17**(11): 4606-4618.

Wolozin, B. (2012). "Regulated protein aggregation: stress granules and neurodegeneration." Mol Neurodegener **7**: 56.

Wong, N. K., B. P. He and M. J. Strong (2000). "Characterization of neuronal intermediate filament protein expression in cervical spinal motor neurons in sporadic amyotrophic lateral sclerosis (ALS)." J Neuropathol Exp Neurol **59**(11): 972-982.

Writing Group (2017). "Safety and efficacy of edaravone in well defined patients with amyotrophic lateral sclerosis: a randomised, double-blind, placebo-controlled trial." Lancet Neurol **16**(7): 505-512.

Wu, C. H., C. Fallini, N. Ticozzi, P. J. Keagle, P. C. Sapp, K. Piotrowska, P. Lowe, M. Koppers, D. McKenna-Yasek, D. M. Baron, J. E. Kost, P. Gonzalez-Perez, A. D. Fox, J. Adams, F. Taroni, C. Tiloca, A. L. Leclerc, S. C. Chafe, D. Mangroo, M. J. Moore, J. A. Zitzewitz, Z. S. Xu, L. H. van den Berg, J. D. Glass, G. Siciliano, E. T. Cirulli, D. B. Goldstein, F. Salachas, V. Meininger, W. Rossoll, A. Ratti, C. Gellera, D. A. Bosco, G. J. Bassell, V. Silani, V. E. Drory, R. H. Brown, Jr. and J. E. Landers (2012). "Mutations in the profilin 1 gene cause familial amyotrophic lateral sclerosis." Nature **488**(7412): 499-503.

Xia, Q., H. Wang, Z. Hao, C. Fu, Q. Hu, F. Gao, H. Ren, D. Chen, J. Han, Z. Ying and G. Wang (2016). "TDP-43 loss of function increases TFEB activity and blocks autophagosome-lysosome fusion." EMBO J **35**(2): 121-142.

Xiao, S., L. MacNair, J. McLean, P. McGoldrick, P. McKeever, S. Soleimani, J. Keith, L. Zinman, E. Rogaeva and J. Robertson (2016). "C9orf72 isoforms in Amyotrophic Lateral Sclerosis and Frontotemporal Lobar Degeneration." Brain Res **1647**: 43-49.

Xue, Y. C., R. Feuer, N. Cashman and H. Luo (2018a). "Enteroviral Infection: The Forgotten Link to Amyotrophic Lateral Sclerosis?" Front Mol Neurosci **11**: 63.

Xue, Y. C., C. M. Ruller, G. Fung, Y. Mohamud, H. Deng, H. Liu, J. Zhang, R. Feuer and H. Luo (2018b). "Enteroviral Infection Leads to Transactive Response DNA-Binding Protein 43 Pathology in Vivo." Am J Pathol **188**(12): 2853-2862.

Yamashita, S., A. Mori, H. Sakaguchi, T. Suga, D. Ishihara, A. Ueda, T. Yamashita, Y. Maeda, M. Uchino and T. Hirano (2012). "Sporadic juvenile amyotrophic lateral sclerosis caused by mutant FUS/TLS: possible association of mental retardation with this mutation." J Neurol **259**(6): 1039-1044.

Yamazaki, T., S. Chen, Y. Yu, B. Yan, T. C. Haertlein, M. A. Carrasco, J. C. Tapia, B. Zhai, R. Das, M. Lalancette-Hebert, A. Sharma, S. Chandran, G. Sullivan, A. L. Nishimura, C. E. Shaw, S. P. Gygi, N. A. Shneider, T. Maniatis and R. Reed (2012). "FUS-SMN protein interactions link the motor neuron diseases ALS and SMA." Cell Rep **2**(4): 799-806.

Yamazaki, T. and T. Hirose (2015). "The building process of the functional paraspeckle with long non-coding RNAs." Front Biosci (Elite Ed) **7**: 1-41.

Yamazaki, T., S. Souquere, T. Chujo, S. Kobelke, Y. S. Chong, A. H. Fox, C. S. Bond, S. Nakagawa, G. Pierron and T. Hirose (2018). "Functional Domains of NEAT1 Architectural lncRNA Induce Paraspeckle Assembly through Phase Separation." Mol Cell **70**(6): 1038-1053 e1037.

Yan, J., H. X. Deng, N. Siddique, F. Fecto, W. Chen, Y. Yang, E. Liu, S. Donkervoort, J. G. Zheng, Y. Shi, K. B. Ahmeti, B. Brooks, W. K. Engel and T. Siddique (2010). "Frameshift and novel mutations in FUS in familial amyotrophic lateral sclerosis and ALS/dementia." Neurology **75**(9): 807-814.

Yang, X., Y. Shen, E. Garre, X. Hao, D. Krumlinde, M. Cvijovic, C. Arens, T. Nystrom, B. Liu and P. Sunnerhagen (2014). "Stress granule-defective mutants deregulate stress responsive transcripts." PLoS Genet **10**(11): e1004763.

Yang, Y., A. Hentati, H. X. Deng, O. Dabbagh, T. Sasaki, M. Hirano, W. Y. Hung, K. Ouahchi, J. Yan, A. C. Azim, N. Cole, G. Gascon, A. Yagmour, M. Ben-Hamida, M. Pericak-Vance, F. Hentati and T. Siddique (2001). "The gene encoding alsin, a protein with three guanine-nucleotide exchange factor domains, is mutated in a form of recessive amyotrophic lateral sclerosis." Nat Genet **29**(2): 160-165.

Yasuda, K. and S. Mili (2016). "Dysregulated axonal RNA translation in amyotrophic lateral sclerosis." Wiley Interdiscip Rev RNA **7**(5): 589-603.

Yasuda, K., H. Zhang, D. Loiselle, T. Haystead, I. G. Macara and S. Mili (2013). "The RNA-binding protein Fus directs translation of localized mRNAs in APC-RNP granules." J Cell Biol **203**(5): 737-746.

Zhang, F., A. L. Strom, K. Fukada, S. Lee, L. J. Hayward and H. Zhu (2007). "Interaction between familial amyotrophic lateral sclerosis (ALS)-linked SOD1 mutants and the dynein complex." J Biol Chem **282**(22): 16691-16699.

Zhang, K., J. G. Daigle, K. M. Cunningham, A. N. Coyne, K. Ruan, J. C. Grima, K. E. Bowen, H. Wadhwa, P. Yang, F. Rigo, J. P. Taylor, A. D. Gitler, J. D. Rothstein and T. E. Lloyd (2018a). "Stress Granule Assembly Disrupts Nucleocytoplasmic Transport." Cell **173**(4): 958-971 e917.

Zhang, L. and A. Wang (2012). "Virus-induced ER stress and the unfolded protein response." Front Plant Sci **3**: 293.

Zhang, M., W. B. Wu, Z. W. Wang and X. H. Wang (2017). "lncRNA NEAT1 is closely related with progression of breast cancer via promoting proliferation and EMT." Eur Rev Med Pharmacol Sci **21**(5): 1020-1026.

Zhang, Q., C. Y. Chen, V. S. Yedavalli and K. T. Jeang (2013a). "NEAT1 long noncoding RNA and paraspeckle bodies modulate HIV-1 posttranscriptional expression." MBio **4**(1): e00596-00512.

Zhang, T., Y. C. Wu, P. Mullane, Y. J. Ji, H. Liu, L. He, A. Arora, H. Y. Hwang, A. F. Alessi, A. G. Niaki, G. Periz, L. Guo, H. Wang, E. Elkayam, L. Joshua-Tor, S. Myong, J. K. Kim, J. Shorter, S. E. Ong, A. K. L. Leung and J. Wang (2018b). "FUS Regulates Activity of MicroRNA-Mediated Gene Silencing." Mol Cell **69**(5): 787-801 e788.

Zhang, Y. J., T. F. Gendron, M. T. W. Ebbert, A. D. O'Raw, M. Yue, K. Jansen-West, X. Zhang, M. Prudencio, J. Chew, C. N. Cook, L. M. Daughrity, J. Tong, Y. Song, S. R. Pickles, M. Castanedes-Casey, A. Kurti, R. Rademakers, B. Oskarsson, D. W. Dickson, W. Hu, A. D. Gitler, J. D. Fryer and L. Petrucelli (2018c). "Poly(GR) impairs protein translation and stress granule dynamics in C9orf72-associated frontotemporal dementia and amyotrophic lateral sclerosis." Nat Med **24**(8): 1136-1142.

Zhang, Z., S. Almeida, Y. Lu, A. L. Nishimura, L. Peng, D. Sun, B. Wu, A. M. Karydas, M. C. Tartaglia, J. C. Fong, B. L. Miller, R. V. Farese, Jr., M. J. Moore, C. E. Shaw and F. B. Gao (2013b). "Downregulation of microRNA-9 in iPSC-derived neurons of FTD/ALS patients with TDP-43 mutations." PLoS One **8**(10): e76055.

Zhang, Z. and G. G. Carmichael (2001). "The fate of dsRNA in the nucleus: a p54(nrb)-containing complex mediates the nuclear retention of promiscuously A-to-I edited RNAs." Cell **106**(4): 465-475.

Zhang, Z., F. Lotti, K. Dittmar, I. Younis, L. Wan, M. Kasim and G. Dreyfuss (2008). "SMN deficiency causes tissue-specific perturbations in the repertoire of snRNAs and widespread defects in splicing." Cell **133**(4): 585-600.

Zhong, J., L. Jiang, Z. Huang, H. Zhang, C. Cheng, H. Liu, J. He, J. Wu, R. Darwazeh, Y. Wu and X. Sun (2017). "The long non-coding RNA Neat1 is an important mediator of the therapeutic effect of bexarotene on traumatic brain injury in mice." Brain Behav Immun **65**: 183-194.

Zhou, Y., S. Liu, G. Liu, A. Ozturk and G. G. Hicks (2013). "ALS-associated FUS mutations result in compromised FUS alternative splicing and autoregulation." PLoS Genet **9**(10): e1003895.

Zinszner, H., J. Sok, D. Immanuel, Y. Yin and D. Ron (1997). "TLS (FUS) binds RNA in vivo and engages in nucleo-cytoplasmic shuttling." J Cell Sci **110 (Pt 15)**: 1741-1750.

Zou, Z. Y., Z. R. Zhou, C. H. Che, C. Y. Liu, R. L. He and H. P. Huang (2017). "Genetic epidemiology of amyotrophic lateral sclerosis: a systematic review and meta-analysis." J Neurol Neurosurg Psychiatry **88**(7): 540-549.

Zu, T., Y. Liu, M. Banez-Coronel, T. Reid, O. Pletnikova, J. Lewis, T. M. Miller, M. B. Harms, A. E. Falchook, S. H. Subramony, L. W. Ostrow, J. D. Rothstein, J. C. Troncoso and L. P. Ranum (2013). "RAN proteins and RNA foci from antisense transcripts in C9ORF72 ALS and frontotemporal dementia." Proc Natl Acad Sci U S A **110**(51): E4968-4977.